Studies of Low Oxidation State Main Group Complexes:

Their Syntheses and Reactivities

by

Richard P Rose

This thesis is presented for the degree Doctor of Philosophy to the Faculty of Science,

Cardiff University, October 2006

UMI Number: U584840

Dissertation Publishing

DECLARATION

This work has not been previously accepted in substance for any degree and is not being concurrently submitted in candidature for any degree.

Signed ....(candidate)

Date ....13 Nov 2006.....

STATEMENT 1

This thesis is the result of my own investigations, except where otherwise stated. Where correction services have been used, the extent and nature of the corrections is clearly marked in a footnote(s).

Other sources are acknowledged by footnotes giving explicit references. A bibliography is appended.

Signed ....(candidate)

Date ....13 Nov 2006...

STATEMENT 2

I hereby give consent for my thesis, if accepted, to be available for photocopying and for inter-library loan, and for the title and summary to be made available to outside organisations.

Signed ....(candidate)

Date ......13 Nov 2006......

Abstract

The work presented in this thesis describes the synthesis, structure and reactivities of a range of low oxidation state main group metal complexes. The work upon this subject is divided into six chapters.

Chapter 1 provides a general introduction to the group 13 elements, low oxidation state group 13 chemistry and group 13 diyls. This chapter also describes the synthesis, theoretical treatments and reactivities of N-heterocyclic carbenes and their main group 13, 14 and 15 analogues, with a focus on the group 13 N-heterocyclic carbene analogues.

Chapter 2 describes an investigation into the formation of transition metal complexes of an anionic gallium(I) N-heterocyclic carbene analogue, [K(tmeda)][Ga{[N(Ar)C(H)]$_2$}], Ar = 2,6-diisopropylphenyl. These studies highlighted three different mechanistic pathways by which complexes could be isolated. Initially, substitution of a carbonyl ligand by the gallium carbene analogue in transition metal half sandwich carbonyl complexes was investigated. This yielded, for example, the first structurally authenticated Ga-V bond in [K(tmeda)][CpV(CO)$_3$[Ga{[N(Ar)C(H)]$_2$}]], Cp = cyclopentadienyl. Secondly, the direct donation of the gallium carbene analogues lone pair of electrons towards a manganese dialkyl fragment gave the complex [K(tmeda)][Mn{CH(SiMe$_3$)$_2$}$_2$[Ga{[N(Ar)C(H)]$_2$}]]. Finally, the salt metathesis reactions of the gallium carbene analogue with a series of Lewis base stabilised transition metal di-halides were explored. Results include, a series of complexes taking the structural form [M(tmeda)[Ga{[N(Ar)C(H)]$_2$}]$_2$], M = Mn, Fe, Co, Ni, Zn; and the first structurally authenticated Ga-Cu bond in [Cu(dppe)[Ga{N(Ar)C(H)}$_2$]], dppe = Bis(diphenylphosphino)ethane-P,P'.

Chapter 3 details a study into the reactions of a gallium(III) heterocycle, [I$_2$Ga{[N(Ar)C(H)]$_2$˙}], by the group 2 metals calcium or magnesium. A series of gallium-group 2 metal bonded complexes have been isolated including, for example the first structurally authenticated group 13-group 2 bond in the complex [Ca{Ga[(N(Ar)C(H))$_2$]}$_2$(THF)$_4$]. Furthermore, a subsequent investigation into the reactivity of an anionic gallium(I) N-heterocyclic carbene analogue, [K(tmeda)][Ga{[N(Ar)C(H)]$_2$}], towards N-heterocyclic carbenes and imidazolium cations gave, in one case, the novel group 13 hydride complex [HGa{[N(Ar)C(H)]$_2$}(IMes)], IMes = 1,3-bis(2,4,6-trimethylphenyl)imidazol-2-ylidene.

Chapter 4 describes the reactions of a paramagnetic gallium(II) dimeric complex, [{(Bu^t-DAB˙)GaI}$_2$], with the alkali metal pnictides, [ME(SiMe$_3$)$_2$] (M = Li or Na; E = N, P or As). These reactions have led to a series of paramagnetic gallium(III)-pnictide complexes, [(Bu^t-DAB)Ga{E(SiMe$_3$)$_2$}I] (E = N, P, As) and [(Bu^t-DAB)Ga{E(SiMe$_3$)$_2$}$_2$] (E = P, As). The complex [(Bu^t-DAB)Ga{As(SiMe$_3$)$_2$}I] possesses the shortest Ga-As single bond yet recorded.

Chapter 5 details an investigation into the reactivity of a amidinato germanium chloride complex, [(Cl)Ge{N(Ar)C(Bu^t)N(Ar)}]. This complex has been shown to participate in a range of different reactions. These are, salt metathesis giving, for example, the complex [{(CO)$_2$Fe(η^5-Cp)}Ge{N(Ar)C(Bu^t)N(Ar)}] and donation of a lone pair of electrons giving [{(CO)$_5$W}(Cl)Ge{N(Ar)C(Bu^t)N(Ar)}]. Furthermore, an investigation into the synthesis of a range of amidinato bismuth complexes by salt metathesis is described. The first structurally characterised amidinato bismuth complexes, for example [[(μ^2-Br)Bi(Br)[{(2,6-^{i}Pr$_2$C$_6$H$_3$)N}$_2$C(H)](THF)]$_2$], have been isolated and subsequent reductions have been attempted in some cases.

Finally, chapter 6 describes some aspects of group 13 hydride chemistry and details the attempted syntheses of group 13 metal(II)-metal(II) bonded species. Complexes, for example QuinAl(H)$_2$[tempo], Quin = 1-azabicyclo[2.2.2]octane, tempo = 2,2,6,6-Tetramethyl-1-piperidinyloxy; were isolated from reactions of a radical abstraction agent with Lewis base adducts of group 13 trihydrides.

Acknowledgements

Table of Contents

Chapter 1
General Introduction

Chapter 2
Complexes of a Anionic Gallium(I) Heterocycle with Transition Metal Fragments

Chapter 3

Main Group Chemistry of an Anionic Gallium(I) N-Heterocyclic Carbene Analogue

Chapter 4

Reactions of a Paramagnetic Gallium(II) Dimer Towards a Series of Pnictide Complexes

Chapter 5

Group 14 and 15 Amidinate Complexes

Chapter 6

Synthesis and Characterisation of Tempo-Group 13 Hydride Complexes

Abbreviations

Å	Angstrom, 1 x 10^{-10} meter
Ad	1-adamantyl
a_{iso}	Hyperfine coupling value
Ar	A general aryl substitutent
Ar-DAB	N,N'-bis(2,6-diisopropylphenyl)diazabutadine
BM	Bohr magneton, J T^{-1}
Br	Broad
Bu^t	Tertiary butyl
Bu^t-DAB	N,N'-bis(2,6-ditertiarybutyl)diazabutadiene
Bu^n	Normal butyl
ca.	Circa
cm^{-1}	Wavenumber, unit of frequency (= v/c)
Cp	Cyclopentadienyl, η^5-C_5H_5
Cp*	Pentamethylcyclopentadienyl, η^5-C_5Me_5
Cy	Cyclohexyl
δ	Chemical shift in NMR (ppm)
d	Doublet
dd	Double doublet
dec.	Decomposition temperature
DFT	Density Functional Theory
Dipp	Diisopropylphenyl
DPPE	Bis(diphenylphosphino)ethane-P,P'
E	Element
EPR	Electron Paramagnetic Resonance
ESR	Electron Spin Resonance
Et_2O	Diethyl ether
FTIR	Fourier Transform Infrared Spectroscopy
gem	Geminal, two function groups situated on one atom
g_{iso}	Isotropic g value
HOMO	Highest Occupied Molecular Orbital

Hz	Hertz, s^{-1}
IMes	1,3-bis(2,4,6-trimethylphenyl)imidazol-2-ylidene
ipso	ipso-substituent
IR	Infrared
$^{n}J_{xy}$	Coupling constant between nuclei X and Y, over n bonds, in Hz
J	Joule, $Kg\,m^2\,s^{-2}$
kcal	Kilocalorie (1 kcal = 4.184 kJ)
kJ	Kilojoule
L	A general ligand
M	A general metal or Molar ($mol\,dm^{-3}$)
M^{+}	Molecular ion
Me	Methyl
m/z	Mass / charge ration
Mes	Mesityl (2,4,6-trimethylphenyl)
MOCVD	Metal Organic Chemical Vapour Deposition
MS(APCI)	Atmospheric Pressure Chemical Ionisation Mass Spectroscopy
MS(EI)	Electron Ionisation Mass Spectroscopy
m	Multiplet, medium
meta	meta-substituent
m.p.	Melting point
NBO	Natural Bond Orbital
NMR	Nuclear Magnetic Resonance
ortho	ortho-substituent
Ph	Phenyl
Pr^{i}	Isopropyl
para	Para-substituent
ppm	Parts per million
q	Quartet
quin	quinuclidine, 1-azabicyclo[2.2.2]octane
R	General organic substituent
s	Singlet or strong
sept	Septet

sh	Sharp
TEMPO	2,2,6,6-Tetramethyl-1-piperidinyloxy
THF	Tetrahydrofuran
TMEDA	N,N,N',N'-tetramethylethylene-1,2-diamine
t	Triplet
18-crown-6	1,4,7,10,13,16-hexaoxacyclooctadecane
III/V	Semiconductor material derived from group 13/15 elements (1:1)
v	Frequency in Hz
X	A general halide

Thermal ellipsoids are shown at 25% probability level unless otherwise indicated

Chapter 1

General Introduction

1. Group 13 Elements

The elements of group 13 are boron, aluminium, gallium, indium and thallium. Their ground state valence electronic configuration is $ns^2\,np^1$. On descent of the group the physical properties of the elements vary greatly.

Table 1 displays some of the selected properties of these elements.

Table 1

Some Physical Properties of the Group 13 Elements[1-5]

Property	B	Al	Ga	In	Tl
Electronic configuration	$[He]2s^22p^1$	$[Ne]3s^23p^1$	$[Ar]3d^{10}4s^24p^1$	$[Kr]4d^{10}5s^25p^1$	$[Xe]4f^{14}5d^{10}6s^26p^1$
Atomic Number	5	13	31	49	81
Covalent Radii (Å)	0.81	1.25	1.25	1.50	1.55
1st Ionisation Energy (kJ mol^{-1})	800.3	564.2	564.2	558.3	589
2nd Ionisation Energy (kJ mol^{-1})	2427	1816	1979	1820	1970
3rd Ionisation Energy (kJ mol^{-1})	3658	2744	2962	2705	2975
Electronegativity (Pauling)	2.04	1.61	1.81	1.78	2.04
Electronegativity (Allred-Rochow)	2.01	1.47	1.82	1.49	1.44
Melting Point (^{o}C)	2300	660	29.8	157	303

In group 13 only boron is non-metallic. Boron is too electronegative to be a metal and as a result does not participate in delocalised metallic bonding. However, boron has four valence orbitals and only three valence electrons that form more localised covalent bonds in its compounds. However, due to the electron deficiency of the element, multicentre bonds tend to form in preference to 2-centre-2-electron bonds. This deficiency in electrons allows boron to have a wide and varied chemistry and it is often more closely related to its neighbour carbon and diagonal neighbour silicon than the rest of the elements in Group 13.[1]

The other four elements of group 13, Al, Ga, In and Tl, are classed as metals. After the rare gas core electronic configuration, there is a filled d^{10} valence shell for Ga and In, and in the case of Tl there is also a filled f^{14} valence shell.[2] Irregularities that occur in the physical properties, as descent through group 13 is made, can be attributed to effects on the valence electrons from these additional orbitals.[3]

The increase in the effective nuclear charge and size contraction, due to the filling of the proceeding orbitals, accounts for valence electrons of Ga, In and Tl to be held more strongly than expected. This effect can be seen from the differences in their ionisation energies. From boron to aluminium, there is a drop in the energy required to remove an electron. From aluminium to gallium there is little change in the ionisation energy. This inconsistency is caused by the 'd-block contraction', which describes the fall in atomic radii after the filling of the d-orbitals. This reduction in size increases the effective nuclear charge seen by the valence electrons, so makes them harder to remove. In turn, the decrease in the atomic size means the electronegativity of the elements increases from aluminium to gallium. This trend is confirmed from the Pauling and Allred-Rochow classifications.[4]

The covalent radii of aluminium and gallium are both 1.25 Å, because of the d-block contraction. An electron in the gallium $4s$ orbital is effectively less shielded from the nuclear charge by the filled $3d$ orbital, therefore $4s$ electrons contract towards the nucleus. Indium and thallium have larger radii, 1.50 and 1.55 respectively. A similar situation arises for thallium in respect to its $4f$ orbitals being filled, and thus the covalent radii of the two elements are similar.[1]

The prevailing oxidation state for group 13 compounds is +3. However as descent of the group is made toward the heavier elements the +1 oxidation state becomes more prominent. The 'inert pair effect' can explain this observation. As you descend the group, the energy gap between the valence s and p orbitals increases, consequently it is found that the s electrons are more reluctant to participate in bonding, and so remain paired. In addition for thallium, and to

2

some extent indium, the energy gained from forming 3 covalent bonds is less than the energy required to promote the s electrons to allow this. Mono halides for InX and TlX, X = Cl, Br, and I, are known. The lighter group 13 mono-halides are also known, AlCl is encountered only at high temperatures in the gas phase, as is GaX for X = Cl, Br, and I.[3,5,6] Relativistic effects can also contribute to the inert pair effect causing a predominance of the +1 oxidation state in complexes of the heaviest element. As the velocity of a $1s$ electron increases towards the speed of light, its mass increases, and it, and the higher energy s-orbitals, all contract towards the nucleus.[1]

2.   Low Oxidation State Group 13 Halide Chemistry

In the past 20 years there has been much interest in the low oxidation state chemistry of lighter group 13 element compounds, and rapid progress has been made. The stabilisation of metastable aluminium(I) and gallium(I) halide complexes, [{MX(L)}$_n$], M = Al or Ga; X = halide; L = Lewis base, has allowed explorative chemistry into the formation of novel alkyl, silyl and amido low-oxidation state metal and cluster complexes. These low-oxidation state halides have been prepared by use of a specialist reactor. HX$_{(g)}$ X = halogen, is reacted with liquid Al or Ga at high temperatures, $ca.$ 1000°C, and vacuum 5 x 10^{-5} mbar. The resultant MX vapour is condensed at −196°C on the surface of the reactor chamber. To access the material the liquid nitrogen cooling is removed and the melting condensate can be collected in a Schlenk vessel. However, disproportionation of the melting condensate can occur, and thus solvents are added in order to stabilise these species. One example is the synthesis of "AlBr" where the addition of a triethylamine / toluene mix yields the complex [Al$_4$Br$_4$(NEt$_3$)$_4$] which has been crystallographically characterised and shown to be a cyclic tetramer.[7-9]

In 1990 a facile synthesis of "Ga(I)I" was reported.[10] The ultrasonic activation of gallium metal and 0.5 equivalents of iodine in toluene resulted in a pale green powder. The reactivity of this material suggested that it was a gallium mono iodide species. This preparation has allowed access to a source of gallium(I) halide without specialised reactors or techniques. The molecular structure of "GaI" is unknown, however Raman spectroscopy studies have suggested a mixture of sub halides, predominiated by [Ga]$_2^+$ [Ga$_2$I$_6$]$^{2-}$.[11] The chemistry of this species is now being

widely explored and this has led to an array of novel compounds, for example from the reaction of "GaI" with Fp^*_2, $Fp^* = Cp^*Fe(CO)_2$, which gave $[Cp^*Fe(CO)_2GaI_2]_2$.[12]

Complexes containing gallium and indium in the +II oxidation state have also received attention in the mid part of the last century.[13,14] Early attempts to synthesise these compounds resulted in disproportionation to mixed valence species such as gallium(I) tetraiodogallate(III), $[Ga]^+ [GaI_4]^-$.[15,16] About twenty years later a neutral gallium(II) compound was isolated $Ga_2Cl_4 \cdot 2(\text{diox})$, diox $= C_4H_8O_2$, which was crystallographically characterised and found to be a discrete molecule containing a Ga-Ga bond.[17] Related In(II) complexes have also been synthesised and structurally characterised, for example $[InI_2(PPr^n_3)]_2$.[18]

3.   Group 13 Diyl Chemistry

Group 13 diyls take the form :E(I)R, where E = Al, Ga, In, Tl; R = alkyl, aryl. The fragment is isolobal with CO, therefore it has the ability to act as a σ-donor as well as a potential π-acceptor in its transition metal complexes. It can also be thought of analogous to acyclic carbenes. There is a *sp*-hybridised orbital where a lone-pair of electrons reside, as well as two vacant *p*-orbitals. The organic substituent R can affect the π-accepting ability of the group 13 centre in that when R = Cp^* ($Cp^* = C_5Me_5$), there is orbital overlap of the ligand π-system with the empty metal *p*-orbitals. This diminishes the π-accepting ability of E when the diyl acts as a ligand.[19]
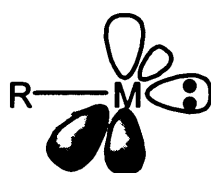
R = alkyl, aryl
M = Al, Ga, In, Tl

Density Functional Theory (DFT) studies have been performed on a series of model group 13 diyl transition metal complexes to gain an insight into the effect of the group 13 substituent on the π-accepting ability of the group 13 metal.[20] The model complex $[(CO)_4Fe\{GaCp\}]$, (where Cp $= C_5H_5$), where there is overlap of the empty gallium *p*-orbitals by

the filled p-orbitals of the Cp substituent, possesses a Ga-Fe dissociation energy of 32.89 kcal mol^{-1}. In addition, charge decomposition analysis (CDA) calculations on this showed that the Ga$\rightarrow$Fe σ-donation (0.413 electrons) is clearly stronger than the Ga$\leftarrow$Fe π-back donation (0.039 electrons). Comparing these values with the model [(CO)$_4$Fe{GaPh}], Ph = C$_6$H$_5$; where there is little p-orbital overlap between the gallium and Ph substituent, the Ga-Fe bond dissociation energy is significantly increased to 55.03 kcal mol^{-1}. CDA calculations also showed that a significantly higher bonding contribution comes from Ga$\leftarrow$Fe π-back donation (0.264 electrons) but this is still smaller than the Ga$\rightarrow$Fe σ-donation (0.383 electrons). This trend is present for all the analogous group 13 compounds.

The heavier group 13 diyls E(I)R, where E = Tl, In; R = Cp; have been known for some time and will not be further discussed here.[21,22] There are two general routes employed in the synthesis of the lighter gallium and aluminium diyls. Firstly, salt metathesis, for example in the synthesis of **1**, (scheme 1),[23] and secondly the reduction of REX$_2$ species with a suitable alkali metal, e.g. in the synthesis of **2**, (scheme 1).[24]

Scheme 1

$$M(I)Cl \quad + \quad [MgCp^*{}_2] \xrightarrow{\text{toluene / ether}} 0.5[Cp^*MgCl.Et_2O]_2 + [MCp^*]$$
1

$$M(I)Cl \quad + \quad [LiCp^*] \xrightarrow{\text{toluene / ether}} LiCl + [MCp^*]$$
1

M = Al, Ga, In, Tl; Cp* = C$_5$Me$_5$

$$(Me_3Si)_3CAlI_2.THF + Na / K \xrightarrow[\text{-NaI \quad -KI \quad -THF}]{\text{toluene}} 0.25[(Me_3Si)_3CAl]_4$$
2
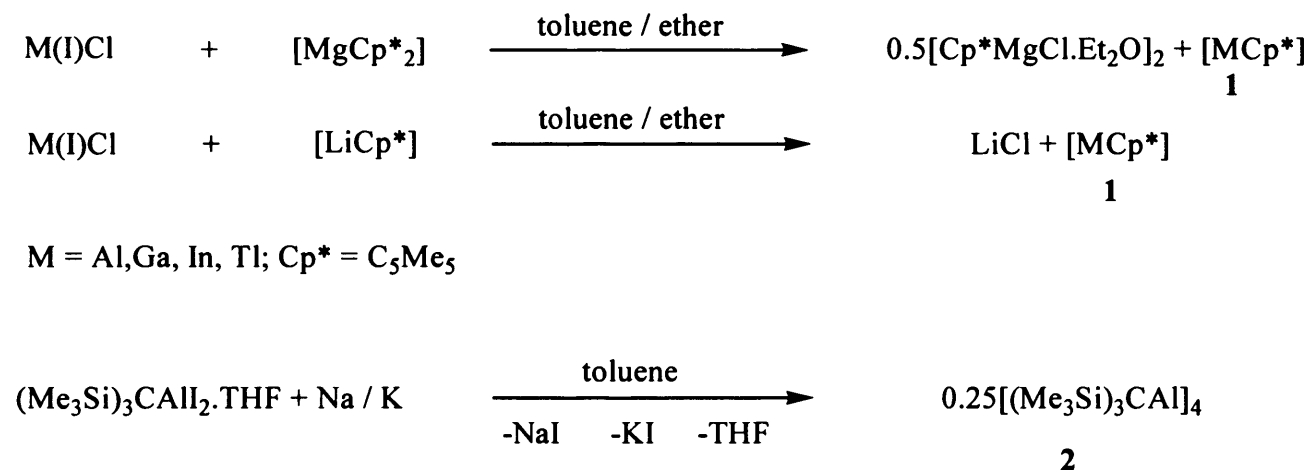
Oligomerisation is seen to occur for the metal diyls, and is most apparent in the solid state.[7] For example, TlCp* is found to crystallise with a polymeric zig zag chain where the Tl atoms and Cp* rings alternate. The structure of the analogous AlCp* is, however, quite different where the structure has been formulated as [Al$_4$Cp$^*{}_4$], and contains a central Al$_4$ tetrahedron. These observed differences in the solid state structures are attributed to a decreasing ionic bonding contribution between the ligand and the metal for the lighter elements of group 13. As a

result, stronger metal-metal interactions are expected for the lighter elements. Oligomerisation is found to occur to a much greater extent by replacing the Cp* ligand with ligands such as {C(SiMe₃)₃}. The Cp* ligand stabilises the formation of monomeric diyl units by forming π-interactions between the ligand and the metal. This does not occur for the {C(SiMe₃)₃} ligand. Tetrameric structures have been identified for [M₄{C(SiMe₃)₃}₄], M = Al, Ga, In. The most notable difference between these compounds is that the tetrameric In compound retains its structure in solution. This is believed to be due to a lower steric strain between the indium's substituents, due to the larger size of the M₄ tetrahedron.[7]

Metal diyls have been shown to participate in a range of different chemistries. Early investigations involved reactions with homoleptic transition metal carbonyl complexes. The reactions giving, for example, [Co₂(CO)₆(μ²-ECp*)₂], 3, E = Al, Ga; where the diyl fragment acts as a bridging ligand. Alternatively, the diyl fragment can act as a terminal ligand, as in 4, and can be synthesised by substitution of a labile olefin, for example in the reaction of Cp*Ga with Cr(CO)₅(C₈H₁₄) giving [(Cp*Ga)Cr(CO)₅].[19a,b] As a result, metal diyls can be thought of as isolobal analogues of CO.

E = Al, Ga; Cp* = C₅Me₅
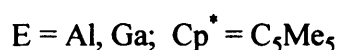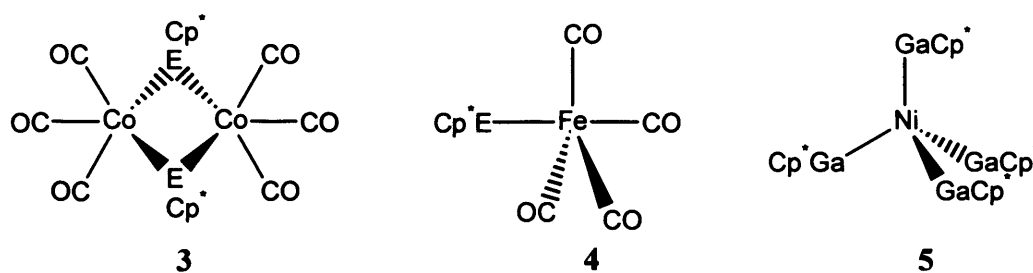
Homoleptic transition metal diyls can be synthesised by the total substitution of olefins. For example, in the reaction of Ni(COD)₂, COD = 1,5-cyclooctadiene; with 4 equivalents of GaCp*, the homoleptic complex 5 is formed.[25]

Insertion reactions have also been observed for group 13 diyls. In these reactions the Cp* moiety can change from an η⁵ binding to η¹-bonding to the group 13 metal. This change in binding mode allows for the formation of complexes such as 6 and highlights the reducing ability of metal diyls.[19a]

Scheme 2

E = Ga, In

6 ECp*

toluene, RT

6
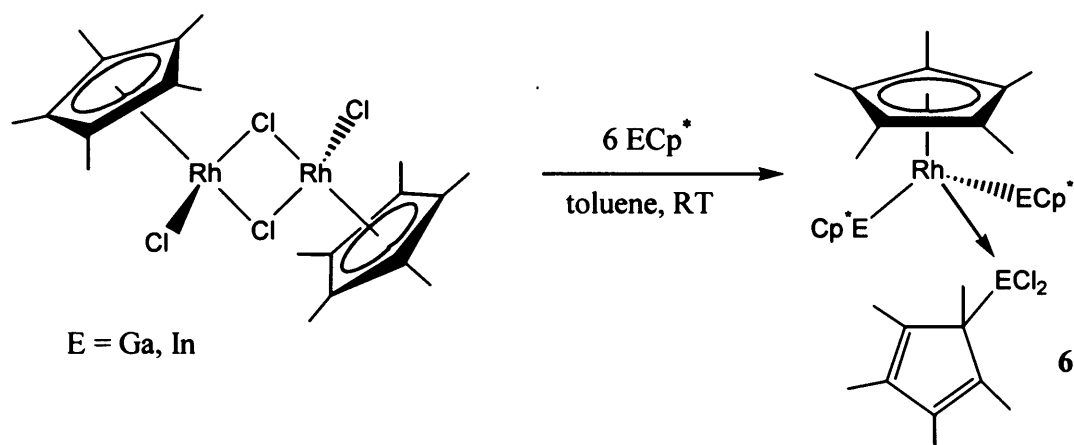
The use of more sterically bulky substituents on the group 13 metal diyls has also been explored. Scheme 3 shows one example where two possible pathways to a complex with bulky diyl ligands can be employed. Firstly, the direct substitution of a ligand and secondly the salt metathesis of a higher oxidation state starting material. Complex **7** was originally described as a ferrogallyne i.e. possessing a triple bond.[26] However, it has also been described, more convincingly, as a strong σ-donor complex, with little iron to gallium π-donation.[27]

Scheme 3

Ga + Fe(CO)₅ → Toluene, - CO

[Ar*GaCl₂] + Na₂[Fe(CO)₄] → Ether, -2 NaCl

7
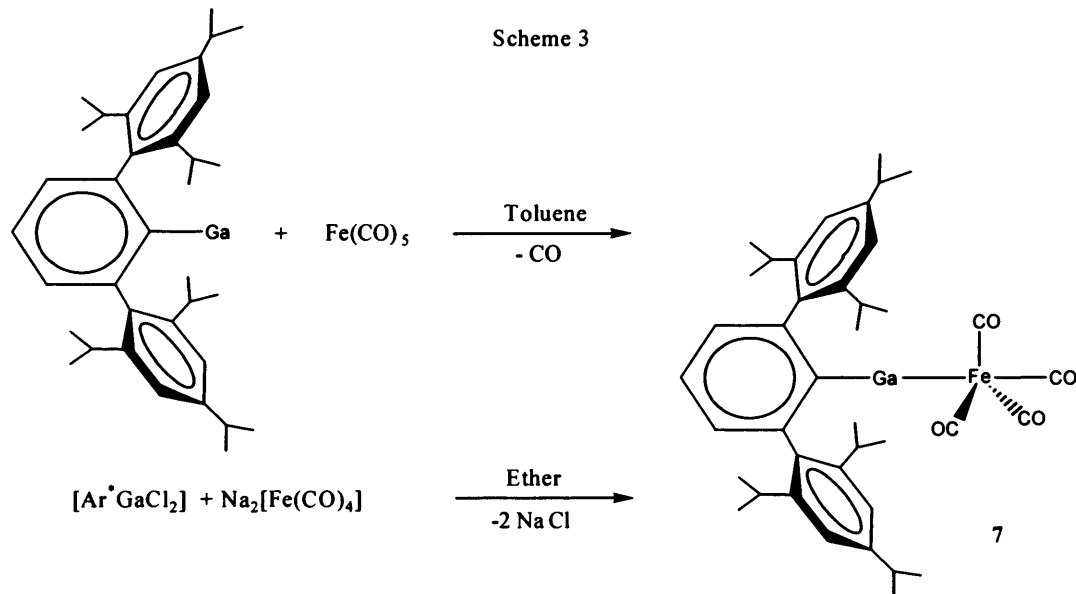
Numerous theoretical investigations have investigated **7** and related complexes. Current perspectives suggest minimal metal-metal π-back-bonding, with strong σ-donation in this complex.[28,20] However, this is not always the case. Homoleptic complexes such as

7

[Ni{GaC(SiMe$_3$)$_3$}$_4$], **8**, where the diyl ligand does not compete with other ligands for metal d-electron density, have been shown to have significant π-back-bonding by calculations.[29]

$$GaC(SiMe_3)_3$$

$$(Me_3Si)_3CGa \diagdown \overset{Ni}{\underset{GaC(SiMe_3)_3}{\big|}} \diagup GaC(SiMe_3)_3$$

8
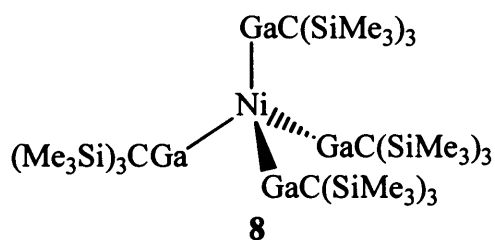
4.   N-Heterocyclic Carbenes

Carbenes have been known for many years and can be classified as divalent carbon compounds of the general form :CR$_2$. These are often transient intermediates in organic syntheses and to some extent can be considered as analogues of group 13 diyls, :MR.[30] Research into the chemistry of carbenes during the mid 1950's and 1960's was carried out by, for example, Doering[31] and Fischer[32] and allowed for research into a broad range of applications for such species. Wanzlick[33,34] and Öfele[35] later discovered synthetic pathways to N-heterocyclic carbenes (NHC), and were able to derive transition metal carbene complexes such as **9** and **10**.

Scheme 4
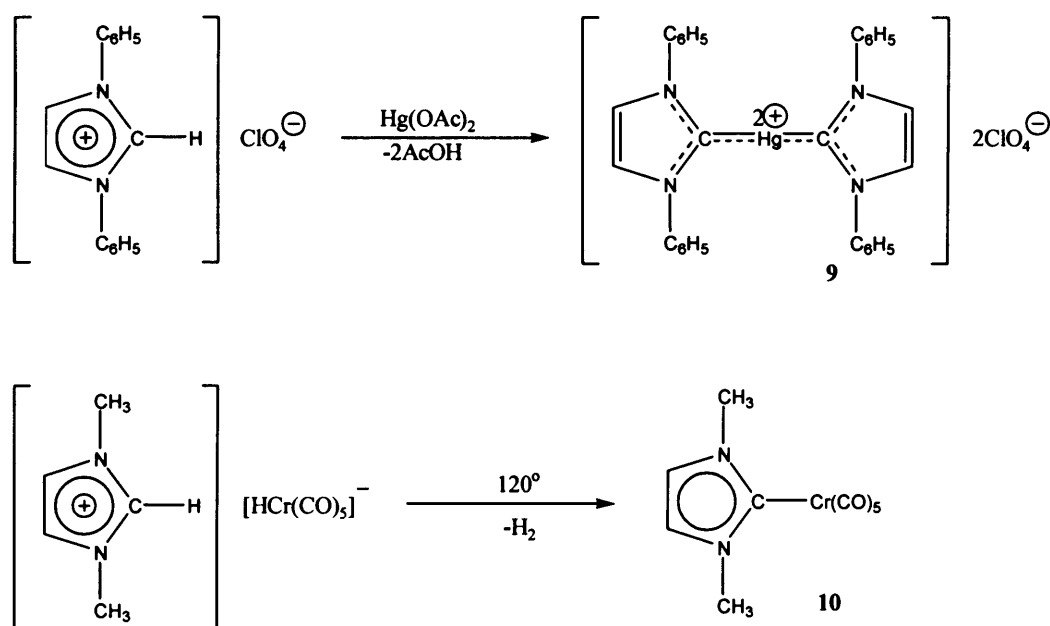
Both reactions involved an imidazolium salt being deprotonated by a metal precursor of significant basicity. Little further progress with isolating free carbene fragments was made until 1991 when Arduengo and co-workers[36] synthesised and crystallographically characterised 1,3-di-1-adamantyl-imidazol-2-ylidene, the first isolated stable N-heterocyclic carbene. This carbene was synthesised by the deprotonation of 1,3-di-1-adamantylimidazol chloride using sodium hydride. Further studies have allowed for the isolation of many stable NHC's.[37,38] Suffice to say, since 1991 a rapid expansion into the chemistry of NHC has been carried out, giving numerous main group and transition metal complexes. These studies have allowed for the exploration of the catalytic behaviour of NHC complexes in which the NHC ligand often acts as a phosphine mimic.[39a,40] Indeed, in some cases the NHC ligand has enhanced catalytic activity in place of phosphines.[40]

In NHC-transition metal complexes it is thought that the NHC is not able to participate in π-bonding with filled metal d-orbitals to any significant extent.[41] The interaction of the carbene centre with the π-donating, σ-attracting amino substituents is believed to cause this.[38,39b]
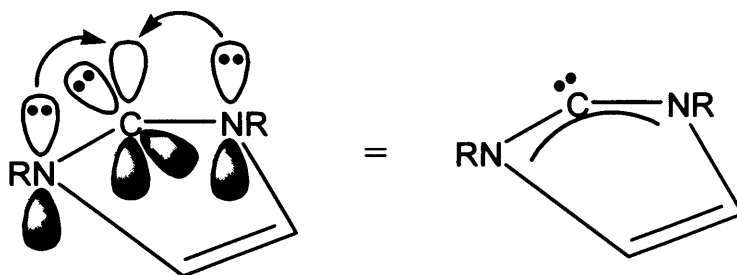
The donation of p-electron density from the nitrogens into the empty p-orbitals of the carbene effectively removes the possibility of π-back bonding from a transition metal taking place. The filled p-orbital of the carbene can, therefore, not accept any significant electron density from filled metal d-orbitals. However, this p-electron density donation does aid the stabilisation of the carbene species.[38] The NHCs have been described as 'diaza-allyl systems' with little π-aromaticity.[39a,b]

5.   Theoretical Treatment of Group 13 Metal(I) Heterocycles

Since the isolation of the first crystalline N-heterocyclic carbene in 1991, there has been a drive to expand this area of research to include heterocycles including main group elements other than carbon. Group 13 heterocycles have received attention and in 1997 Schoeller *et al.*[42]

performed density functional theory calculations (DFT) on model compounds [E{N(H)C(H)}$_2$]$^-$, where E = B, Al, Ga, In, **11**. Quantitative considerations were set in place to determine whether the group 13 carbene analogues would be experimentally accessible. These were (a) the singlet-triplet energy gap must be large so facile radical reactions would not take place, (b) the electron affinities of the metal must be large so preparation of the carbene analogues might be possible. Results from the calculations indicated for E = B, a non-bonding lone pair is present, but this diminishes when E = Al - In in favour of increased *p*-electron density at the neighbouring nitrogen atoms. These findings suggest for higher element homologues, a cyclic delocalisation of electrons does not occur.

11(A)   **11(B)**

E = Al, Ga or In
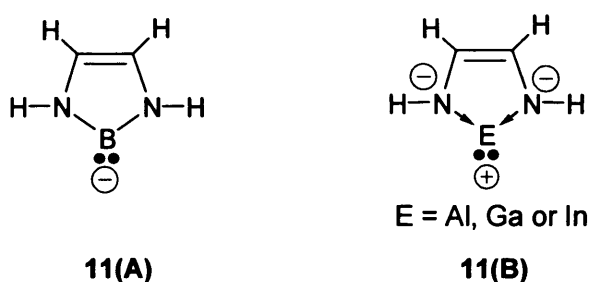
A further calculation was performed to include another feasible structure where a 1,2-hydrogen shift from a neighbouring N to the group 13 metal, E, had taken place. The results indicated the lowest energy structure for B was when the proton migration had occurred. For Al and Ga the proton migrations were disfavoured. Other fundamental differences were found on descent of the group for the heterocycles. When E = B, the E-N bond is almost single where for E = Al it is almost half a bond. The results suggest the predominance of structure **11(A)** for E = B, and a donor-acceptor formulation **11(B)** for E = Al, Ga, In. Structure **11(B)** becomes more prominent in the order E = Al < Ga < In. Concluding, group 13 carbene analogues are worthy synthetic targets. Very recently, an anionic boryl complex has been synthesised, [B{[N(Ar)C(H)]$_2$}], where Ar = 2,6-Pr$^i_2$C$_6$H$_3$. The solid state structure indicates the anionic boryl component takes the form **11(A)**.[86]

Similar results were gained from *ab initio* studies on the same model heterocycles. These indicated that for E = B and Al there is an appreciable aromatic stabilisation, albeit less compared with normal NHCs at the same level of theory. This stabilisation is derived from an aromatic ring current. The current is found to be greater with E = B compared with E = Al. Consequently, the lone pair at Al should have more *s*-character. A molecular orbital treatment

found that the lone pair resides in the highest occupied molecular orbital (HOMO) for both compounds, and is at high energy. The empty Al p-orbital was found not to participate in delocalisation of the π system, whereas for B, the p-orbital was largely incorporated in the ring delocalisation.[43]

Additionally, Schoeller *et al.*[44] have extended their investigations to include P-heterocyclic group 13 carbene analogues. The ligand diphosphabutadiene, (HPCH=CHPH) was studied using the same methodology as for the diazabutadiene ligand system in **11**. It was found that the P-E bonding in $[E\{P(H)C(H)\}_2]^{-1}$ E = B, Al, Ga; becomes more covalent, than the E-N bonding in **11**, as P is less electronegative than N. Concluding, the heterocycles would be worthy targets for synthesis.[45]

Neutral 6-membered N-heterocyclic group 13 metal(I) carbene analogues have also been investigated by DFT calculations on the model complexes $[E\{HC(CR'NR'')_2\}]$ E = B, Al, Ga, In; R' = H; R" = H or Me.[46] The higher group 13 homologues (E = Al - In) carry a partial positive charge at the metal, whereas B possesses a partial negative charge in its heterocycle. The N-E bonds have substantial ionic character as a result. Electron Localisation Function calculations revealed the presence of a lone pair for all group 13 elements. The singlet-triplet energy gaps were found to be close for B but for the heavier homologues, E = Al - In, the triplet states lie more than 150 kJmol^{-1} above the singlet state. For E = Al - In polar E-N bonds typical of donor acceptor complexes are seen. The structure is best represented as an anionic chelating ligand and a positively charged group 13 metal in the +I oxidation state (scheme 5). In contrast, when E = B the complex exhibits more covalent B-N bonds and is best described as a di-radical species with B in the +II oxidation state.

Scheme 5

E = B, Al, Ga, In
R' = H; R" = H or Me
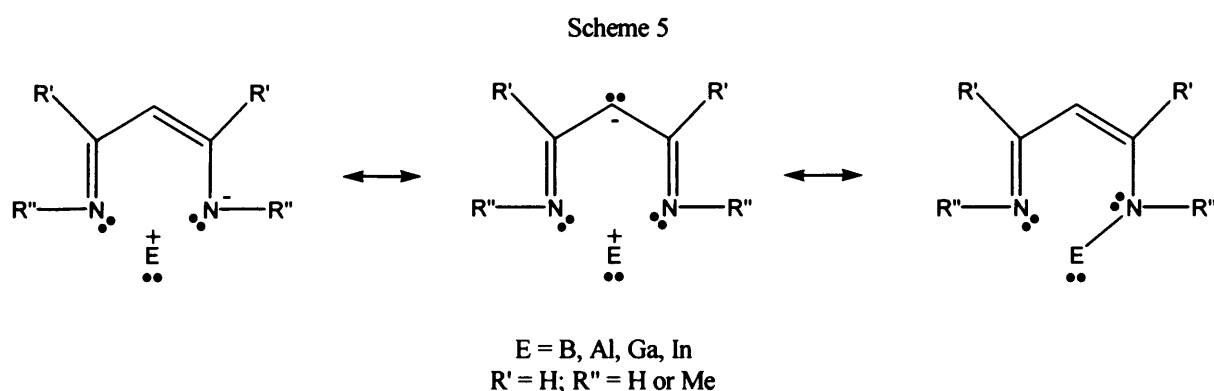
Power and co-workers[47] have examined the model gallium heterocycle [:Ga{(N(Me)C(Me))$_2$CH}], where the HOMO was found to correspond to the gallium lone pair,

and the lowest unoccupied molecular orbital (LUMO) surprisingly is not based on the empty Ga $4p$-orbital, but instead it is largely a N-C π^*-orbital located on the N_2C_3 skeleton of the β-diketiminate ligand. The LUMO is separated from the HOMO by 110 kcal mol^{-1}. These observations suggest that such complexes should act as strong σ-donors but would be poor π-acceptors. A study using Hartree-Fock and DFT calculations was carried out on the model compound, [:Ge{(N(H)C(H))$_2$CH}]$^+$, which is isoelectronic to the previous Ga model. The results indicated that the HOMO is associated with Ge-N and C-C π-bonding within the ring. The Ge lone pair resides in the HOMO-1 orbital and the LUMO is associated with the empty Ge $4p$-orbital. Replacing Ga with Ge$^+$ lowered the HOMO and LUMO energy levels.[48]

Roesky *et al.* have investigated [:Al{(N(Me)C(Me))$_2$CH}] by *ab initio* calculations.[49] The results of this study largely agree with the previous investigation.[46] This study indicates that the lone pair at the Al resides in an *sp*-like orbital and is stereo-chemically active. Similarly, Hill and co-workers[50] have investigated model In(I) and Tl(I) heterocycles, [:M{(N(Ar)C(R))$_2$CH}], M = In; R = Me, CF$_3$; M = Tl; R = Me; Ar = 2,6-^{i}Pr$_2$C$_6$H$_3$; by DFT calculations. When M = In, in both cases the HOMO corresponds to a lone-pair on the metal which has prominent *sp*-character, and is stereo-chemically active. The LUMO in each case is entirely ligand based and of π symmetry. The LUMO+1 (indium empty p-orbitals) are separated from the HOMO by 98.5 and 104.8 kcal mol^{-1} respectively. In the Tl complex there is a significant reordering of orbital energies. The HOMO is entirely ligand based and the lone-pair is found to be 17 kcal mol^{-1} lower in energy. The LUMO is represented by a metal based p-orbital.

Theoretical investigations of neutral 6-membered N-heterocyclic group 13 metal(I) carbene analogues have now been extended to include the reactivity of such a species. Su and co-workers[51] investigated C-H bond insertions with methylene, cycloadditions with ethylene and kinetic stability with respect to dimerization. Their analysis of the models [:E{(N(Ph)C(Me))$_2$CH}] E = B, Al, Ga, In, Tl; suggested that when E = B, the heterocycle can readily undergo C-H bond insertion and cycloaddition reactions. In particular, no barrier to dimerization was found. However, findings indicated the B compound to be unstable and potentially unobtainable synthetically. In the cases of E = Al, Ga, In and Tl, the aforementioned reactions were found to all be energetically unfavourable with the likelihood of such reactions taking place diminishing with increasing atomic number.

Neutral 4-membered N-heterocyclic group 13 metal(I) carbene analogues have recently been the subject of DFT investigations.[52,53] These showed that in [:M{η^2-N-N'-

(Ph)NC(NMe$_2$)N(Ph)}], M = Al, Ga, Tl (see below); the metal lone pair is associated with the HOMO and the LUMO with the empty metal p-orbital. The lone pairs possess sp-character and the HOMO-LUMO energy separations were found to be significant (M = Al 61.8, Ga 67.4, In 63.5 kJmol^{-1}). These values suggest the heterocycles will be good σ-donors but weak π-acceptor ligands. The N-M bonds have high ionic character so little overlap of the N p-orbital lone-pair with the metal was found.[52]

M = Al, Ga or Tl
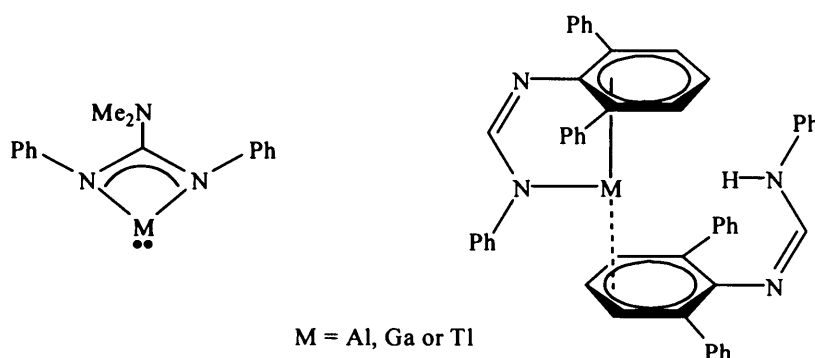
The model [In{PhNC(H)NPh}] · {PhN(H)C(H)NPh}, which contains an isomer of the 4-membered neutral group 13 indium(I) carbene analogue, was also used for the study. Binding energies between the two fragments was found to be very weak at 7.20 kJmol^{-1}. This study also revealed the lone pair at the In centre to be essentially of s-character.[53]

6.   Synthesis of Group 13, 14, and 15 N-Heterocyclic Carbene Analogues, Including Structural Analyses of Group 13 Analogues

In 1991 Arduengo and co-workers[36] isolated the first crystalline NHC and since, there has been much interest in synthesising other main group heterocyclic carbene analogues. This area of research has not been exclusive to 5-membered NHC systems but also includes 4- and 6-membered heterocycles. The ligands used to prepare these heterocycles take the general form shown below and stabilise the metal centre of the heterocycle by promoting kinetic inertness through steric bulk of the N-substituent.[41]
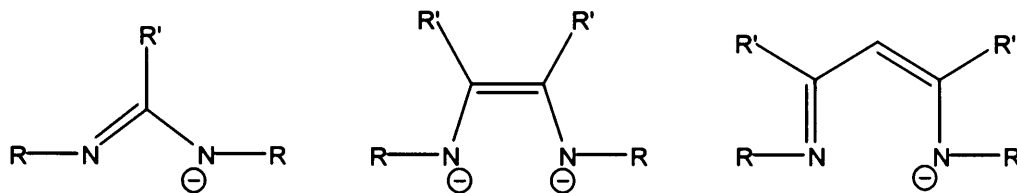
6.1   Four-Membered NHC Analogues

Jones and co-workers have recently synthesised a series of 4-membered group 13(I) carbene analogues.

Scheme 6

K[Piso] $\xrightarrow{\text{MX}}$

Piso =[(Ar)NC(Bu^t)N(Ar)]

12 M = In
13 M = Tl
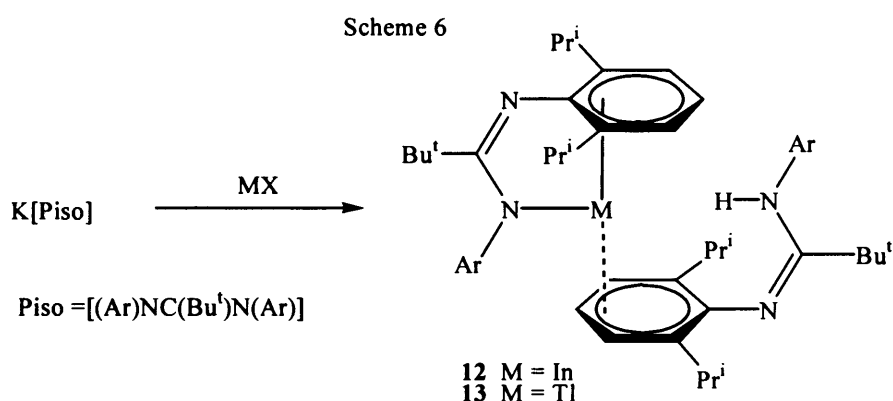
Following on from previous successes isolating In(I), **12**, and Tl(I), **13**, isomers of neutral 4-membered carbene analogues, scheme 6,[53] the modification of the back-bone substituent from ^{t}Bu to bulkier NCy$_2$, Cy = cyclohexyl, employing similar synthetic procedures, afforded the group 13(I) NHC analogues **14** and **15**, scheme 7.[52]

Scheme 7

"GaI" or InCl
Toluene

14 M = Ga (35%)
15 M = In (48%)

Ar = C$_6$H$_3$Pr^i$_2$-2,6
Cy = cyclohexyl

TlBr
Toluene

16 (68%)

14
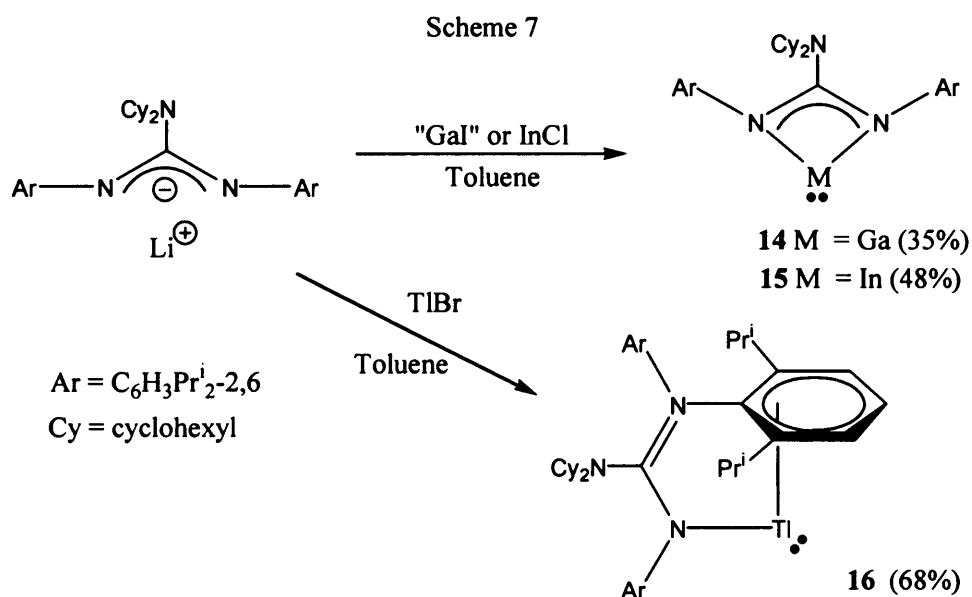
Treatment of group 13 metal(I) halides with the lithium guanidinate, Li[Giso], Giso⁻ = [(Ar)NC(NCy₂)N(Ar)]⁻, in toluene led to the guanidinate complexes **14, 15**, and **16** in moderate to good yields, scheme 7. In the gallium and indium complexes, N,N-chelation is preferred over N,arene-chelation, as is seen in thallium complex. These differences were attributed to the increasing ionic radii in the series Ga^+-Tl^+. There are no close intermolecular metal-element contacts (< 3.4 Å) in either structure. The M-N distances of the heterocycles are slightly longer than those in related five- and six-membered rings[49,50,55,58,68,71] but the N-M-N angles are significantly more acute.[52]

The only group 14 4-membered NHC (or analogue) known is the carbene **17**, which was synthesised via the two step synthesis shown in scheme 8.[54] As yet no group 15 analogues have been published.

<div align="center">Scheme 8</div>
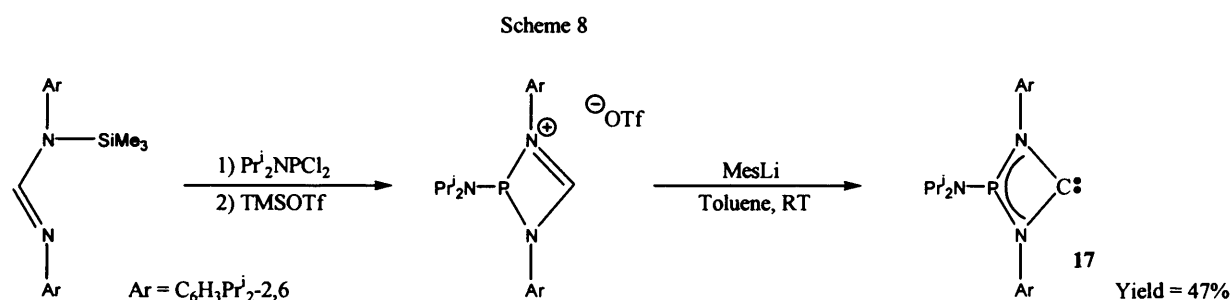
6.2 Five-Membered NHC Analogues

There are five-membered NHC analogues known for group 13, 14, and 15 elements. The only group 13 element that has been successfully incorporated into an NHC analogue is gallium. Synthesis of such a heterocycle was first reported by Schmidbaur *et al.* in 1999.[55] Two synthetic routes to this gallium(I) heterocycle are depicted in scheme 9. The synthesis involves the treatment of a dilithiated diazabutadiene ligand with GaCl₃ to give a chlorogalla-imidazole, **18**. This was then reduced over a period of five days, in two steps, in the presence of a crown ether to give, **19**, as a potassium salt in poor yield (4%). Alternatively, reduction in the presence of tetramethylethylenediamine (tmeda) gave complex, **20**, in low yield (18%).[56] Both complexes were fully characterised. The digallane intermediate had been previously isolated.[57]

Scheme 9

Bu^t
NLi
NLi
Bu^t

GaCl$_3$
- LiCl

Bu^t
Cl
Ga
Cl
N
Ga
N–Bu^t
N
Bu^t
N–Bu^t

18

K
- KCl

Bu^t
N
Ga—Ga
N
Bu^t

Bu^t
N
N
Bu^t

K, THF,
18-crown-6

K, THF,
tmeda

Bu^t
N
Ga$^-$
N
Bu^t

19

[K(18-crown-6)(THF)$_2$]
Yield = 4%

Bu^t
N
Ga
N
Bu^t

Me Me
N
K—N
Me Me

Me Me
N—K
Me

Bu^t
Ga
N
Bu^t

20

Yield = 18%
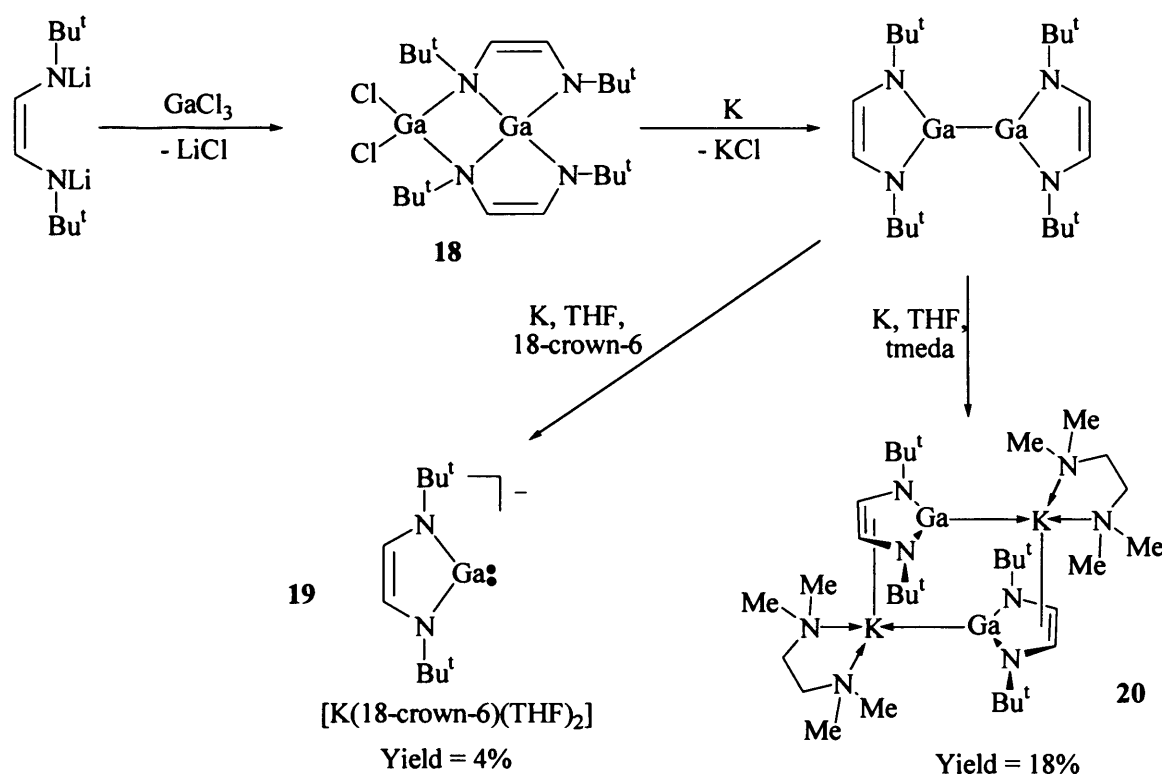
The heterocycle, **20**, has a N-Ga-N angle of 81.8(3)°, Ga-N average bond lengths of 1.985(6) Å, a backbone C-C bond length of 1.985(6) Å, and is relatively planar. These metric parameters compare favourably with those for the model system previously mentioned.[42] The complex is dimeric in the solid state, but can be considered as two monomeric units in which a gallium heterocycle is η^5-coordinated to a K(tmeda) fragment. The gallium lone pair of the neighbouring unit interacts with the K(tmeda) fragment causing aggregation of the units. Intra-ring parameters are similar to those in **19** and the intermolecular Ga-K contact is 3.4681(5) Å. The potassium forms an angle of 20.8° with the C$_2$N$_2$Ga ring plane which indicates that the lone pair at the gallium is orientated towards the potassium counter-ion.

Higher yielding syntheses ca. 75%, of three potassium complexes, **22-24**, incorporating bulkier 2,6-diisopropylphenyl N-substituents have been reported (scheme 10).[58] This route involves the use of "GaI" reacting with {(Ar)N=C(H)}$_2$, ArDAB (Ar = 2,6-diisopropylphenyl), which leads to a one-electron reduction of the DAB ligand, a disproportionation reaction and formation of the paramagnetic Ga(III) compound **21**. This is then cleanly reduced by excess potassium in ether to give **22** in 75% yield.

Scheme 10

Ar = C₆H₃Pr^{i}₂-2,6
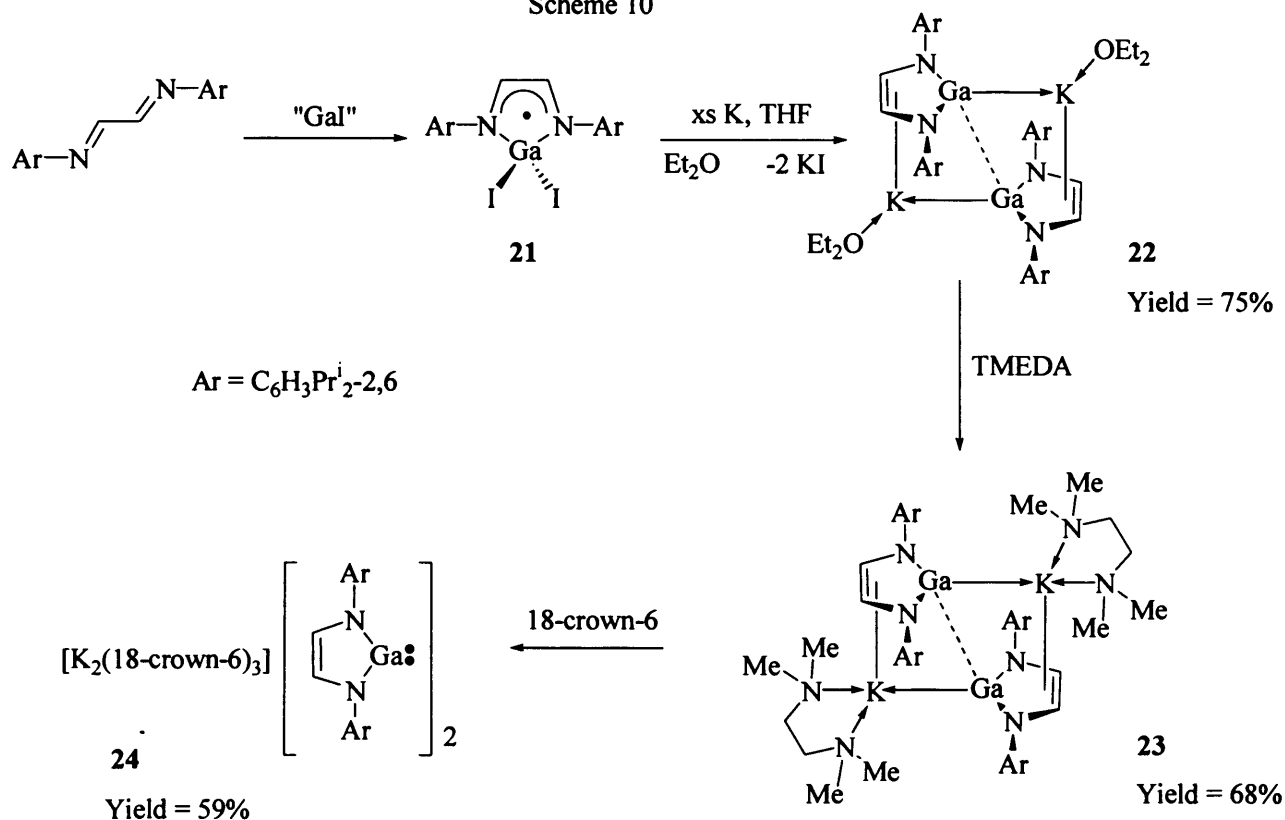
The crystal structure of **22** showed similarities to that of **20**, however significant differences were also seen. The heterocycle potassium interaction angle is only 3.4° (20.8° in **20**), and the Ga-Ga separation closes from 4.21 Å in **20**, to 2.8640(13) Å in **22**. This is outside the normal Ga-Ga single bond range but it could indicate that aggregation is not only caused by electrostatics, but also from partial donation of electron density from the lone pair on each gallium centre into the empty *p*-orbital on the other.[41] The direct analogue of **20** can be made by treatment of **22** with tmeda. A short Ga-Ga separation is still observed, 2.8746(15) Å. This interaction is not strong, as the charge separated species, **24**, can be synthesised by treatment of **23** with 18-crown-6.

Some good to high yielding syntheses of group 14 NHCs and their analogues are summarised in scheme 11.

17

Scheme 11

$$\text{Ad} = \text{adamantyl}$$

$$\xrightarrow[\text{THF} \quad -H_2, -Na\,Cl]{\text{NaH} \quad \text{cat. DMSO}}$$

$$\mathbf{25^{36}}$$
Yield = 96%

$$\xrightarrow[\text{THF} \quad -2KCl]{\text{3K} \quad 60^0\text{C}}$$

$$\mathbf{26^{59}}$$
Yield = 78%

$$\xrightarrow[\text{THF} \quad -2LiCl]{\text{GeCl}_2.\text{L}}$$

L = 1,4-dioxane

$$\mathbf{27^{60}}$$
Yield = 85%

$$\xrightarrow[\text{THF} \quad -2\ LiCl]{\text{Et}_3\text{NHCl}}$$

$$\xrightarrow[-\text{HN(SiMe}_3)_2]{\text{[Sn(N(SiMe}_3)_2)]}}$$

$$\xleftarrow{-\text{HN(SiMe}_3)_2}$$

$$\mathbf{28^{61}}$$

R = ^{t}Bu (35 %), Mes (50 %)

$$\xrightarrow[\text{Ether}]{\text{Pb[N(SiMe}_3)_2]_2}$$

$$\mathbf{29^{62}} \quad R = CH_2Bu^t$$

18

Some synthetic procedures for group 15 carbene analogues are summarised in scheme 12.

Scheme 12

$$CH_3I \quad 3d, RT$$
acetone, ether

30
Yield = 70%

$$PCl_3$$
Benzene - $SiCl_4$

31
Yield = 65%

$$ECl_3 \quad -78\ ^\circ C$$
Toluene -2 LiCl

E = P, Yield = 55%   **31**
E = As, Yield = 40%   **32**

$$ECl_3 \text{ or } Me_3SiOSO_2CF_3$$
Ether

33

E = Al, Ga, Sb

X = AlCl$_4^-$(73%), GaCl$_4^-$(70%), SbCl$_4^-$(51%), SO$_4$CF$_3^-$(72%)
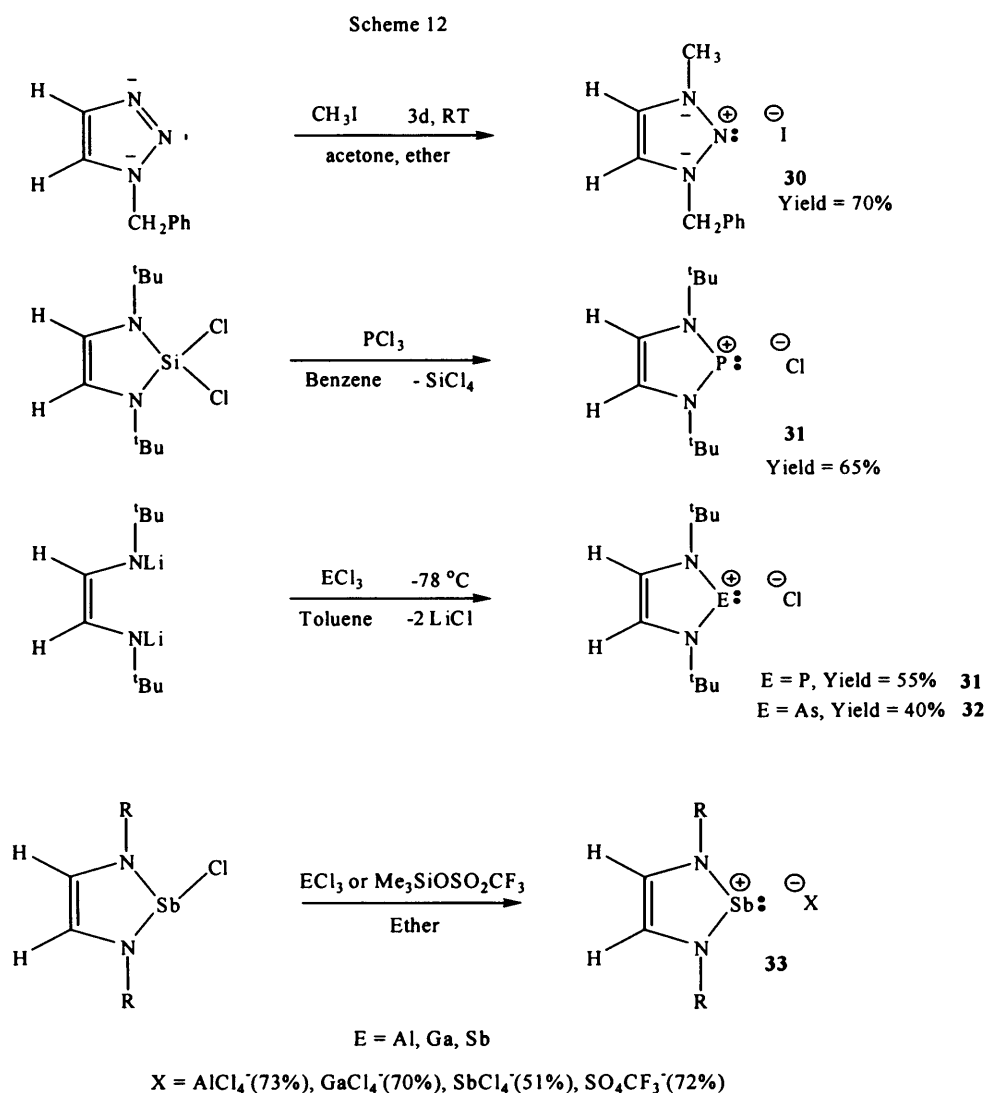
The nitrenium cation **30**,[63] phosphenium cation **31**,[64,65] arseneium cation **32**,[65] and stibenium cation **33**,[66] can all be formed in good yield. The phosphenium cation was first prepared by Denk et al.[64] by reacting a dichlorosilene with 1 equivalent of PCl$_3$ in benzene. An alternative procedure was published by Cowley et al.[65] using a salt metathesis path way, using toluene as a solvent. Denk had unsuccessfully attempted this route using THF as the solvent.

A five-membered bismuth NHC analogue has not yet been reported.

19

6.3 Six-Membered NHC Analogues

There are six-membered NHC analogues incorporating groups 13 and 14 elements, but as yet there are no known group 15 analogues. For group 13 these species are neutral and the metal is in the +1 oxidation state. Syntheses are available for the aluminium **34**,[67] gallium **35**,[68] indium **36**,[69] and thallium heterocycles **37**.[70,71] Examples are summarised in scheme 13.

Scheme 13
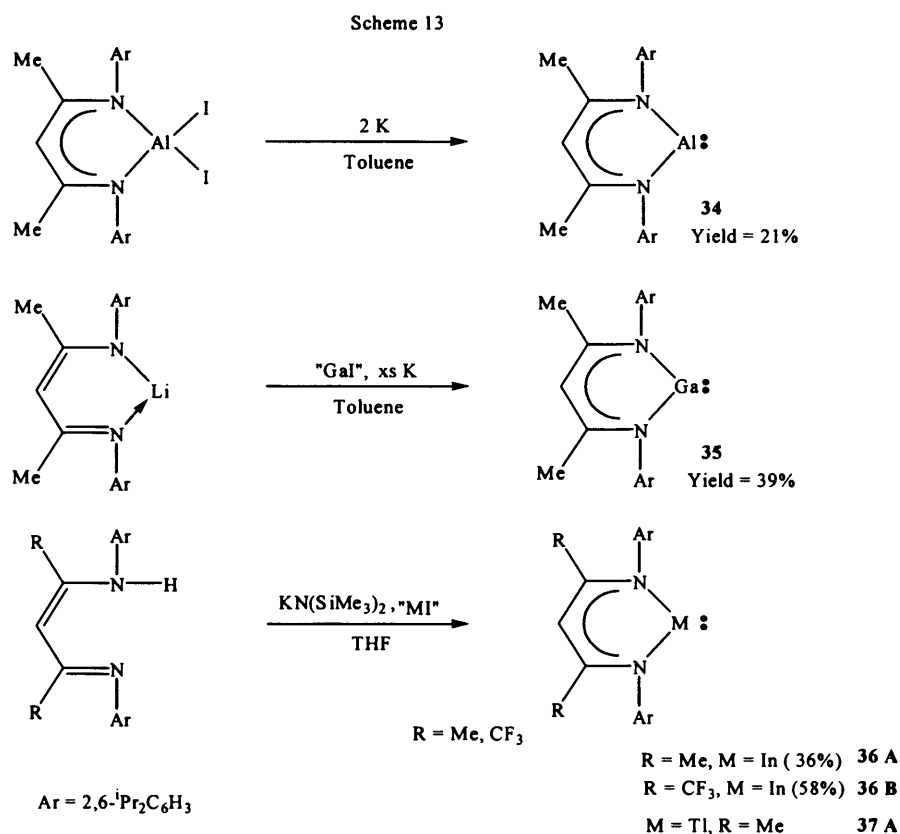
These heterocycles are derived from the β-diketiminate ligand, [HC(C(Me)N(Ar))₂]⁻ Ar = 2,6-diisopropylphenyl. The reduction of [{HC(C(Me)N(Ar)₂}AlI₂] with potassium in toluene over a period of three days gives **34**, a monomeric Al(I) carbene analogue, in 21% yield. The aluminium diiodide precursor is formed from the reaction of I₂ with the corresponding parent aluminium dimethyl species. The crystal structure of the compound shows a monomeric heterocycle with no close contacts with Al, thus **34** is the first example of a complex containing a two coordinate aluminium centre. Its Al-N bond lengths are 1.957(2), 1.957(2) Å, and the N-Al-N angle is 89.86(8)°. The bond lengths are longer and the angle more acute than seen in the parent dimethyl Al(III) complex (1.922 Å average and 96.18(9)°, respectively). This observation

indicates that two $3p$-orbitals on the Al are essentially involved in bonding with the two nitrogen atoms, leading to a more covalent Al-N bond for the longer Al(I) centre.[67]

The gallium homologue was synthesised by salt metathesis from a β-diketiminate lithium salt and "GaI" in toluene. The mixture was stirred overnight then potassium added to reduce any $I_2Ga\{(N(Ar)C(Me))_2CH\}$ formed, giving a two coordinate Ga(I) complex, **35**, in 39% yield. The solid state structure was determined to be monomeric with average Ga-N bond lengths of 2.054(2) Å, and a N-Ga-N angle of 87.56(6)°. The structure is best viewed as possessing a Ga(I) cation complexed by the bidentate monoanionic ligand $[HC(C(Me)N(Ar))_2]^-$.[68]

Indium and thallium homologues were synthesised in one pot reactions between $K[N(SiMe_3)_2]$, MI, M = In, Tl; and the required β-diketimine ligand precursor $[H(N(Ar)C(R))_2CH]$, R = Me or CF_3. Where R = Me, the indium complex, **36 A**, shows In-N bond lengths of 2.268(3) Å and 2.276(3) Å with an N-In-N angle of 81.12(10)°. When R = CF_3, **36 B**, there is a lengthening of In-N bond lengths to 2.357(4) Å, and 2.364(4) Å, with a significantly more acute N-In-N angle of 78.23(14)°. Although these changes can be attributed to minor adjustments in steric demands of the ligand, computational studies suggest that a minor modification to the ligand electron density distribution may also play a role. For thallium, R = Me, **37 A**, the Tl-N bond lengths are 2.428(4) Å and 2.403(4) Å, with the N-Tl-N angle being 76.67(15)°. All crystallise as distinct monomeric units with no close M-M contacts.

Previous to the above Tl(I) carbene analogue, two related complexes had been reported, scheme 14.[71] These were synthesised using salt metathesis with a β-diketiminate salt and Tl(I)Cl, giving **37 B** and **37 C** in good yield.[71] Both crystallise as discrete monomeric units with long Tl-Tl contacts found at 4.21 Å and 3.76 Å respectively, both well outside possible bonding distances. The Tl-N bond lengths for **37 B** were found to be 2.456(3) Å and 2.449(3) Å, with an N-Tl-N angle of 78.0(1)°. For **37 C**, Tl-N bond lengths of 2.471(3) Å and 2.423(3) Å, and a N-Tl-N angle of 76.20(9)° were found.

Scheme 14
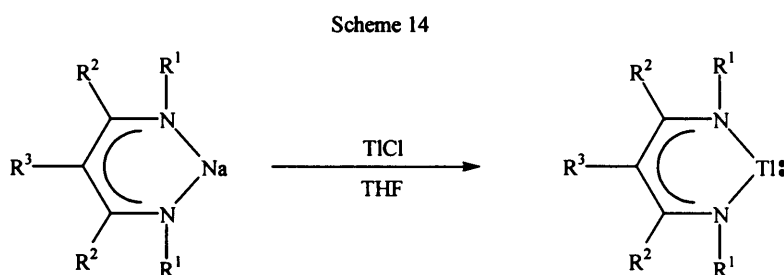
37 B = R^1 = SiMe$_3$, R^2 = Ph, R^3 = H, Yield = 82%

37 C = R^1 = 2,6-^{i}Pr$_2$C$_6$H$_3$, R^2 = H, R^3 = Ph, Yield = 80%

For the heterocyclic series when descending group 13, the E-N bond lengths become significantly longer and the N-E-N angles become more acute, compared to values seen in related β-diketiminate group 13(III) complexes. This trend has been ascribed to a larger covalent radii of the group 13 metals in the +1 oxidation state.[41]

Group 14 NHC analogues have been synthesised by extraction of chloride from 6-membered precursors (scheme 15), yielding salt species. Tin and germanium are the only reported group 14 elements incorporated into 6-membered NHC analogues and can be isolated in good yield.[72]

Scheme 15
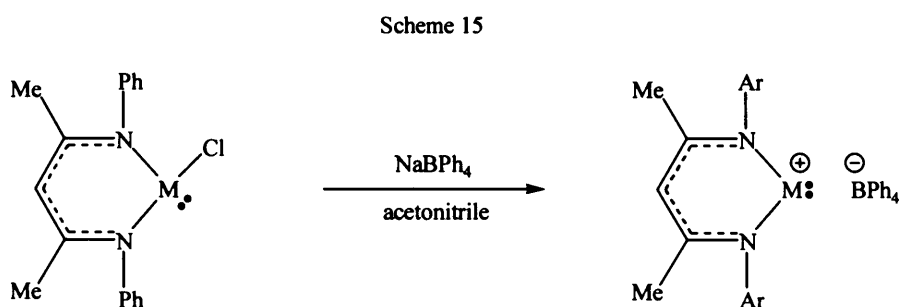
38 M = Ge, Yield = 82%

39 M = Sn, Yield = 67%

7. Reactions of 6-Membered Group 13 Metal(I) NHC Analogues

The reactions of five-membered anionic gallium(I) NHC and six-membered neutral group 13 metal(I) NHC analogues towards transition metal and main group fragments has been explored. Only the reactivity of 6-membered metal(I) heterocycles will be summarised in this section. The reactivity of anionic 5-membered heterocycles will be reviewed in the introductions

to chapters 2 and 3. It is of note that no further chemistry has yet been reported for 4-membered group 13(I) NHC analogues.

The reactions of six-membered heterocycles with transition metal complexes are limited. There have only been a handful of reactions reported which are summarised in scheme 16. The first was from the treatment of **35** with $Fe(CO)_5$ which led to the isolation of $[(CO)_4FeGa\{(N(Ar)C(Me))_2CH\}]$, **40**, via CO displacement, in moderate yield (26%).[27]

In another, **35** was reacted with $[(PPh_3)AuCl]$ and yielded the first characterised Ga-Au bond in the complex $[(PPh_3)Au\{Ga[(N(Ar)C(Me))CH]_2Cl\}]$, **41**.[73] This is formed by the oxidative insertion of a Ga(I) centre into the Au-Cl bond of the precursor. Further insertion reactions into rhodium halide bonds have been reported in the formation of $[(PPh_3)_2Rh\{Ga[\{N(Ar)C(Me)\}_2C(H)]\}(\mu\text{-}Cl)]$, **42**, and $[(COE)(benzene)Rh\{[\{N(Ar)C(Me)\}_2C(H)]GaCl\}]$, **43**, COE = cyclooctene; Ar = $2,6\text{-}Pr^i_2C_6H_3$; being the most recent.[74]

Scheme 16
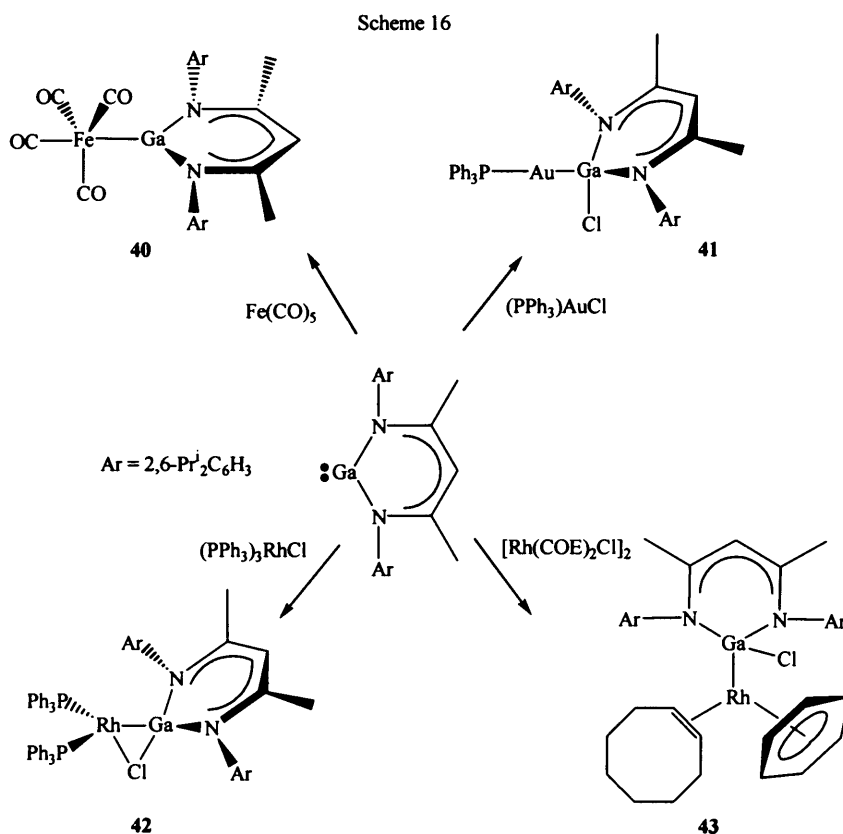
The majority of reactivity investigations with 6-membered heterocycles have been based on main group fragments. However, there is only one report of a group 13-group 13 bonded complex, **44**, where **35** was treated with $B(C_6F_5)_3$ leading to a dative Ga→B interaction in the

complex, $HC[(Me)C(Ar)N]_2Ga \rightarrow B(C_6F_5)_3$, scheme 17.[75] The heterocycle Ga-N bond-lengths are 1.942 Å (average) once coordinated to the $B(C_6F_5)_3$, compared with 2.054 Å (average) in the free heterocycle. This was said to be consistent with the decrease in the partial anti-bonding character of these bonds once the gallium lone-pair is donated, and by development of positive and negative charges on the Ga and B atoms respectively.

There is only one report of the reaction of a group 13 heterocycle with a group 14 precursor. When **34** was treated with the NHC, $[:C\{N(^iPr)C(Me)\}_2]$, crystalline $[\{HC[C(CH_3N(Ar)](C(Me)N(Ar)\}AlH\{CN(^iPr)C_2Me_2N(^iPr)\}]$, **45**, was afforded in moderate yield (48%).[76] The Al-H hydrogen comes from one of the terminal methyl groups of the β-diketiminate ligand. The authors were unable to suggest a mechanism for this process.

Group 15 precursors have been more extensively reacted with **34** and **35**. Scheme 17 summarises the results of these reactions. There are currently no reports involving the reactivity of the heavier In and Tl heterocycles, with such precursors.

Scheme 17

45 Yield = 47%

$[C\{N(Pr^i)C(Me)\}_2]$

E = Ga (19%) **46**
E = Al (58%) **47**

N_3SiMe_3

N_3SiMe_3

Yield = 54%
48

N_3Ar^*

E = Al(52%) **49**
E = Ga(74%) **50**

$B(C_6F_5)_3$

44 Yield = 81%

N_3Ar'

N_3Ar'

Heat

51
Yield = 42%

52
Yield = 24%

$Ar^* = C_6H_3(C_6H_2Pr^i_3-2,4,6)_2-2,6$
$Ar' = C_6H_3(C_6H_3Pr^i_2-2,6)_2-2,6$
$Ar = 2,6-Pr^i_2C_6H_3$

24
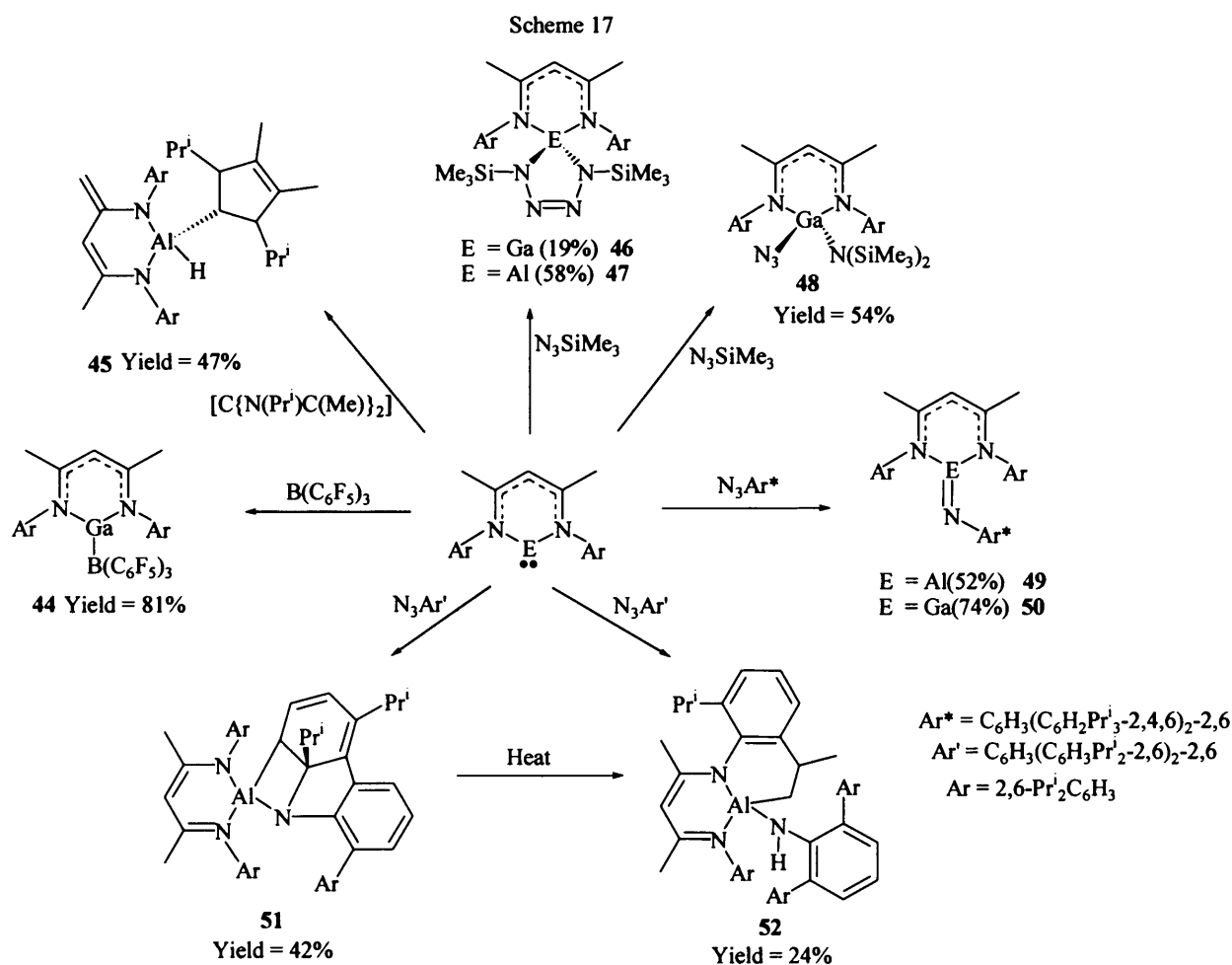
The reaction of **35** with two equivalents of Me$_3$SiN$_3$ gave the tetrazole and amide / azide complexes **46** and **48**, respectively, which were isolated through fractional crystallisation.[77] Additionally, when **34** was treated with Me$_3$SiN$_3$, the analogous aluminium tetrazole **47** was produced.[78] It is suggested that **47** was formed via the initial formation of the intermediate [HC{(C(Me)N(Ar)}$_2$]Al=NSiMe$_3$ with the loss of N$_{2(g)}$, before the second equivalent of Me$_3$SiN$_3$ reacts.

Bulkier azides, 2,6-Trip$_2$C$_6$H$_3$N$_3$ (Ar*N$_3$), Trip = 2,4,6-^{i}Pr$_3$C$_6$H$_2$, were used to react with **34** and **35** to give complexes **49**[79] and **50**,[80] in good yields. The steric bulk of the azide stabilised the monomeric species and prevented dimerization from occurring. The solid state structure of **50** showed a short Ga-N imide bond-length of 1.742(3) Å. A suggestion of multiple bonding character was made. The imide nitrogen possesses a bent coordination geometry, with a Ga-N-C angle of 134.6(3)°, which is consistent with the presence of a stereochemically active lone pair, which is further evidence for this suggestion. Hartree-Fock calculations on the model [HN=Ga{[N(H)C(H)]$_2$CH}] were carried out. Results of these showed favourable comparisons of Ga-N bond-lengths and Ga-N-H orientation, so suggesting there is Ga-N π-bond character, although weak. Concluding, there is strong σ-donation from gallium to nitrogen with weaker π-donation from nitrogen to gallium.[80]

In a similar reaction of **34** using a different terphenylazide, N$_3$Ar', Ar' = 2,6-Ar$_2$C$_6$H$_3$, Ar = 2,6-Pr$^i_2$C$_6$H$_3$; complexes **51** and **52**, instead of terminal azides, were formed. Complex **51** is presumed to form by a [2+2] cycloaddition of a phenyl ring of the Ar' substituent with an intermediate Al=N bond, while **52** might form by an intramolecular C-H activation and migration from the methyl group of the isopropyl aryl substituent. Complex **52** can also be accessed by thermal conversion of **51**.[81]

There have been two publications on reactions of 6-membered heterocycles with other group 15 precursors. This work is summarised in scheme 18.

Scheme 18

53
Yield = 69%

[Ph₂P(PPh₃)]
[SO₃CF₃]

54
Yield = 79%

N₂O or S₈   E = Al, Ga   ⁶/₈ S₈

A = O (62%) **55**
A = S (34%) **56**

57
Yield = 22%
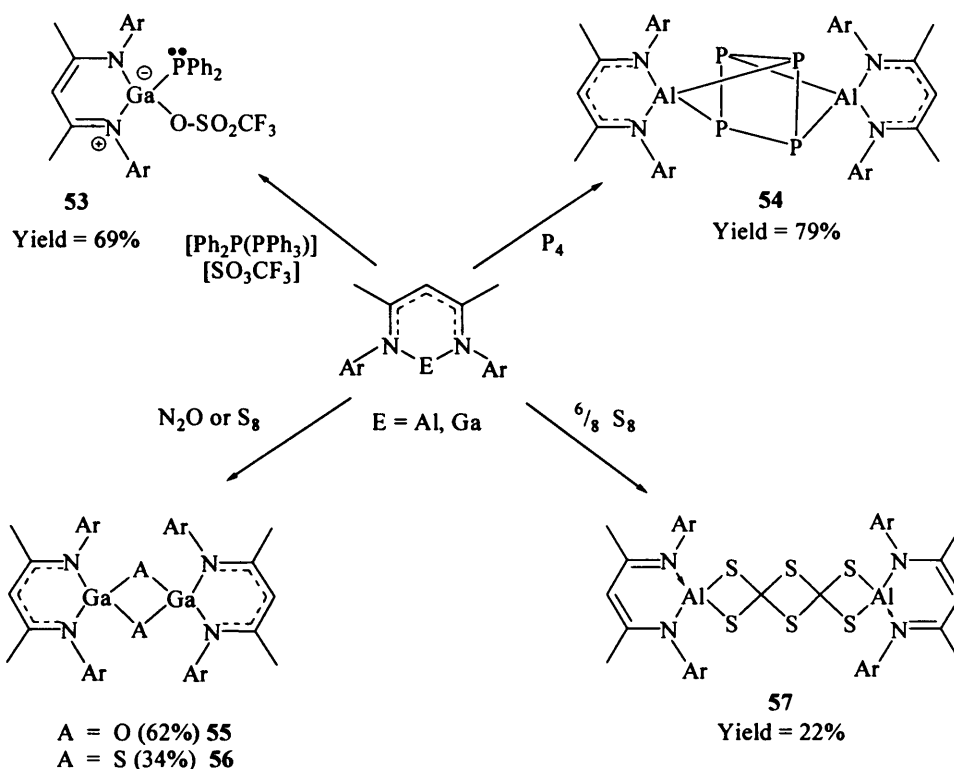
One paper described the reaction of **35** with [Ph₂P-PPh₃][SO₃CF₃] which yielded **53** in good yield. Compound **53** was described as a coordination Umpolung. The structure also revealed the association of a triflate oxygen to the gallium centre. The Umpolung involves the donation of electron density from the gallium, usually an electron acceptor, to the phosphorus centre, usually an electron donor. This was the first example of gallane-phosphine coordination.[82] The other report involved the reaction of **34** with white phosphorous, {P₄}, to give **54** in good yield. The solid state structure reveals that the P-P edges of the P₄ tetrahedron have opened and each is bridged by an LAl moiety.[83]

Finally, two papers report group 13 heterocycle-group 16 element reactivity. In one, **35** reacts with N₂O giving complex **55** in good yield. The solid state structure revealed a Ga-Ga separation of 2.5989(3) Å, though the Ga-Ga interaction was said to be negligible. The treatment of **35** with S₈ gave the related complex **56**, in a moderate yield. The Ga-S-Ga angles are more acute than the analogous Ga-O-Ga angle of **55** ca. 90.82(4) and 96.51(2) respectively. The Ga-Ga separations in **56** are 3.0127(6), which are outside the normal bonding ranges for Ga-Ga bonds.[84]

In a similar reaction, treating two equivalents of **34** with ⁶/₈ S₈ yielded **57** in low yield. The structure encompasses an eight-membered Al₂S₆ ring with two (μ-S₃) chains connecting the Al atoms.[85]

8. References

1. N. C. Norman, *"Periodicity and the s- and p-Block Elements"*, Oxford University Press, Oxford, 1997.

2. A. G. Massey, *"Main Group Chemistry"*, John Wiley & Sons, 2nd edn., 2000.

3. D. F. Shriver, P. W. Atkins, C. H. Langford, *"Inorganic Chemistry"*, Oxford University Press, 2nd edn., 1998.

4. J. E. Huheey, E. A. Keiter, R. L. Keiter, *"Inorganic Chemistry, Principles of Structure and Reactivity"*, Harper Collins College Publishers, 4th edn., 1993.

5. *"Chemistry of Aluminium, Gallium, Indium and Thallium"* Ed. A. J. Downs, Blakie, Glasgow, 1993.

6. F. A. Cotton, G. Wilkinson, *"Advanced Inorganic Chemistry"*, John Wiley & Sons, 5th edn., 1988.

7. C. Dohmeier, D. Loos, H. Schnöckel, *Angew. Chem. Int. Ed. Engl.*, 1996, **35**, 129.

8. G. Linti, H. Schnöckel, *Coord. Chem. Revs.*, 2000, **206-207**, 285.

9. A. Schnepf, H. Schnöckel, *Angew. Chem. Int. Ed.*, 2002, **41**, 3532.

10. M. L. H. Green, P. Mountford, G. J. Smout, S. R. Speel, *Polyhedron.*, 1990, **9**, 2763.

11. M. Kehrwald, W. Köstler, A. Rodig, G. Linti, *Organometallics*, 2001, **20**, 860.

12. R. J. Baker, C. Jones, *Dalton Trans.*, 2005, 1341.

13. J. R. Chadwick, A. W. Atkinson, B. G. Huckstepp, *J. Inorg. Nucl. Chem.*, 1966, **28**, 1021.

14. J. D. Corbett, R. K. McMullan, *J. Am. Chem. Soc.*, 1955, **77**, 4214.

15. L. A. Woodward, G. Garton, H. L. Roberts, *J. Chem. Soc.*, 1956, 3723.

16. G. Garton, H. M. Powell, *J. Inorg. Nucl. Chem.*, 1957, **4**, 84.

17. J. C. Beamish, R. W. H. Small, I. J. Worrall, *Inorg. Chem.*, 1979, **18**, 220.

18. S. M. Godfrey, K. J. Kelly, P. Kramkowski, C. A. McAuliffe, R. G. Pritchard, *Chem. Commun.*, 1997, 1001.

19. a) C. Gemel, T. Steinke, M. Cokoja, A. Kempter, R. A. Fischer, *Eur. J. Inorg. Chem.*, 2004, 4161, and references therein. b) P. Jutzi, B. Neumann, H. Stammler, *Organometallics*, 1998, **17**, 1305.

20. C. Boehme, J. Uddin, G. Frenking, *Coord. Chem. Revs.*, 2000, **197**, 249, and references therein.

21. E. O. Fischer, *Angew. Chem.,* 1957, **69**, 207.

22. E. O. Fischer, H. P. Hofmann, *Angew. Chem.,* 1957, **69**, 639.

23. D. Loos, H. Schnöckel, *J. Organomet. Chem.,* 1993, **463**, 37.

24. C. Schnitter, H. W. Roesky, C. Röpken, R. Herbst-Irmer, H. Schmidt, M. Noltemeyer, *Angew. Chem. Int. Ed.,* 1998, **37**, 1952.

25. P. Jutzi, B. Neumann, L. O. Schebaum, A. Stammler, H. Stammler, *Organometallics,* 1999, **18**, 4462.

26. J. Su, X. Li, R. C. Crittendon, C. F. Campana, G. H. Robinson, *Organometallics,* 1997, **16**, 4511.

27. N. J. Hardman, R. J. Wright, A. D. Phillips. P. P. Power, *J. Am. Chem. Soc.,* 2003, **125**, 2667.

28. F. A. Cotton, X. Feng, *Organometallics,* 1998, **17**, 128.

29. W. Uhl, M. Benter, S. Melle, W. Saac, *Organometallics,* 1999, **18**, 3778.

30. W. Kirmse, "*Carbene Chemistry*", Academic Press, New York and London, 2nd edn., 1971.

31. W. von E. Doering, A. K. Hoffmann, *J. Am. Chem. Soc.,* 1954, **76**, 6162.

32. E. O. Fischer, A. Maasböl, *Angew. Chem. Int. Ed.,* 1964, **3**, 580.

33. H. W. Wanzlick, *Angew. Chem. Int. Ed.,* 1962, **1**, 75.

34. H. W. Wanzlick, H. J. Schönherr, *Angew. Chem. Int. Ed.,* 1968, **7**, 141.

35. K. Öfele, *J. Organomet. Chem.,* 1968, **12**, 42.

36. A. J. Arduengo, R. L. Harlow, M. Kline, *J. Am. Chem. Soc.,* 1991, **113**, 361.

37. A. J. Arduengo, H. V. R. Dias, R. L. Harlow, M. Kline, *J. Am. Chem. Soc.,* 1992, **114**, 5530.

38. D. Bourissou, O. Guerret, F. P. Gabbaï, G. Bertrand, *Chem. Rev.,* 2000, **100**, 39.

39. a) W. A. Herrmann, *Angew. Chem. Int. Ed.,* 2002, **41**, 1290. b) M. Tafipolsky, W. Scherer, K. Öfele, G. Artus, B. Pedersen, w. A. Herrmann, G. S. McGrady, *J. Am. Chem. Soc.,* 2002, **124**, 5865.

40. C. M. Crudden, D. P. Allen, *Coord. Chem. Revs.,* 2004, **248**, 2247.

41. R. J. Baker, C. Jones, *Coord. Chem. Revs.,* 2005, **249**, 1857, and references therein.

42. A. Sundermann, M. Reiher, W. W. Schoeller, *Eur. J. Inorg. Chem.,* 1998, 305.

43. N. Metzler-Nolte, *New J. Chem.,* 1998, 793.

44. W. W. Schoeller, D. Eisner, *Inorg. Chem.,* 2004, **43**, 2585.

45. D. Martin, A. Baceiredo, H. Gornitzka, W. W. Schoeller, G. Bertrand, *Angew. Chem. Int. Ed.*, 2005, **44**, 1700.

46. M. Reiher, A. Sundermann, *Eur. J. Inorg. Chem.*, 2002, 1854.

47. N. J. Hardmann, A. D. Phillips, P. P. Power, *ACS Symp. Ser.*, 2002, 2.

48. M. Stender, A. D. Phillips, P. P. Power, *Inorg. Chem.*, 2001, **40**, 5314.

49. C. Cui, H. W. Roesky, H. Schmidt, M. Noltemeyer, H. Hao, F. Cimpoesu, *Angew. Chem. Int. Ed.*, 2000, **39**, 4274.

50. M. S. Hill, P. B. Hitchcock, R. Pongtavornpinyo, *Dalton Trans.*, 2005, 273.

51. C. Chen, M. Tsai, M. Su, *Organometallics*, 2006, **25**, 2766.

52. C. Jones, P. C. Junk, J. A. Platts, A. Stasch, *J. Am. Chem. Soc.*, 2006, **128**, 2206.

53. C. Jones, P. Junk, J. A. Platts, D. Rathmann, A. Stasch, *Dalton Trans.*, 2005, 2497.

54. E. Despagnet-Ayoub, R. H. Grubbs, *J. Am. Chem. Soc.*, 2004, **126**, 10198.

55. E. S. Schmidt, A. Jockisch, H. Schmidbaur, *J. Am. Chem. Soc.*, 1999, **121**, 9758.

56. E. S. Schmidt, A. Schier, H. Schmidbaur, *J. Chem. Soc., Dalton Trans.*, 2001, 505.

57. D. S. Brown, A. Decken, A. H. Cowley, *J. Am. Chem. Soc.*, 1995, **117**, 5421.

58. R. J. Baker, R. D. Farley, C. Jones, M. Kloth, D. M. Murphy, *J. Chem. Soc., Dalton Trans.*, 2002, 3844.

59. M. Denk, R. Lennon, R. Hayashi, R. West, A. V. Belyakov, H. P. Verne, A. Haaland, M. Wagner, N. Metzler, *J. Am. Chem. Soc.*, 1994, **116**, 2691.

60. W. A. Herrmann, M. Denk, J. Behm, W. Scherer, F. Klingan, H. Bock, B. Solouki, M. Wagner, *Angew. Chem. Int. Ed.*, 1992, **31**, 1485.

61. T. Gans-Eichler, D. Gudat, M. Nieger, *Angew. Chem. Int. Ed.*, 2002, **41**, 1888.

62. B. Gehrhus, P. B. Hitchcock, M. F. Lappert, *J. Chem. Soc., Dalton Trans.*, 2000, 3094.

63. a) R. H. Wiley, K. F. Hussung, J. Moffat, *J. Am. Chem. Soc.*, 1955, **77**, 1703. b) G. Boche, P. Andrews, K. Harms, M. Marsch, K. S. Ranhappa, M. Schimeczek, C. Willeke, *J. Am. Chem. Soc.*, 1996, **118**, 4925.

64. M. K. Denk, S. Gupta, R. Ramachandran, *Tetrahedron Let.*, 1996, **37**, 9025.

65. C. J. Carmalt, V. Lomeli, B. G. McBurnett, A. H. Cowley, *Chem. Commun.*, 1997, 2095.

66. D. Gudat, T. Gans-Eichler, M. Nieger, *Chem Commun.*, 2004, 2434.

67. C. Cui, H. W. Roesky, H. Schmidt, M. Noltemeyer, H. Hao, F. Cimpoesu, *Angew. Chem. Int. Ed.*, 2000, **39**, 4274.

68. N. J. Hardman, B. E. Eichler, P. P. Power, *Chem. Commun.*, 2000, 1991.

69. M. S. Hill, P. B. Hitchcock, *Chem. Commun.,* 2004, 1818.

70. M. S. Hill, P. B. Hitchcock, R. Pongtavornpinyo, *Dalton Trans.,* 2005, 273.

71. Y. Cheng, P. B. Hitchcock, M. F. Lappert, M. Zhou, *Chem. Commun.,* 2005, 752.

72. A. Akkari, J. J. Byrne, I. Saur, G.Rima, H. Gornitzka, J. Barrau, *J. Organomet. Chem.,* 2001, **622**, 190.

73. A. Kempter, C. Gemel, R. A. Fischer, *Inorg. Chem.,* 2004, **44**, 163.

74. A.Kempter, C. Gemel, N. J. Hardmen, R. A. Fischer, *Inorg. Chem.,* 2006, **45**, 3133.

75. N. J. Hardman, P. P. Power, J. D. Gorden, C. L. B. Macdonald, A. H. Cowley, *Chem. Commun.,* 2001, 1866.

76. H. Zhu, J. Chai, A. Stasch, H. W. Roesky, T. Blunck, D. Vidovic, J. Magull, H. Schmidt, M. Noltemeyer, *Eur. J. Inorg. Chem.,* 2004, 4046.

77. N. J. Hardman, P. P. Power, *Chem. Commun.,* 2001, 1184.

78. C. Cui, H. W. Roesky, H. Schmidt, M. Noltemeyer, *Angew. Chem. Int. Ed.,* 2000. **39**, 4531.

79. C. Cui, S. Köpke, R. Herbst-Irmer, H. W. Roesky, M. Noltemyer, H. Schmidt, B. Wrackmeyer, *J. Am. Chem. Soc.,* 2001, **123**, 9091.

80. N. J. Hardman, C. Cui, H. W. Roesky, W. H. Fink, P. P. Power, *Angew. Chem. Int. Ed.,* 2001, **40**, 2172.

81. H. Zhu, J. Chai, V. Chandrasekha, H. W. Roesky, J. Magull, D. Vidovic, H. Schmidt, M. Noltemeyer, P. P. Power, W. A. Merrill, *J. Am. Chem. Soc.,* 2004, **126**, 9472.

82. N. Burford, P. J. Ragogna, K. N. Robertson, T. S. Cameron, N. J. Hardman, P. P. Power, *J. Am. Chem. Soc.,* 2002, **124**, 382.

83. Y. Peng, H. Fan, H. Zhu, H. W. Roesky, J. Magull, C. E. Hughes, *Angew. Chem. Int. Ed.,* 2004, **43**, 3443.

84. N. J. Hardman, P. P. Power, *Inorg. Chem.,* 2001, **40**, 2474.

85. Y. Peng, H. Fan, V. Jancik, H. W. Roesky, R. Herbst-Irmer, *Angew. Chem. Int. Ed.,* 2004, **43**, 6190.

86. Y. Segawa, M. Yamashita, K. Nozaki, *Science,* 2006, **314**, 113.

Chapter 2

Complexes of an Anionic Gallium(I) Heterocycle with Transition Metal Fragments

1.   Introduction

The coordination chemistry of the N-heterocyclic carbene (NHC) class of ligand has been extensively explored and complexes of these heterocycles have found a variety of applications.[1] Of most note are transition metal-NHC complexes, many of which show high activity and/or selectivity as catalysts in a number of processes. This has led to NHCs being widely regarded as phosphine mimics, as they are strong σ-donors but very poor π-acids, a result of considerable N p-orbital lone pair overlap with the p-orbital of the carbene carbon. We are interested in preparing group 13 metal(I) analogues of NHCs and comparing the coordination and further chemistry of the two ligand classes. Most success has come with the anionic five-membered heterocycle **1**, which is valence isoelectronic with NHCs.[2] The s- and p-block coordination chemistry[3,4] of this heterocycle has shown similarities with that of NHCs in that it is very nucleophilic and can stabilise thermally labile fragments, e.g. indium hydrides. The transition metal coordination chemistry of **1** has and is continuing to be systematically investigated by Jones *et al.*[3] A number of complexes have been synthesised via a variety of routes.

Scheme 1 shows a number of the reported complexes and their synthetic routes. The iron complex [Fe(CO)$_4${Ga[N(Ar)C(H)]$_2$}]$^-$, **2**,[5] was synthesised by ligand substitution, whereby a carbonyl ligand on the iron centre was replaced by the gallium(I) carbene analogue. Theoretical and spectroscopic studies on **2** and a model complex have shown that, although the p-orbital at the gallium centre interacts minimally with the N centres' p-orbital lone pairs and is therefore effectively unoccupied, there is negligible Fe$\rightarrow$Ga back-bonding in this complex. This is not surprising considering the likely high energy of the gallium p-orbital relative to the $\pi*$ acceptor orbitals of the CO ligand *trans*- to the heterocycle.

Scheme 1

2
Yield = 54%

Ar = 2,6-Pr$^i_2$C$_6$H$_3$

M = Ni (46%) **3**
M = Co **4**

5
Yield = 63%
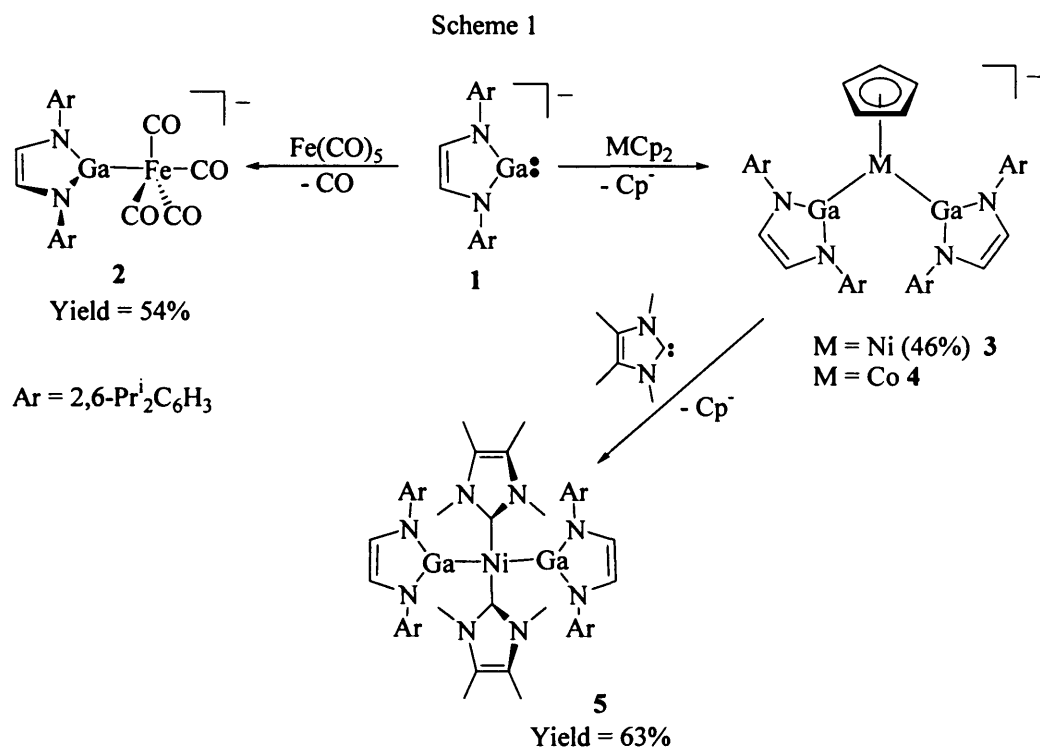
In similar work, the transition metal metallocenes, Cp$_2$M, M = Ni, Co; have been reacted with **1** to give [(tmeda)(Et$_2$O)K(μ-η^5-Cp)M{Ga[N(Ar)C(H)]$_2$}$_2$], M = Ni **3** or Co **4**.[6] KCp is eliminated during the reaction, which is closely related to reported reactions of NHCs with metallocenes, in which cationic complexes [CpM(NHC)$_2$]$^+$ are formed with elimination of Cp$^-$.[7] Bonding of the gallium(I) heterocycle to late transition metal complexes, free of competing π-electron accepting ligands, could potentially lead to metal-gallium back bonding. Very short Ni-Ga bond-lengths (2.218 Å, avg.) were found in **3**, which are only longer than those in the homoleptic gallium diyl complex [Ni{Ga-C(SiMe$_3$)$_3$}$_4$], (2.1700(4) Å) for which significant Ni-Ga back bonding has been suggested.[8] A model of the complex **3**, [CpNi{Ga[N(Ph)C(H)]$_2$}$_2$]$^-$, was examined by DFT using the Amsterdam Density Function (ADF). This study found a 28 % π-component for the Ni-Ga bonds, which suggests some back-bonding in this complex.[3] Complex **3** can be treated with an excess of the NHC, [:C{N(Me)C(Me)}$_2$], which leads to the elimination of KCp and the formation of the neutral complex, **5**, in good yield.

A related bis(gallyl)-zirconium(III) complex, **6**, has also been accessed *via* the oxidative insertion of the *in situ* generated "Cp$_2$Zr" fragment into the Ga-Ga bond of the digallane, [Ga{[N(Ar)C(H)]$_2$}]$_2$, (**7**) (Ar = C$_6$H$_3$Pr$^i_2$-2,6), in the presence of Bu^{n}Li.[9] Although the exact mechanism of the reaction is unknown, the nature of the product highlights the ability of the gallium heterocycle to stabilise low oxidation state early transition metal fragments.

$[Li(THF)_4]^+$ **6**

$Ar = C_6H_3Pr^i_2\text{-}2,6$
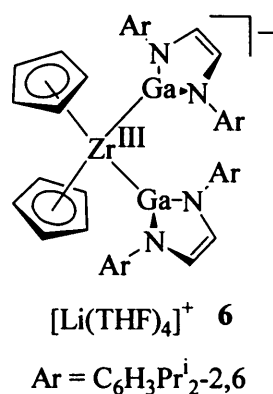
Further work related to complex **6** has been published, whereby neutral metallocene-gallyl complexes have been accessed via the oxidative insertion of metallocenes into the Ga-Ga bond of the digallane **7**.[10] The 1:1 reactions of the metallocenes, Cp'$_2$M, (Cp' = C$_5$H$_4$Me), M = V or Cr, with **7** afforded the neutral mono-gallyl complexes, [Cp'$_2$M[Ga{[N(Ar)C(H)]$_2$}]], M = V **9** or Cr **10**; in low yield, scheme 2. Presumably the mechanism for the reactions involve an initial oxidative insertion of the transition metal centre into the Ga-Ga bond of **7** to give bis-gallyl complexes, **8**, which then undergo comproportionation reactions with Cp'$_2$M, to give the observed products.

Scheme 2

[K(tmeda)(OEt$_2$)]$^+$ **11**

M = V **9**
M = Cr **10**
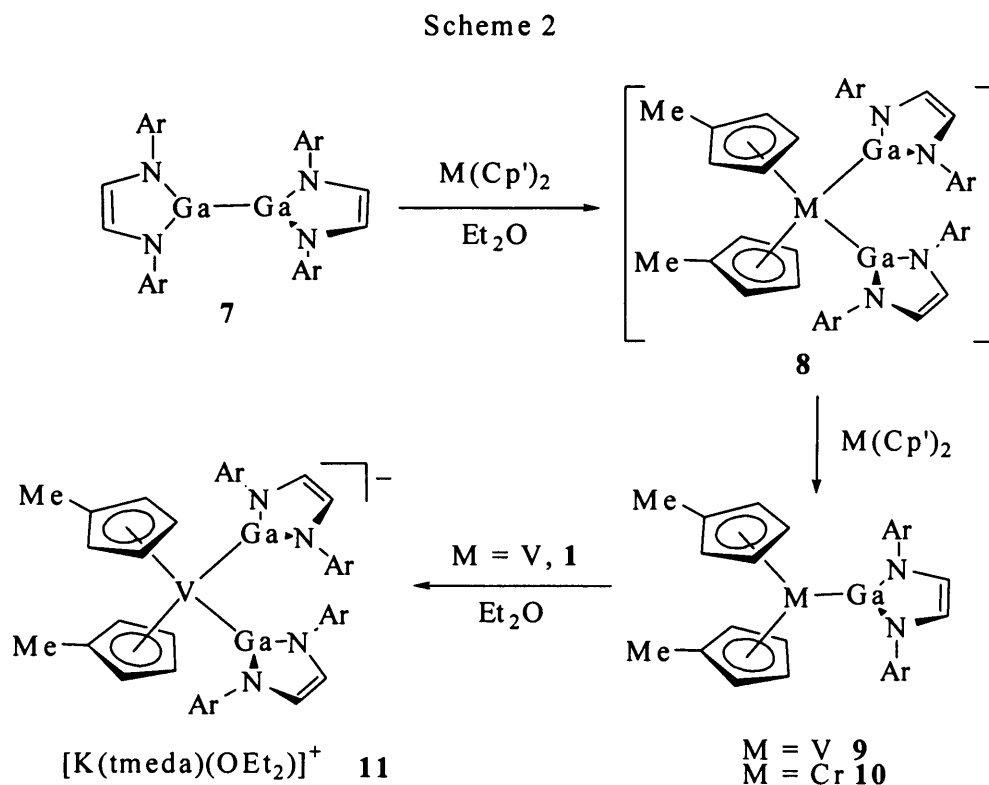
When **9** or **10** were treated with the same NHC as was **3**, [:C{N(CH₃)C(CH₃)}], no reaction occurred. However, when **9** or **10** were treated with the gallium(I) NHC analogue, **1**, a reaction occurred with **9** to give the anionic complex **11** (scheme 2) but no reaction was observed with **10**. Compound **11** is analogous to the zirconium complex **6**.

2.   Research Proposal

Considering the great importance of transition metal-NHC chemistry, and the fact that the coordination chemistry of related acyclic group 13 metal(I) compounds (e.g. metal diyls, :M(I)R, M = Al, Ga or In) has been widely studied,[11] it seemed appropriate to systematically extend the use of **1** as a ligand towards d-block metal fragments. In previous studies, the chemistry of the gallium(I) heterocycle, **1**, has been shown to mimic that of the important *N*-heterocyclic carbene class of ligand. Despite there being many similarities, there are also significant differences between the gallium heterocycle and the NHC class of ligand. To further understand the reactivity of the gallium heterocycle towards transition metal fragments, reactions of half sandwich, metal dialkyl, and metal dihalide fragments were proposed to be carried out. Comparisons with related NHC complexes were to be made where possible.

3.   Results and Discussion

3.1   Reactions with half sandwich complexes

In recent years a number of neutral or cationic half sandwich complexes of the type, $[CpM(CO)_n(NHC)]^{0 \text{ or } +1}$, have been reported and their use in catalysis has been suggested.[12] In attempts to form related neutral transition metal-gallyl complexes, either $[CpFe(CO)_2I]$ or $[CpMo(CO)_3Cl]$ were reacted with **1** in a 1:1 stoichiometery. The only isolated products of these reactions were, however, the paramagnetic gallium(II) dimers, $[GaX\{[N(Ar)C(H)^{\cdot}]_2\}]_2$, X = I or Cl,[13] which suggests the reactions proceed *via* an initial insertion of the gallium(I) centre of **1** into the M-X bond of the transition metal complex, followed by decomposition of the formed intermediate. It is worth noting that gallium diyls, :GaR, and the neutral six-membered gallium

34

heterocycle, [:Ga{[N(Ar)C(Me)]₂CH}], are now well known to insert into transition metal-halide bonds.[11,14] In order to circumvent this problem and to form related anionic complexes, **1** was reacted with a series of cyclopentadienyl-metal carbonyl half sandwich compounds which afforded the gallium heterocycle complexes, **12 - 14**, in moderate to good yields (Scheme 3). When the reactions were carried out in a greater than 1:1 stoichiometry, only the 1:1 complexes resulted and the excess of **1** remained unreacted.

Scheme 3

[K(tmeda)]⁺

1

[K(tmeda)]⁺

12 M = V,   n = 4, R = H
13 M = Mn, n = 3, R = Me
14 M = Co, n = 2, R = H
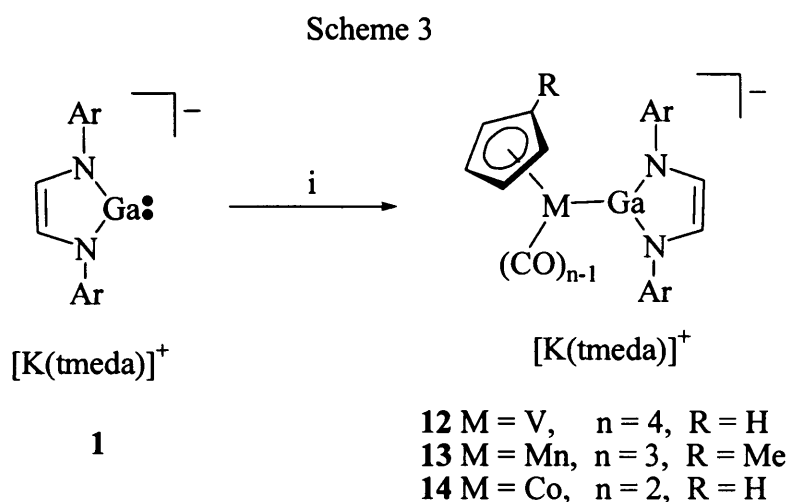
i) (C₅H₄R)M(CO)ₙ, -CO

Ar = 2,6-diisopropylphenyl

Complexes **12 - 14** have been characterised by solution state multinuclear NMR (^{1}H, ^{13}C{^{1}H} and ^{51}V for **12**) and IR spectroscopy. The ^{1}H and ^{13}C{^{1}H} NMR spectra of all complexes are more symmetrical than would be expected if their oligomeric/polymeric solid state structures (*vide infra*) were retained in solution. Therefore, it seems that in C₆D₆ solutions the associated forms of these compounds are not retained and there is free rotation of the gallium heterocycle about the M-Ga bonds. The ^{51}V NMR spectrum of **12** exhibits a signal at −1809 ppm ($v_{1/2}$ = 494 Hz) which is, not surprisingly, considerably upfield of the signal for the neutral starting material, [CpV(CO)₄] (-1533 ppm). It is also upfield of the resonance for the related anionic complex, [CpV(CO)₃H]⁻ (-1730 ppm),[15] which might indicate that the gallium heterocycle is a better σ-donor than the hydride ligand.

The infrared spectra of **12 - 14** were acquired in THF/18-crown-6 solutions to minimise interactions between the cationic and anionic components of the complexes, as are seen in the

solid state (*vide infra*). The positions of the CO stretching bands for these complexes (**12**: ν 1962, 1891, 1785 cm^{-1}; **13**: 1877, 1812 cm^{-1}; **14**: 1690 cm^{-1}) are consistent with anionic complexes and that for **14** can be compared to the position of the band in the directly analogous neutral NHC complex, [CpCo(CO)(IPr)], IPr = :CN$_2$(Ar)$_2$C$_2$(H)$_2$ (ν 1921 cm^{-1}); for which less M-CO back bonding would be expected.[12(d)] A comparison of the CO stretching absorptions of **12** and **13** with those of the related hydride complexes, [CpM(CO)$_n$H]$^-$ (M = V, n = 3, ν CO = 1889, 1775 cm^{-1};[15] M = Mn, n = 2, ν CO =1860, 1770 cm^{-1} [16]), show that the latter appear at significantly lower wavenumbers which could suggest that the hydride ligand is a better σ-donor than the gallium heterocycle and/or that the gallium heterocycle has some π-acceptor capability. The first suggestion is at odds with our tentative assumption from the ^{51}V NMR spectrum of **12** that the gallium heterocycle is actually a better σ-donor than the hydride ligand.

X-ray crystallographic studies were carried out on **12 - 14** and their molecular structures are depicted in Figures 1 - 3 respectively. All three complexes are associated in the solid state. Complex **12** forms 1-dimensional polymeric strands *via* η^1-O-coordination of the potassium cation by two carbonyl ligands, chelation by a molecule of tmeda and an η^2-interaction with one arene substituent of the heterocycle. Both **13** and **14** form cyclic dimers, though that for **13** is held together with η^1-O-interactions from both carbonyl ligands of each monomeric unit to potassium centres, whilst the single carbonyl ligands of the monomeric units of **14** bridge the two K centres in an η^1-O:η^2-CO-fashion. The geometries of the coordinated gallium heterocycle in each complex are similar to each other and to the geometries in the majority of previously reported complexes of this heterocycle.[3-6] In addition, the least squares plane of the gallium heterocycle in each complex subtends a relatively acute angle with the Cp centroid-M-Ga containing plane (**12** 28.3° avge., **13** 28.1°, **14** 34.9°). This angle in **14** is significantly more acute than the related angle in its direct NHC analogue, [CpCo(CO)(IPr)] (45.9°).[12(d)] In addition, the angles in both **13** and **14** potentially allow the HOMO of the transition metal fragment[17] to overlap with the empty *p*-orbital at gallium, giving rise to π-bonding as shown below in a model of **13**.
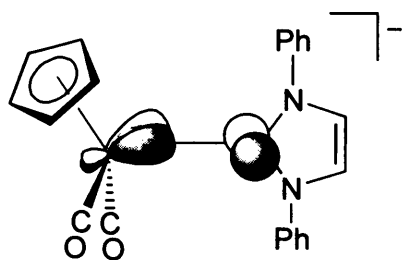
An examination of the Cambridge Crystallographic Database (CCD) revealed that complex **12** contains the first structurally authenticated V-Ga bond in a molecular compound. The Mn-Ga and Co-Ga bonds in **13** and **14** are shorter than any other examples of such bonds by more than 0.1 Å in each case (reported ranges Mn-Ga: 2.424 – 2.680 Å; Co-Ga: 2.342 – 2.708 Å[18]) and may also indicate M-Ga π-bonding.[18] The shortness of these bonds is significant as previously reported examples of each include systems containing three coordinate gallium centres, e.g. [Mes*Ga(Cl){Mn(CO)$_5$}] and [Mes*Ga{Co(CO)$_4$}$_2$], Mes* = C$_6$H$_2$Bu$^t_3$-2,4,6.[19]
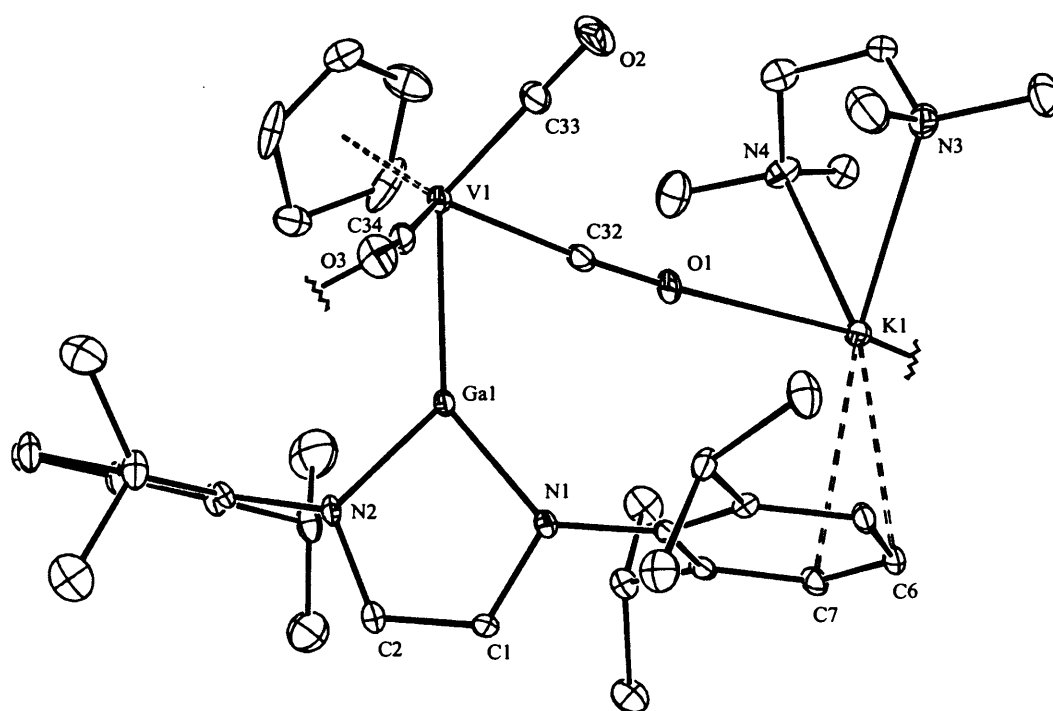
Figure 1. Molecular Structure of **1**. Selected bond lengths (Å) and angles (°): Ga(1)-V(1) 2.4618(13), Ga(1)-N(1) 1.900(5), Ga(1)-N(2) 1.883(5), V(1)-C(32) 1.893(6), V(1)-C(33) 1.918(8), V(1)-C(34) 1.904(8), C(32)-O(1) 1.167(7), C(33)-O(2) 1.148(8), C(34)-O(3) 1.173(8), K(1)-O(1) 2.622(4), K(1)-N(4) 2.804(6), K(1)-N(3) 2.866(6), K(1)-C(6) 3.185(7), K(1)-C(7)

K(1)-C(6) 3.185(7), K(1)-C(7) 3.190(6), C(1)-N(1) 1.403(7), C(2)-N(2) 1.387(8), C(1)-C(2) 1.355(7), N(2)-Ga(1)-N(1) 86.9(2), N(2)-Ga(1)-V(1) 131.61(15), N(1)-Ga(1)-V(1) 141.47(14), C(32)-V(1)-C(34) 107.7(3), C(32)-V(1)-C(33) 79.6(3), C(34)-V(1)-C(33) 76.9(3), C(32)-V(1)-Ga(1) 67.96(19), C(34)-V(1)-Ga(1) 70.89(19), C(33)-V(1)-Ga(1) 123.2(3), N(4)-K(1)-N(3) 65.32(18), C(32)-O(1)-K(1) 173.0(5), O(1)-C(32)-V(1) 175.7(6), O(2)-C(33)-V(1) 178.4(8), O(3)-C(34)-V(1) 175.2(6).
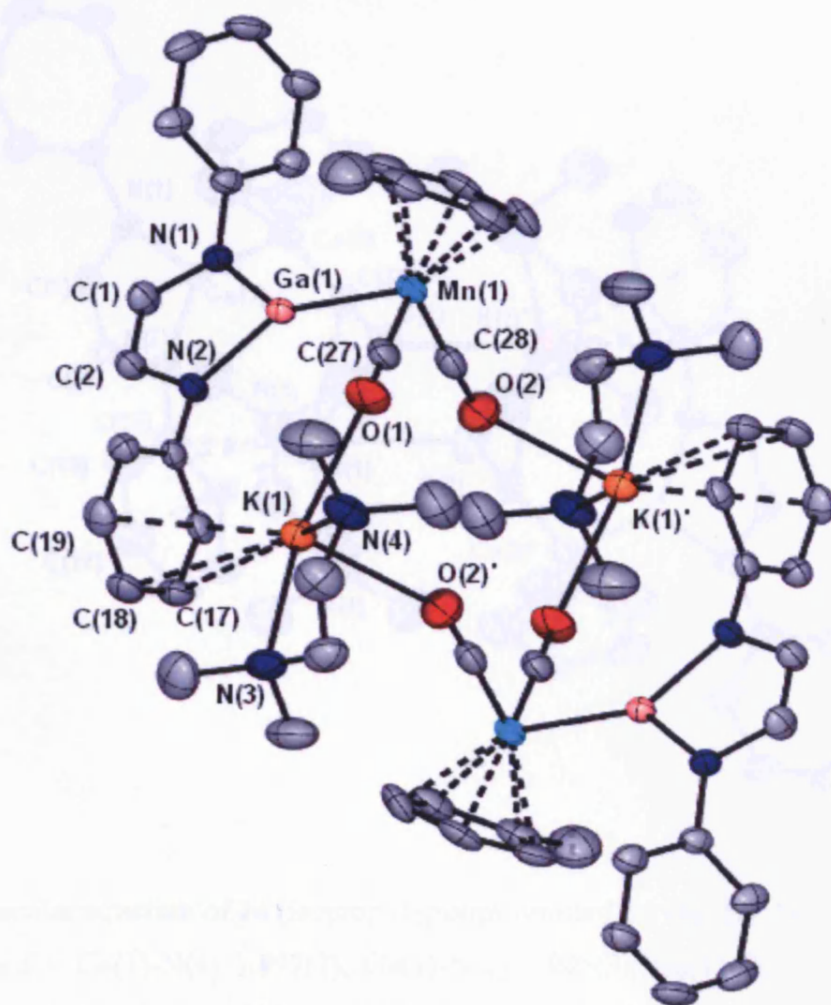
Figure 2. Molecular structure of **13** (isopropyl groups omitted for clarity). Selected bond lengths (Å) and angles (°): Ga(1)-N(1) 1.902(4), Ga(1)-N(2) 1.906(4), Ga(1)-Mn(1) 2.3105(9), Mn(1)-C(27) 1.749(6), Mn(1)-C(28) 1.752(6), K(1)-O(1) 2.627(4), K(1)-O(2)' 2.663(4), K(1)-N(4) 2.840(5), K(1)-N(3) 2.855(4), K(1)-C(17) 3.187(5), K(1)-C(18) 3.102(5), K(1)-C(19) 3.193(5),

O(1)-C(27) 1.174(6), O(2)-C(28) 1.175(6), O(2)-K(1)' 2.663(4), N(1)-C(1) 1.388(6), N(2)-C(2) 1.400(6), C(1)-C(2) 1.339(7), N(1)-Ga(1)-N(2) 85.87(16), N(1)-Ga(1)-Mn(1) 133.78(12), N(2)-Ga(1)-Mn(1) 140.14(12), C(27)-Mn(1)-C(28) 92.5(3), C(27)-Mn(1)-Ga(1) 89.90(16), C(28)-Mn(1)-Ga(1) 85.80(17), O(1)-K(1)-O(2)' 95.05(13), O(1)-K(1)-N(4) 78.40(13), N(4)-K(1)-N(3) 65.70(14), C(1)-N(1)-Ga(1) 110.8(3), C(2)-N(2)-Ga(1) 109.8(3), O(1)-C(27)-Mn(1) 176.5(5), O(2)-C(28)-Mn(1) 178.0(5). Symmetry transformations used to generate equivalent atoms: ' -x+1/2, -y+3/2, -z+1/2.
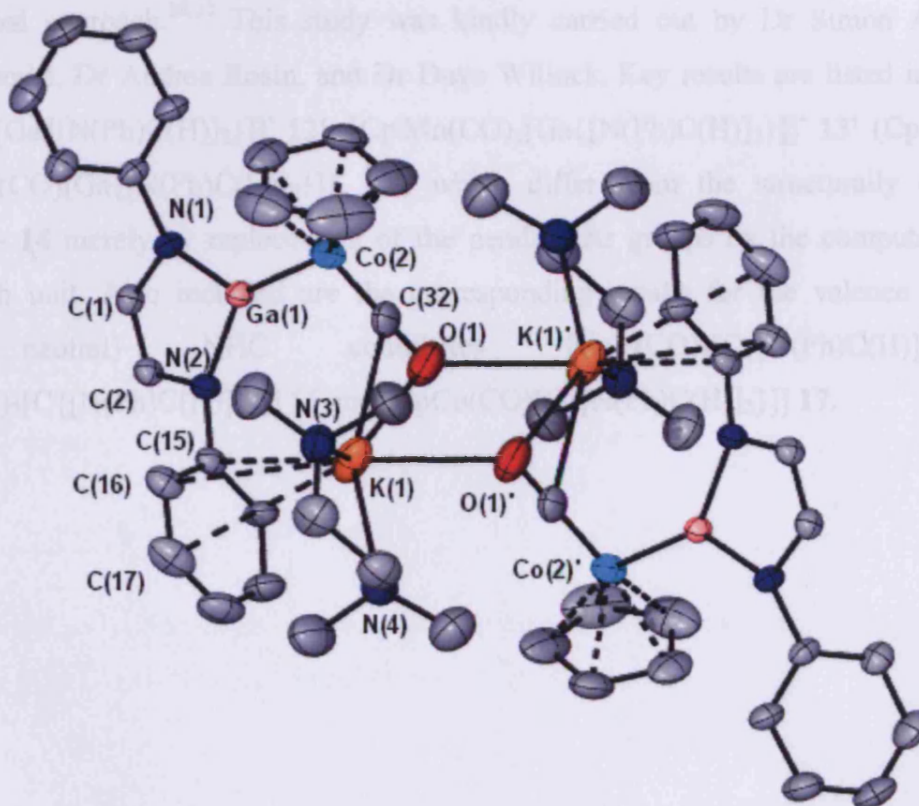

Figure 3. Molecular structure of **14** (isopropyl groups omitted for clarity). Selected bond lengths (Å) and angles (°): Ga(1)-N(1) 1.897(2), Ga(1)-N(2) 1.905(3), Ga(1)-Co(2) 2.2347(7), Co(2)-C(32) 1.677(4), K(1)-O(1)' 2.758(3), K(1)-N(4) 2.899(3), K(1)-N(3) 2.954(3), K(1)-C(32) 3.121(4), K(1)-O(1) 3.167(4), K(1)-C(15) 3.669(3), K(1)-C(16) 3.609(4), K(1)-C(17) 3.698(4), O(1)-C(32) 1.186(5), N(1)-C(1) 1.400(4), N(2)-C(2) 1.397(4), C(1)-C(2) 1.339(4), N(1)-Ga(1)-N(2) 86.96(11), N(1)-Ga(1)-Co(2) 135.10(8), N(2)-Ga(1)-Co(2) 137.80(8), C(32)-Co(2)-Ga(1) 83.19(13), N(4)-K(1)-N(3) 61.20(9), O(1)'-K(1)-C(32) 75.24(10), O(1)'-K(1)-O(1) 60.92(10),

Ga(1) 109.50(19), C(2)-N(2)-Ga(1) 109.2(2), O(1)-C(32)-Co(2) 178.2(4), O(1)-C(32)-K(1) 81.3(3). Symmetry transformations used to generate equivalent atoms: ' -x+1, -y+1, -z.


In consideration of the very short M-Ga bonds in all complexes, the orientation of the heterocycle planes in **13** and **14**, and the possibility that the positions of the CO stretching bands in the infrared spectra of **12** - **14** suggest M-Ga π-bonding in these compounds, it was decided to carry out DFT theoretical studies of models of these compounds using a well precedented computational approach.[20,21] This study was kindly carried out by Dr Simon Aldridge, Ms Natalie Coombs, Dr Andrea Rosin, and Dr Dave Willock. Key results are listed in Table 1 for [CpV(CO)₃[Ga{[N(Ph)C(H)]₂}]]⁻ **12'**, [Cp'Mn(CO)₂[Ga{[N(Ph)C(H)]₂}]]⁻ **13'** (Cp' = C₅H₄Me) and [CpCo(CO)[Ga{[N(Ph)C(H)]₂}]]⁻ **14'**, which differ from the structurally characterized species **12** - **14** merely by replacement of the pendant Ar groups by the computationally less intensive Ph unit. Also included are the corresponding results for the valence isoelectronic (charge neutral) NHC complexes [CpV(CO)₃[C{[N(Ph)C(H)]₂}]] **15**, [Cp'Mn(CO)₂[C{[N(Ph)C(H)]₂}]] **16** and [CpCo(CO)[C{[N(Ph)C(H)]₂}]] **17**.

Table 1: Calculated and measured structural and bonding parameters for compounds **12'-14'** and **15 - 17**.

Compound	σ:π ratio	r(Ga-M)/ Å [a]	Angle between heterocycle and Cp centroid-M-Ga containing planes/ °[a]	Compound	σ:π ratio	r(C-M)/ Å [a]	Angle between heterocycle and Cp centroid-M-C containing planes / °[a]
12'	87:13	2.554 [2.461(mean)]	33.3 [28.3]	**15**	86:14	2.315	36.7
13'	82:18	2.396 [2.311(1)]	29.4 [28.1]	**16**	79:21	2.061	27.3
14'	73:27	2.304 [2.235(1)]	41.5 [34.9]	**17**[b]	74:26	1.918 [1.888(3)]	47.9 [45.9]

[a] Calculated values given; experimental values in parentheses where applicable. [b] Experimental values for [CpCo(CO)(IPr)] taken from reference 12(d).

In general, the agreement between calculated and experimentally observed molecular geometries is good, with the 2 - 3% over-estimate in the lengths of the metal-metal bonds for **12'** - **14'** mirroring the results of previous studies.[20,21] Such phenomena have been ascribed to a combination of solid-state effects leading to the shortening of donor/acceptor bonds, and a general over-estimate of bond lengths by generalized gradient approximation (GGA) methods.[22] The generally good reproduction of the experimentally observed values for the angles between the gallium heterocycle and the Cp centroid-M-Ga containing least squares planes is reassuring, given that rotation around the metal-ligand axis in related systems has been shown to involve motion across a very shallow potential energy surface.[20]

The calculated σ:π ratios for **12'** - **14'** show the expected trend of increasing M→Ga π back-bonding on moving to more electron-rich late transition metal systems containing a decreasing number of competing π acidic carbonyl ligands. However, in each case the calculated π contribution is similar to that found for the corresponding valence isoelectronic NHC system, and similar in magnitude to values calculated for related half-sandwich boryl complexes (typically 10–20%).[21] NHC and boryl ligand systems have typically been described as strong σ donor ligands with minor π acid capabilities.[23] Thus, the σ:π ratios for **12'** - **14'** can be put into the appropriate context by comparing them with the corresponding ratios of 86:14 and 66:33 for model systems containing formal M-Ga single and M=Ga double bonds, respectively.[20,24]

3.2   Reactions with dialkylmanganese complexes

As little success was had in the reactions of **1** with manganocenes, the gallium compound, **1**, and the digallane, **7**, were treated with the manganese dialkyls, [Mn{C(SiMe3)3}2] and [Mn{CH(SiMe3)2}2]. No reactions were observed with the bulkier dialkyl complex and similarly no reaction occurred between [Mn{CH(SiMe3)2}2] and the digallane, **7**. In contrast, the reaction between [Mn{CH(SiMe3)2}2] and **1** afforded the anionic complex, **18**, in moderate yield (Scheme 4). The complex is related to other adducts of manganese dialkyls, most notably the three coordinate monomeric complex, [Mn{CH(SiMe3)2}2(THF)].[25] The paramagnetic nature of **18** meant that little meaningful NMR data could be obtained on this compound. Although the magnetic moment of **18** in solution is lower than expected (5.92 BM) for a high spin d^5 octahedral complex (μ_{eff} = 4.62 BM by the Evans' method), it is in the range previously observed for high spin complexes of manganese(II) alkyls.[25] However, the solid state structure of **18** indicates a distorted trigonal planar geometry at the manganese centre. This would give rise to a different crystal field splitting pattern which may complicate the observed magnetic moment for **18**.

Scheme 4

$$\text{Ar} \quad \overset{\displaystyle -}{\underset{\displaystyle \text{N}}{\Big\lceil}} \quad \overset{\text{N}}{\underset{\text{N}}{\Big[}} \text{Ga:} \qquad \xrightarrow{\ i\ } \qquad \overset{\text{Ar}}{\underset{\text{N}}{\Big[}} \text{Ga—Mn} \overset{\text{CH(SiMe}_3)_2}{\underset{\text{CH(SiMe}_3)_2}{}}$$

[K(tmeda)]$^+$ [K(tmeda)]$^+$

1   **18**
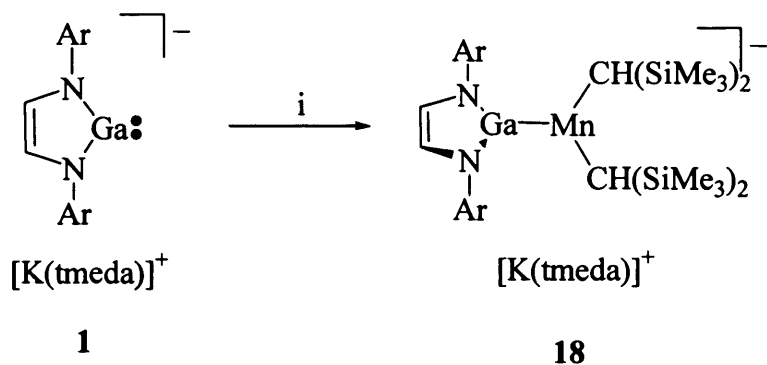
i) $Mn\{CH(SiMe_3)_2\}_2$, OEt_2

Ar = 2,6-diisopropylphenyl

The molecular structure of **18** is depicted in Figure 4. This shows it to be monomeric with a three coordinate distorted trigonal planar manganese centre. The anionic gallium heterocycle has an η^5-interaction with the potassium counter-ion which is additionally chelated by a molecule of tmeda. The structure of this heterocycle-potassium ion pair is very similar to that seen in **1** itself,[2] though in that compound two such ion pairs form a dimer through two intermolecular Ga lone pair-K interactions. It is of interest that the Ga-Mn distance in **18** is more than 0.3 Å longer than that in the half sandwich complex, **13**. Despite this, it lies in the normal range.[18] In addition, it can be surmised that the gallium heterocycle is a significantly stronger σ-donor than THF as the C-Mn-C angle in **12** is more than 25° narrower than in the related adduct, $[Mn\{CH(SiMe_3)_2\}_2(THF)]$ 160.1(9)°.[25] Finally, the gallium heterocycle is not co-planar with the manganese dialkyl fragment and forms an angle of 28.3° with the least squares plane containing the C_2MnGa fragment.
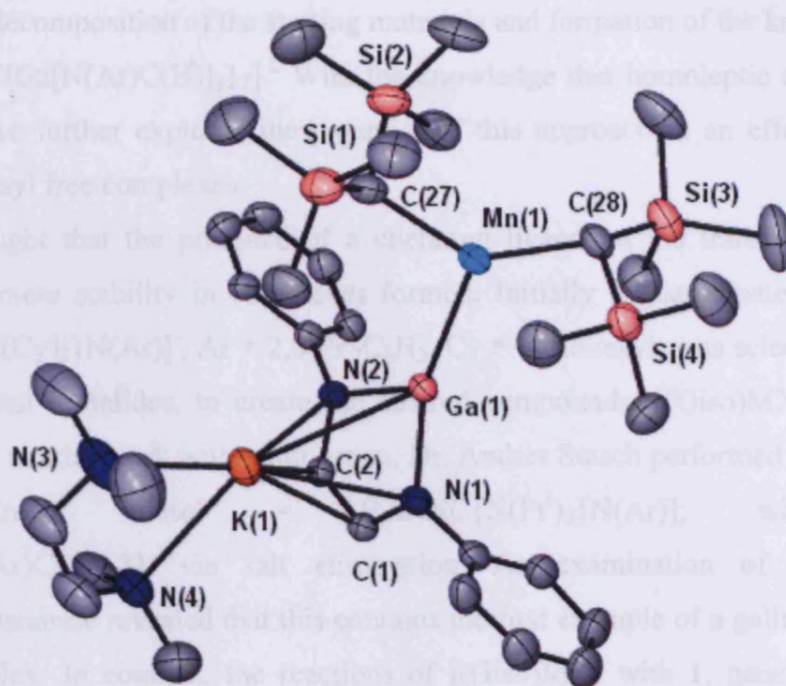
Figure 4. Molecular structure of **18** (isopropyl groups omitted for clarity). Selected bond lengths (Å) and angles (°): Ga(1)-N(1) 1.940(3), Ga(1)-N(2) 1.946(3), Ga(1)-Mn(1) 2.6658(10), Ga(1)-K(1) 3.4925(15), Mn(1)-C(28) 2.143(4), Mn(1)-C(27) 2.158(5), K(1)-N(4) 2.839(4), K(1)-N(3) 2.863(5), K(1)-C(2) 3.052(4), K(1)-C(1) 3.081(5), K(1)-N(2) 3.093(4), K(1)-N(1) 3.150(4), N(1)-Ga(1)-N(2) 84.16(14), N(1)-Ga(1)-Mn(1) 147.69(11), N(2)-Ga(1)-Mn(1) 125.93(10), C(28)-Mn(1)-C(27) 134.12(18), C(28)-Mn(1)-Ga(1) 122.97(14), C(27)-Mn(1)-Ga(1) 102.88(12).

3.3 Reactions with transition metal halide complexes

It was believed that the minimal M-Ga back-bonding seen in **12-14** could be increased by synthesising neutral carbonyl free transition metal gallyl complexes. An example of a homoleptic transition metal gallium complex, [Ni{Ga-C(SiMe₃)₃}₄], where there are no competing π acidic ligands on the transition metal, has been shown to have significant π-back-bonding by calculations.[8] It was thought that salt metathesis reactions with **1** may allow homoleptic complexes to be synthesised. Subsequently, attempts were made to synthesise homoleptic

complexes by reacting **1** with a variety of first row transition metal chlorides. However, this exclusively led to decomposition of the starting materials and formation of the known gallium(II) chloride dimer [{ClGa[N(Ar)C(H)]$_2$}$_2$].[2] With the knowledge that homoleptic complexes could not be accessed, we further explored the potential of this approach in an effort to synthesise heterolyptic, carbonyl free complexes.

It was thought that the presence of a chelating ligand on the transition metal halide fragment may promote stability in complexes formed. Initially a guanidinate ligand, [Giso]$^-$, Giso = [(Ar)NC{N(Cy)$_2$}N(Ar)]$^-$, Ar = 2,6-Pr$^i_2$C$_6$H$_3$, Cy = cyclohexyl; was selected, and reacted with transition metal di-halides, to create the desired compounds, [(Giso)MX], M = 1st row transition metal. In similar work within our group, Dr. Andres Stasch performed the reaction of **1** with [(Giso')ZnCl], Giso' = [(Ar)NC{N(Pr^i)$_2$}N(Ar)]; which yielded [(Giso')Zn{Ga[N(Ar)C(H)]$_2$}], via salt elimination. An examination of the Cambridge Crystallographic Database revealed that this contains the first example of a gallium-zinc bond in a molecular complex. In contrast, the reactions of [(Giso)MX] with **1**, generally resulted in intractable mixtures of products. However, the reaction of **1** with [(Giso)CoCl] led to the crystallisation, after work up, of [(tmeda)Co{Ga(N(Ar)C(H))$_2$}$_2$], Ar = 2,6-^{i}Pr$_2$C$_6$H$_3$; **21** in low yield. Presumably, the formation of this complex occurs by initial displacement of Giso as GisoH (via solvent proton abstraction) and the subsequent coordination of tmeda in place of it. As a consequence, a series of [(tmeda)$_n$MX$_2$] compounds were synthesised and reacted with **1**. Specifically the 1:2 reactions of [(tmeda)$_n$MX$_2$], M = Mn, Fe, Co, Ni, Zn; X = Br, Cl; with **1** afforded a series of neutral, covalently bound, transition metal bis-gallyl complexes, [(tmeda)M{:Ga(N(Ar)C(H))$_2$}$_2$], M = Mn, Fe, Co, Ni, Zn; Ar = 2,6-^{i}Pr$_2$C$_6$H$_3$; **19 - 23**, in low to good yields (scheme 5). The reaction of [(tmeda)CuCl$_2$] with **1** led to isolation of the known digallane, [{Ga(N(Ar)C(H))$_2$}$_2$], via the oxidative coupling of the gallium fragments as evident by the deposition of copper metal in the reaction.[26]

Scheme 5

$$[(tmeda)_nMX_2] \quad + \quad \underset{\substack{Ar \\ [K(tmeda)]^+ \\ \mathbf{1}}}{\overset{Ar}{\bigcirc}}Ga\colon \quad \xrightarrow[\text{- KCl}]{\text{THF}}$$
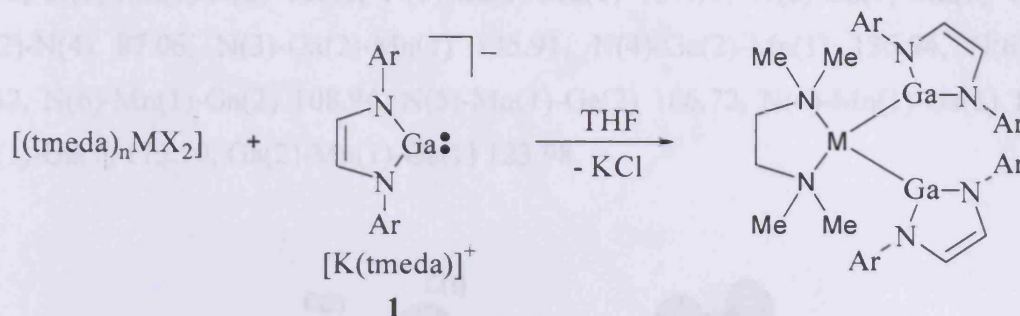
tmeda = N,N,N',N'-tetramethylethylene diamine

Ar = 2,6-^{i}Pr$_2$C$_6$H$_3$

n = 1, M = Mn **19**, Co **21**, Zn **23**, X = Cl

n = 2, M = Fe **20**, X = Cl

n = 2, M = Ni **22**, X = Br

X-ray crystallographic studies were carried out on **19 - 23** and their molecular structures are depicted in figures 5-9 respectively.
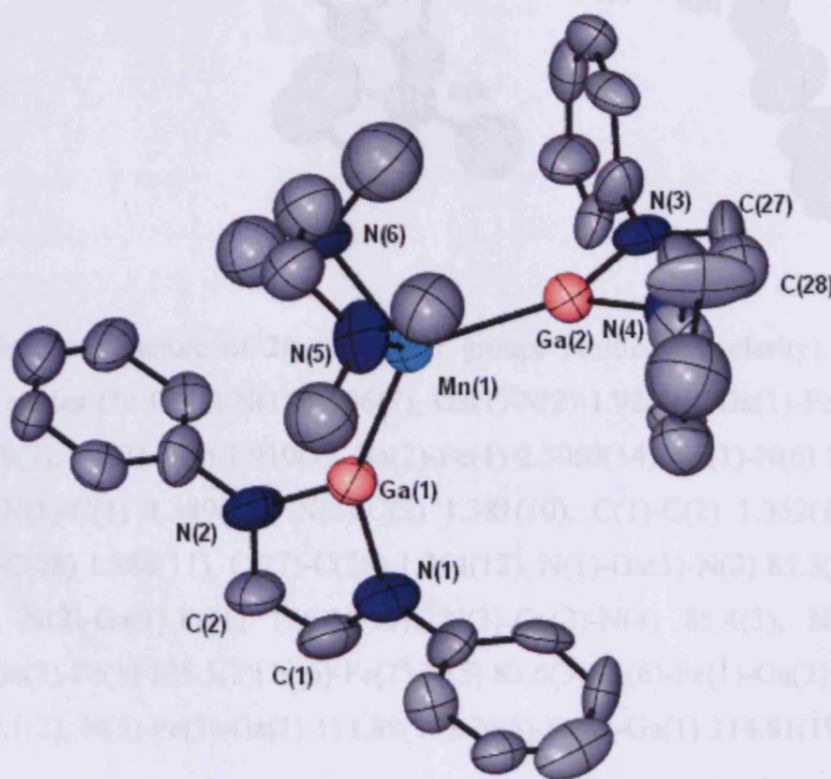
Figure 5. Molecular structure of **19** (isopropyl groups omitted for clarity). Selected bond lengths (Å) and angles (°): Ga(1)-N(1) 1.918, Ga(1)-N(2) 1.929, Ga(1)-Mn(1) 2.595, Ga(2)-N(3) 1.938, Ga(2)-N(4) 1.868, Ga(2)-Mn(1) 2.508, Mn(1)-N(6) 2.205, Mn(1)-N(5) 2.240, N(1)-C(1) 1.316, N(2)-C(2) 1.396, C(1)-C(2) 1.425, N(3)-C(27) 1.392, N(4)-C(28) 1.469, C(27)-C(28)

1.266, N(1)-Mn(1)-N(2) 85.40, N(1)-Ga(1)-Mn(1) 137.79, N(2)-Ga(1)-Mn(1) 136.78, N(3)-Ga(2)-N(4) 87.06, N(3)-Ga(2)-Mn(1) 135.91, N(4)-Ga(2)-Mn(1) 136.94, N(6)-Mn(1)-N(5) 84.42, N(6)-Mn(1)-Ga(2) 108.94, N(5)-Mn(1)-Ga(2) 106.72, N(6)-Mn(1)-Ga(1) 109.87, N(5)-Mn(1)-Ga(1) 115.79, Ga(2)-Mn(1)-Ga(1) 123.98.
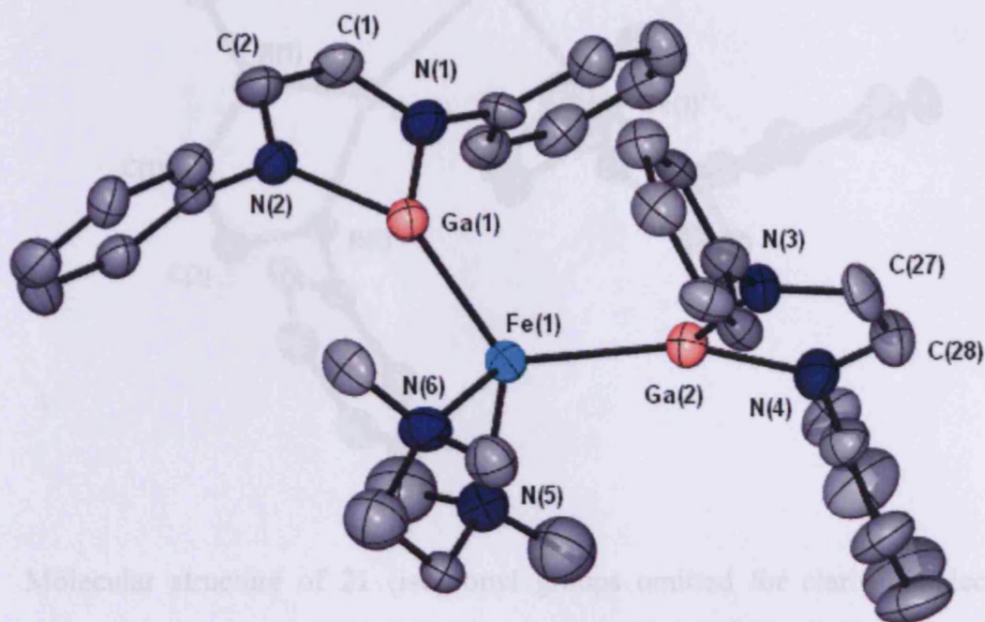
Figure 6. Molecular structure of **20** (isopropyl groups omitted for clarity). Selected bond lengths (Å) and angles (°): Ga(1)-N(1) 1.906(7), Ga(1)-N(2) 1.920(6), Ga(1)-Fe(1) 2.5245(14), Ga(2)-N(3) 1.898(7), Ga(2)-N(4) 1.910(7), Ga(2)-Fe(1) 2.5063(14), Fe(1)-N(6) 2.107(7), Fe(1)-N(5) 2.174(8), N(1)-C(1) 1.389(10), N(2)-C(2) 1.381(10), C(1)-C(2) 1.352(12), N(3)-C(27) 1.382(10), N(4)-C(28) 1.388(11), C(27)-C(28) 1.354(12), N(1)-Ga(1)-N(2) 85.3(3), N(1)-Ga(1)-Fe(1) 138.6(2), N(2)-Ga(1)-Fe(1) 136.04(19), N(3)-Ga(2)-N(4) 85.4(3), N(3)-Ga(2)-Fe(1) 135.9(2), N(4)-Ga(2)-Fe(1) 138.5(2), N(6)-Fe(1)-N(5) 83.6(3), N(6)-Fe(1)-Ga(2) 108.3(2), N(5)-Fe(1)-Ga(2) 109.1(2), N(6)-Fe(1)-Ga(1) 111.89(19), N(5)-Fe(1)-Ga(1) 114.81(19), Ga(2)-Fe(1)-Ga(1) 122.32(5).
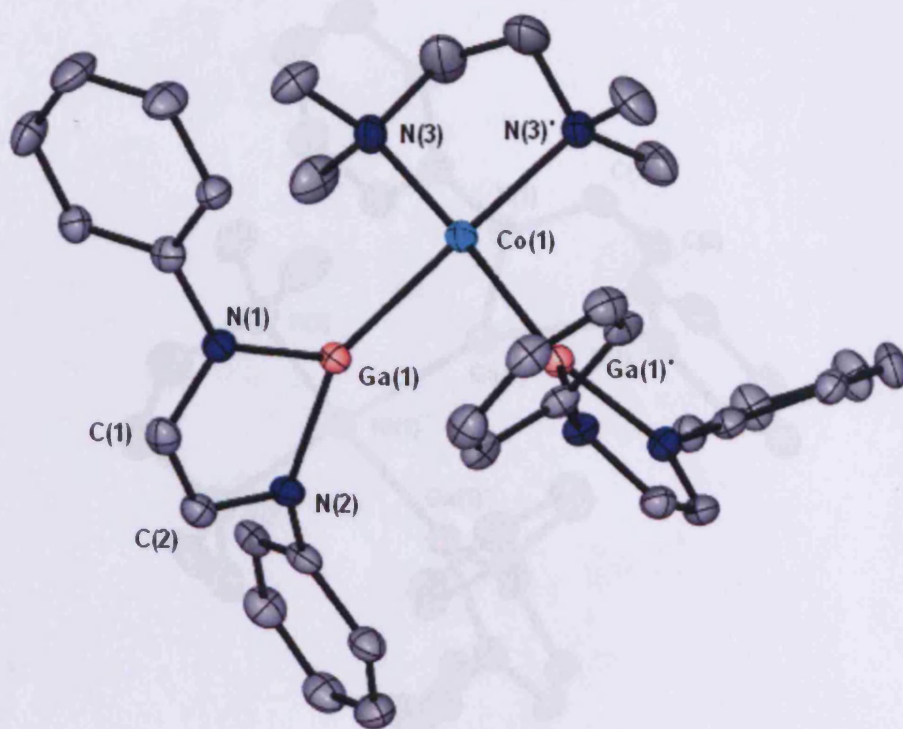
Figure 7. Molecular structure of **21** (isopropyl groups omitted for clarity). Selected bond lengths (Å) and angles (°): Ga(1)-N(1) 1.915(2), Ga(1)-N(2) 1.898(2), Ga(1)-Co(1) 2.3331(6), N(1)-C(1) 1.396(3), N(2)-C(2) 1.404(3), C(1)-C(2) 1.333(4), Co(1)-N(3) 2.085(2), N(2)-Ga(1)-N(1) 86.84(9), N(2)-Ga(1)-Co(1) 145.66(6), N(1)-Ga(1)-Co(1) 127.50(7), N(3)-Co(1)-N(3)' 84.84(13), Ga(1)-Co(1)-Ga(1)' 79.06(3), N(3)-Co(1)-Ga(1) 98.12(6), N(3)-Co(1)-Ga(1)' 175.99(6).
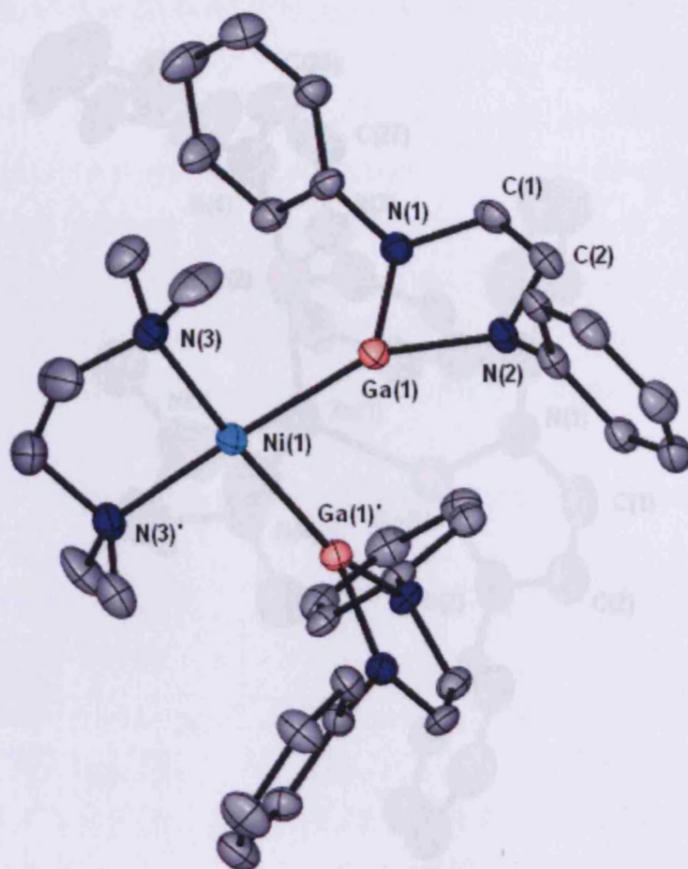
Figure 8. Molecular structure of **22** (isopropyl groups omitted for clarity). Selected bond lengths (Å) and angles (°): Ga(1)-N(1) 1.911(3), Ga(1)-N(2) 1.897(3), Ga(1)-Ni(1) 2.3051(8), N(1)-C(1) 1.401(4), N(2)-C(2) 1.405(4), C(1)-C(2) 1.335(5), Ni(1)-N(3) 2.047(3), N(2)-Ga(1)-N(1) 87.00(12), N(2)-Ga(1)-Ni(1) 145.48(9), N(1)-Ga(1)-Ni(1) 127.47(9), N(3)-Ni(1)-N(3)' 86.41(18), Ga(1)-Ni(1)-Ga(1)' 78.27(3), N(3)-Ni(1)-Ga(1) 97.76(9), N(3)-Ni(1)-Ga(1)' 147.69(9).

Figure 9. Molecular structure of **23** (isopropyl groups omitted for clarity). Selected bond lengths (Å) and angles (°): Ga(1)-N(1) 1.903(9), Ga(1)-N(2) 1.905(10), Ga(1)-Zn(1) 2.4491(17), Ga(2)-N(3) 1.895(8), Ga(2)-N(4) 1.886(10), Ga(2)-Zn(1) 2.4037(17), Zn(1)-N(6) 2.168(9), Zn(1)-N(5) 2.177(10), N(1)-C(1) 1.403(13), N(2)-C(2) 1.408(13), C(1)-C(2) 1.339(16), N(3)-C(27) 1.396(14), N(4)-C(28) 1.409(14), C(27)-C(28) 1.359(17), N(1)-Zn(1)-N(2) 86.2(4), N(1)-Ga(1)-Zn(1) 136.3(3), N(2)-Ga(1)-Zn(1) 137.5(3), N(3)-Ga(2)-N(4) 86.7(4), N(3)-Ga(2)-Zn(1) 133.9(3), N(4)-Ga(2)-Zn(1) 139.1(3), N(6)-Zn(1)-N(5) 84.7(3), N(6)-Zn(1)-Ga(2) 107.3(2), N(5)-Zn(1)-Ga(2) 109.0(3), N(6)-Zn(1)-Ga(1) 111.0(2), N(5)-Zn(1)-Ga(1) 111.1(3), Ga(2)-Zn(1)-Ga(1) 126.00(6).

The solid state structures of these compounds do not display any unusually short gallium – transition metal bond-lengths, indicating that there is no π-back-donation from the transition metal *d*-orbitals to the empty gallium *p*-orbitals. The Ga-Mn bond-length in **19** 2.3565 Å is significantly longer than that of **13**, 2.3105(9) Å, but is slightly shorter than that of **18**,

2.6658(10) Å. Similarly, the Ga-Co bond-lengths in **21** are *ca.* 0.1 Å longer than that in **14**. In all **19-23** the gallium heterocycle Ga-N bond-lengths and N-Ga-N angles are significantly shorter and more obtuse compared with those of the free heterocycle, **1**, see Table 2. This is consistent with the gallium heterocycle being a strong σ-electron donor. Once donation is made, there is a development of a partial positive charge on the gallium, causing a greater ionic bonding component between the gallium and the nitrogens of the diazabutadiene ligand. Consequently, the Ga-N bond lengths are reduced. This is similar to findings for the six-membered gallium heterocycle, [Ga{[N(Ar)C(Me)]₂C(H)}], once its coordination takes place.[27]

Table 2: Selected bond lengths and angles for **1**, **19-23**. Bond lengths and angles are averages (ave) where indicated.

Bond	Free Heterocycle	Mn(Td) 19	Fe(Td) 20	Co(Sp) 21	Ni(Sp) 22	Zn(Td) 23
Ga-N (Å)	1.9695(ave)	1.9210(ave)	1.9085(ave)	1.9065(ave)	1.904(ave)	1.8975(ave)
N-Ga-N (°)	83.02(11)	86.5(ave)	85.35(ave)	86.84(9)	87.00(12)	86.45(ave)
M-Ga	-	2.5515(ave)	2.5154(ave)	2.3331(6)	2.3051(8)	2.4264(ave)

Td – tetrahedral, Sp – square planar.

The apparent trend of the shortening of the Ga-N bond lengths for the gallium heterocycle once coordination has occurred, is observed for all the complexes **19-23**. As we proceed across the transition from Mn-Zn there is a shortening of the Ga-M bond lengths in line with a contraction of the covalent radii of the transition metal. However, all the observed Ga-M bond lengths fall within the normal bonding ranges for single M-Ga bonds.

The solid state structures of **19-23** show that there is a geometry change, at the transition metal centre, from distorted tetrahedral (Mn, Fe) to distorted square planar (Co, Ni) and finally a return to tetrahedral (Zn). The metals are all in the +II oxidation state and with these geometries, the crystal field splitting diagrams indicate that only the nickel and zinc complexes should be diamagnetic. The zinc complex crystallises with a tetrahedral geometry with filled *d*-orbitals and hence it is diamagnetic. The nickel complex is d^8, and with a square planar geometry is therefore diamagnetic. The remaining complexes are all paramagnetic and so no useful information from their NMR spectra could be gained. In order to gauge the magnetic susceptibility of these complexes the Evans' method was applied to their analysis. The resulting effective magnetic

moments (μ_{eff}) were found to be 2.64 BM for **19**, 2.17 BM for **20**, and 1.48 BM for **21**. For comparison, the transition metal di-halide starting materials, used in the synthesis of these complexes, posses μ_{eff} values of 5.89 BM (Mn)[28], 5.3 BM (Fe)[29], and 4.83 BM (Co)[28], and are described as having typical high spin values, for the assumed geometries, in each case. However, the number of unpaired electrons expected for low spin configurations, would be 1 unpaired e⁻ for **19** (Td, Mn, d^5), 2 unpaired e⁻ for **20** (Td, Fe, d^6), and 1 unpaired e⁻ for **21** (Sp, Co, d^7). The μ_{eff} values found for the transition metal di-gallyl complexes indicate that low spin configurations for the valence electrons at the transition metal centre are present. The gallium heterocycle is known to be a strong σ-donor, and so may increase the Δ_{Td} for the Mn and Fe complexes, and Δ_{Sp} for the Co complex, so increasing the possibility of the transition metal adopting a low spin configuration for its valence electrons.[30] Square planar cobalt(II) is described as always possessing a low spin configuration with typical μ_{eff} values of 2.2-2.7 BM.[31] To the best of our knowledge there are no reported complexes containing tetrahedral Mn(II) or Fe(II) that possess a low spin configuration. They are found exclusively to be high spin, with 'spin only' μ_{eff} values, for tetrahedral Mn(II) and Fe(II), of 5.92, and 4.90 respectively.[32] With this in mind, despite a reproducible outcome for the μ_{eff} values found using the Evans' method for **19-21**, we feel that these results are inconclusive and we can provide no explanation for these observations at present.

The ^1H and $^{13}C\{^1H\}$ NMR spectra of the zinc complex, **23**, are as would be expected if the solid state structure was retained in solution. However, complex **22** displays unusual splitting patterns in its ^1H NMR spectra. The spectrum suggests in-equivalent back-bone heterocycle protons, as an AB pattern is seen in the expected region. Presumably, this weak coupling arises from the backbone protons sitting in two slightly different chemical environments caused by restricted rotation around the Ni-Ga bond. This phenomenon is further exacerbated by the presence of two septets for the CH protons and four doublets for the CH_3 protons of the ^iPr aryl substituents respectively. This ^1H NMR spectra suggests that the solid state structure is retained in solution and that free rotation of the gallium heterocycle is restricted. If free rotation was allowed the diastereotopic nature of the CH_3 protons of the ^iPr aryl substituents would give rise to only two doublets and a pseudo septet for the CH proton in the ^1H NMR.

It was thought that reduced pressure sublimation of complex **20** could lead to elimination of the tmeda ligand and formation of a ferrocene analogue with a η^5-coordinated gallium heterocycles, $[Fe\{\eta^5\text{-}Ga[N(Ar)C(H)]_2\}_2]$. In this respect, the Ga(I) heterocycle is known to have

η^5-interaction with the K$^+$ cation in **1**. The experiment was carried out at 6×10^{-6} bar and 110°C during which a red powder was seen to sublime, leaving a black involatile residue. An ^{1}H NMR analysis of the sublimate revealed it to be the known digallane, [{Ga[N(Ar)C(H)]$_2$}$_2$], presumably formed through the reductive elimination of the gallium heterocycles to form the digallane and leaving an elemental iron deposit.

Following on from these successes, the reactions of the analogous dppe metal di-halide complexes, [(dppe)MX$_2$] dppe = bis(diphenylphosphino)ethane; M = Mn, Fe, Co, Ni, Cu, Zn; X = Cl, Br, I; were carried out with **1** in 1:2 ratios. These led to mixtures of free dppe and the tmeda complexes, mentioned above. The reaction of **1** with [(dppe)CuCl$_2$] led to total decomposition of the starting materials, presumably by reduction to copper metal. One further attempt was made to synthesise a copper-gallium complex, this time by reacting **1** with ½[(dppe)$_2$Cu$_2$I$_2$]. This reaction resulted in the formation of **24**, in moderate yield. Decomposition to copper metal presumably did not occur in this case due to the low oxidation state of the copper precursor. The solid state structure is shown in figure 10.
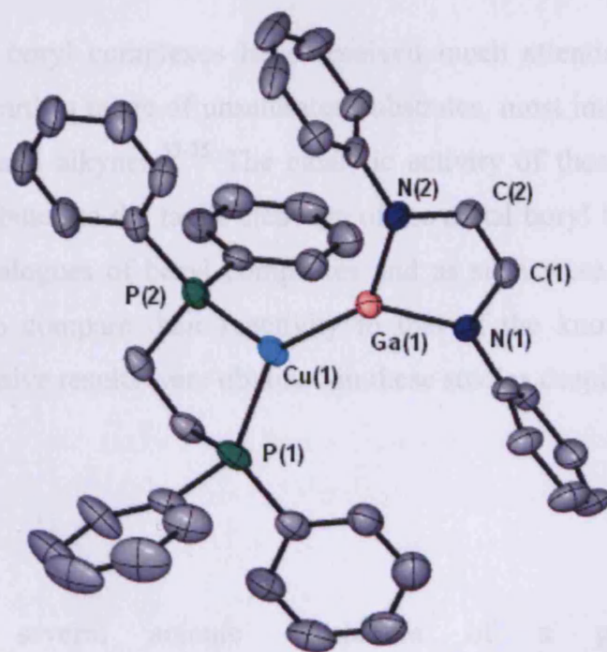
Figure 10. Molecular structure of **24** (isopropyl groups omitted for clarity). Selected bond lengths (Å) and angles (°): Ga(1)-N(1) 1.898(3), Ga(1)-N(2) 1.901(2), Ga(1)-Cu(1) 2.3054(9), N(1)-C(1) 1.392(4), N(2)-C(2) 1.386(4), C(1)-C(2) 1.345(4), Cu(1)-P(1) 2.2613(10), Cu(1)-P(2)

2.706(11), N(1)-Ga(1)-N(2) 85.22(11), N(2)-Ga(1)-Cu(1) 138.03(8), N(1)-Ga(1)-Cu(1) 134.25(8), C(1)-N(1)-Ga(1) 111.27(19), C(2)-N(2)-Ga(1) 111.11(19), P(1)-Cu(1)-P(2) 89.90(4), P(1)-Cu(1)-Ga(1) 139.88(3), P(2)-Cu(2)-Ga(2) 127.74(4).

The ^{1}H and ^{13}C$\{^1$H$\}$ NMR spectra of the copper complex, 24, are as would be expected if the solid state structure was retained in solution. An examination of the Cambridge Crystallographic Database revealed that complex 24 contains the first example of a gallium-copper bond (2.3054(9) Å) in a molecular compound. The coordinated gallium heterocycle Ga-N bond-lengths are found to be 1.898(3) and 1.901(2) Å, with an N-Ga-N angle of 85.22(11), which, as seen with the complexes before, are significantly shorter and more obtuse, respectively, than those of the free heterocycle 1. The solid state structure of 24 reveals a distorted trigonal planar geometry of the copper centre which is not unusual for copper(I) complexes.[31]

4. Further reactivity

Transition metal boryl complexes have received much attention as they have shown interesting reactivity towards a range of unsaturated substrates, most importantly in the catalytic diborylation of alkenes and alkynes.[33-35] The catalytic activity of these boryl transition metal complexes has been attributed to the facile cleavage of the metal boryl bonds. Complexes 19-24 can be thought of as analogues of boryl complexes and as such were treated with a range of unsaturated substrates to compare their reactivity to that of the known di-boryl complexes. Unfortunately, no conclusive results were obtained in these studies despite considerable effort.

5. Conclusion

In summary, several anionic complexes of a gallium(I) heterocycle, [Ga{[N(Ar)C(H)]₂}]⁻, with transition metal half sandwich fragments have been prepared by reaction of the heterocycle with suitable metal precursors. Although there is crystallographic and some spectroscopic evidence to suggest the possibility of significant M-Ga π-bonding in these species, a theoretical study on models of these compounds suggests they exhibit no more back-bonding than do analogous neutral NHC complexes. An anionic complex of the gallium

heterocycle with a manganese dialkyl has also been prepared by reaction of a metal dialkyl with the anionic gallium(I) heterocycle. This complex displays a Mn-Ga bond length that is not suggestive of any π-bonding. A series of neutral complexes of the gallium heterocycle were also accessed via salt metathesis reactions. The M-Ga bond lengths of these complexes are also not suggestive of any M-Ga π-bonding. In this study, complexes containing the first examples of V-Ga, Cu-Ga, and Zn-Ga bonds have been formed. Future studies will examine the use of the prepared complexes as potential reagents for catalytic or stoichiometric organic transformations, as has been reported for transition metal boryl complexes.

6. Experimental

General experimental procedures can be found in appendix 1. The magnetic moment determination was carried out using the Evans' method.[36] The compounds $[K(tmeda)][Ga\{[N(Ar)C(H)]_2\}]^2$, $[Mn\{CH(SiMe_3)_2\}_2]^{37}$, $[MnCl_2(tmeda)]^{28}$, $[FeCl_2(tmeda)_2]^{29}$, $[CoCl_2(tmeda)]^{28}$, $[NiCl_2(tmeda)_2]^{38}$, $[Cu_2(dppe)_2I_2]^{39}$ and $[ZnCl_2(tmeda)]^{40}$, were synthesized according to literature procedures, whilst all other reactants were obtained commercially and used as received.

Preparation of $[K(tmeda)][CpV(CO)_3[Ga\{[N(Ar)C(H)]_2\}]]$ 12. To a solution of $[K(tmeda)][:Ga\{[N(Ar)C(H)]_2\}]$ (0.30g, 0.50 mmol) in THF (15 cm^3) was added a solution of $[CpV(CO)_4]$ (0.11g, 0.50 mmol) in THF (15 cm^3) at −78 °C over 5 minutes. The resultant yellow solution was warmed to room temperature and stirred overnight. Volatiles were removed *in vacuo* and the residue extracted with hexane (20 cm^3). Filtration, concentration and cooling to − 30 °C overnight yielded yellow/orange crystals of **12** (0.22g, 54%). Mp 164-166°C; ^{1}H NMR (400MHz, C$_6$D$_6$, 298K): δ = 0.96 (d, $^3J_{HH}$ = 6.8 Hz, 12H, CH(CH_3)$_2$), 0.99 (d, $^3J_{HH}$ = 6.8 Hz, 12H, CH(CH_3)$_2$), 1.75 (s, 12H, NCH$_3$), 1.94 (s, 4H, NCH$_2$), 3.80 (v. sept, $^3J_{HH}$ = 6.8 Hz, 4H, CH(CH$_3$)$_2$), 4.51 (s, 5H, CpH), 6.26 (s, 2H, NC$_2$H$_2$N), 6.71 (t, $^3J_{HH}$ = 7.7 Hz, 2H, *p*-ArH), 8.89 (d, $^3J_{HH}$ = 7.7 Hz, 4H, *m*-ArH); ^{13}C{^{1}H} NMR (75MHz, C$_6$D$_6$, 298K): δ = 23.7 (CH(CH_3)$_2$), 24.1 (CH(CH_3)$_2$), 25.9 (CH(CH$_3$)$_2$), 45.0 (NCH$_3$), 56.8 (NCH$_2$), 87.6 (Cp), 117.0 (N$_2$C$_2$H$_2$), 122.9 (*m*-ArC), 123.7 (*p*-ArC), 147.2 (*o*-ArC), 148.7 (*ipso*-ArC), CO resonance not observed; ^{51}V NMR

(79MHz, C_6D_6, 298K): δ = -1809 ppm (s); IR v/cm^{-1} (THF/18-crown-6): 1962(s), 1891(s), 1785(br.s); m/z (CI/-ve): 645.2 [[CpV(CO)$_3$[Ga{[N(Ar)C(H)]$_2$}]]$^-$, 40%], 617.0 [[CpV(CO)$_2$[Ga{[N(Ar)C(H)]$_2$}]]$^-$, 55%], 376 [{N(Ar)C(H)}$_2^-$, 100%]; Acc. mass (CI/-ve): calc. for $C_{34}H_{41}O_3N_2{}^{69}Ga^{51}V$: 645.1818; obsvd. 645.1816.

Preparation of [K(tmeda)][Cp'Mn(CO)$_2$[Ga{[N(Ar)C(H)]$_2$}]] 13. To a solution of [K(tmeda)][:Ga{[N(Ar)C(H)]$_2$}] (0.20g, 0.34 mmol) in THF (15 cm^3) was added a solution of [Cp'Mn(CO)$_3$] (0.07g, 0.33 mmol) in THF (35 cm^3). The mixture was irradiated with a UV lamp for 2 hours at −78 °C. The resultant solution was warmed to room temperature and stirred overnight to yield a yellow solution. Volatiles were removed *in vacuo* and the residue extracted with hexane (20 cm^3). Filtration, concentration and cooling to −30 °C overnight yielded yellow/orange crystals of **13** (0.12g, 46%). Mp 255-257°C; ^{1}H NMR (300MHz, C_6D_6, 298K): δ = 1.11 (d, 12H, $^3J_{HH}$ = 6.6 Hz, CH(CH_3)$_2$), 1.15 (d, 12H, $^3J_{HH}$ = 6.6 Hz, CH(CH_3)$_2$), 1.51 (s, 3H, C$_5$H$_4$(CH_3)), 1.82 (s, 12H, NCH$_3$), 1.96 (s, 4H, NCH$_2$), 3.15 (v. sept, $^3J_{HH}$ = 6.6 Hz, 4H, CH(CH$_3$)$_2$), 3.87 (m, 2H, CpH), 4.06 (m, 2H, Cp), 6.24 (s, 2H, N$_2$C$_2$H$_2$), 6.80-7.20 (m, 6H, ArH); ^{13}C{^{1}H} NMR (75MHz, C_6D_6, 298K): δ = 23.4 (C$_5$H$_4$(CH$_3$)), 23.8 (CH(CH$_3$)$_2$), 25.9 (CH(CH$_3$)$_2$), 28.4 (CH(CH$_3$)$_2$), 44.8 (NCH$_3$), 56.7 (NCH$_2$), 76.7, 78.9, 96.8 (Cp), 122.3 (NC$_2$H$_2$), 122.8 (*m*-ArC), 123.7 (*p*-ArC), 147.7 (*o*-ArC), 150.4 (*ipso*-ArC), 238.3 (CO); IR v/cm^{-1} (THF/18-crown-6): 1877(s), 1812(s); m/z (APCI): 377 [{N(Ar)C(H)}$_2$H$^+$, 100%].

Preparation of [K(tmeda)][CpCo(CO)[Ga{[N(Ar)C(H)]$_2$}]] 14. To a solution of [K(tmeda)][:Ga{[N(Ar)C(H)]$_2$}] (0.30g, 0.50 mmol) in diethyl ether (15 cm^3) was added a solution of [CpCo(CO)$_2$] (0.09g, 0.50 mmol) in diethyl ether (15 cm^3) at −78 °C over 5 minutes. The resultant solution was warmed to room temperature and stirred overnight to yield a red solution. Volatiles were removed *in vacuo* and the residue extracted with hexane (20 cm^3). Filtration, concentration and cooling to −30 °C overnight yielded red crystals of **14** (0.26g, 66%). Mp 118-120°C; ^{1}H NMR (250MHz, C_6D_6, 298K): δ = 1.49 (v. t, $^3J_{HH}$ = 6.6 Hz, 24H, CH(CH_3)$_2$), 1.89 (s, 12H, NCH$_3$), 2.03 (s, 4H, NCH$_2$), 3.77 (v. sept, $^3J_{HH}$ = 6.6 Hz, 4H, CH(CH$_3$)$_2$), 4.40 (s, 5H, CpH), 6.18 (s, 2H, N$_2$C$_2$H$_2$), 6.90-7.26 (m, 6H, ArH); ^{13}C{^{1}H} NMR (75MHz, C_6D_6, 298K): δ = 24.2 CH(CH$_3$)$_2$, 25.2 CH(CH$_3$)$_2$, 28.0 CH(CH$_3$)$_2$, 45.2 (NCH$_3$), 57.1 (NCH$_2$), 77.1 (Cp),

121.8 (N₂C₂H₂), 122.7 (*m*-ArC), 123.7 (*p*-ArC), 147.2 (*o*-ArC), 149.2 (*ipso*-ArC), 209.1 (CO); IR v/cm⁻¹ (THF/18-crown-6): 1690(s); m/z (APCI): 377 [{N(Ar)C(H)}₂H⁺, 75%].

Preparation of [K(tmeda)][Mn{CH(SiMe₃)₂}₂[Ga{[N(Ar)C(H)]₂}]] 18. To a solution of [K(tmeda)][:Ga{[N(Ar)C(H)]₂}] (0.41 g, 0.68 mmol) in diethyl ether (25 cm³) was added a solution of [Mn{CH(SiMe₃)₂}₂] (0.26 g, 0.68 mmol) in diethyl ether (25 cm³) at −78 °C over 15 min. The resultant red solution was warmed to room temperature over 1 hour and stirred overnight. Volatiles were removed *in vacuo* and the residue extracted with hexane (20 cm³). Filtration, concentration and cooling to −30 °C overnight yielded red crystals of **18** (0.30 g, 45 %). Mp = 85 − 87 °C; IR v/cm⁻¹ (Nujol): 1854(s), 1251(s), 1091(s), 1033(s), 851(s); m/z (APCI): 377 [{N(Ar)C(H)}₂H⁺, 100%]; μ_eff = 4.62 BM; C₄₆H₉₀N₄GaKMnSi₄ requires: C 56.65%, H 9.30%, N 5.74%; found: C 56.51%, H 8.96%, N 5.58%.

Preparation of [Mn(tmeda)[Ga{N(Ar)C(H)}₂]₂] 19. To a solution of [K(tmeda)][:Ga{[N(Ar)C(H)]₂}] (0.25 g, 0.42 mmol) in THF (20 cm³) was added a solution of [(tmeda)MnCl₂] (0.05 g, 0.21 mmol) in THF (20 cm³) at −78 °C. The solution was warmed to room temperature and stirred for one hour to yield a green solution. Volatiles were removed *in vacuo* and the residue washed with hexane (15 cm³) and extracted with diethyl ether (40 cm³). Filtration, concentration and cooling to −30 °C overnight yielded green crystals of **19** (0.06 g, 27 %). Mp = 127 − 129 °C; μ_eff = 2.64 BM; IR v/cm⁻¹ (Nujol): (m) 1580 (s) 1213, (s) 1116, (s) 944, (s) 897, (s) 802, (s) 762; m/z (EI): 1063 [M⁺, 4%], 446 [ArDABGa⁺, 43%], 377 [ArDAB⁺, 80 %]; Acc. mass (EI): calc. for C₅₈H₈₈N₆MnGa₂: 1061.4957, obsvd. 1061.4955.

Preparation of [Fe(tmeda)[Ga{N(Ar)C(H)}₂]₂] 20. To a solution of [K(tmeda)][:Ga{[N(Ar)C(H)]₂}] (0.34 g, 0.56 mmol) in THF (20 cm³) was added to solution of [(tmeda)₂FeCl₂] (0.10 g, 0.28 mmol) in THF (20 cm³) at −78 °C. The solution was warmed to room temperature and stirred for one hour to yield a green solution. Volatiles were removed *in vacuo* and the residue washed with hexane (15 cm³) and extracted with diethyl ether (40 cm³). Filtration, concentration and cooling to −30 °C overnight yielded green crystals of **20** (0.09 g, 30 %). Mp = 166 − 168 °C; μ_eff = 2.17 BM; IR v/cm⁻¹ (Nujol): (s) 1586, (s) 1259, (s) 1212, (s) 1115,

(s) 943, (s) 933, (br) 800, (s) 762, (s) 681; m/z (EI): 1064 [M$^+$, 6%], 446 [ArDABGa$^+$, 36%], 377 [ArDAB$^+$, 100 %]; Acc. mass (EI): calc. for $C_{58}H_{88}N_6FeGa_2$: 1062.4926, obsvd. 1062.4925.

Preparation of [Co(tmeda)[Ga{N(Ar)C(H)}_2]_2] 21. To a solution of [K(tmeda)][:Ga{[N(Ar)C(H)]_2}] (0.50 g, 0.82 mmol) in THF (20 cm^3) was added to solution of [(tmeda)CoCl_2] (0.10 g, 0.41 mmol) in THF (20 cm^3) at −78 °C. The solution was warmed to room temperature and stirred for one hour to yield a green / red solution. Volatiles were removed *in vacuo* and the residue washed with hexane (15 cm^3) and extracted with diethyl ether (20 cm^3). Filtration, concentration and cooling to −30 °C overnight yielded red crystals of **21** (0.04 g, 9 %). Mp = 220 - 223 °C; μ_{eff} = 1.48 BM; IR v/cm^{-1} (Nujol): (m) 1585, (s) 1318, (s) 1252, (s) 1112, (s) 804, (s) 764, (s) 750; m/z (EI): 446 [ArDABGa$^+$, 100%], 377 [ArDAB$^+$, 42 %].

Preparation of [Ni(tmeda)[Ga{N(Ar)C(H)}_2]_2] 22. To a solution of [K(tmeda)][:Ga{[N(Ar)C(H)]_2}] (0.25 g, 0.42 mmol) in THF (20 cm^3) was added to solution of [(tmeda)_2NiBr_2] (0.09 g, 0.21 mmol) in THF (20 cm^3) at −78 °C. The solution was warmed to room temperature and stirred for one hour to yield a red solution. Volatiles were removed *in vacuo* and the residue washed with hexane (15 cm^3) and extracted with diethyl ether (20 cm^3). Filtration, concentration and cooling to −30 °C overnight yielded red crystals of **22** (0.03 g, 13 %). Mp = 188 - 190 °C; ^{1}H NMR (400MHz, C_6D_6, 298K): δ = 1.28 (s, 4H, NCH_2), 1.34 (d, $^3J_{HH}$ = 6.83 Hz, 9H, ^{i}PrCH_3), 1.37 (d, $^3J_{HH}$ = 6.81 Hz, 9H, ^{i}PrCH_3), 1.45 (d, $^3J_{HH}$ = 6.49 Hz, 9H, ^{i}PrCH_3), 1.49 (d, $^3J_{HH}$ = 6.49 Hz, 9H, ^{i}PrCH_3), 1.55 (s, 12H, NCH_3), 3.32 (sept, $^3J_{HH}$ = 6.67 Hz, 4H, ^{i}PrCH), 4.12 (sept, $^3J_{HH}$ = 6.72 Hz, 4H, ^{i}PrCH), 6.08 (d, $^3J_{HH}$ = 3.61 Hz, 2H, NCH), 6.31 (d, $^3J_{HH}$ = 3.71 Hz, 2H, NCH), 7.19 − 7.47 (m, ArH, 12H); Low solubility of sample and its instability in solution precluded acquisition of useful ^{13}C{^{1}H} NMR data; IR v/cm^{-1} (Nujol): (m) 1560, (s) 1260, (br) 1098, (br) 1019, (s) 802, (s) 722; m/z (EI): 1067 [MH$^+$, 2%], 446 [ArDABGa$^+$, 76%], 377 [ArDAB$^+$, 23 %].

Preparation of [Zn(tmeda)[Ga{N(Ar)C(H)}_2]_2] 23. To a solution of [K(tmeda)][:Ga{[N(Ar)C(H)]_2}] (0.50 g, 0.82 mmol) in THF (20 cm^3) was added a solution of [(tmeda)ZnCl_2] (0.11 g, 0.41 mmol) in THF (20 cm^3) at −78 °C. The solution was warmed to

room temperature and stirred for one hour to yield a yellow solution. Volatiles were removed *in vacuo* and the residue extracted with hexane (60 cm^3). Filtration, concentration and cooling to – 30 °C overnight yielded yellow crystals of **23** (0.32 g, 72 %). Mp = 85 – 87 °C; ^{1}H NMR (400MHz, C$_6$D$_6$, 298K): δ = 1.18 (d, $^3J_{HH}$ = 6.8 Hz, 24H, ^{i}PrCH$_3$), 1.33 (d, $^3J_{HH}$ = 6.8 Hz, 24H, ^{i}PrCH$_3$), 1.42 (s, NCH$_2$, 4H), 1.47 (s, NCH$_3$, 12H), 3.64 (sept, $^3J_{HH}$ = 6.8 Hz, ^{i}PrCH, 8H), 6.37 (s, NCH, 4H), 7.13 – 7.18 (m, ArH, 12H); ^{13}C NMR (75MHz, C$_6$D$_6$, 298K): δ = 23.5 (^{i}PrCH$_3$), 24.4 (^{i}PrCH$_3$), 26.7 (^{i}PrCH), 47.7 (NCH$_3$), 55.8 (NCH$_2$), 121.5 (CN), 121.7 (*m*-ArC), 123.3 (*p*-ArC), 144.1 (*o*-ArC), 146.3 (*ipso*-ArC); IR v/cm^{-1} (Nujol): (s) 1587, (s) 1259, (br) 1100, (br) 1020, (s) 800, (s) 762; m/z (EI): 446 [ArDABGa$^+$, 12%], 377 [ArDAB$^+$, 100 %].

Preparation of [Cu(dppe)[Ga{N(Ar)C(H)}$_2$]] 24. To a solution of [K(tmeda)][:Ga{[N(Ar)C(H)]$_2$}] (0.25 g, 0.42 mmol) in Et$_2$O (20 cm^3) was added a solution of [(dppe)$_2$Cu$_2$I$_2$] (0.24 g, 0.21 mmol) in Et$_2$O (20 cm^3) at –78 °C. The solution was warmed to room temperature and stirred overnight to yield a red solution. Volatiles were removed *in vacuo* and the residue washed with hexane (20 cm^3) and extracted with diethyl ether (30 cm^3). Filtration, concentration and cooling to –30 °C overnight yielded red crystals of **24** (0.09 g, 46 %). Mp = 148 – 149 °C; ^{1}H NMR (250MHz, C$_6$D$_6$, 298K): δ = 1.38 (d, $^3J_{HH}$ = 6.9 Hz, 12H, ^{i}PrCH$_3$), 1.56 (d, $^3J_{HH}$ = 6.9 Hz, 12H, ^{i}PrCH$_3$), 1.91 (br. m, PCH$_2$, 4H), 4.28 (sept, $^3J_{HH}$ = 6.9 Hz, ^{i}PrCH, 4H), 6.83 (s, NCH, 2H), 7.08 – 7.48 (m, ArH, 26H); ^{13}C NMR (75MHz, C$_6$D$_6$, 298K): δ = 23.5 (PCH$_2$), 24.0 (^{i}PrCH$_3$), 25.7 (^{i}PrCH$_3$), 28.2 (^{i}PrCH), 122.8 (NCH), 123.7 (*m*-PhC), 128.5 (*m*-ArC), 128.6 (*p*-ArC), 128.9 (*m*-PhC), 132.8 (*o*-PhC), 146.1 (*o*-ArC), *ipso*-PhC and *ipso*-ArC not observed; ^{31}P NMR (121MHz, C$_6$D$_6$, 298K): δ = -3.25 (dppe); IR v/cm^{-1} (nujol): (s) 1585, (s) 1259, (s) 1101, (s) 803, (s) 761, (s) 745, (s) 693; m/z (EI): 908 [MH$^+$, 2%], 446 [ArDABGa$^+$, 76%], 377 [ArDAB$^+$, 24 %].

7. References

1. e.g. (a) N. Kuhn and A. Al-Sheikh, *Coord. Chem. Rev.*, 2005, **249**, 829; (b) W. Kirmse, *Eur. J. Org. Chem.*, 2005, 237; (c) W. A. Herrmann, *Angew. Chem. Int. Ed.*, 2002, **41**, 1291; (d) C. J. Carmalt and A. H. Cowley, *Adv. Inorg. Chem.*, 2000, **50**, 1; (e) D.

Bourissou, O. Guerret, F. P. Gabai and G. Bertrand, *Chem. Rev.*, 2000, **100**, 39, and references therein.

2. R. J. Baker, R. D. Farley, C. Jones, M. Kloth and D. M. Murphy, *J. Chem. Soc., Dalton Trans.*, 2002, 3844;

3. R. J. Baker and C. Jones, *Coord. Chem. Rev.*, 2005, **149**, 1857, and references therein.

4. (a) C. Jones, D. P. Mills, J. A. Platts and R. P. Rose, *Inorg. Chem.*, 2006, **45**, 3146; (b) R. J. Baker, C. Jones, D. P. Mills, D. M. Murphy, E. Hey-Hawkins and R. Wolf, *Dalton Trans.*, 2006, 64; (c) R. J. Baker, C. Jones and M. Kloth, *Dalton Trans.*, 2005, 2106; (d) R. J. Baker, C. Jones, M. Kloth and J.A. Platts, *Organometallics*, 2004, **23**, 4811; (e) R. J. Baker, C. Jones, M. Kloth and J. A. Platts, *Angew. Chem. Int. Ed.*, 2003, **43**, 2660.

5. R. J. Baker, C. Jones and J. A. Platts, *Dalton Trans.*, 2003, 3673.

6. R. J. Baker, C. Jones and J. A. Platts, *J. Am. Chem. Soc.*, 2003, **125**, 10534.

7. C. D. Abernerthy, J. A. C. Clyburne, A. H. Cowley, R. A. Jones, *J. Am. Chem. Soc.*, 1999, **121**, 2329.

8. W. Uhl, M. Benter, S. Melle, W. Saac, *Organometallics*, 1999, **18**, 3778.

9. R. J. Baker, C. Jones and D. M. Murphy, *Chem. Commun.*, 2005, 1339.

10. S. Aldridge, R. J. Baker, N. D. Coombs, C. Jones, R. P. Rose, A. Rossin, D. J. Willock, *Dalton Trans.*, 2006, 3313.

11. e.g. (a) X.-J. Yang, Y. Wang, B. Quillian, P. Wei, Z. Chen, P. v. R. Schleyer and G. H. Robinson, *Organometallics*, 2006, **25**, 925; (b) G. Gemel, T. Steinke, M. Cokoja, A. Kempter and R.A. Fischer, *Eur. J. Inorg. Chem.*, 2004, 4161, and references therein.

12. e.g. (a), E. Fooladi, B. Dalhus and M. Tilset, *Dalton Trans.*, 2004, 3909; (b) P. Buchgraber, L. Toupet and V. Guerchais, *Organometallics*, 2003, **22**, 5144; (c) V. K. Dioumaev, D.J. Szalda, J. Hanson, J. A. Franz and R.M. Bullock, *Chem. Commun.*, 2003, 1670; (d) R.W. Simms, M.J. Drewitt and M.C. Baird, *Organometallics*, 2002, **21**, 2958.

13. R.J. Baker, R.D. Farley, C. Jones, D.P. Mills, M. Kloth, D.M. Murphy, *Chem. Eur. J.*, 2005, **11**, 2972.

14. A. Kempter, C. Gemel, N. J. Hardman and R. A. Fischer, *Inorg. Chem.*, 2006, **45**, 3133.

15. U. Phttfarcken and D. Rehder, *J. Organomet. Chem.*, 1980, **185**, 219.

16. V. S. Leong and N. J. Cooper, *Organometallics*, 1988, **7**, 2080.

17. (a) B. E. R. Schilling, R. Hoffmann and D. Lichtenberger, *J. Am. Chem. Soc.*, 1979, **101**, 585; (b) P. Hoffman and M. Padmanabhan, *Organometallics*, 1983, **2**, 1273.

18. As determined by a survey of the Cambridge Crystallographic Database, April, 2006.

19. A. H. Cowley, A. Decken, C. A. Olazabal and N. C. Norman, *Inorg. Chem.*, 1994, **33**, 3435.

20. S. Aldridge, A. Rossin, D. L. Coombs and D .J. Willock, *Dalton Trans.*, 2004, 2649.

21. A. A. Dickinson, D. J. Willock, R. J. Calder and S. Aldridge, *Organometallics*, 2001, **21**, 1146.

22. e.g.: (a) E. A. McCullough, Jr., E. Aprà and J. Nichols, *J. Phys. Chem. A*, 1997, **101**, 2502; (b) C. L. B. Macdonald and A. H. Cowley, *J. Am. Chem. Soc.*, 1999, **121**, 12113; (c) J. Uddin, C. Boehme and G. Frenking, *Organometallics*, 2000, **19**, 571; (d) J. Uddin and G. Frenking, *J. Am. Chem. Soc.*, 2001, **123**, 1683.

23. J. Zhu, Z. Lin and T. B. Marder, *Inorg. Chem.*, 2005, **44**, 9384.

24. N. R. Bunn, S. Aldridge, D. L. Coombs, A. Rossin, D. J. Willock, C.Jones and L.-L. Ooi, *Chem. Commun.*, 2004, 1732.

25. P. B. Hitchcock, M. F. Lappert and W.-P. Leung, *J. Organomet. Chem.*, 1990, **394**, 57, and references therein.

26. D. S. Brown, A. Decken, A. H. Cowley, *J. Am. Chem. Soc.*, 1995, **117**, 5421.

27. N. J. Hardman, P. P. Power, J. D. Gorden, C. L. B. Macdonald, A. H. Cowley, *Chem. Commun.*, 2001, 1971.

28. P. Sobota, J. Utko, S. Szafert, Z. Janas, T. Glowiak, *J. Chem. Soc., Dalton. Trans.*, 1996, 3469.

29. S. C. Davies, D. L. Hughes, G. J. Leigh, J. R. Sanders, J. S. de Souza, *J. Chem. Soc., Dalton. Trans.*, 1997, 1981.

30. D. F. Shriver, P. W. Atkins, C. H. Langford, "*Inorganic Chemistry*", Oxford University Press, 2nd edn., 1998.

31. F. A. Cotton, G. Wilkinson, "*Advanced Inorganic Chemistry*", John Wiley & Sons, 5th edn., 1988.

32. J. E. Huheey, E. A. Keiter, R. L. Keiter, "*Inorganic Chemistry, Principles of Structure and Reactivity*", Harper Collins College Publishers, 4th edn., 1993.

33. H. Braunschweig, *Angew. Chem. Int. Ed.*, 1998, **37**, 1786.

34. G. J. Irvine, M. J. G. Lesley, T. B. Marder, N. C. Norman, C. R. Rice, E. G. Robins, W. R. Roper, G. R. Whittell, L. J. Wright, *Chem. Rev.*, 1998, **98**, 2685.

35. H. Braunschweig, M. Colling, *Coord. Chem. Revs.*, 2001, **223**, 1.

36.   (a) D. F. Evans, *J. Chem. Soc.*, 1959, 2003; (b) E. M. Schubert, *J. Chem. Ed.*, 1992, **69**, 62.

37.   R. A. Anderson, D. J. Berg, L. Ferholt, K. Faegri, J. C. Green, A. Haaland, M. F. Lappert, W. P. Leung and K. Rypdal, *Acta. Chem. Scand.*, 1988, **A42**, 554.

38.   D. A. Handley, P. B. Hitchcock, G. J. Leigh, *Inorganica. Chimica. Acta.*, 2001, **314**, 1.

39.   P. Comba, C. Katsichtis, B. Nuber, H. Pritzkow, *Eur. J. Inorg. Chem.*, 1999, 777.

40.   K. G. Caulton, *Inorg. Nucl. Chem. Lett.*, 1973, **9**, 533.

Chapter 3

Main Group Chemistry of an Anionic Gallium(I) N-Heterocyclic Carbene Analogue

1.   Introduction

1.1   Main Group N-heterocyclic carbene chemistry

Since 1991, when the first stable N-heterocyclic carbene (NHC) 1,3-di-1-adamantylimidazol-2-ylidene was isolated,[1] 1 where R^1 = adamantly, R^2 = H, there has been an extensive exploration of the reactivity of these species towards main group metal precursors which has been recently comprehensively reviewed.[2] A brief summary of this field of research will be presented here.
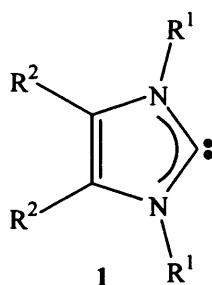
There are very few examples of adducts of NHCs with group 1 alkali metal fragments. Some compounds that have been isolated and characterised containing NHC-group 1 interactions and are shown in scheme 1.

Scheme 1
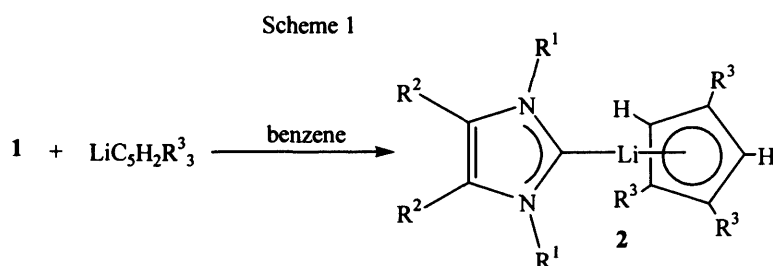
R^1 = ^{t}Bu (72 %), Ad (41 %), Mes (77 %); R^2 = H; R^3 = SiMe$_3$;

M = Li, Na, K; R^1 = Pr^i; R^2 = H; R^3 = SiMe$_3$;
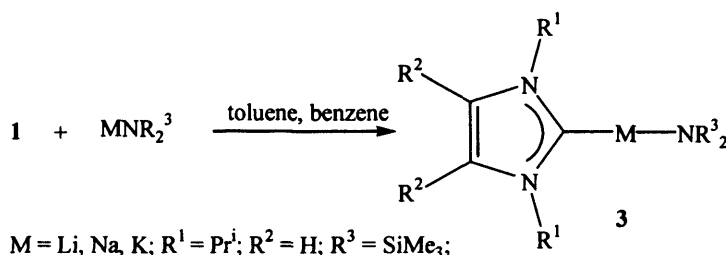
The reaction of **1** with lithium-1,2,4-tris(trimetylsilyl)cyclopentadienide gave complexes of the form **2**, in moderate to good yields. The central lithium atom possesses an almost symmetrical η^5-coordinated cyclopentadienyl ring (0.7° off plane) and a single σ-interaction between the lithium and the carbene fragment.[3] Evidence for the existence of further group 1 alkali metal carbene complexes have been reported.[4] Complexes of the type **3** were formed from the reaction of **1** with $MN(SiMe_3)_2$, M = Li, Na, K. ^{13}C NMR data were presented to support formation of such complexes whereby the carbene carbon signal was seen to have an upfield shift once the reactant was introduced. However, these complexes could not be crystallised so no further evidence to support these findings was given.

Scheme 2

1 + BeCl₂ ⟶

R¹ = Me; R² = H;

1 + Cp*₂M $\xrightarrow{\text{toluene / benzene}}$

M = Mg **5**; R¹ = Me, Pr^i; R² = Me;

M = Ca **6**; R¹ = Me, Pr^i; R² = Me;

M = Sr **7**; R¹ = Me, Pr^i; R² = Me;

M = Ba **8**; R¹ = Me, Pr^i; R² = Me;
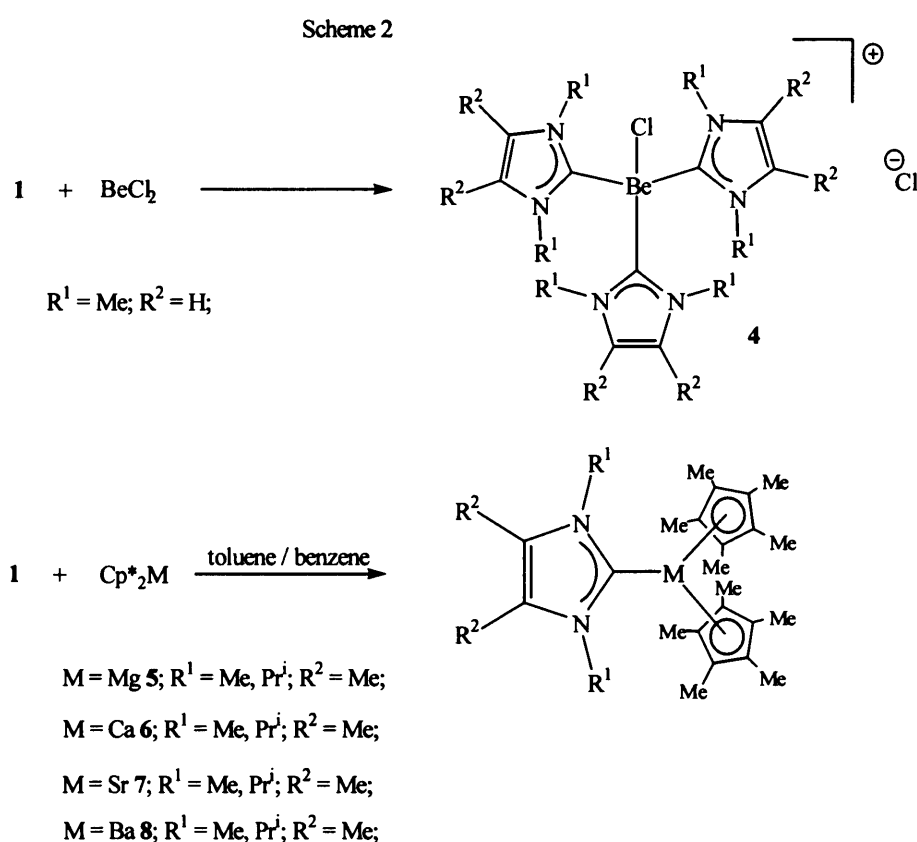
With group 2 precursors there is only 1 example of a beryllium-NHC complex. This was obtained from the reaction of **1** with $BeCl_2$, scheme 2, whereby the nucleophlicity of the NHC causes cleavage of polymeric $(BeCl_2)_n$ followed by heterolysis to yield the ionic complex **4**.[5] Further group 2 NHC complexes have been obtained through, for example, the reactions of **1** with bis(pentamethylcyclopentadienyl)magnesium, -calcium, strontium and -barium yielding complexes **5, 6, 7** and **8** respectivly.[6] In the solid state, the Mg complex **5** was found to possess 1

η^5-bound Cp* ligand with the other having a ligation between η^3- and σ-bonding. For the heavier group 2 complexes, **6-8**, both Cp* ligands were found to possess η^5-interactions. The carbene-metal bond lengths were found to be somewhat covalent for Mg (2.194(2) Å) progressing to rather ionic for barium (2.951(3) Å).

NHC complexes containing boron fragments are known and examples are shown in scheme 3. The reactions of a solvated boron tri-halide or tri-hydride with **1** yielded complexes **9** and **10** in good yields.[7,8] Complex **9** (where R^1 = Mes (2,4,6-trimethylphenyl), R^2 = H) possesses a surprisingly high melting point of 296 - 300°C. This was attributed to a strong intermolecular interaction in the solid state. A theoretical study of this complex revealed the hydrogen atoms attached to the boron to possess a partial negative charge, and the back-bone protons of the carbene fragment to exhibit a partial positive charge.[8]

Scheme 3

$$1 \quad + \quad S.BX_3 \quad \longrightarrow$$

S = C_4H_8O, Et_2O, SMe_3;
X = H **9**; R^1 = Me, Et, Pr^i, Mes; R^2 = Me, H;
X = F **10**; R^1 = Me, Mes; R^2 = Me, H, Cl;

$$1 \quad + \quad \longrightarrow$$

R^1 = Me, Pr^i; R^2 = H, Me; R^3 = Bu^t;

11
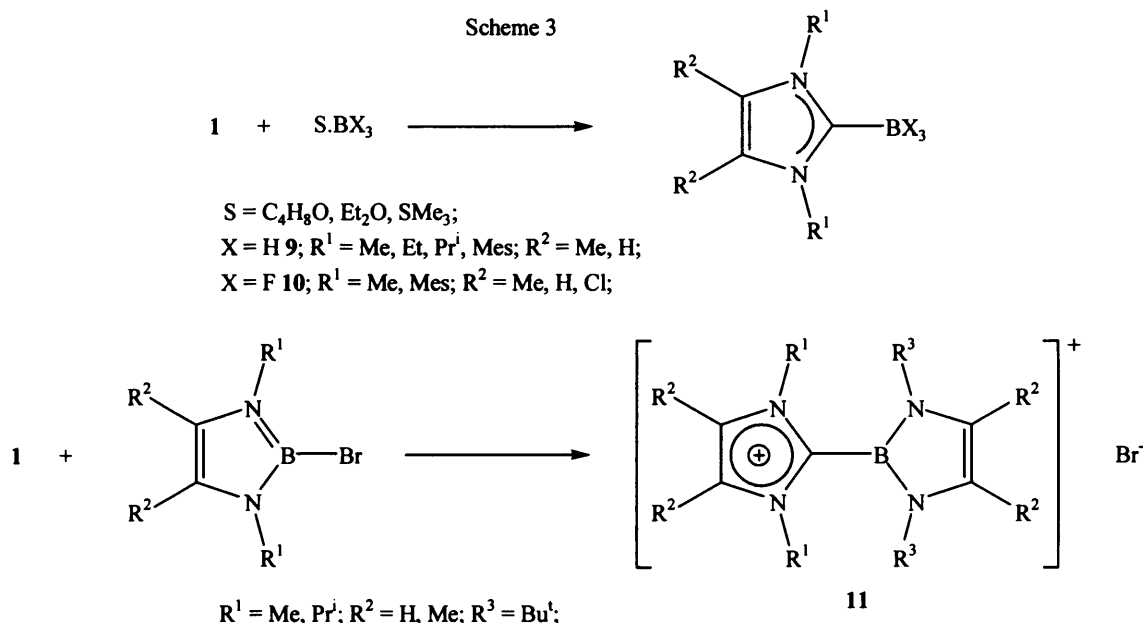
NHC fragments have also been coordinated to boryl substituents through the reaction of **1** with 2-bromo-1,2,3-diazaboroles giving, for example, compound **11** in moderate yield. The reaction proceeds via a halide displacement to afford the borolyimidazolium salt.[9]

The stabilisation of thermally labile late group 13 metal hydride fragments has also been achieved using NHCs, scheme 4. The reactions of $LiMH_4$, M = Al, Ga, In; with **1** leads to the isolation of complexes **12**, **13** and **14** respectively in good yield with the subsequent loss of LiH.[2,10,11] Alternatively, these compounds could be accessed via ligand substitution, for example, in the reaction of **1** with $InH_3(NMe_3)$ which also produces **14**, whereby NMe_3 is replaced by the

NHC.[11] When R^1 = mesityl, for complex **14**, the decomposition temperature in the solid state was found to be 115°C which is upwards of 100°C greater than those found for tertiary amine-indane adducts. For example, InH$_3$(quinuclidine) was found to decompose above *ca.* -5°C.[10]

Scheme 4

$$ \textbf{1} \ + \ LiMH_4 \ \xrightarrow[- LiH]{} \ $$

M = Al **12**; R^1 = Mes, Pr^i, 2,6-Pr$^i_2$C$_6$H$_3$; R^2 = H, Me;

M = Ga **13**; R^1 = Mes, Pr^i; R^2 = H, Me;

M = In **14**; R^1 = Mes; R^2 = H;

$$ \textbf{1} \ + \ TlX_3 \ \longrightarrow \ $$

R^1 = Mes; R^2 = H, Br; X = Cl, Br;   **15**
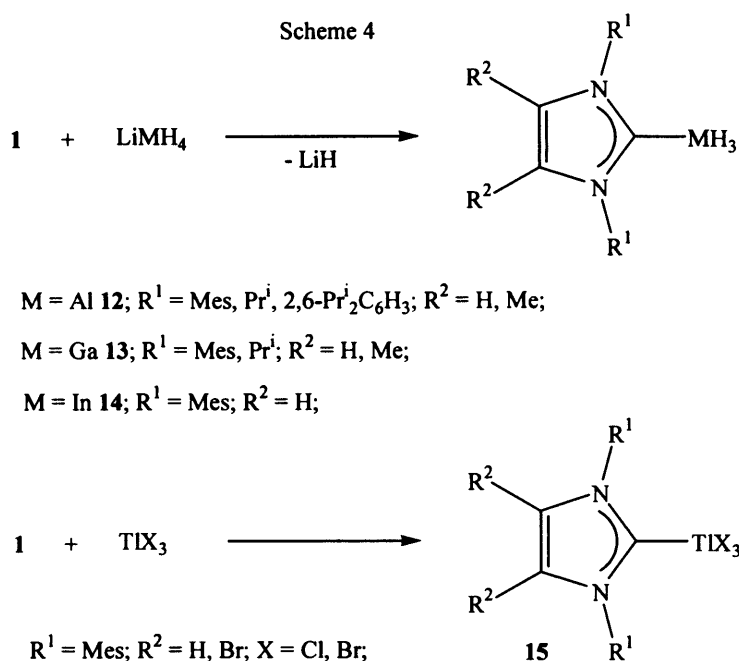
The stability of the NHC-group 13 tri-hydrides has been attributed to a combination of the large steric bulk of the NHC ligand and its high nucleophilicity. The steric bulk protects the central metal atom from attack by oxygen and moisture as well as preventing the formation of intermolecular hydride bridges. The nucleophilicity of the NHC circumvents the formation of these bridges by satisfying the metal centres electronically.[11] To the best of my knowledge there have been no reports of an isolated thallane complex (LTlH$_3$ where L = Lewis base). This, however, does not mean that Tl-NHC bonds are unknown. The reaction of TlX$_3$, X = Cl or Br; with **1** led to the coordination of **1** giving complexes **15** in good yield.[12]

Scheme 5 shows some examples of NHC group 14 chemistry. The reaction of **1** with 2-fluoro-1,3-diisopropyl-4,5-dimethylimidazolium tetrafluoroborate gives the dicationic salt **16** after a subsequent addition of BF$_3$.Et$_2$O.[2]

66

Scheme 5

R¹ = Pr'; R² = Me;

16

17   18

M = Si **19**, Ge **20**, Sn **21**, Pb **22**; R¹ = CH₂CMe₃
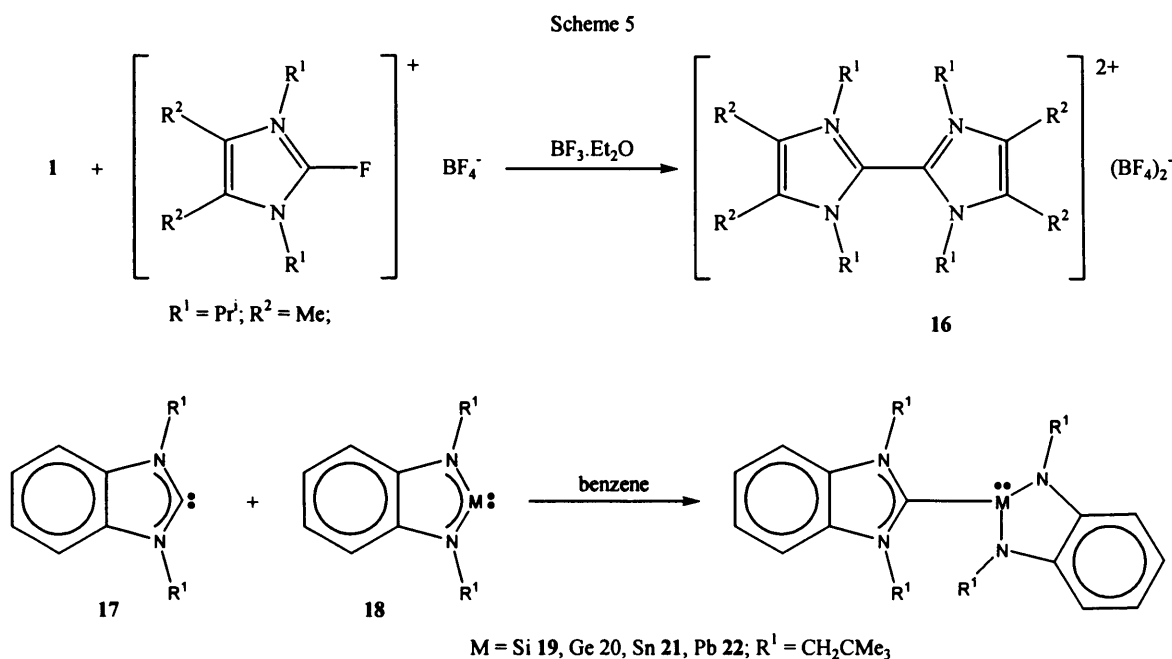
Further group 14 NHC complexes have been synthesised from the reactions of **1** with group 14 analogues of carbenes, **18**, giving complexes **19 - 22** in good yield.[13,14] Crystallographic and spectroscopic studies of these complexes point towards the carbene metal bond being very weak, and the interaction between the carbene and metal being largely electrostatic.[14] This has also been confirmed by Density Functional Theory (DFT) on a model of **19**, [(CH₂)₂(NH)₂C-Si[(NH)₂(CH₂)₂], which revealed a C-Si bond dissociation energy of -13.4 kJ mol^{-1}, with a partial negative charge on the Si atom.[14]

Scheme 6

1 + H₂C=N⁺=N⁻ ⟶

R¹ = Mes; R² = H;   **23**

1 + MF₅ ⟶

M = P **24**; R¹ = Mes; R² = H, Cl;

M = As **25**, Sb **26**; R¹ = Mes; R² = Cl;
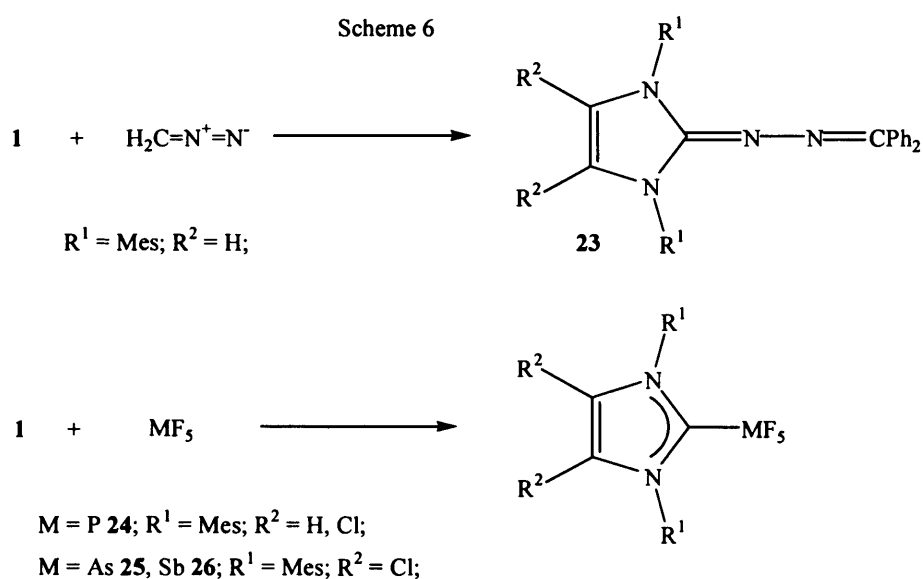
Group 15 NHC complexes can be formed and some examples are presented above in scheme 6. The reaction of **1** with the diazo compound, $(C_6H_5)_2CN_2$, gives rise to the azine compound **23** in moderate yield.[15] In addition, a series of pnictogen pentafluorides have been reacted with **1** giving complexes **24 - 26** in good yield.[16,17] To the best of our knowledge there have been no bismuth-NHC complexes reported.

Group 16 NHC complexes are known and some examples are shown in scheme 7. Carbenes of the type **1** appear to be inert to O_2 attack, whilst the treatment of **1** with N_2O led to complete oxidation giving **27** in good yield.[2,18] Complexes **28** and **29** were synthesised from the direct reaction of **1** with elemental sulfur or tellurium respectively.[2,19]

Scheme 7

$$
\begin{array}{c}
N_2O \\
\mathbf{1} \quad + \quad S \\
Te
\end{array}
\longrightarrow
$$

E = O **27**; R^1 = ^{t}Bu; R^2 = H
E = S **28**; R^1 = Me, H; R^2 = H
E = Te **29**; R^1 = Mes, Me, Et, ^{i}Pr; R^2 = H, Cl, Me

$$
\begin{array}{c}
SF_4 \text{ or } SO_2F_2 \\
\mathbf{1} \quad + \quad CCl_4 \text{ or } 1,2\text{-}Cl_2C_2H_4 \text{ or } C_2Cl_6 \\
Br_2 \text{ or } 1,2\text{-}Br_2C_2H_4 \\
I_2
\end{array}
\longrightarrow
$$

X^1 = F **30**; R^1 = ^{i}Pr; R^2 = Me; X^2 = SF$_3$
X^1 = Cl **31**; R^1 = Mes, Me, Et, ^{i}Pr; R^2 =H, Cl; X^2 = Cl
X^1 = Br **32**; R^1 = Mes, ^{i}Pr; R^2 =H, Me; X^2 = Br
X^1 = I **33**; R^1 = Mes, Et; R^2 =H, Me; X^2 = I
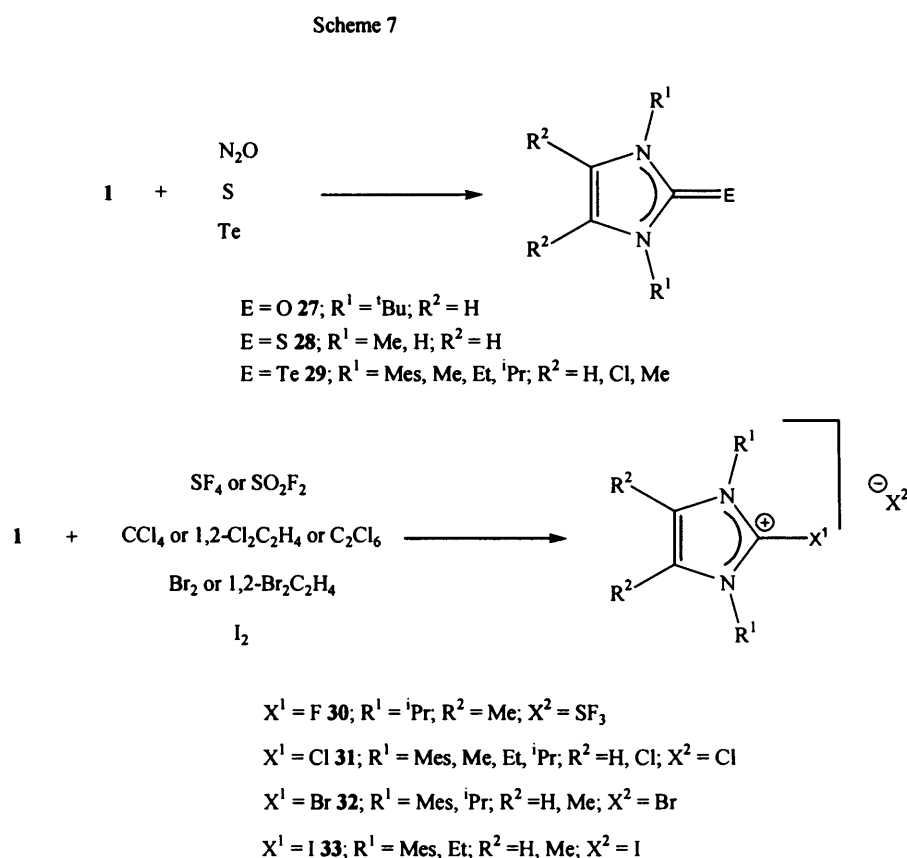
Group 17 NHC complexes are known and examples are shown in scheme 7. The halogenations of **1** proceed readily and give the complexes **30 - 33** in good yields.[2,20-24]

1.2 Main group-gallium(I) NHC analogue chemistry

The coordination chemistry of compounds containing a Lewis basic gallium(I) centre with a singlet lone pair has rapidly expanded. The most widely studied compounds in this respect are gallium diyls, :GaR, R = alkyl, aryl, substituted cyclopentadiene etc., which have been utilised in the formation of a fascinating array of transition metal complexes.[25] Similarly, the coordination chemistry of the neutral six membered heterocycle, [:Ga{[N(Ar)C(Me)]$_2$CH}], Ar = 2,6-Pr$^i_2$C$_6$H$_3$;[26] is starting to emerge and has been reviewed in chapter 1.[27] In recent years Jones and co-workers have been systematically studying the main group coordination chemistry of the anionic gallium(I) heterocycle, [Ga{N(Ar)C(H)}$_2$]$^-$, **34**, which is a valence isoelectronic analogue of the N-heterocyclic carbene (NHC) class of ligand. The results of their studies are summarised here.

<div align="center">Scheme 8</div>
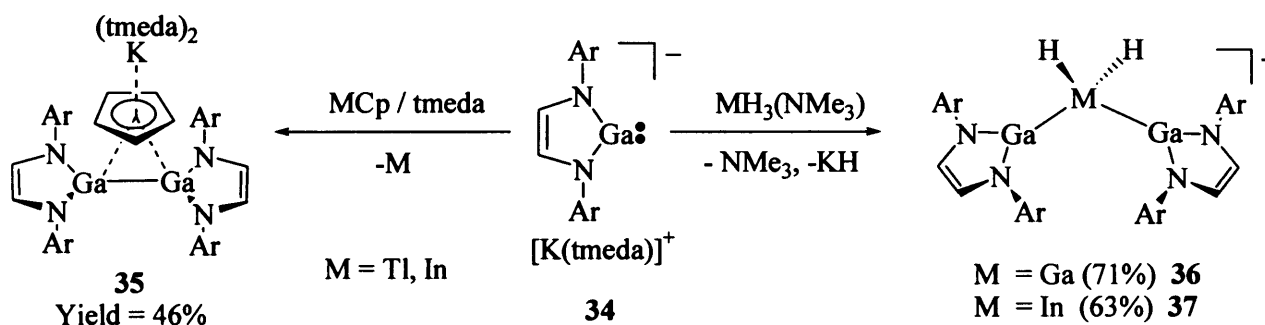
The treatment of **34** with main group cyclopentadienyl complexes, MCp, M = In, Tl, led to elemental metal deposition (In or Tl), and isolation of a cyclopentadienyl-bridged digallane complex **35**, in good yield. Presumably, the mechanism of this reaction involves an oxidative coupling of **34** to give the known digallane, [{Ga^{II}[N(Ar)C(H)]$_2$}$_2$], followed by complexation by half of the generated KCp to give the observed product.[28] This was the first structurally characterised π-interaction with a Ga(II) centre. To investigate the nature of this interaction Density Functional Theory (DFT) calculations were carried out on the model [{Ga[N(Me)C(H)]$_2$}$_2${μ-CpK(NH$_3$)$_4$}], the results of which indicated a 29 kJmol^{-1} binding energy of the KCp fragment to the digallane moiety and a donation of 0.209 electrons from the π-system of the Cp anion into the empty *p*-orbital of the gallium centres. As a consequence, a

partial pyramidalisation of the Ga centres relative to those in the free digallane was be expected. The solid state structure of **35** confirmed this hypothesis.[27]

The steric and electronic properties of bulky NHCs make them useful as ligands for the stabilisation of thermally labile fragments. For example, group 13 metal trihydrides, [InH$_3$\{C[N(Mes)C(H)]$_2$\}], Mes = mesityl, have been found to be stable, in the solid state, up to *ca.* 115°C.[29] To gauge the stabilising ability of **34**, its reactivity towards [MH$_3$(L)], M = Al, Ga or In, L = Lewis base; has been investigated. However, the reaction of **34** with [AlH$_3$(NMe$_3$)] led to significant metal deposition of Al and Ga, during warming of the reaction mixture, and formation of an ionic tetraamido gallium complex [Ga\{[N(Ar)C(H)]$_2$\}$_2$][K(DME)$_4$]. Interestingly, when **34** was reacted with tertiary amine adducts of GaH$_3$ and InH$_3$, thermally stable novel tri-metalic complexes, **36** and **37**, were formed in high yields (scheme 8).[30] These complexes possessed remarkable thermal stability with melting points of 128-131°C and 116-118°C respectively. It is thought that the mechanism of formation initially involved KH elimination to form neutral intermediates, [MH$_2$(Ga\{N(Ar)C(H)\}$_2$)], M = Ga or In; followed by coordination of a second equivalent of the gallium(I) heterocycle to give the observed products. Complex **37** contains the first example of a gallium-indium bond.

Investigations into the reactivity of **34** with group 15 and group 16 precursors has also been performed and is summarised in scheme 9. Two papers by Jones and co-workers have been published regarding the reactivity of **34** towards a range of group 15 precursors. In one of these publications, attempts were made to synthesise gallium-terminal pnictinidene complexes. However, a variety of novel heterocyclic gallium-group 15 complexes were instead isolated.[31] The reaction of **34** with *cyclo*-(PPh)$_5$, gave complex **38** in moderate yield. This complex was formed by the oxidative insertion of the gallium(I) centre into one of the P-P bonds of (PPh)$_5$, with concomitant loss of one PPh fragment. The reaction of **34** with azobenzene, PhN=NPh, yielded the ionic spirocyclic system, **39**, in good yield. The formation of this is thought to proceed by a [4+1] cyclo-addition of the Ga(I) centre with the azobenzene followed by a rapid 1,3 migration of the *ortho*-aryl proton to the N-centre bearing the metallated phenyl group. Some evidence for this mechanism was presented as the reaction of MesN=NMes, which is devoid of *ortho*-aryl protons, with **34** was found not to proceed. The other publication reports the reaction of **34** with 1,3,5-triphosphabenzene, P$_3$C$_3$Bu^t$_3$. This led to the isolation of a potassium salt of the 1,3-diphosphacyclopentadienyl anion, **40**. This product was formed via the abstraction of phosphorus from the triphosphabenzene. Compound **40** has also been synthesised via the

reduction of 1,3,5-triphosphabenzene with potassium metal, which highlights the strong reducing nature of **34**.[32]

Scheme 9

39   Yield = 57%

38

Yield = 31%

(PPh)$_5$

PhN=NPh

P$_3$C$_3$Bu$^t_3$

40

N$_2$O or
Et$_3$P=Te

34

(PhE)$_2$

E) = O (19%) **41**
E) = Te (68%) **42**

E = Se (48%) **43**
E = Te (57%) **44**
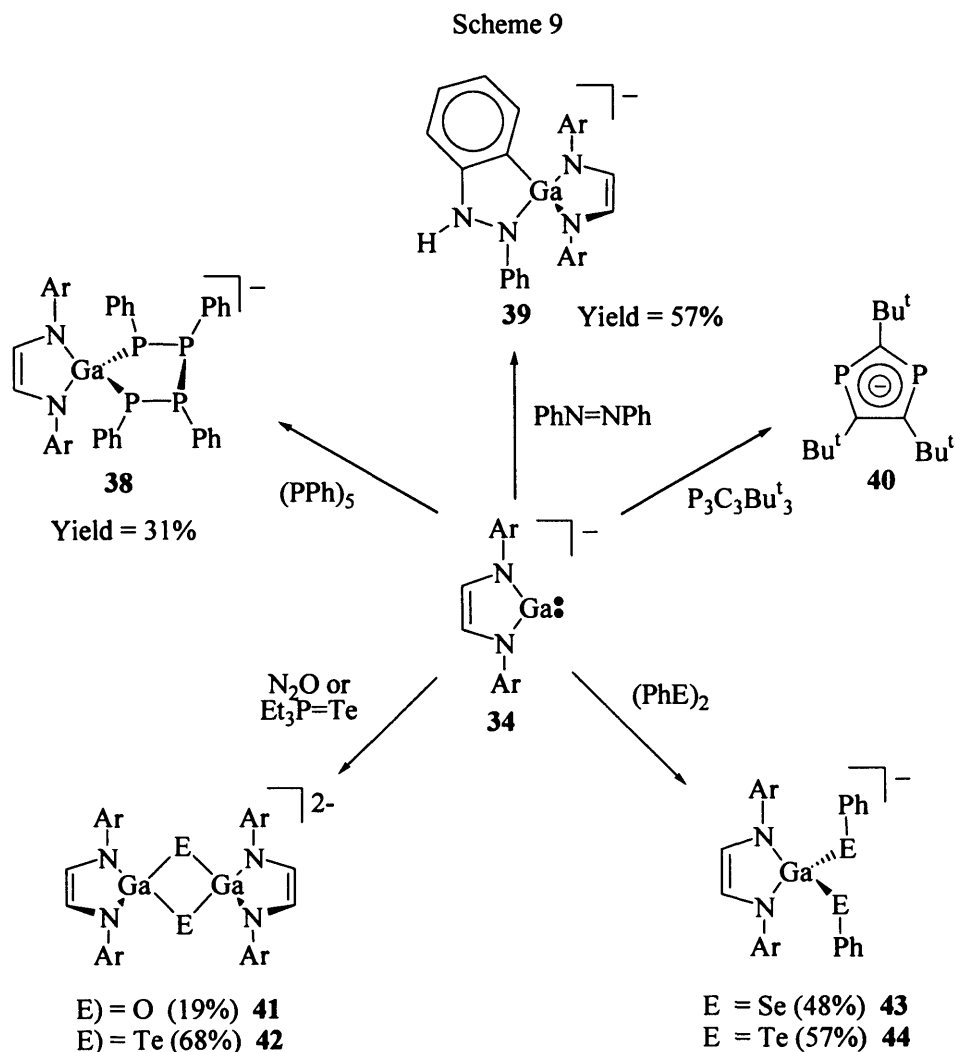
The reactivity of **34** towards group 16 elements and diorgano-dichalcogenides has been explored.[33] When complex **34** was treated with oxygen, decomposition occurred. However, this was prevented by using stoichiometric quantities of N$_2$O, resulting in the isolation of the dimeric, dianionic complex, **41**, in moderate yield. Complex **41** possesses Ga-O bond-lengths of 1.814(3) and 1.905(3) Å. The shorter bond-length is thought to be suggestive of some Ga-O double bond character. However, the heterocycle-Ga-O bond angle was found to be more acute (126.2°) than the ideal angle for Ga-O π-bonding (180°). Due to the electronegativity differences between Ga and O, bonding is presumed to be largely ionic in character. The Ga···Ga separation was found to be 2.608 Å, which is at the upper range for a Ga-Ga single bond. It was postulated that the shortness of this separation does not constitute an interaction, but could be due to ligation of the

71

Ga centres by electronegative N- and O-atoms, so increasing their relative ionic nature and decreasing the effective radii of the Ga-centres. The tellurium homologue of **41** was formed from the reaction of **34** with (Te)PEt$_3$, giving **42** in good yield. The Ga···Ga separation was found to be 3.408 Å, which is much larger than that in **41**. This is consistent with the larger covalent radii of Te (1.37 Å) compared to that of O (0.66 Å). Finally, complexes **43** and **44** were formed from the reaction of **34** with PhE-EPh, E = Se or Te. The resultant complexes were isolated in good yields. The mechanism of formation was thought to involve the Ga(I) centre of **34** oxidatively inserting into the E-E bond of the precursor to give the anionic complexes. The treatment of **44** with a stoichiometric amount of oxygen led to decomposition and subsequent re-formation of the ditelluride precursor, Ph$_2$Te$_2$.

2. Research Proposal

Considering the propensity of NHCs to form complexes with main group metal fragments,[2] it was felt that extending the s-block coordination chemistry of [:Ga{(N(Ar)C(H))$_2$}]⁻ to the alkaline earth metals warranted investigation. Further to this, NHCs have been previously shown to form adducts with some heavier group 14 NHC analogues (scheme 5).[13,14] As a result it seemed appropriate that the reactivity of [:Ga{(N(Ar)C(H))$_2$}]⁻ towards strong nucleophiles, in particular NHCs deserved investigation.

3. Results and discussion

3.1 Reactions of gallium(III) heterocycles with group 2 metals

Initially, the reactivity of [K(tmeda)][:Ga{[N(Ar)C(H)]$_2$}]⁻, **34**, towards anhydrous MI$_2$, M= Mg, Ca or Sr, was explored but in all cases intractable mixtures of products were obtained. More success was had by reducing the paramagnetic gallium(III) heterocycles, **45**, with a large excess of either magnesium or calcium metal in the presence of mercury. These reactions afforded the bis(gallyl)-magnesium and calcium complexes, **46 - 48**, in low to good yields (Scheme 10). It is apparent that the mechanisms of the reactions involve the step wise reduction

of **45**, firstly to the paramagnetic Ga(II) dimer, **49**,[31] and then the diamagnetic dimer, **50**.[34] The group 2 metal then oxidatively inserts into the Ga-Ga bond of **50** to give the observed products. Evidence for this proposal comes from the fact that both **49** and **50** can be isolated from these reactions if they are worked up in their early stages (after *ca.* 3 hours). In addition, when pure samples of **49** or **50** (R = H) were reacted with Mg or Ca metal in THF, complexes **46** and **47** were formed in similar yields to the reactions with **45** (R = H).

Surprisingly, when **45** (R = H) was treated with excesses of either strontium or barium metal in the presence of mercury, the reactions did not proceed past the doubly reduced product, **50** (R = H), even when they were carried out over extended periods (1 week), at elevated temperatures (*ca.* 50°C) and under ultrasonic conditions. This seems counter-intuitive as the heavier elements are more electropositive than the lighter metals. It is not known why these differences occur but they cannot be due to the inactivity of the surfaces of the metals as reduction of **45** (R = H) to **50** (R = H) occurs as readily as in the reactions that gave **46** and **47**.

Scheme 10

Ar = C$_6$H$_3$Pr$^i_2$-2,6

47 R = H
48 R = Me
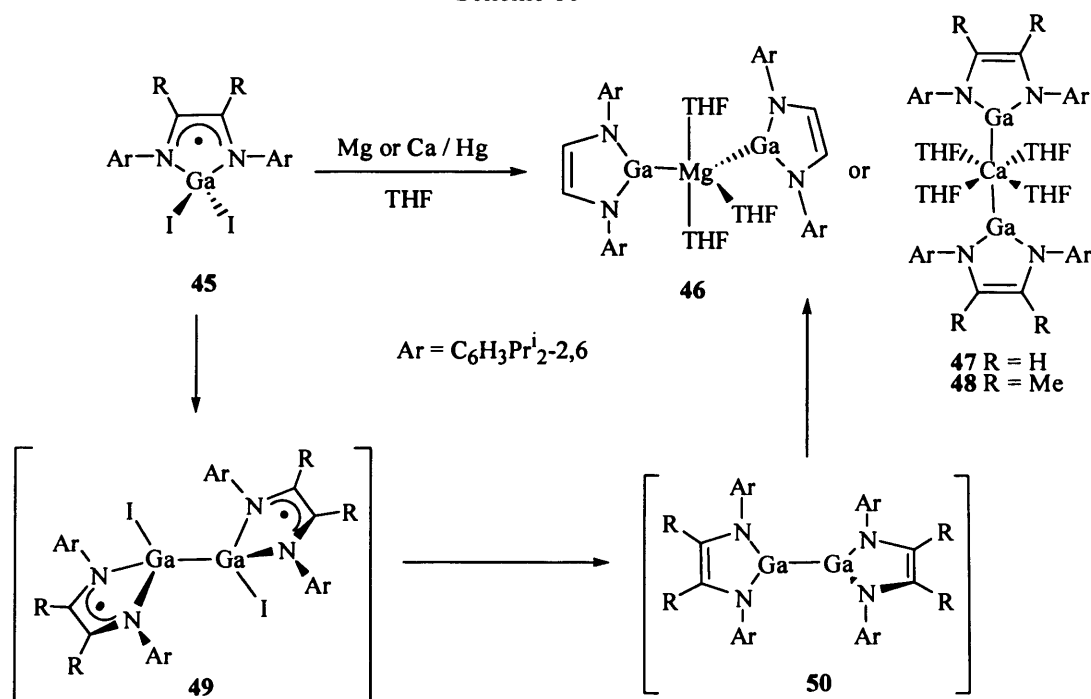
Compounds **46** - **48** are extremely oxygen and moisture sensitive but are thermally robust. Their ^{1}H and ^{13}C NMR spectroscopic data are consistent with their proposed formulations. An X-ray crystal structure of each complex was obtained and the molecular structures of **46** - **48** are depicted in Figures 1 - 3 respectively. The magnesium centre of **46** possesses a distorted trigonal bipyramidal geometry with both gallyl ligands in equatorial sites and O(2) and O(3) in axial positions. In contrast, the calcium centres of **47** and **48** have

octahedral coordination environments with the gallyl ligands *trans-* to each other. These differences presumably result from the greater covalent radius of the heavier metal. The geometries of the coordinated gallium heterocycles in each complex are similar to each other but possess Ga-N bond lengths and N-Ga-N angles that are intermediate between those of the free heterocycle (*ca.* 2.0 Å and 82° respectively) and the majority of previously reported complexes of this heterocycle (*ca.* 1.9 Å and 87° respectively).[27,28,30,31,33] This indicates significant ionic character for the metal-gallium bonds. Although there have been no previously reported examples of gallium-magnesium or gallium-calcium bonds, those in **46** and **47** are slightly longer than the sums of covalent radii for these element pairs (Ga-Mg 2.61 Å; Ga-Ca 2.91Å).[36]
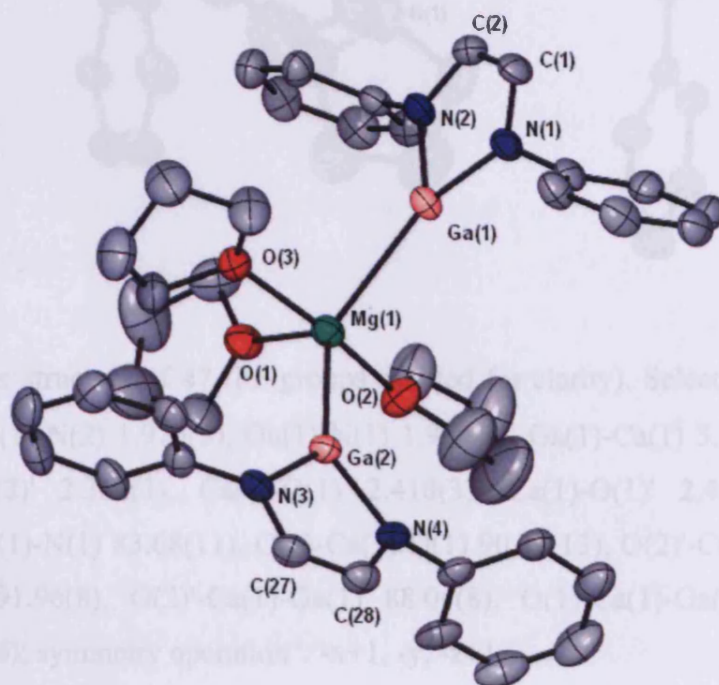

Figure 1. Molecular structure of **46** (Pr[i] groups omitted for clarity). Selected bond lengths (Å) and angles (°): Ga(1)-N(2) 1.918(3), Ga(1)-N(1) 1.921(3), Ga(1)-Mg(1) 2.7174(15), Ga(2)-N(4) 1.916(3), Ga(2)-N(3) 1.923(3), Ga(2)-Mg(1) 2.7269(14), Mg(1)-O(1) 2.056(3), Mg(1)-O(2) 2.135(3), Mg(1)-O(3) 2.158(3), N(2)-Ga(1)-N(1) 84.56(15), N(4)-Ga(2)-N(3) 84.09(15), O(1)-Mg(1)-O(2) 83.12(14), O(1)-Mg(1)-O(3) 83.66(13), O(2)-Mg(1)-O(3) 166.63(14), O(1)-Mg(1)-Ga(1) 116.91(10), O(2)-Mg(1)-Ga(1) 92.71(10), O(3)-Mg(1)-Ga(1) 91.51(9), O(1)-Mg(1)-Ga(2) 115.75(11), O(2)-Mg(1)-Ga(2) 94.25(9), O(3)-Mg(1)-Ga(2) 93.26(9), Ga(1)-Mg(1)-Ga(2) 127.32(6).
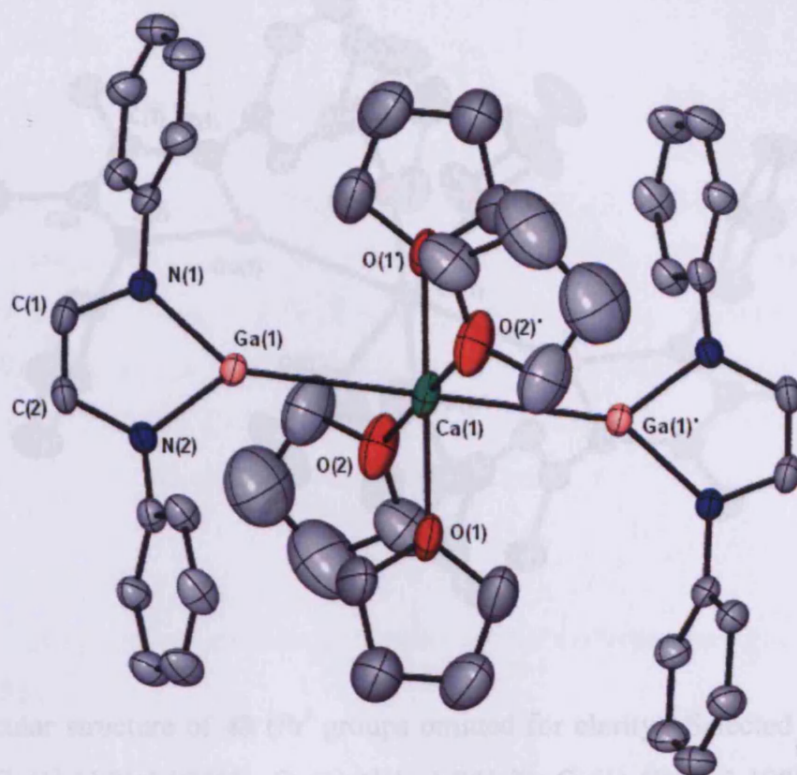
Figure 2. Molecular structure of **47** (Pr^i groups omitted for clarity). Selected bond lengths (Å) and angles (º): Ga(1)-N(2) 1.919(3), Ga(1)-N(1) 1.955(3), Ga(1)-Ca(1) 3.1587(6), Ca(1)-O(2) 2.352(3), Ca(1)-O(2)' 2.352(3), Ca(1)-O(1) 2.410(3), Ca(1)-O(1)' 2.410(3), Ca(1)-Ga(1)' 3.1587(6), N(2)-Ga(1)-N(1) 83.68(11), O(2)-Ca(1)-O(1) 90.37(13), O(2)'-Ca(1)-O(1) 89.63(13), O(2)-Ca(1)-Ga(1) 91.96(8), O(2)'-Ca(1)-Ga(1) 88.04(8), O(1)-Ca(1)-Ga(1) 92.03(6), O(1)'-Ca(1)-Ga(1) 87.97(6); symmetry operation ': -x+1, -y, -z+1.

and [Ca(OMe₂)₂{Ga(MeNCH₂)₂}₂] **52**. For sake of comparison, calculations were also performed on the strontium complex, [Sr(OMe₂)₂{Ga(MeNCH₂)₂}₂] **53**. The magnesium and calcium complexes converged with geometries similar to those from the experimental study (M-Ga distances: 51 2.715 Å mean; 52 3.232 Å mean; M-O distances: 51 axial 2.208 Å mean, equat. 2.046 Å; 52 2.441 Å mean), though the trigonal bipyramidal geometry of 51 is significantly more distorted than that of 46 (e.g. Ga-Mg-Ga 46 177.32(6)°; 51 135.81°). As with 52, the geometry of 53 converged with an octahedral geometry and mono-gallyl ligands [Sr-Ga 3.364 Å mean; Sr-O 2.591 Å mean]. Considering the electronegativity differences between the group 2 metals and gallium, it is not surprising that the M-Ga bonds in 51 – 53 have significant ionic character which increases from M = Mg – Sr (NBO charges: 51 Mg +1.49, Ga -0.33 mean; 52

Figure 3. Molecular structure of **48** (Pr^i groups omitted for clarity). Selected bond lengths (Å) and angles (°): Ga(1)-N(2) 1.926(3), Ga(1)-N(1) 1.941(3), Ga(1)-Ca(1) 3.1988(12), Ca(1)-O(2) 2.355(2), Ca(1)-O(1) 2.383(3), N(2)-Ga(1)-N(1) 82.47(13), N(2)-Ga(1)-Ca(1) 137.01(9), N(1)-Ga(1)-Ca(1) 140.40(9), O(2)-Ca(1)-O(1) 93.56(10), O(2)-Ca(1)-O(1)' 86.44(10), O(2)'-Ca(1)-Ga(1) 91.52(7), O(2)'-Ca(1)-Ga(1) 88.48(7), O(1)-Ca(1)-Ga(1) 86.64(8), O(1)'-Ca(1)-Ga(1) 93.36(8).

In order to further probe the nature of the metal bonds in **46 - 48**, DFT calculations were kindly carried out by Dr Jamie Platts on the model complexes, [Mg(OMe$_2$)$_3${Ga(MeNCH)$_2$}$_2$] **51** and [Ca(OMe$_2$)$_4${Ga(MeNCH)$_2$}$_2$] **52**. For sake of comparison, calculations were also performed on the strontium complex, [Sr(OMe$_2$)$_4${Ga(MeNCH)$_2$}$_2$] **53**. The magnesium and calcium complexes converged with geometries similar to those from the experimental study (M-Ga distances: **51** 2.715 Å mean; **52** 3.232 Å mean; M-O distances: **51** axial 2.208 Å mean, equat. 2.066 Å; **52** 2.443 Å mean), though the trigonal bipyramidal geometry of **51** is significantly more distorted than that of **46** (e.g. Ga-Mg-Ga: **46** 127.32(6)°; **51** 138.41°). As with **52**, the geometry of **53** converged with an octahedral geometry and *trans*-gallyl ligands (Sr-Ga 3.363 Å mean; Sr-O 2.591 Å mean). Considering the electronegativity differences between the group 2 metals and gallium, it is not surprising that the M-Ga bonds in **51 - 53** have significant ionic character which increases from M = Mg – Sr (NBO charges: **51** Mg +1.35, Ga -0.33 mean; **52**

Ca +1.54, Ga -0.27 mean; **53** Sr +1.58, Ga -0.23 mean; M-Ga Wiberg bond indices (mean): **51** 0.377, **52** 0.240, **53** 0.232).

Calculations were also carried out to assess the total energies of the neutral fragment combinations, $[M(OMe_2)_4\{Ga(MeNCH)_2\}_2]$ + OMe_2, M = Ca or Sr, relative to the ion combinations, $[M(OMe_2)_5\{Ga(MeNCH)_2\}]^+$ + $[Ga(MeNCH)_2]^-$. The rationale here was that these calculations would shed light on the relative strengths of the M-Ga bonds and thus might point to a thermodynamic reason why **50** (R = H) reacts with calcium to give **48** but is unreactive towards strontium. The energy differences between these combinations are, however, very similar (M = Ca +348.9 kJ/mol; Sr +358.4 kJ/mol) which perhaps indicates that the lack of reactivity of **50** towards strontium is due to kinetic reasons.

3.2 Reactions of an anionic gallium(I) N-heterocyclic carbene analogue with NHCs and imidazolium cations

The reactions of $[K(tmeda)][:Ga\{[N(Ar)C(H)]_2\}]^-$, **34**, with either a hindered or an unhindered NHC, $:C\{N(R)C(R')\}_2$, R=R'=Me or R = mesityl, R' = H, were attempted in toluene. In both cases only the starting materials were recovered from the reaction mixture. Despite earlier theoretical studies which suggested the heterocycle's gallium centre should be electrophilic,[37] this result is perhaps not surprising considering the overall anionic nature of the ring. Similarly, attempts to form complexes of $[:Ga\{[N(Ar)C(H)]_2\}]^-$ with a range of unhindered strong Lewis bases, e.g. quinuclidine, also met with failure.

Accordingly, attention was shifted to an examination of the reactivity of **34** towards imidazolium salts. Although a reaction was observed with $[HC\{N(Me)C(Me)\}_2]Cl$, only an intractable mixture of products was obtained. In contrast, the 1:1 reaction of the bulkier imidazolium salt, $[HC\{N(Mes)C(H)\}_2]Cl$, IMesHCl, Mes = $C_6H_2Me_3$-2,4,6, with **34** in THF led to a mixture of the gallium hydride complexes, **54** and **55**, in low (5%) and moderate yields (41%) respectively (Scheme 11). It seems likely that **54** was formed *via* the oxidative insertion of the Ga(I) centre of **34** into the imidazolium C-H bond. To the best of our knowledge this represents the first example of such a reaction, though a number of related C-H, C-C, Si-H and M-Cl activation reactions have been recently reported for transition metal complexes of the metal(I) diyls, $:M(C_5Me_5)$, M = Al or Ga.[25a] It is apparent that **55** arose from the partial

77

hydrolysis of **54** with 0.5 equivalents of water which preferentially attacks the coordinated IMes ligand of **54** over its hydride ligand. A recent paper[38] has shown that the earlier patent preparation of IMesHCl,[39] can lead to a product contaminated with significant amounts of its monohydrate, IMesHCl.H$_2$O, which is difficult to dry due to strong Cl···HO hydrogen bonding in the crystal lattice. When IMesHCl was recrystallised from dichloromethane and dried *in vacuo* for 24 hrs at 130°C it was sufficiently water free to repeat the reaction with **34**. This led to a moderate isolated yield (44%) of **54** with no evidence for the concomitant formation of **55**. When a pure sample of **54** was treated with trace amounts of water in THF, the characteristic Ga-H stretching absorption of **55** (*vide infra*) was observed in the infrared spectrum of the product mixture.

Scheme 11
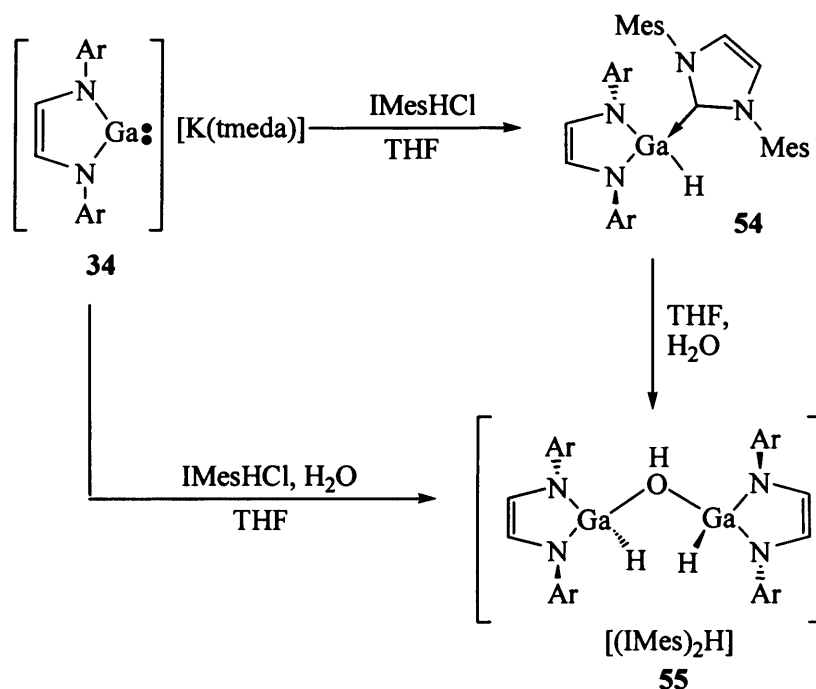
The molecular structure of **54** and the structure of the anionic component of **55** are depicted in Figures 4 and 5 respectively. In both, the hydride ligands were located from difference maps and refined isotropically, thus confirming that the coordination geometries of all gallium centres are distorted tetrahedral. In monomeric **54**, the carbene-Ga distance is similar to those in other NHC-gallium hydride complexes and the geometry of the GaN$_2$C$_2$ ring is suggestive of the presence of a localised C-C double bond.[40] Of note is the fact that one of the Ar substituents of that ring (that attached to N(1)) is bent out of the least squares plane of the

78

heterocycle by 34.8°. This most likely arises from steric buttressing between it and one of the mesityl substituents of the NHC ligand. As far as we are aware, the only gallium heterocycle related to that in **54** can be found in the complex, $[HGa\{[N(Bu^t)C(H)]_2\}]_2$, which is dimeric through N-Ga interactions.[41] The anion of **55** contains a bent Ga-O(H)-Ga moiety with Ga-O bond lengths that are in the normal range for such fragments, though with a significant difference between the two.[42] The cation of **55** has been previously structurally characterised and shows the imidazolium proton to bridge the two IMes carbene centres.[3] The sterically protected nature of this proton may provide an explanation for why it is stable to reaction with either Ga-H fragment.
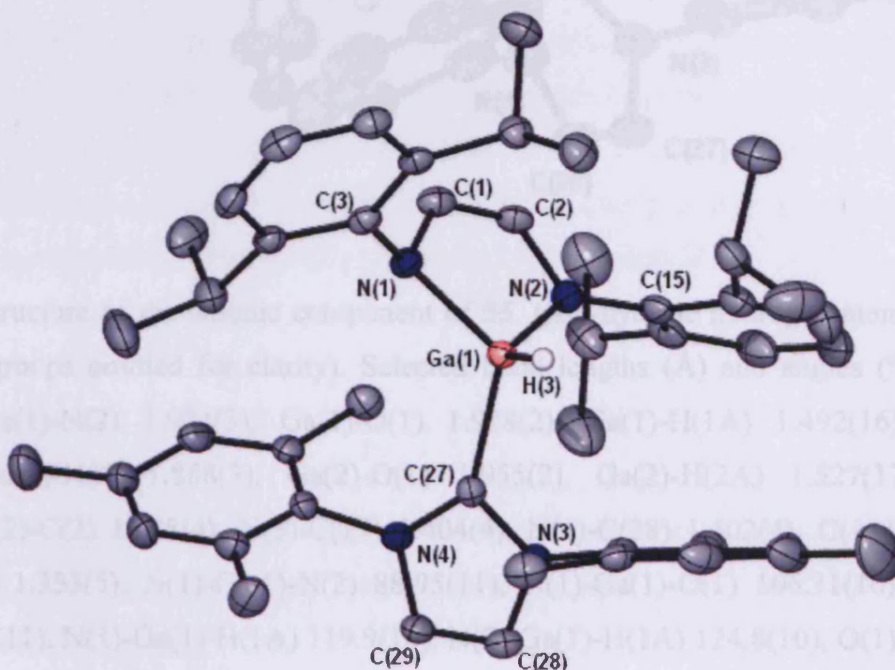
Figure 4. Molecular structure of **54** (non-hydride hydrogen atoms omitted for clarity). Selected bond lengths (Å) and angles (°): Ga(1)-N(1) 1.923(3), Ga(1)-N(2) 1.924(3), Ga(1)-C(27) 2.095(3), Ga(1)-H(3) 1.498(16), N(1)-C(1) 1.418(4), N(2)-C(2) 1.405(4), N(3)-C(27) 1.358(4), N(3)-C(28) 1.379(4), N(4)-C(27) 1.369(4), N(4)-C(29) 1.378(4), C(1)-C(2) 1.337(4), C(28)-C(29) 1.342(4), N(1)-Ga(1)-N(2) 89.40(11), N(1)-Ga(1)-H(3) 112.8(10), N(2)-Ga(1)-H(3) 121.2(10), C(27)-Ga(1)-H(3) 104.9(10), N(3)-C(27)-N(4) 103.3(2).
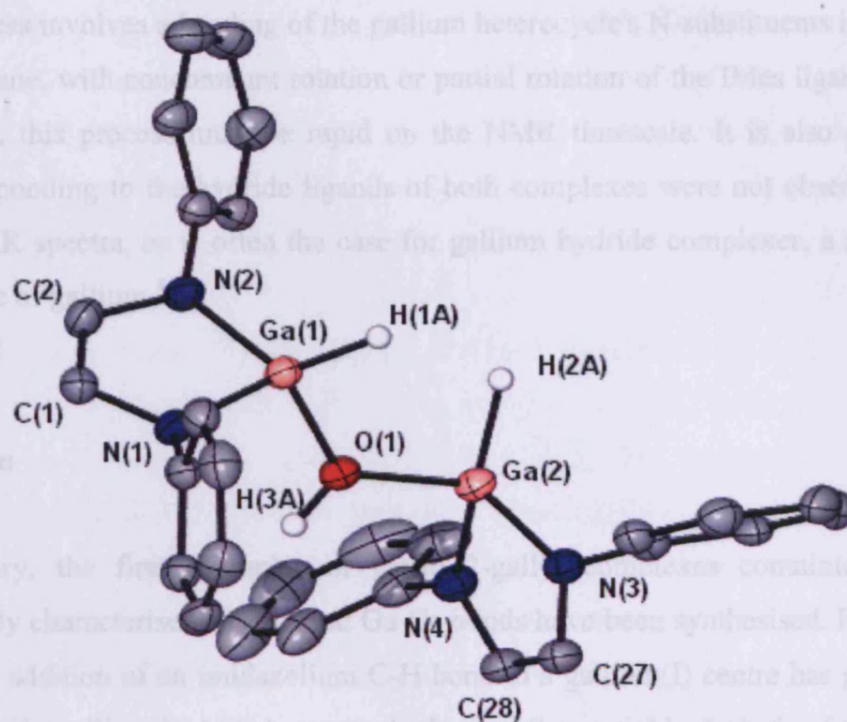
Figure 5. Structure of the anionic component of **55**. (non-hydride hydrogen atoms omitted for clarity, Pr^i groups omitted for clarity). Selected bond lengths (Å) and angles (°): Ga(1)-N(1) 1.884(3), Ga(1)-N(2) 1.904(3), Ga(1)-O(1) 1.928(2), Ga(1)-H(1A) 1.492(16), Ga(2)-N(3) 1.887(3), Ga(2)-N(4) 1.888(3), Ga(2)-O(1) 1.955(2), Ga(2)-H(2A) 1.527(17), N(1)-C(1) 1.400(4), N(2)-C(2) 1.408(4), N(3)-C(27) 1.404(4), N(4)-C(28) 1.402(4), C(1)-C(2) 1.347(4), C(27)-C(28) 1.333(5), N(1)-Ga(1)-N(2) 88.95(11), N(1)-Ga(1)-O(1) 106.31(10), N(2)-Ga(1)-O(1) 114.21(11), N(1)-Ga(1)-H(1A) 119.9(10), N(2)-Ga(1)-H(1A) 124.8(10), O(1)-Ga(1)-H(1A) 102.0(10), N(3)-Ga(2)-N(4) 88.49(11), N(3)-Ga(2)-O(1) 110.67(11), N(4)-Ga(2)-O(1) 103.20(11), N(3)-Ga(2)-H(2A) 123.8(11), N(4)-Ga(2)-H(2A) 128.3(11), O(1)-Ga(2)-H(2A) 100.9(11), Ga(1)-O(1)-Ga(2) 130.32(12).

The spectroscopic data for **54** and **55** are consistent with their formulations. Of most note are their infra-red spectra which exhibit strong, broad Ga-H stretching absorptions (**54**: 1854 cm⁻¹; **55**: 1902 cm⁻¹) in the normal range.[43] In addition, a broad O-H stretching absorption (3510 cm⁻¹) was observed in the spectrum of **55**. The ¹H and ¹³C{¹H} NMR spectra of **54** are more symmetrical than might be expected if its solid state structure is retained in solution and are suggestive of a fluxional process occurring. Although cooling solutions of **55** to the point of

precipitation in D$_8$-toluene (*ca.* –30°C) led to no visible change in the spectrum, it is likely that the fluxional process involves a bending of the gallium heterocycle's N-substituents in and out of the heterocycle plane, with concomitant rotation or partial rotation of the IMes ligand about the Ga-C bond. If so, this process must be rapid on the NMR timescale. It is also of note that resonances corresponding to the hydride ligands of both complexes were not observed in their respective ^{1}H NMR spectra, as is often the case for gallium hydride complexes, a result of the quadrupolar nature of gallium.[43]

4. Conclusion

In summary, the first examples of group 2-gallyl complexes containing the first crystallographically characterised Ga-Mg and Ga-Ca bonds have been synthesised. Furthermore, the first oxidative addition of an imidazolium C-H bond to a gallium(I) centre has given rise to an NHC complex of a gallium hydride heterocycle. In turn, the partial hydrolysis of this complex has afforded an unusual hydroxide bridged gallium hydride complex.

5. Experimental

General experimental procedures can be found in appendix 1. Compound 34,[44] IMes[1] and IMesHCl[38,39] were synthesised by literature methods. All other chemicals were obtained commercially and used as received.

Preparation of [Mg{Ga[(N(Ar)C(H))$_2$]}$_2$(THF)$_3$] 46. To a mixture of Mg metal (1.00 g, 42 mmol) and Hg (3 drops) in THF (20 cm^3) was added a solution of [I$_2$Ga{(N(Ar)C(H))$_2$}] (2.00 g, 2.87 mmol) in THF (40 cm^3) at –78 °C. The resultant suspension was warmed to room temperature and stirred for four days. Upon filtration and removal of volatiles from the filtrate *in vacuo*, the residue was extracted with hexane (30 cm^3). The extract was then filtered and the filtrate cooled to –30 °C overnight yielding orange crystals of 46 (0.41 g, 25 %). Mp = 109 – 113 °C; ^{1}H NMR (400MHz, C$_6$D$_6$, 298K): δ = 0.87 (d, $^3J_{HH}$ = 6.9 Hz, 24H, CHC*H*$_3$), 1.05 (d, $^3J_{HH}$ =

6.9 Hz, 24H, CHCH_3), 1.50 (br, 12H, THF), 3.11 (br, 12H, THF), 3.46 (sept, $^3J_{HH}$ = 6.9 Hz, 8H, CHCH$_3$), 6.16 (s, 4H, NCH), 6.76 – 6.89 (m, 12H, ArH); ^{13}C NMR (75MHz, C$_6$D$_6$, 298K): δ = 24.9 (THF), 25.1 (CHCH_3), 25.5 (CHCH_3), 27.9 (CHCH$_3$), 68.9 (THF), 122.5 (N=CH), 122.6,124.1, 145.3, 147.8 (ArC); m/z (EI): 378 [{(ArNCH)$_2$}H$^+$, 32%], 448 [Ga{(ArNCH)$_2$}H$^+$, 42%];

Prepration of [Ca{Ga[(N(Ar)C(H))$_2$]}$_2$(THF)$_4$] 47. To a mixture of Ca metal (2.00 g, 50 mmol) and Hg (3 drops) in THF (10 cm^3) at –78 °C was added a solution of [I$_2$Ga{(N(Ar)C(H))$_2$·}] (2.00 g, 2.87 mmol) in THF (30 cm^3). The resultant suspension was warmed to room temperature and stirred for four days. Upon filtration and removal of volatiles from the filtrate *in vacuo*, the residue was washed with hexane (30 cm^3) and then extracted with ether (100 cm^3). Filtration, concentration to *ca.* 50 cm^3 and cooling to –30 °C overnight yielded yellow crystals of **47** (1.00 g, 57%). Mp = 225 – 230 °C; ^{1}H NMR (400MHz, D$_8$THF, 298K): δ = 1.01 (d, $^3J_{HH}$ = 6.7 Hz, 24H, CHCH_3), 1.08 (d, $^3J_{HH}$ = 6.7 Hz, 24H, CHCH_3), 1.66 (br, 16H, THF), 2.86 (sept, $^3J_{HH}$ = 6.7 Hz, 8H, CHCH$_3$), 3.50 (br, 16H, THF), 5.78 (s, 4H, NCH), 6.60 – 7.13 (m, 12H, ArH); ^{13}C NMR (75MHz, D$_8$THF , 298K): δ = 23.7 (THF), 24.6 (CHCH_3), 25.5 (CHCH_3), 28.0 (CHCH$_3$), 65.4 (THF), 122.6 (NC$_2$H$_2$), 122.8, 123.3, 144.7, 146.2 (ArC); m/z (EI): 448 [Ga{(ArNCH)$_2$}H$^+$, 60%], 378 [{(ArNCH)$_2$}H$^+$, 10%];

Preparation of [Ca{Ga[(N(Ar)C(CH$_3$))$_2$]}$_2$(THF)$_4$] 48: To a mixture of Ca metal (2.00 g, 50 mmol) and Hg (3 drops) in THF (10 cm^3) at –78 °C was added a solution of [I$_2$Ga{(N(Ar)C(CH$_3$))$_2$·}] (2.00 g, 2.87 mmol) in THF (30 cm^3). The resultant suspension was warmed to room temperature and stirred for four days. Upon filtration and removal of volatiles from the filtrate *in vacuo*, the residue was washed with hexane (30 cm^3) and then extracted with toluene (100 cm^3). Filtration, concentration to *ca.* 50 cm^3 and cooling to –30 °C overnight yielded yellow crystals of **48** (0.18 g, 9 %). Mp = 108 - 127 °C; ^{1}H NMR (400MHz, C$_6$D$_6$, 298K): δ = 0.95 (d, $^3J_{HH}$ = 6.5 Hz, 24H, CHCH_3), 1.08 (d, $^3J_{HH}$ = 6.5 Hz, 24H, CHCH_3), 1.85 (br, 16H, THF), 2.01 (s, 12H, NCCH_3), 3.22 (br, 16H, THF), 3.45 (sept, $^3J_{HH}$ = 6.5 Hz, 8H, CHCH$_3$), 6.66 – 6.86 (m, 12H, ArH); ^{13}C NMR (75MHz, C$_6$D$_6$, 298K): δ = 21.2 (N=CCH_3), 23.7 (THF), 25.3 (CHCH_3), 25.7 (CHCH_3), 27.6 (CHCH$_3$), 68.6 (THF), 122.17, 123.20, 146.1, 149.4 (ArC),

N=C not observed: m/z (EI): 475 [Ga{(ArNCMe)$_2$}H$^+$, 68%], 810 [(THF)$_4$CaGa{(ArNCMe)$_2$}$^+$, 35%].

Preparation of [HGa{[N(Ar)C(H)]$_2$}(IMes)] 54. [K(tmeda)][:Ga{[N(Ar)C(H)]$_2$}] (0.15 g, 0.25 mmol) in THF (10 cm^3) was added over 5 mins to a suspension of rigorously dried IMesHCl (0.08 g, 0.25 mmol) in THF (30 cm^3) at −78 °C. The mixture was warmed to room temperature overnight to yield a red solution. Volatiles were removed *in vacuo* and the residue extracted with hexane (20 cm^3). Filtration, concentration and cooling to −30 °C overnight yielded red crystals of **54** (0.08 g, 44 %). Mp = 95 − 100 °C; ^{1}H NMR (400MHz, C$_6$D$_6$, 298K): δ 0.87 (d, $^3J_{HH}$ = 5 Hz, 12H, CHC*H*$_3$), 0.94 (d, $^3J_{HH}$ = 5 Hz, 12H, CHC*H*$_3$), 1.51 (s, 12H, *o*-CH$_3$), 1.83 (s, 6H, *p*-CH$_3$), 3.29 (sept, $^3J_{HH}$ = 5 Hz, 4H, C*H*CH$_3$), 5.39 (s, 2H, GaN$_2$C$_2$*H*$_2$), 5.58 (s, 2H, CN$_2$C$_2$*H*$_2$), 6.36 − 6.91 (m, 10H, ArH); ^{13}C NMR (75MHz, C$_6$D$_6$, 298K): δ 17.5 (*o*-CH$_3$), 20.7 (*p*-CH$_3$), 24.8 (CHCH$_3$), 25.7 (CHCH$_3$), 31.7 (*C*HCH$_3$), 122.5 (CN$_2$*C$_2$*H$_2$), 122.8 (GaN$_2$*C$_2$*H$_2$), 123.6, 124.0, 129.6, 134.6, 135.0, 139.2, 146.9, 149.7 (ArC), 171.8 (NCN); IR v/cm^{-1} (Nujol): 1854(s, Ga-H), 1251(s), 1091(s), 1033(s), 804(s); m/z (EI): 303 [IMesH$^+$, 100%], 378 [(ArNCH)$_2$H$^+$, 35%], 447 [Ga(ArNCH)$_2$, 16%], 750 [M$^+$, 3%]; Accurate Mass MS (EI$^+$) Calc. For M$^+$: C$_{47}$H$_{61}$N$_4$Ga: 750.4147; Found: 750.4141.

Preparation of [{HGa[N(Ar)C(H)]$_2$}$_2$OH][(IMes)$_2$H] 55. [K(tmeda)][:Ga{[N(Ar)C(H)]$_2$}] (0.25 g, 0.42 mmol) in THF (20 cm^3) was added to a suspension of IMesHCl (containing water of crystallisation) (0.14 g, 0.41 mmol) in THF (20 cm^3) at −78 °C over 5 mins. The mixture was warmed to room temperature overnight to yield a brown / red solution. Volatiles were removed *in vacuo* and the residue washed with hexane (20 cm^3) and extracted with diethyl ether (30 cm^3). Filtration, concentration and cooling to −30 °C overnight yielded yellow crystals of **55** (0.13 g, 41 %). Mp = 118 − 126 °C; ^{1}H NMR (400MHz, D$_8$-THF, 298K): δ 0.93 (d, $^3J_{HH}$ = 6 Hz, 24H, CHC*H*$_3$), 1.12 (d, $^3J_{HH}$ = 6 Hz, 24H, CHC*H*$_3$), 1.85 (s, 24H, *o*-CH$_3$), 2.23 (s, 12H, *p*-CH$_3$), 3.40 (sept, $^3J_{HH}$ = 6 Hz, 8H, C*H*CH$_3$), 4.80 (br s, 1H, OH), 5.55 (s, 2H, GaN$_2$C$_2$*H*$_2$), 6.89 - 7.60 (m, 24H, ArH and CN$_2$C$_2$*H*$_2$), 10.81 (br s, 1H, IMesH$^+$); ^{13}C NMR (125MHz, D$_8$-THF, 298K): δ 18.4 (*o*-CH$_3$), 20.5 (*p*-CH$_3$), 22.9, 23.8 (CHCH$_3$), 28.01 (*C*HCH$_3$), 118.5 (GaN$_2$*C$_2$*H$_2$), 122.2 (CN$_2$*C$_2$*H$_2$), 125.9, 126.7, 132.5, 138.2, 140.8 , 142.0, 145.4, 146.8 (ArC), 172.8 (NCN); IR

v/cm^{-1} (Nujol): 3510(br, OH), 1902(s, Ga-H) 1258(s), 1101(s), 927(s), 761(s); m/z (-ve CI): 462 [H(OH)Ga(ArNCH)$_2$, 8%], 907 [{HGa(ArNCH)$_2$}$_2$OH, 15%]; Accurate Mass MS (CI) Calc. For {HGa(ArNCH)$_2$}$_2$OH: C$_{52}$H$_{73}$ON$_4$Ga$_2$: 907.4301; Found: 907.4333.

6. References

1.   A. J. Arduengo, R. L. Harlow, M. Kline, *J. Am. Chem. Soc.,* 1991, **113**, 361.

2.   (a) N. Kuhn, A. Al-Sheikh, *Coord. Chem. Revs.,* 2005, **249**, 829, and references therein. (b) D. Bourissou, O. Guerret, F. P. Gabbaï, G. Bertrand, *Chem. Rev.,* 2000, **100**, 39.

3.   A. J. Arduengo, M. Tamm, J. C. Calabrese, F. Davidson, W. J. Marshall, *Chem. Lett.,* 1999, 1021.

4.   R. W. Alder, M. E. Blake, C. Bortolotti, S. Bufali, C. P. Butts, E. Linehan, J. M. Oliva, A. G. Orpen, M. J. Quayle, *Chem. Commun.,* 1999, 241.

5.   W. A. Herrmann, O. Runte, G. Artus, *J. Organomet. Chem.,* 1995, **501**, C1.

6.   A.J. Arduengo, F. Davidson, R. Krafczyk, W. J. Marshall, M. Tamm, *Organometallics,* 1998, **17**, 3375.

7.   N. Kuhn, G. Henkel, T. Kratz, J. Kreutzberg, R. Boese, A. H. Maulitz, *Chem. Ber.,* 1993, **126**, 2041.

8.   T. Ramnial, H. Jong, I. D. McKenzie, M. Jennings, J. A. C. Clyburne, *Chem. Commun.,* 2003, 1722.

9.   L. Weber, E. Dobbert, H. Stammler, B. Neumann, R. Boese, D. Bläser, *Chem. Ber.,* 1997, **130**, 705.

10. (a) C. Jones, *Chem. Commun.,* 2001, 2293, (b) M. L. Cole. C. Jones, M. Kloth, *Inorg. Chem.,* 2005, **44**, 4909.

11. C. D. Abernethy, M. L. Cole, C. Jones, *Organometallics,* 2000, **19**, 4852.

12. M. L. Cole, A. J. Davies, C. Jones, *J. Chem. Soc., Dalton Trans.,* 2001, 2451.

13. W. M. Boesveld, B. Gehrhus, P. B. Hitchcock, M. F. Lappert, P von R. Schleyer, *Chem. Commun.,* 1999, 755.

14. B. Gehrhus, P. B. Hitchcock, M. F. Lappert, *J. Chem. Soc., Dalton Trans.,* 2000, 3094.

15. J. M. Hopkins, M. Bowdridge, K. N. Robertson, T. S. Cameron, H. A. Jenkins, J. A. C. Clyburne, *J. Org. Chem.,* 2001, **66**, 5713.

16. A. J. Arduengo, R. Krafczyk, W. J. Marshall, R. Schmutzler, *J. Am. Chem. Soc.*, 1997, **119**, 3381.

17. A. J. Arduengo, F. Davidson, R. Krafczyk, W. J. Marshall, R. Schmutzler, *Monatsh.*, 2000, **131**, 251.

18. M. K. Denk, J. M. Rodezno, S. Gupta, A. J. Lough, *J. Organomet. Chem.*, 2001, **617-618**, 242.

19. A. J. Arduengo, E. M. Burgess, *J. Am. Chem. Soc.*, 1977, **99**, 2376.

20. A. J. Arduengo, F. Davidson, H. V. R. Dias, J. R. Goerlich, D. Khasnis, W. J. Marshall, T. K. Prakasha, *J. Am. Chem. Soc.*, 1997, **119**, 12742.

21. N. Kuhn, A. Abu-Rayyan, M. Göhner, M. Steimann, *Z. Anorg, Allg, Chem.*, 2002, **628**, 1721.

22. N. Kuhn, A. Abu-Rayyan, K. Eichele, S. Schwarz, M. Steimann, *Inorg. Chem. Acta.*, 2004, **357**, 1799.

23. N. Kuhn, T. Kratz, G. Henkel, *J. Chem. Soc., Chem. Commun.*, 1993, 1778.

24. A. J. Arduengo, M. Tamm, J. C. Calabrese, *J. Am. Chem. Soc.*, 1994, **116**, 3625.

25. (a) G. Gemel, T. Steinke, M. Cokoja, A. Kempter, R. A. Fischer, *Eur. J. Inorg. Chem.*, 2004, 4161. (b) A. H. Cowley, *Chem. Commun.*, 2004, 2369 and references therein.

26. N. J. Hardman, B. E. Eichler, P. P. Power, *Chem. Commun.*, 2000, 1991.

27. R. J. Baker, C. Jones, *Coord. Chem. Reves.*, 2005, **249**, 1857, and references therein.

28. R. J. Baker, C. Jones, M. Kloth, J. A. Platts, *Organometallics*, 2004, **23**, 4811.

29. C. Jones, *Chem. Commun.*, 2001, 2293.

30. R. J. Baker, C. Jones, M. Kloth, J. A. Platts, *Angew. Chem. Int. Ed.*, 2003, **42**, 2660.

31. R. J. Baker, C. Jones, D. P. Mills, D. M. Murphy, E. Hey-Hawkins, R. Wolf, *Dalton Trans.*, 2006, 64.

32. C. Jones, M. Waugh, *Dalton Trans.*, 2004, 1971.

33. R. J. Baker, C. Jones, M. Kloth, *Dalton Trans.*, 2005, 2106.

34. T. Pott, P. Jutzi, W. W. Schoeller, A. Stammler, H. Stammler, *Organometallics*, 2001, **20**, 5492.

35. (a) R. J. Baker, C. Jones, D. M. Murphy, *Chem. Commun.*, 2005, 1339; (b) R. J. Baker, C. Jones, J. A. Platts, *Dalton Trans.*, 2003, 3673; (c). R. J. Baker, C. Jones, J. A. Platts, *J. Am. Chem. Soc.*, 2003, **125**, 10534.

36. J. Emsley, "The Elements" 2nd edition, Clarendon Press, Oxford, 1995.

37.   A. Sunderman, M. Reiher, W. W. Schoeller, *Eur. J, Inorg. Chem.*, 1998, 305.

38.   M. L. Cole, P. C. Junk, *Cryst. Eng. Comm.*, 2004, **6**, 173.

39.   A. J. Arduengo, US Patent, 1991, 5 077 414.

40.   J. D. Gorden, C. L. B. Macdonald, A. H. Cowley, *J. Organomet. Chem.*, 2002, **487**, 643, and references therein.

41.   E. S. Schmidt, A. Jockisch, H. Schmidbaur, *J. Chem. Soc., Dalton Trans.*, 2000, 1039.

42.   As determined by a survey of the Cambridge Crystallographic Database, February, 2006.

43.   (a) S. Aldridge, A. J. Downs, *Chem. Rev.*, 2001, **101**, 3305; C. Jones, G. A. Koutsantonis, C. L. Raston, *Polyhedron*, 1993, **12**, 1829, and references therein.

44.   R. J. Baker, R. D. Farley, C. Jones, M. Kloth, D. M. Murphy, *J. Chem. Soc., Dalton Trans.*, 2002, 3844.

Chapter 4

Reactions of a Paramagnetic Gallium(II) Dimer Towards a Series of Pnictide Complexes

1. Introduction

1.1 Gallium(III)-pnictides

The chemistry of group 13 metal(III) pnictides has been extensively investigated and is well developed.[1] In particular, the synthesis of gallium(III) pnictides and their subsequent use as materials precursors has received much attention.[1,2] Due to the extensive nature of this field of research only a brief summary of this area will be presented here.

Gallium in the +III oxidation state has predominantly featured in the synthesis of gallium-pnictide compounds. For example, the reactions shown in scheme 1 all make use of gallium(III) starting materials. The synthesis of gallium(III) pnictide complexes has been achieved via different routes. For instance, complex 1 was prepared by RX, R = silyl or alkyl; X = Br or Cl; elimination whereas complex 2 has been accessed via salt metathesis.[2,3] It is worthy of note that the oxidation state of the gallium centres remains unchanged from the starting materials to the products.[3] It is apparent that a common feature of these gallium pnictide materials is their aggregation into dimeric forms.[3] Gallium(III) complexes with mixed pnictide ligands have also been synthesised. For example, complex 3 was the first molecular compound containing a P(μ-Ga)$_2$Sb core (scheme 1).[4]

Scheme 1

X = Cl, R = SiMe$_3$, SiMe$_2$Ph, Bu^t, SiMe$_3$;
X = Br, R = SiMe$_3$;

X = Cl   E = P or As
R = Me or ^{n}Bu

$$Et_2GaCl \quad + \quad P(SiMe_3)_3 \quad + \quad Sb(SiMe_3)_3 \xrightarrow{-SiMe_3Cl}$$
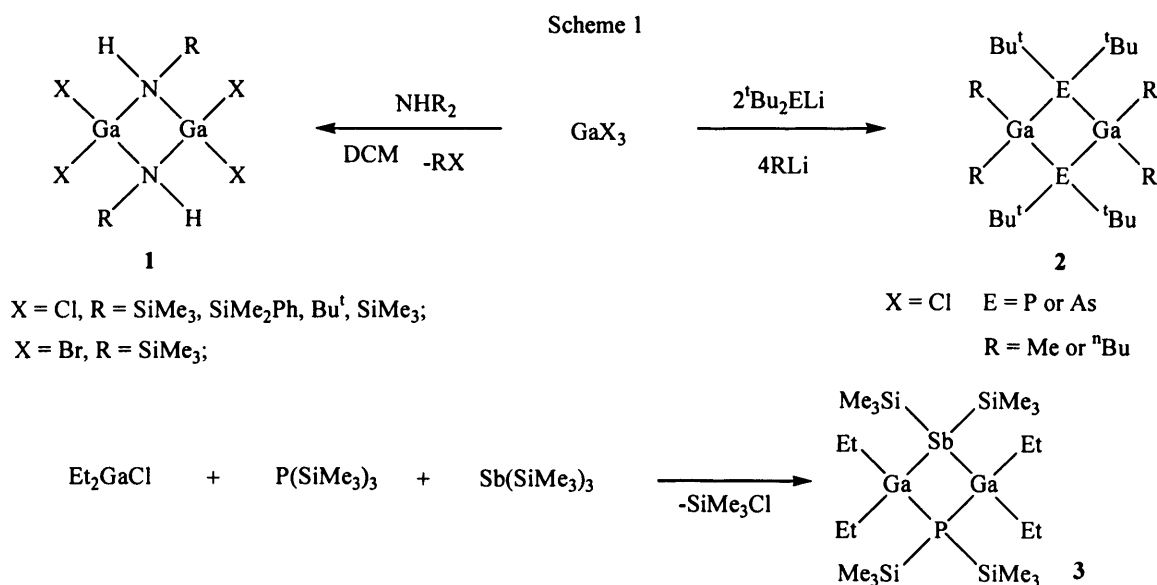
Group 13 pnictides have wide ranging uses within the materials and electronics industries.[5] Their importance arises from their physical properties where compounds of Al, Ga and In with N, P, As and Sb based ligands have been described as possessing properties intermediate between those of ionic and covalent materials.[5] An important aspect of the group 13 metal(III) pnictide materials has been highlighted in their use as precursors to binary group 13-pnictide materials.[3,6] In this field, the bis(silyl)pnictide ligands, [E(SiMe$_3$)$_2$]$^-$, E = N, P, As or Sb, are especially important, as their gallium complexes have been widely used as precursors to the binary gallium pnictides, GaE.[1,2] Such compounds are highly sort after due to their electronic and optical properties. In particular, binary group 13-pnictide compounds have found uses in type III-V semiconductors which have been utilised in the production of light emitting diodes (LEDs).[7,8] These materials have commonly been accessed through the following methods (a) the thermal decomposition of ammonia adducts i.e. AlCl$_3$.NH$_3$ or GaX$_3$.NH$_3$, X = Cl, Br or I; which at 900°C leads to the deposition of AlN or GaN, (b) the reaction of Ga or Ga$_2$O$_3$ with ammonia gas at 600 – 1000°C which gave GaN and (c) pyrolysis under vacuum at 700°C of (NH$_4$)$_3$[MF$_6$] which gave MN, M = Ga or In.[3,6] The importance of these materials is very apparent[7] and research into new gallium-pnictide material precursors is ongoing. For example, it has been demonstrated that the thermolysis of complex 2 led to the deposition of a GaAs thin film.[3]

Scheme 2

2
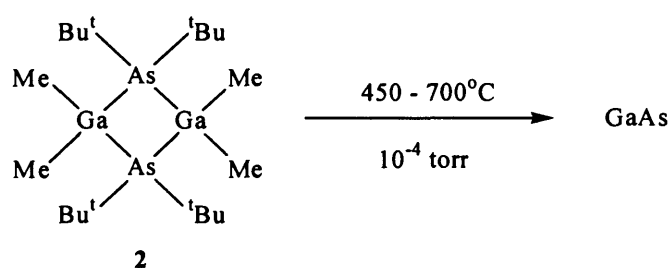
It is also possible to access binary group 13-pnictides via the direct reactions of group 13 metal(III) alkyl with a group 15 hydride (scheme 3).[3,5,6]

Scheme 3

$$MR_3 \ + \ EH_3 \ \longrightarrow \ ME \ + \ 3RH$$

M = Al, Ga or In   E = P or As   R = Cl, Br, Ph or alkyl

1.2 Low valent gallium-pnictide complexes

Recently, the chemistry of gallium-pnictide complexes has been extended to gallium(I) with the reactions of [LiN(SiMe$_3$)$_2$] with "metastable" gallium(I) halides, [{GaX(L)}$_n$], X = halide, L = ether, amine or phosphine. These lead to an array of remarkable sub-oxidation state "metalloid" cluster compounds, e.g. [Ga$_{84}${N(SiMe$_3$)$_2$}$_{20}$]$^{4-}$, via controlled disproportionation reactions.[9] Related clusters derived from the dialkyl phosphide ligand, [PBu$^t_2$]$^-$, have also been described in the last two years, e.g. [Ga$_{16}$(PBu$^t_2$)$_{10}$]^{10} and [Ga$_{51}$(PBu$^t_2$)$_{14}$Br$_6$]$^{3-}$.[11] In gallium(II) chemistry, amide complexes are rare,[12] e.g. [Ga{[N(Ar)C(H)]$_2$}]$_2$, Ar = C$_6$H$_3$Pr$^i_2$-2,6; and to the best of our knowledge, there is only one structurally characterized phosphide complex[13] [(Ar')$_2$C$_6$H$_3$]Ga{H$_2$PGa(H)PH$_2$Ga[C$_6$H$_2$(Ar')$_2$], Ar' = 2,4,6-Pr$^i_3$C$_6$H$_3$ and no known arsenides.

The ability of the diazabutadiene (DAB) class of ligand to stabilise gallium centres in a variety of oxidation states has been demonstrated, as for example in 4 - 7.[12(c),14-17]

R = Bu^t or C$_6$H$_3$Pr$^i_2$-2,6
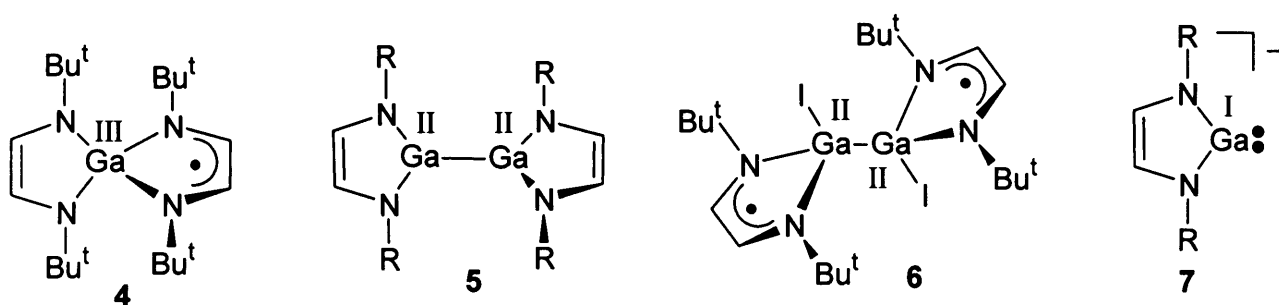
In addition, the ability of the DAB class of ligand to form stable complexes with the DAB in either a singly or doubly reduced form allows for the synthesis of a variety of novel compounds with interesting magnetic properties.[14] For example, the reaction of 1,4-di-t-butyl-

1,4-diazabuta-1,3-diene (^{t}Bu-DAB) with gallium vapour gave the paramagnetic complex **4** in low yield (scheme 4).[14(a)] An initial investigation into the electronic structure of this complex using Electron Paramagnetic Resonance (EPR), and its solid state structure using X-ray crystallography, allowed the authors to deduce the oxidation state of the metal centre to be formally gallium(II) with the unpaired electron residing on the Ga centre. A subsequent re-investigation of the EPR spectra of **4** concluded that the complex was best represented as [(DAB^{2-})Ga(III)(DAB$^-$)], with the unpaired electron localised on the DAB ligand and with the metal centre formally in the +III oxidation state.[14(b)]

Scheme 4

4

6
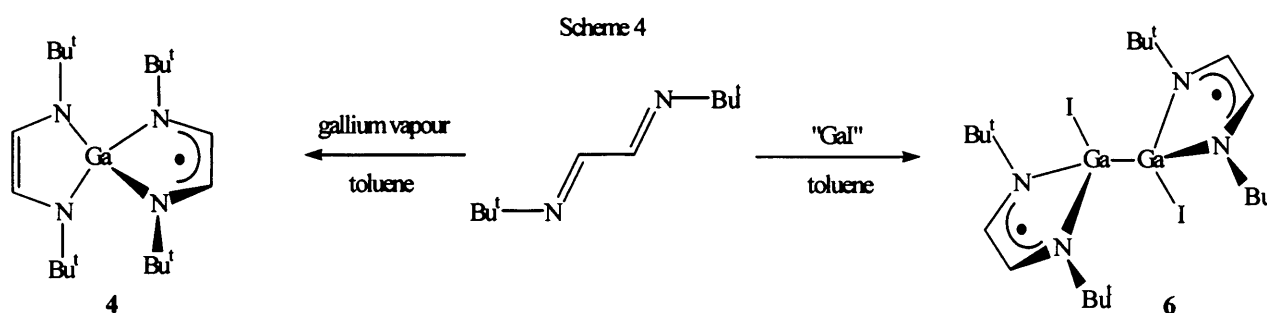
The paramagnetic complex, **6**, was formed from the reaction of ^{t}Bu-DAB with "GaI" in moderate yield (32%), scheme 4.[16] This complex is presumably formed via a 1-electron reduction of the DAB ligand by the gallium(I) starting material.

The diamagnetic digallane complexes, **5**, can be synthesised in a variety of ways. The first reported occurrence of this complex type was from the reaction of di-lithio-Bu^{t}DAB with Ga$_2$Cl$_2$·2dioxane.[15] Alternatively, this compound, R = Ar, has be accessed via a photochemical cleavage of the Cp* moiety in the compound (Ar-DAB)GaCp*, Ar = 2,6-Pr$^i_2$C$_6$H$_3$; Cp* = pentamethylcyclopentadienyl; to yield complex **5**.[12(c)] In our group, and that of Schmidbaur's, the ability of DAB ligands to stabilise low oxidation state gallium centres has been most evidently exploited in the formation of the valence isoelectronic N-heterocyclic carbene analogues, **7**, the coordination chemistry of which is currently emerging and has been reviewed in chapters 1, 2 and 3.[18] As a component of those studies Jones and co-workers have developed a synthetic route to **6**, which has been used as a precursor to **7**, R = Bu^t.[16]

EPR investigations of the above complexes (where applicable) have revealed that the unpaired electron density generally resides within the delocalised DAB ligand back bone, with very little spin density residing on the metal centres.[14-16]

2. Research proposal

Of the known crystallographically authenticated gallium(II) complexes, $[E(SiMe_3)_2]^-$ ligands have not featured. Considering their importance to Ga(III) chemistry and the amide's ability to stabilize sub-oxidation state gallium clusters, it was our intention to prepare gallium(II)-bis(silyl)pnictide complexes and investigate their structural properties. Additionally, we saw **6** as a potential precursor to gallium(II) pnictide complexes. To this end, the reactivity of $[\{(Bu^t\text{-DAB})GaI\}_2]$, **6**, towards $[ME(SiMe_3)_2]$ (M = Li or Na; E = N, P or As) has been examined. The unexpected results of this study are reported here.

3. Results and discussion

The reactions of **6** with two equivalents of $[ME(SiMe_3)_2]$ (M = Li or Na; E = N, P or As) afforded good yields of the mono-pnictido gallium(III) complexes, **8 - 10** (Scheme 5). It is unsure what the mechanism of formation of these compounds is but it must involve salt elimination, Ga-Ga bond cleavage and disproportionation reactions. In this respect, it is noteworthy that related reactions of organo-digallium(II) diiodides, $[\{GaI(R)\}_2]$, R = $C(SiMe_3)_3$, with carboxylate salts do not lead to Ga-Ga bond cleavage but to salt elimination and the formation carboxylate bridged gallium(II) complexes, e.g. $[\{Ga(R)\}_2\{\mu\text{-}O_2C(Ph)\}_2]$.[19] In the formation of **8 - 10**, the only identified by-products were gallium metal and small amounts of the known Ga(III) complex $[Ga(Bu^t\text{-DAB})_2]$, **4**.[14] It is interesting that when the reactions were carried out in 1:1 stoichiometries, **8 - 10** were formed in reduced yields and significant amounts of **6** were recovered unreacted. Therefore, it appears that the mechanism of formation of these compounds requires two equivalents of the alkali metal pnictide. Moreover, due to the observed disproportionation processes, it is clear that each dimeric molecule of **6** can give rise to only one molecule of monomeric **8 - 10** in these reactions. It should also be mentioned that attempts to prepare the antimonide analogue of **8 - 10** by reaction of **6** with $[LiSb(SiMe_3)_2]$ were not successful and led to the formation of the known distibine, $\{Sb(SiMe_3)_2\}_2$,[20] via an oxidative coupling of the antimonide fragment.

Scheme 5

M = Li or Na

2 ME(SiMe₃)₂

4 NaN(SiMe₃)₂

E = N (8), P (9), As (10)

6

4 LiE(SiMe₃)₂

E = P (11), As (12)

13
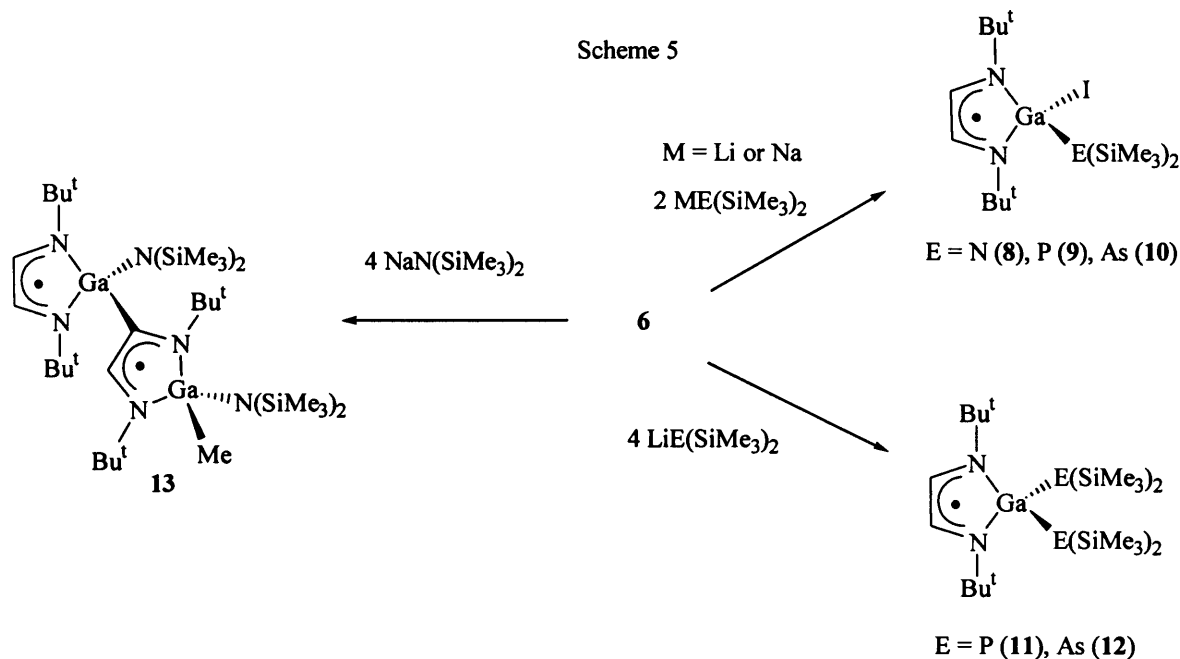
Due to their paramagnetic nature, no meaningful NMR spectroscopic data could be obtained for **8 - 10**. Consequently, X-ray crystallographic studies were required to elucidate their structures. The molecular structures of **8, 9** and **10** are depicted in Figures 1, 2 and 3. The geometries of the diazabutadiene ligands in **8 - 10** (Table 1) are similar to each other and are suggestive of significant delocalisation, as has been found in related paramagnetic complexes, e.g. [GaI₂(Buᵗ-DAB)].[10] Likewise, the geometries about the gallium centres of the complexes are comparable and are distorted tetrahedral in each case. The only obvious trend in the series involves the angles about the pnictide centres. As would be expected, the amido N-centre in **8** is trigonal planar, whilst the geometries of the P- and As-centres in **9** and **10** tend towards pyramidal. The Ga-N(amide) bond length of 1.868(2) Å in **8** is greater than its Ga-N(Buᵗ-DAB) interactions but identical to the Ga-N distances in [Ga{N(SiMe₃)₂}₃].[21] Complexes **9** and **10** contain rare examples of terminal phosphido- and arsenido-gallane fragments, respectively. The Ga-P bond in **9** [2.2991(11) Å] is one of the shortest yet reported and can be compared with the mean Ga-P(terminal phosphide) distance for all previously reported structures [2.39 Å].[22] Moreover, it is very close to that in [(Buᵗ)₂Ga{P(Mes*)SiPh₃}] (Mes* = C₆H₂Buᵗ₃-2,4,6) [2.295(3) Å] which has been postulated as having a weak Ga-P π-contribution to the bond.[23] Clearly, in **9** this cannot be the case as the gallium and phosphorus centres do not have trigonal planar geometries. Importantly, **10** possesses the shortest Ga-As single bond yet reported [2.3893(12) Å], which is significantly shorter than in related complexes, e.g. 2.421 Å avge. in

[Ga{As(SiMe$_3$)$_2$}$_3$].[23] The only shorter Ga-As interactions are the resonance stabilized double bonds [2.318(1) Å] in [{Li(THF)$_3$}$_2$Ga$_2${As(SiPr$^i_3$)}$_4$].[25]
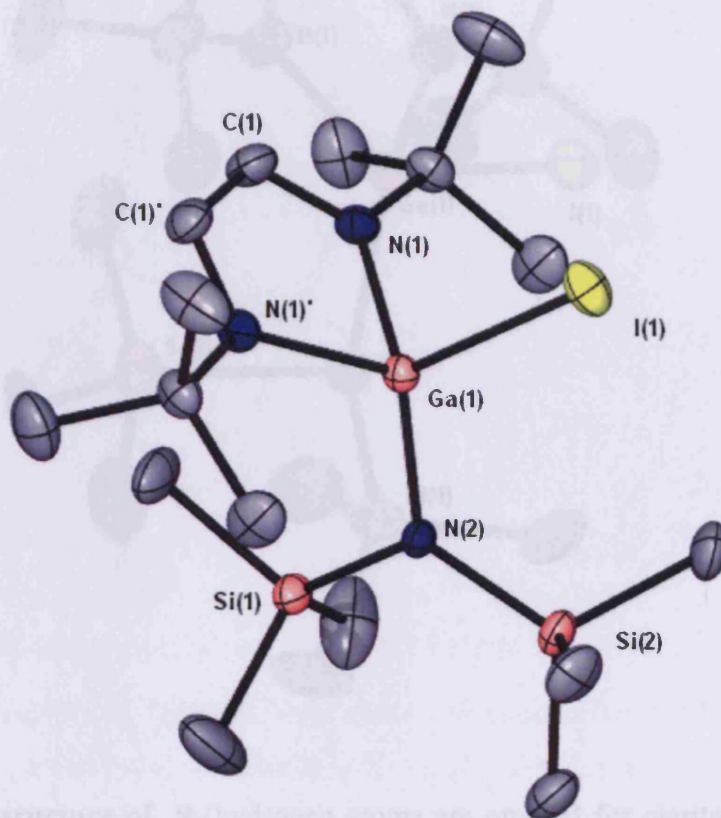

Figure 1. Molecular structure of 8 (hydrogen atoms are omitted for clarity). Selected bond lengths (Å) and angles (°): I(1)-Ga(1) 2.5906(5), Ga(1)-N(2) 1.868(2), Ga(1)-N(1) 1.9559(average), Si(1)-N(2) 1.740(3), Si(2)-N(2) 1.744(3), N(1)-C(1) 1.329(average), C(1)-C(1)' 1.406(5), N(2)-Ga(1)-N(1) 119.32(7), N(1)-Ga(1)-N(1)' 85.86(11), N(2)-Ga(1)-I(1) 118.02(8), N(1)-Ga(1)-I(1) 104.51(6), C(1)-N(1)-Ga(1) 108.59(15), Si(1)-N(2)-Si(2) 121.67(15), Si(1)-N(2)-Ga(1) 117.60(13), Si(2)-N(2)-Ga(1), N(1)-C(1)-C(1)' 118.28(13). Symmetry transformation used to generate equivalent atoms ':x, -y+1/2, -z'.
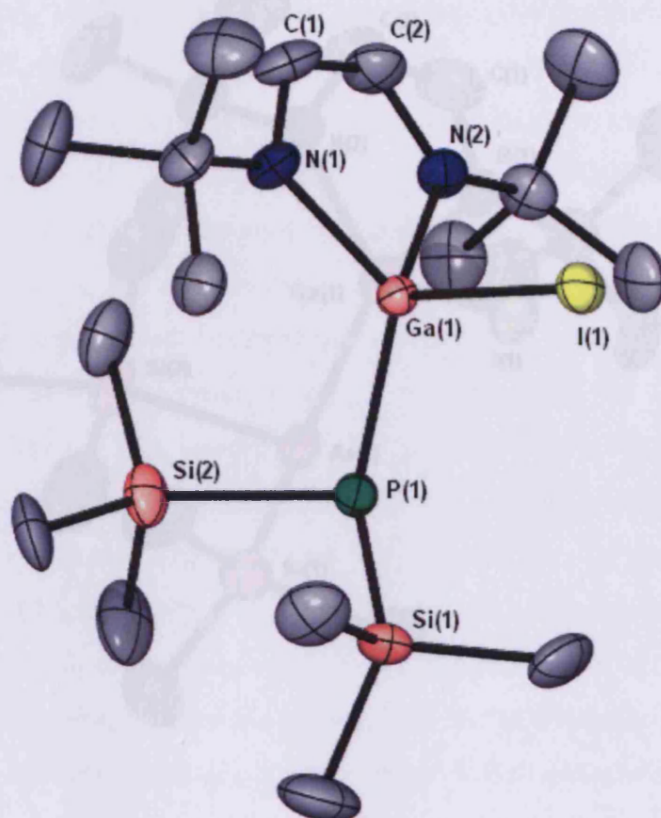
Figure 2. **Molecular structure of 9** (hydrogen atoms are omitted for clarity). Selected bond lengths (Å) and angles (°): I(1)-Ga(1) 2.5893(8), Ga(1)-N(1) 1.955(3), Ga(1)-N(2) 1.972(3), Ga(1)-P(1) 2.2991(11), P(1)-Si(1) 2.2437(16), P(1)-Si(2) 2.2466(16), N(1)-C(1) 1.335(5), N(1)-C(3) 1.480(5), N(2)-C(2) 1.318(5), C(1)-C(2) 1.395(6), N(1)-Ga(1)-N(2) 85.88(13), N(1)-Ga(1)-P(1) 128.30(10), N(2)-Ga(1)-P(1) 111.08(10), N(1)-Ga(1)-I(1) 104.69(10), N(2)-Ga(1)-I(1) 106.60(10), P(1)-Ga(1)-I(1) 115.20(3), Si(1)-P(1)-Si(2) 107.78(6), Si(1)-P(1)-Ga(1) 109.17(5), Si(2)-P(1)-Ga(1) 106.36(5), C(1)-N(1)-C(3) 119.3(3), C(1)-N(1)-Ga(1) 108.2(3), C(2)-N(2)-Ga(1) 108.1(3), N(1)-C(1)-C(2) 118.6(4), N(2)-C(2)-C(1) 119.1(4).

Figure 3. Molecular structure of **10** (hydrogen atoms are omitted for clarity). Selected bond lengths (Å) and angles (°): As(1)-Si(1) 2.346(2), As(1)-Si(2) 2.349(2), As(1)-Ga(1) 2.3893(12), Ga(1)-N(1) 1.956(6), Ga(1)-N(2) 1.959(6), N(1)-C(1) 1.305(11), N(2)-C(2) 1.330(10), C(1)-C(2) 1.411(12), Si1 As1 Si2 105.64(9), Si(1)-As(1)Ga(1) 107.04(7), Si(2)-As(1)-Ga(1) 104.07(7), N(1)-Ga(1)-N(2) 85.6(3), N(1)-Ga(1)-As(1) 110.48(19), N(2)-Ga(1)-As(1) 129.1(2), N(1)-Ga(1)-I(1) 106.66(18), N(2)-Ga(1)-I(1) 104.87(19), As(1)-Ga(1)-I(1) 114.86(4), C(1)-N(1)-Ga(1) 109.4(6), C(2)-N(2)-Ga(1) 108.2(5), N(1)-C(1)-C(2)0 118.1(8), N(2)-C(2)-C(1) 118.5(8).

Considering the formation of **8 - 10**, it is perhaps not surprising that the treatment of **6** with four equivalents of [LiE(SiMe₃)₂] (E = P, As) affords compounds of the type [(Bu^t-DAB)Ga{E(SiMe₃)₂}₂], E = P **11**, As **12**, in moderate yields (Scheme 5). Similarly, treating **9** or **10** with one equivalent of [LiE(SiMe₃)₂] leads to these complexes. More unexpected was the result of the related reaction of **6** with four equivalents of [NaN(SiMe₃)₂]. This led, reproducibly, to a moderate yield of the unusual coupled diradical product, **13**, as the only identifiable product.

The mechanism of formation of **13** has been investigated and it is believed that the initial reaction product is [(Bu^t-DAB)Ga{N(SiMe₃)₂}₂] (cf. **11** and **12**). This is then thought to undergo

an intramolecular transmethylation reaction to give the intermediate [(Bu^t-DAB)Ga{N(SiMe₃)₂}Me], **14**. This proposal has precedent in the reactions of $GaCl_3$ with either [LiN(SiMe₃)₂][26] or N(SiMe₃)₃[27] which both give rise to Si-C bond scissions and methyl migrations to the gallium centres. It must be said that in the reaction mixture that gave **13**, we have not been able to isolate the expected elimination product, {(Me₃Si)NSi(Me)₂}₂. The final product, **13**, could be formed by deprotonation of the diazabutadiene backbone of one molecule of the intermediate, **14** by the GaMe moiety of another (i.e. CH_4 elimination). This has been disproved by intentionally preparing **14** from the reaction of **8** with MeLi. The product was found to be stable towards the formation of **13**. Alternatively, **13** could be formed by deprotonation of the backbone of the intermediate, **14**, with excess [NaN(SiMe₃)₂] in the reaction mixture. The resulting carbanion could then attack [(Bu^t-DAB)Ga{N(SiMe₃)₂}I] **8**, which must also be a reaction intermediate, to give **13** *via* NaI elimination. To test this hypothesis, an equimolar mixture of **8**, **14** and [NaN(SiMe₃)₂] in diethyl ether was warmed from −78°C to 25°C. Although the reaction was not clean, compound **13** was isolated from it in a low yield (*ca.* 10%). Presumably, similar coupling reactions were not observed in the preparations of **11** and **12** as the pyramidal geometries at their pnictogen centres (*vide infra*) circumvent close interactions between their gallium centres and SiMe₃ groups. This would be a likely prerequisite for methyl migration reactions to occur.
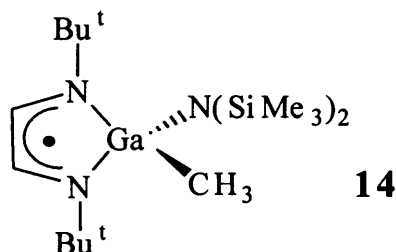
Crystals of **11** - **13** suitable for X-ray diffraction were grown from hexane solutions and the molecular structures of **11**, **12** and **13** are shown in Figures 4, 5 and 6 respectively. The asymmetric units of both **11** and **12** contain 1.5 crystallographically independent molecules which show no significant geometrical differences. Consequently, the structure of only the full independent molecule of each will be discussed here (Table 1). Both are monomeric with distorted tetrahedral geometries about their gallium centres. The geometries of the heterocyclic fragments are similar to those in **8** - **10**, whilst the average Ga-E bond lengths of **11** and **12** are significantly greater than those in **9** and **10**, presumably due to steric reasons.

Table 1. Selected Metrical Parameters for complexes 8 - 12.

|	Ga-N(Bu^t-DAB) (Å avge.)	Ga-I (Å)	Ga-E (Å)	N-Ga-N (°)	Σ angles at E (°)	C-N (in heterocycle) (Å avge.)	C-C (in heterocycle) (Å)
8	1.956	2.5906(5)	1.868(2)	85.86(11)	360.0	1.329	1.406(5)
9	1.963	2.5893(8)	2.2991(11)	85.88(13)	323.3	1.326	1.395(6)
10	1.957	2.5944(12)	2.3893(12)	85.6(3)	316.8	1.318	1.411(12)
11	1.986	-	2.343 (avge.)	84.74(15)	330.4 (avge.)	1.330	1.394(6)
12	1.991	-	2.437 (avge.)	84.62(14)	322.6 (avge.)	1.328	1.382(6)
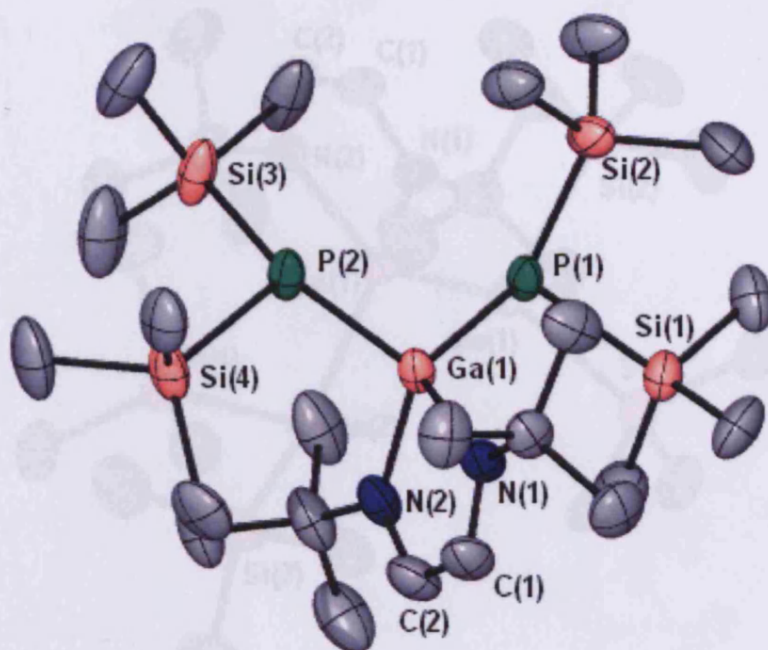
Figure 4. Molecular structure of 11 (hydrogen atoms are omitted for clarity). Selected bond lengths (Å) and angles (°): Ga(1)-N(2) 1.984(4), Ga(1)-N(1) 1.989(3), Ga(1)-P(2) 2.3396(13), Ga(1)-P(1) 2.3457(13), P(1)-Si(1) 2.2468(17), P(1)-Si(2) 2.2551(18), P(2)-Si(3) 2.2381(18), P(2)-Si(4) 2.2585(16), N(1)-C(1) 1.335(5), N(2)-C(2) 1.326(6), C(1)-C(2) 1.394(6), N(2)-Ga(1)-N(1) 84.74(15), N(2)-Ga(1)-P(2) 118.89(10), N(1)-Ga(1)-P(2) 108.55(11), N(2)-Ga(1)-P(1) 108.39(10), N(1)-Ga(1)-P(1) 117.74(10), P(2)-Ga(1)-P(1) 115.25(4), Si(1)-P(1)-Si(2) 104.22(6), Si(1)-P(1)-Ga(1) 108.34(6), Si(2)-P(1)-Ga(1) 113.32(6), Si(3)-P(2)-Si(4) 106.57(6), Si(3)-P(2)-Ga(1) 114.82(6), Si(4)-P(2)-Ga(1) 113.58(7), C(1)-N(1)-Ga(1) 108.9(3), C(2)-N(2)-Ga(1) 108.7(3), N(1)-C(1)-C(2) 118.2(4), N(2)-C(2)-C(1) 119.5(4).
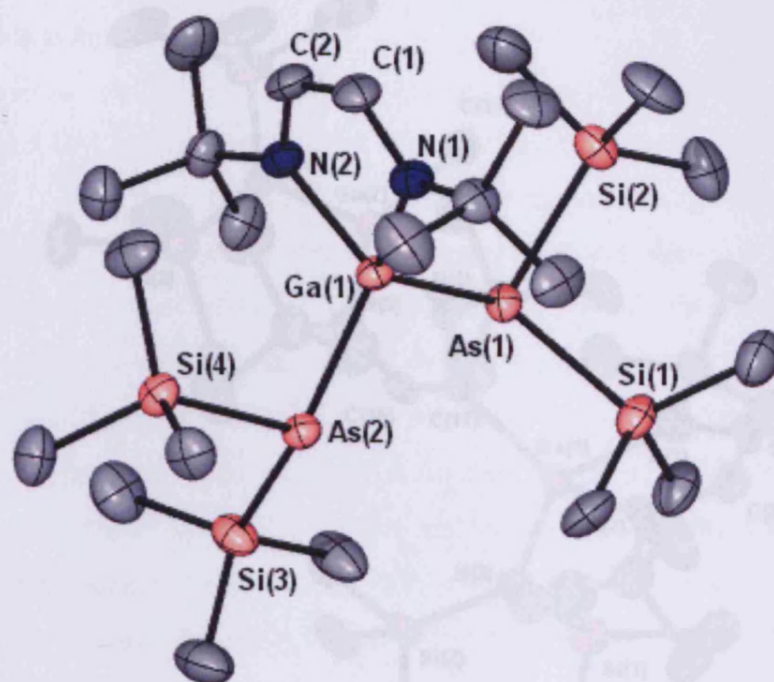
Figure 5. Molecular structure of 12 (hydrogen atoms are omitted for clarity). Selected bond lengths (Å) and angles (°): As(1)-Si(2) 2.3482(14), As(1)-Si(1) 2.3558(13), As(1)-Ga(1) 2.4395(8), As(2)-Si(3) 2.3463(14), As(2)-Si(4) 2.3624(13), As(2)-Ga(1) 2.4350(7), Ga(1)-N(2) 1.989(3), Ga(1)-N(1) 1.993(3), N(1)-C(1) 1.327(5), N(2)-C(2) 1.330(5), C(1)-C(2) 1.382(6), Si(2)-As(1)-Si(1) 102.50(5), Si(2)-As(1)-Ga91) 105.68(4), Si(1)-As(1)-Ga(1) 111.02(4), Si(3)-As(2)-Si(4) 105.09(5), Si(3)-As(2)-Ga(1) 110.15(4), Si(4)-As(2)-Ga(1) 110.76(4), N(2)-Ga(1)-N(1) 84.62(14), N(2)-Ga(1)-As(2) 120.74(10), N(1)-Ga(1)-As(2) 108.35(10), N(2)-Ga(1)-As(1) 107.88(10), N(1)-Ga(1)-As(1) 118.98(10), As(2)-Ga(1)-As(1) 113.68(2), C(1)-N(1)-Ga(1) 108.5(3), C(2)-N(2)-Ga(1) 108.4(3), N(1)-C(1)-C(2) 119.2(4), N(2)-C(2)-C(1) 119.3(4).

Figure 6: Molecular structure of 13 (hydrogen atoms are omitted for clarity). Selected bond lengths (Å) and angles (°): Ga(1)-N(1) 2.036(5), Ga(1)-N(2) 1.986(5), Ga(1)-N(3) 1.910(5), Ga(1)-C(17) 2.023(6), Ga(2)-N(4) 1.990(5), Ga(2)-N(5) 1.972(5), Ga(2)-N(6) 1.909(4), Ga(2)-C(33) 1.981(6), N(1)-C(1) 1.333(8), N(2)-C(2) 1.344(8), N(4)-C(17) 1.359(8), N(5)-C(18) 1.315(8), C(1)-C(2) 1.382(9), C(17)-C(18) 1.432(8), N(1)-Ga(1)-N(2) 84.5(2), N(1)-Ga(1)-N(3) 116.5(2), N(1)-Ga(1)-C(17) 105.1(2), N(2)-Ga(1)-N(3) 107.2(2), N(2)-Ga(1)-C(17) 124.5(2), N(3)-Ga(1)-C(17) 115.5(2), N(4)-Ga(2)-N(5) 83.91(18), N(4)-Ga(2)-N(6) 118.4(2), N(4)-Ga(2)-C(33) 107.6(2), N(5)-Ga(2)-N(6) 115.5(2), N(5)-Ga(2)-C(33) 108.1(3), N(6)-Ga(2)-C(33) 118.1(2).

The molecular structure of **13** confirms that a ligand coupling reaction has occurred in its formation. Both the heterocycles in this compound have similar geometries which imply significant delocalisation over their diazabutadiene backbones (*cf.* **8 - 12**). Moreover, the two Ga-N(amide) bond lengths,1.910(5) Å and 1.909(4) Å, are almost identical but greater than that

in **8**. Finally, both Ga-C bonds [Ga(1)-C(17) 2.023(6) Å, Ga(2)-C(33) 1.981(6) Å] are in the normal range for such interactions.[22]

Electron Paramagnetic Resonance (EPR) spectroscopic studies were kindly carried out by Dr Karen Antcliff and Dr Damien Murphy. The EPR spectra of the paramagnetic complexes, **8** - **10**, were recorded at X-band frequency (9 GHz). The resulting room temperature (298K) X-band spectra, recorded under identical conditions, for the complexes are shown in Figure 7(a-c) . A previous EPR study on the related complex, [(Bu^t-DAB)GaI$_2$], revealed a relatively small degree of spin delocalisation on the gallium nucleus; the observed hyperfine splittings being only 3.64 MHz and 4.62 MHz for ^{69}Ga and ^{71}Ga respectively (representing a 0.03% isotropic unpaired spin density on ^{69,71}Ga).[16] Hyperfine splittings to two equivalent nitrogen nuclei (24.14 MHz), two α protons of the diazabutadiene ligand (3.92 MHz) and very weak couplings to the remote ^{127}I nuclei (3.64 MHz) were also identified in the EPR spectrum of that compound. As a result of these superimposed hyperfine patterns in the isotropic spectrum, the overall width of the final spectrum was 6.0 mT (168 MHz).

By comparison, the EPR spectra for **8** - **10** are much more complex and significantly wider, with spectral widths of 19.5 mT, 20.1 mT and 20.5 mT respectively. Attempts to successfully simulate the spectra using commercial simulation packages (e.g. SIMFONIA) proved very difficult due to slight differences in ^{69,71}Ga hyperfine couplings and isotropic g values. For example, while an excellent fit with the outer lines could be achieved (i.e. essentially due to the wider contribution of the ^{71}Ga isotope), the shape of the inner lines was distorted due to overlap with the smaller ^{69}Ga component. This resulted from slight differences in the isotropic g values which we could not satisfactorily reproduce in the simulation. Nevertheless, the computer simulations did reveal an approximate hyperfine splitting of *ca.* 100 MHz to the ^{69,71}Ga nucleus of each compound, which represents *ca.* 0.7% spin density on the gallium nucleus. This can be rationalized in terms of a preferential polarization of the unpaired electron away from the N$_2$C$_2$H$_2$ fragment and towards the gallium nuclei due to the influence of the N-, P- and As-centers. As a result, a small amount of the unpaired spin density can be found at the N-, P- and As- nuclei, as manifested by a significantly increased number of lines in the EPR spectra. Despite the increased spin density on the gallium nuclei, the unpaired electron remains primarily localized on the diazabutadiene ligands of **8** - **10**, as confirmed by the relatively large ^{14}N and smaller ^{1}H EPR hyperfine splittings of *ca.* 25 MHz and *ca.* 3.59 MHz respectively, which are

similar to those for [(^{t}Bu-DAB)GaI$_2$]. The ^{1}H hyperfine couplings were more accurately determined by ENDOR spectroscopy, as discussed in the next section.
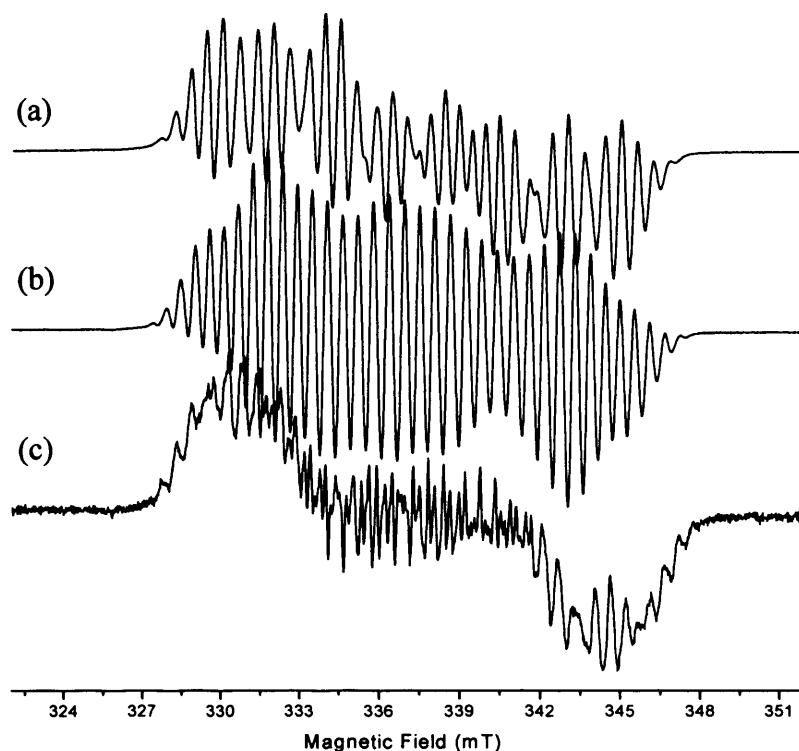

Figure 7. X-Band EPR spectra of (a) **8**, (b) **9** and (c) **10** recorded in hexane at 298 K.

The room temperature EPR spectra of **11** and **12** were also measured and the resulting spectra are shown in Figure 8. The widths of the EPR spectra have decreased to 14.8 mT and 18.1 mT for **11** and **12** respectively (cf. 20.1 mT and 20.5 mT for **9** and **10**). This result indicates that as slightly more electron spin is delocalised towards the two P(SiMe$_3$)$_2$ or As(SiMe$_3$)$_2$ substituents, less spin remains on the gallium nucleus, and therefore smaller ^{69,71}Ga hyperfine splittings are observed, thus producing a decreased spectral width.
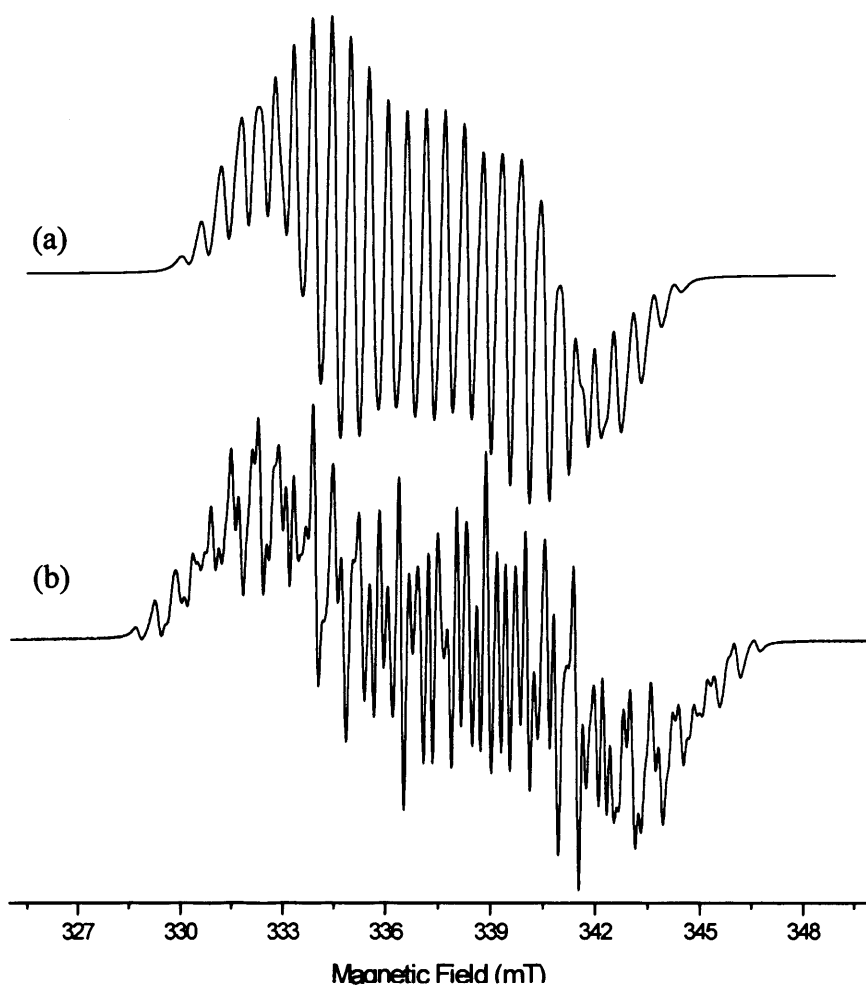
Figure 8. X-Band EPR spectra of (a) **11** and (b) **12** recorded in hexane at 298 K.

Figure 9 depicts the EPR spectrum for **13** recorded at 298K. The spectrum is substantially different compared to the previous spectra, revealing a significantly altered structure for this paramagnetic complex. Despite the presence of two unpaired electrons in the two respective diazabutadiene ligands (i.e. a diradical), the resulting EPR spectrum is not typical of a system with an S=1 triplet ground state and can best be interpreted as a composite spectrum with isotropic contributions from two S=1/2 species. The frozen solution spectrum of **13** (figure 10) revealed an easily identified quartet of *ca.* 3.0 mT (84 MHz) arising from the predominantly isotropic hyperfine splitting to one gallium nucleus, while the room temperature spectrum shows an unmistakable quartet feature (most clearly seen in the expanded outer wings of the spectrum) of 0.13 mT (3.64 MHz) separation which is due to a smaller hyperfine interaction with a second gallium nucleus. The former gallium splitting of *ca.* 84 MHz is approximately of the same order of magnitude as those observed for **8 - 10** while the latter coupling of 3.64 MHz is analogous to

that observed for [(^{t}Bu-DAB)GaI$_2$]. The EPR spectrum, and in particular the discrimination of hyperfine interactions to two independent gallium nuclei, therefore confirms the identity of **13** as a dimeric gallium complex with two non-interacting S=1/2 spin systems.
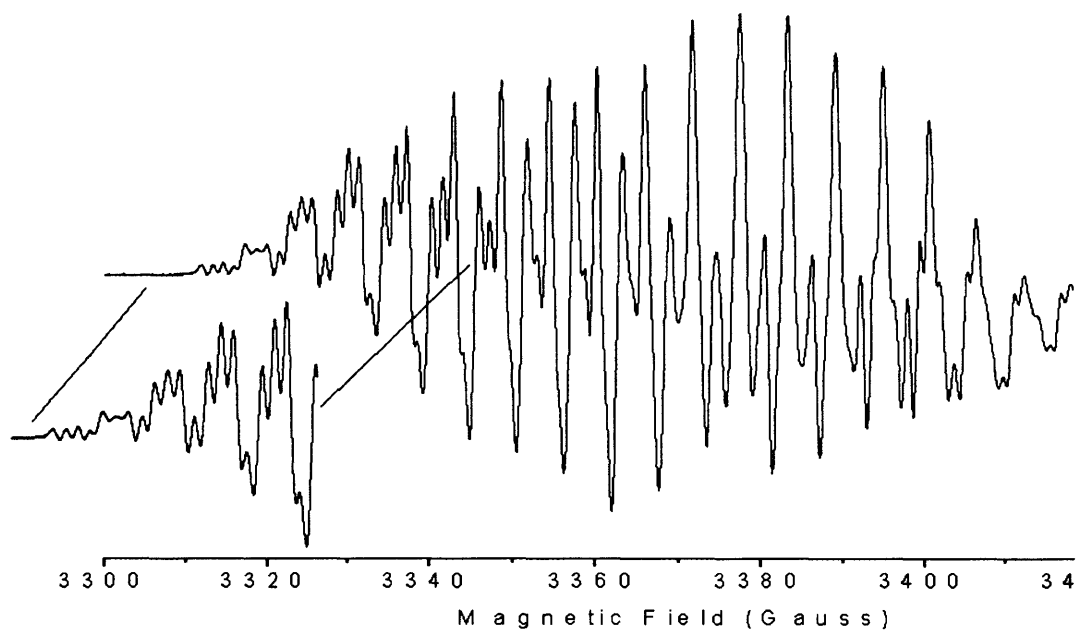

Figure 9. X-Band EPR spectrum of **13** recorded in hexane at 298 K.
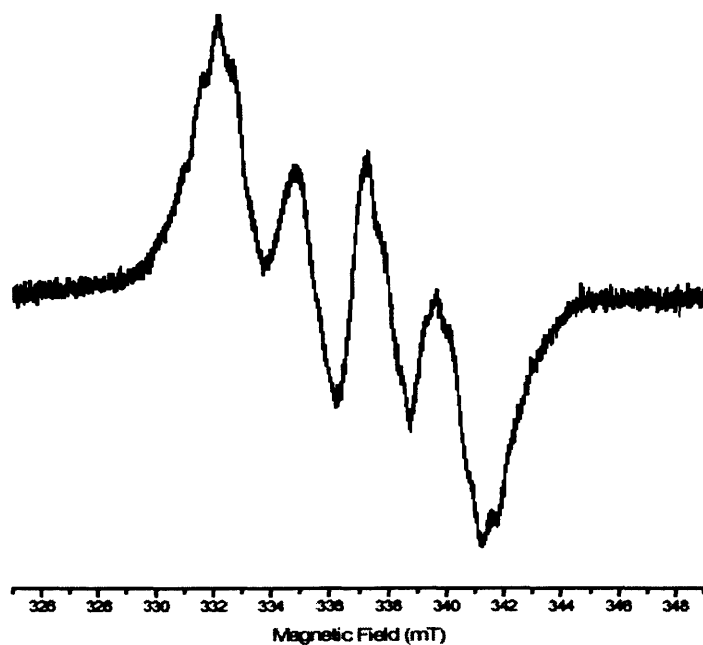

Figure 10. EPR spectrum of **13** recorded in hexane at 100 K.

Electron Nuclear Double Resonance (ENDOR) spectroscopic studies were kindly carried out by Dr Damien Murphy. In order to extract further information on the unpaired spin densities in these complexes, the continuous wave (cw) ENDOR spectra were measured. The ENDOR spectra of the complexes in disordered solids (*i.e.* frozen solutions) are expected to be complicated by the broadened nature of the ENDOR response observed.[28] Due to absorptions from a range of orientations of the radical with respect to the direction of the magnetic field, the ENDOR lines arising from weak superhyperfine interactions to I≠0 nuclei will broaden and may become very weak. Unless the shape of the EPR spectrum is dominated by a particular dipolar interaction, there is little or no orientational selection in the ENDOR experiment and a powder-type spectrum is obtained.[29] This is the typical case expected for carbon-based organic free radicals and narrow lines will only be obtained if the hyperfine anisotropy pertaining to the nucleus is small. For α protons, the anisotropy is about half of the hyperfine coupling, a, so that the principal values of the hyperfine tensor for α protons should occur near $a/2$, a, and $3/2a$. The ENDOR spectra are thus expected to extend over a wider range (from $a/2$ to $3/2a$) but with some build up of intensity at the three principal values of the hyperfine tensor corresponding to those molecules with their respective principal axes oriented along the magnetic field.

The X-band ENDOR spectrum of **10** is shown in Figure 11. As the largest coupling ($3/2a$) is expected to produce a broad and weak signal, the ENDOR spectrum was recorded using a large RF modulation depth of 250 KHz (Figure 11(a)). The three principal values of the hyperfine tensor expected for an α-proton ($a/2$, a, and $3/2a$) are clearly visible; the measured values are 1.897, 3.795 and 5.692 MHz respectively (as shown by the stick diagram in Figure 11(a)). For α-protons the sign of the isotropic hyperfine coupling is expected to be negative, compared to β-protons where a positive sign is predicted.[28(a),29(c)] The reason for the difference in sign relates to the different mechanisms of spin transfer from the π-centre to such protons (spin polarization for α protons and hyperconjugation for β protons). Knowing the isotropic coupling is *ca.* 1.4 G (~3.9 MHz) from the room temperature EPR spectrum, and that this can be assigned a negative value, the three observed hyperfine tensor components of these protons, obtained from the frozen solution ENDOR spectrum, can therefore be assigned negative values (Table 2).

Table 2. Relative Sign and Magnitude (MHz) of the Hyperfine Couplings to the α-Protons and the Remote Protons of the *tert*-Butyl Groups of **7** as Determined by ENDOR Spectroscopy.

protons	A_1	A_2	A_3	a_{iso}
α-H	-1.897	-3.795	-5.692	-3.795
tert-butyl	+2.859	-1.234	-1.234	+0.13
	+2.301	-0.863	-0.863	+0.19

A number of additional peaks can also be detected in the cw ENDOR spectrum with pronounced smaller couplings. These couplings undoubtedly arise from weaker interactions to remote protons of the complex. In order to enhance the resolution of these additional lines, the spectrum was recorded using a lower RF modulation depth of 75 kHz (Figure 11(b)). The unresolved broad line at the nuclear Lamour frequency for ^{1}H (v_N = 14.41 MHz at 3.385mT) is due to a matrix ENDOR line. This line arises from almost purely dipolar couplings of the unpaired electron with surrounding (remote matrix) magnetic nuclei.[28(b)] The remaining lines can then be assigned to weak couplings with the remote protons of the *tert*-butyl groups (shown by the stick diagram in Figure 11(b)). In the case of β-protons, considerably less anisotropy is generally observed compared to α-protons. As a result, these interactions exhibit much stronger ENDOR lines in disordered solids. This is the situation for the remote *tert*-butyl protons in complex **13** which give rise to small hyperfine splittings (Figure 11(b)) which are slightly different for the two *tert*-butyl groups, thus implying a small inequivalency in the unpaired spin distribution on these substituents.
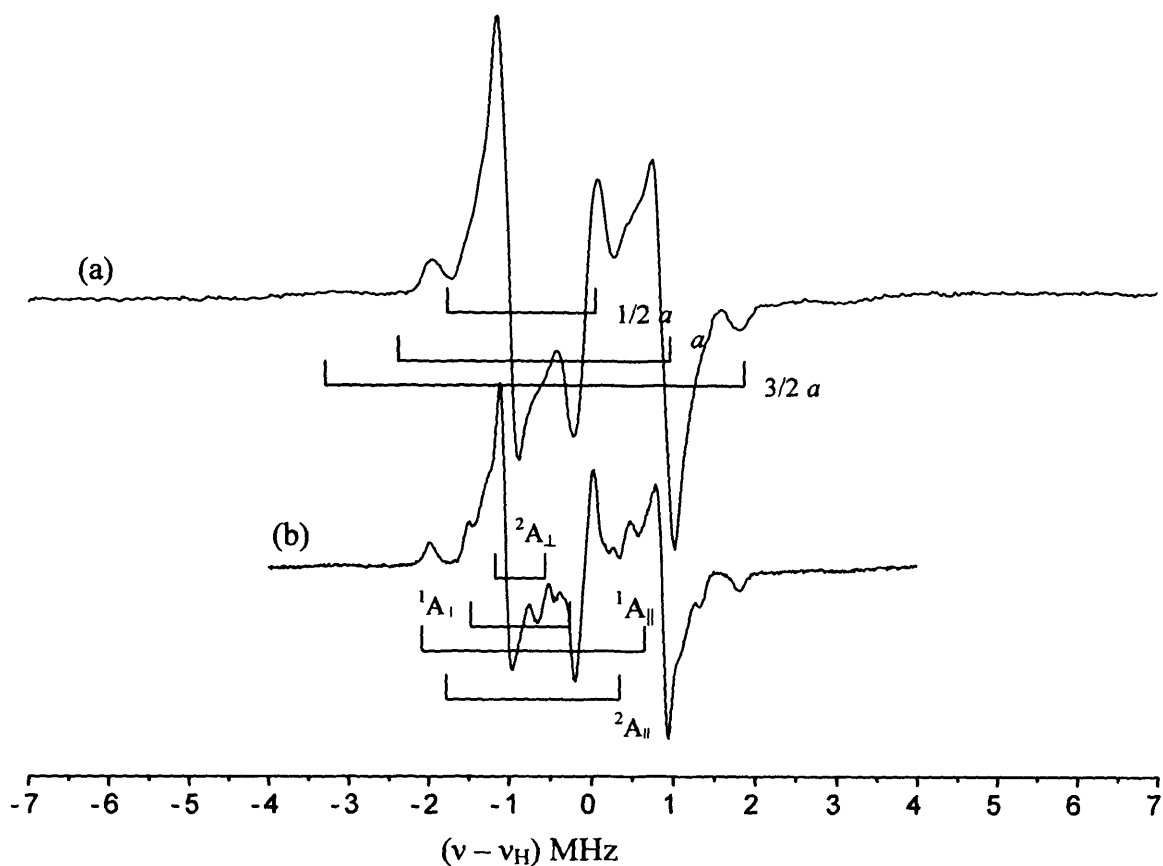
Figure 11. X-Band ENDOR spectrum of **10** at (a) 250 KHz modulation depth and (b) 75 KHz modulation depth (recorded in CD_2Cl_2/C_7D_8 at 10K).

As discussed earlier in the EPR analysis, the presence of the electronegative elements in the $E(SiMe_3)_2$ substituents produced a noticeable redistribution of electron spin density onto the $^{69,71}Ga$, ^{14}N, ^{31}P and ^{75}As nuclei. However, it must be clearly noted that the theoretical isotropic hyperfine couplings of these elements are very large (435.68 mT and 553.58 mT for $^{69,71}Ga$; 64.6 mT for ^{14}N; 474.8 mT for ^{31}P; 523.11 mT for ^{75}As), so even a very small spin density on the nuclei will produce an appreciable hyperfine coupling. We were unable to clearly detect any of these couplings in our cw ENDOR experiment. Despite the apparently large splittings to these nuclei observed in the EPR experiments, the unpaired electron distribution around the diazabutadiene ligand and the *tert*-butyl groups remain very similar for complexes **8** - **12**. This is confirmed by analysis of the ^1H ENDOR spectra for **8** - **10** shown in figure 12, analogous spectra were also recorded for **11** and **12** shown in figure 13. The spectra (and therefore the associated hyperfine couplings responsible for the lines) for all complexes are virtually identical, revealing

that the very weak couplings to the protons of the *tert*-butyl groups and the larger couplings to the α-protons remain predominantly unchanged over the series.
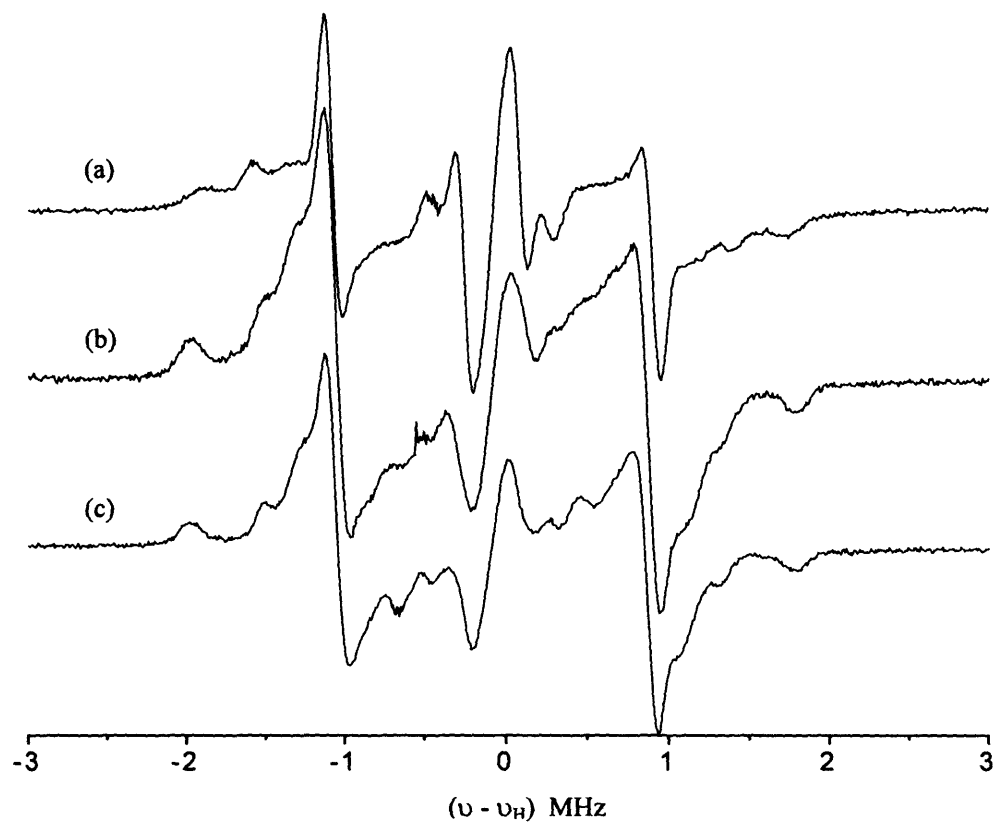

Figure 12. X-Band ENDOR spectra of (a) **8**, (b) **9** and (c) **10** recorded in CD_2Cl_2/C_7D_8 at 10K.

108
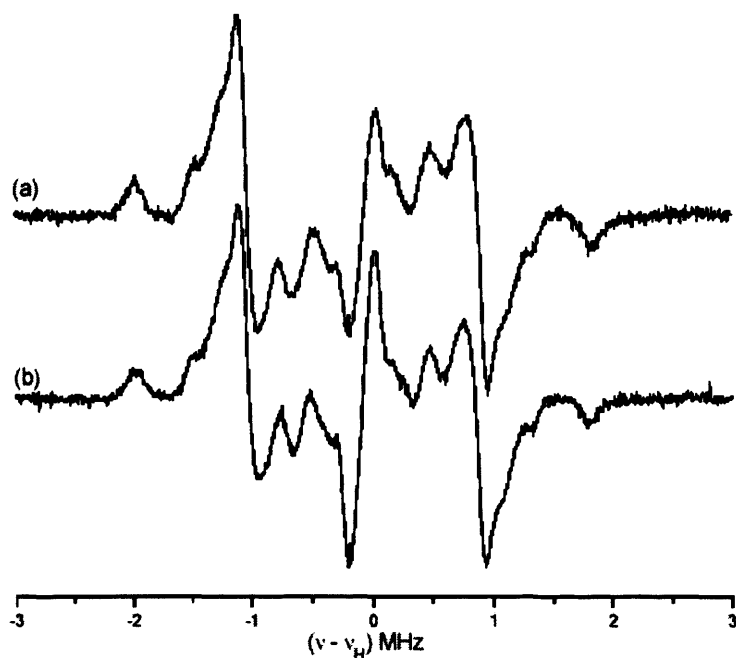
**Figure 13.** X-Band ENDOR spectra of (a) **11** and (b) **12** recorded in CD_2Cl_2/C_7D_8 at 10K.

The cw ENDOR spectrum of **13** (figure 14) is clearly different from those of **8 - 12** and can be interpreted in terms of two superimposed patterns arising, firstly, from the paramagnetic heterocycle containing the gallium centre that bridges to the other heterocycle (producing a spectrum analogous to those observed for **8 - 12**) and, secondly, from the singly deprotonated heterocycle which displays a larger coupling to the remaining α-proton.
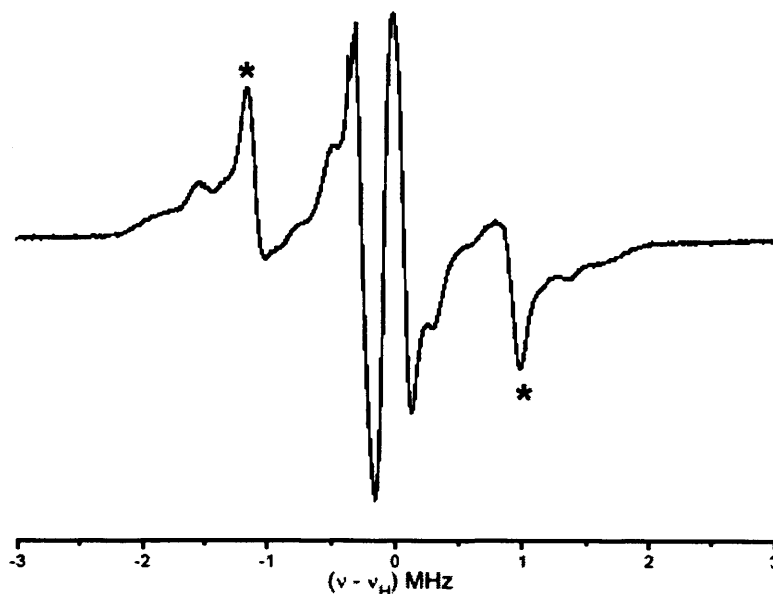
Figure 14. X-Band ENDOR spectra of **13** recorded in CD_2Cl_2/C_7D_8 at 10K.

The ENDOR spectrum supports the earlier claim that the EPR spectrum of **13** (Figure 7) reveals a substantially different structure for **13** compared to those of **8 - 12**.

Recently there has been a publication that challenges the cause of the complexity seen in the EPR spectra for the above complexes.[30] The author used DFT calculations on the model $[(^tBuDAB)Ga(I)\{Pn(SiH_3)_2\}]^-$, (Pn = N, P, As), to simulate the observed EPR spectra. However, from the authors own admission the SiH_3 fragment used in the model would possess steric and electronic differences between itself and the experimentally synthesised complexes. Their results attribute the complexity of the observed EPR spectra, not to the differing isotropic g-values for ^{69}Ga and ^{71}Ga, but from the presence of high order splitting effects and hyperfine coupling constants. Furthermore, these theoretical results demonstrate the occurrence of significant hyperfine coupling to the ^{127}I nucleus in **8, 9**, and **10**. Due to the nature of these complexes, a significant number of lines in the EPR spectra may be observed. However, this does not mean that the lines in the EPR spectra will be resolved and hence the full complexity of the spectra may not be observed.

The lines in the EPR spectra are derived from the interactions of the unpaired electron with spin active nuclei within the complexes. The number of lines in the EPR spectra can be calculated from the equation $2nI + 1$, where n = the number of spin active nuclei and I = the spin of the nuclei. For example, within the heterocycle for complex **9** there are two ^{14}N with spin $I = 1$ which would give rise to 5 lines, two H with $I = 1/2$ which would give 3 lines and one $^{(71\ \&\ 69)}Ga$

with $I = 3/2$ which would give 4 lines. Just considering the heterocycle of **9** it is conceivable that 60 lines in the EPR spectra could be observed. If spin density from the unpaired electron perturbed as far as the ^{31}P and ^{127}I nuclei where $I = 1/2$ and $5/2$ respectively, a further 2 lines for the phosphorus and 6 lines for the iodine could potentially be observed. This would increase the potential number of spectra lines to 720. With regards to simulating EPR spectra the probability of gaining accurate simulations is significantly increased with an increase in the number of theoretical lines that may be observed. To this end, a simulation of the experimentally observed data using 720 lines will be significantly more accurate compared to a simulation based on 60 lines.

In addition, an ^{127}I radical (100% spin density) would possess a hyperfine splitting constant upwards of 14000 gauss (G),[31] and coupled with the fact that spin densities are derived from the equation [experimental G / theoretical G] x 100 = % spin density, even minor amounts of spin density would give rise to large values of G. For example, if 0.1% spin density resides on a ^{127}I atom a value of 14G would be observed in the EPR spectra and more significantly, a hyperfine splitting caused by the ^{127}I would be observed in the ENDOR spectra. It is apparent that despite the authors claim that significant hyperfine coupling to the ^{127}I gives rise to the complexity of the observed EPR spectra, no explanation was provided as to why the ENDOR spectra, for the above complexes, compliments the original interpretation of the EPR data.

4. Conclusions

In summary, the reactions of a gallium(II) dimeric complex, [{(Bu^t-DAB)GaI}$_2$], with the alkali metal pnictides, [ME(SiMe$_3$)$_2$] (M = Li or Na; E = N, P or As), have been carried out under a range of stoichiometries. The reactions have led to a series of paramagnetic gallium(III)-pnictide complexes, [(Bu^t-DAB)Ga{E(SiMe$_3$)$_2$}I] (E = N, P, As) and [(Bu^t-DAB)Ga{E(SiMe$_3$)$_2$}$_2$] (E = P, As). In addition, a novel gallium heterocycle coupling reaction has been observed and its mechanism explored. All prepared complexes have been characterized by X-ray crystallography, which in the case of one compound, **10**, has highlighted the shortest Ga-As single bond yet reported. Moreover, each of the paramagnetic compounds have been characterized in solution by EPR spectroscopy and the frozen solution ^1H ENDOR spectra of several complexes have been acquired and analysed. These spin resonance studies have enabled the estimation of the spin density over the molecular frameworks of the compounds. This has

shown that although the EPR spectra of the various complexes appear very different, the spin densities on the peripheral atoms (e.g. the *tert*-butyl and E(SiMe₃)₂ substituents) do not significantly differ between the complexes, while most of the electron spin remains on their diazabutadiene backbones.

5.   Experimental

General experimental procedures can be found in appendix 1. [{(Bu^t-DAB)GaI}₂],[16] [NaN(SiMe₃)₂],[32] [LiP(SiMe₃)₂.DME][33] and [LiAs(SiMe₃)₂.DME][33] were synthesised by literature procedures.

Preparation of [(Bu^t-DAB)Ga{N(SiMe₃)₂}I], 8. To a solution of [{(Bu^t-DAB)GaI}₂] (0.30 g, 0.41 mmol) in Et₂O (15 cm³) was added [NaN(SiMe₃)₂] (0.15 g, 0.83 mmol) in Et₂O (15 cm³) at −78°C over 5 minutes. The resultant solution was warmed to room temperature and stirred overnight to yield a yellow solution and white precipitate. Volatiles were removed *in vacuo* and the residue extracted with hexane (20 cm³). Filtration, concentration and cooling to −30°C overnight yielded orange crystals of **8** (0.10 g, 46%). Mp 154-156 °C; IR v/cm^{-1} (Nujol): 1262(s), 1202(s), 919(sh), 883(sh), 829(s), 775(w), 760(w), 721(s), 669(w); m/z (APCI): 524 [M$^+$, 100%], 397 [M$^+$-I, 55%], 169 [Bu^t-DABH$^+$, 23%]; C₁₆H₃₈N₃GaSi₂I requires C 36.58%, H 7.29%, N 8.00%; found C 36.11%, H 7.36%, N 8.31%.

Preparation of [(Bu^t-DAB)Ga{P(SiMe₃)₂}I], 9. To a solution of [{(Bu^t-DAB)GaI}₂] (0.30 g, 0.41 mmol) in Et₂O (15 cm³) was added [LiP(SiMe₃)₂.DME] (0.22 g, 0.82 mmol) in Et₂O (15 cm³) at −78°C over 5 minutes. The resultant solution was warmed to room temperature and stirred overnight to yield a red solution. Volatiles were removed *in vacuo* and the residue extracted with hexane (20 cm³). Filtration, concentration and cooling to −30°C overnight yielded red crystals of **9** (0.10 g, 45%). Mp 124-126 °C; IR v/cm^{-1} (Nujol): 1261(m), 1206(w), 1096(w), 1018(w), 719(m); m/z (APCI): 414 [M$^+$ − I, 20%], 365 [M$^+$-P(SiMe₃)₂, 31%], 169 [Bu^t-DABH$^+$, 100%].

Preparation of [(Bu^t-DAB)Ga{As(SiMe₃)₂}I], 10. To a solution of [{(Bu^t-DAB)GaI}₂] (0.30 g, 0.41 mmol) in Et₂O (15cm³) was added [LiAs(SiMe₃)₂.DME] (0.26 g, 0.82 mmol) in Et₂O (15cm³) at −78°C over 5 minutes. The resultant solution was warmed to room temperature and stirred overnight to yield a red solution. Volatiles were removed *in vacuo* and the residue extracted with hexane (20 cm³). Filtration, concentration and cooling to −30°C overnight yielded red crystals of **10** (0.08 g, 33%). Mp 130-132 °C; IR v/cm⁻¹ (Nujol): 1457(s), 1368(s), 1361(s), 1328(sh), 1262(s), 1244(s), 1213(s), 836(m), 776(s), 747(s), 691(s), 620(s); m/z (APCI): 291 [GaAs(SiMe₃)₂⁺, 10%], 221 [As(SiMe₃)₂⁺, 5%], 169 [Bu^t-DABH⁺, 100%]; C₁₆H₃₈N₂GaAsSi₂I: requires C 32.78%, H 6.53%, N 4.78%; found C 32.16%, H 6.59%, N 4.51%.

Preparation of [(Bu^t-DAB)Ga{P(SiMe₃)₂}₂], 11. To a solution of [{(Bu^t-DAB)GaI}₂] (0.30 g, 0.41 mmol) in Et₂O (15 cm³) was added [LiP(SiMe₃)₂.DME] (0.45 g, 1.60 mmol) in Et₂O (15 cm³) at −78°C over 5 minutes. The resultant solution was warmed to room temperature and stirred overnight. Volatiles were removed *in vacuo* and the residue extracted with hexane (20 cm³). Filtration, concentration and cooling to −30°C overnight yielded red crystals of **11** (0.08 g, 33%). Mp 160-162 °C; IR v/cm⁻¹ (Nujol): 1369(s), 1337(s), 1262(sh), 1243(s), 1210(s), 937(s), 832(m), 744(s), 680(s); m/z (APCI): 593 [M⁺, 65%], 415 [M⁺–P(SiMe₃)₂, 75%], 169 [Bu^t-DABH⁺, 100%]; C₂₂H₅₆N₂GaP₂Si₄ requires C 43.58%, H 9.52%, N 4.73%; found C 43.90%, H 9.73%, N 4.84%.

Preparation of [(Bu^t-DAB)Ga{As(SiMe₃)₂}₂], 12. To a solution of [{(Bu^t-DAB)GaI}₂] (0.30 g, 0.41 mmol) in Et₂O (15 cm³) was added a solution of [LiAs(SiMe₃)₂.DME] (0.52 g, 1.60 mmol) in Et₂O (15 cm³) at −78°C over 5 minutes. The resultant solution was warmed to room temperature and stirred overnight to yield a red solution. Volatiles were removed *in vacuo* and the residue extracted with hexane (20 cm³). Filtration, concentration and cooling to −30°C overnight yielded red crystals of **12** (0.15 g, 54%). Mp 158-160°C; IR v/cm⁻¹ (Nujol): 1458(s), 1376(s), 1260(w), 1241(w), 1208(w), 834(m), 722(w); m/z (APCI): 680 [M⁺, 18%], 624 [M⁺-Bu^t, 18%], 459 [M⁺-As(SiMe₃)₂, 32%], 169 [Bu^t-DABH⁺, 100%]; C₂₂H₅₆N₂GaAs₂Si₄ requires C 38.82%, H 8.29%, N 4.12%; found C 38.33%, H 8.37%, N 4.13%.

Preparation of [(Bu^t-DAB)Ga{N(SiMe$_3$)$_2${[CC(H)N$_2$(Bu^t)$_2$]Ga[N(SiMe$_3$)$_2$]CH$_3$}], 13. To a solution of [{(Bu^t-DAB)GaI}$_2$] (0.30 g, 0.41 mmol) in Et$_2$O (15 cm^3) was added [NaN(SiMe$_3$)$_2$] (0.30 g, 1.60 mmol) in Et$_2$O (15 cm^3) at $-78°C$ over 5 minutes. The resultant solution was warmed to room temperature and stirred overnight to yield a brown suspension. Volatiles were removed *in vacuo* and the residue extracted with hexane (20 cm^3). Filtration, concentration and cooling to $-30°C$ overnight yielded olive crystals of **13** (0.10 g, 30%). Mp 123-125 °C; IR v/cm^{-1} (Nujol): 1295(w), 1244(w), 1200(w), 957(s), 904 (w), 875(s), 833(w), 721(w), 669(m); m/z (APCI): 413 [(Bu^t-DAB)Ga(Me){N(SiMe$_3$)$_2$}$^+$, 14%], 398 [(Bu^t-DAB)Ga{N(SiMe$_3$)$_2$}$^+$, 4%], 252 [(Bu^t-DAB)GaMe$^+$, 16%], 161 [N(SiMe$_3$)$_2$H$^+$, 100%].

6. References

1.   e.g. (a) C. J. Carmalt, *Coord. Chem. Revs.* 2001, **223**, 217; (b) S. Schulz, *Coord. Chem. Revs.*, 2001, **215**, 1; (c) R. L. Wells, *Coord. Chem. Revs.*, 1992, **112**, 273; (d) M. J. Taylor, P. J. Brothers, in *Chemistry of Aluminium, Gallium, Indium and Thallium*, Downs, A.J. (ed), Glasgow, 1993, pp. 517 – 524; (e) M. F. Lappert, P. P. Power, A. R. Senger, R. C. Srivastava, *Metal and Metalloid Amides*, Ellis-Horwood, Chichester, 1980, and references therein.

2.   e.g. (a) C. J. Carmalt, J. D. Mileham, A. J. P. White, D. J. Williams, *Dalton Trans.*, 2003, 4255; (b) J. F. Janik, R. A. Baldwin, R. L. Wells, W. T. Pennington, G. L. Schimek, A. L. Rheingold, L. M. Liable-Sands, *Organometallics*, 1996, **15**, 5385; (c) Barry. S.T.; Richeson, D.S. *Chem. Mater.*, 1994, **6**, 2220.

3.   A. H. Cowley, R. A. Jones, *Angew. Chem. Int. Ed. Engl.*, 1989, **28**, 1208.

4.   R. J. Jouet, R. L. Wells, A. L. Rheingold, C. D. Incarvito, *J. Organomet. Chem.*, 2000, **601**, 191.

5.   "*Chemistry of Aluminium, Gallium, Indium and Thallium*" Ed. A. J. Downs, Blakie, Glasgow, 1993.

6.   J. F. Janik, *Powder Tech.*, 2005, **152**, 118.

7.   http://en.wikipedia.org/wiki/LED

8.   J. Kovac, L. Perternai, O. Lengyel, *Thin Solid Films*, 2003, **433**, 22.

9.   A. Schnepf, H. -G. Schnöckel, *Angew. Chem. Int. Ed.,* 2002, **41**, 3532, and references therein.

10.   J. Steiner, G. Stösser, H. -G. Schnöckel, *Angew. Chem. Int. Ed.,* 2003, **42**, 1971.

11.   J. Steiner, G. Stösser, H. -G. Schnöckel, *Angew. Chem. Int. Ed.,* 2004, **43**, 302.

12.   (a) G. Linti, W. Kotsler, A. Rodig, *Z. Anorg. Allg. Chem.,* 2002, **628**, 1319; (b) E. S. Schmidt, A. Schier, N. W. Mitzel, H. Schmidbaur, *Z. Natutforsch. B,* 2001, **56**, 458; (c) T. Pott, P. Jutzi, W. W. Schoeller, A. Stammler, H. G. Stammler, *Organometallics,* 2001, **20**, 5492; (d) G. Linti, R. Frey, M. Schmidt, *Z. Natutforsch. B,* 1994, **49**, 958

13.   W. W. Li, P. Wei, B. C. Beck, Y. Xie, H. F. Schaefer, J. Su, G. H. Robinson, *Chem. Commun.,* 2000, 453.

14.   (a) F. G. N. Cloke, G. R. Hanson, M. J. Henderson, P. B. Hitchcock, C. L. Raston, *J. Chem. Soc., Dalton Trans.,* 1989, 1002; (b) W. Kaim, W. Matheis, *J. Chem. Soc., Chem. Commun.,* 1991, 597; (c) P. P. Power, *Chem. Rev.,* 2003, **103**, 789 and references therein.

15.   D. S. Brown, A. Decken, A. H. Cowley, *J. Am. Chem. Soc.,* 1995, **117**, 5421.

16.   (a) R. J. Baker, R. D. Farley, C. Jones, M. Kloth, D. M. Murphy, *J. Chem. Soc., Dalton Trans.,* 2002, 3844, (b) R. J. Baker, R. D. Farley, C. Jones, D. P. Mills, M. Kloth, D. M. Murphy, *Chem. Eur. J.,* 2005, **11**, 2972.

17.   (a) E. S. Schmidt, A. Jockisch, H. Schmidbaur, *J. Am. Chem. Soc.,* 1999, **121**, 9578; (b) E. S. Schmidt, A. Schier, H. Schmidbaur, *J. Chem. Soc., Dalton Trans.,* 2001, 505.

18.   (a) R. J. Baker, C. Jones, M. Kloth, J. A. Platts, *Angew. Chem. Int. Ed.,* 2003, **42**, 2660; (b) R. J. Baker, C. Jones, J. A. Platts, *J. Am. Chem. Soc.,* 2003, **125**, 10534; (c) R. J. Baker, C. Jones, J. A. Platts, *J. Chem. Soc., Dalton Trans.,* 2003, 3673; (d) R. J. Baker, C. Jones, M. Kloth, J. A. Platts, *Organometallics,* 2004, **23**, 4811; (e) R. J. Baker, C. Jones, M. Kloth, *Dalton Trans.,* 2005, 2106.

19.   (a) W. Uhl, A. El-Hamdan, *Eur. J. Inorg. Chem.,* 2004, 969; (b) W. Uhl, *Chem. Soc. Revs.,* 2000, **29**, 259; (c) W. Uhl, *Adv. Organomet. Chem.,* 2004, **51**, 53.

20.   G. Becker, H. Freudenblum, C. Witthauer, *Z. Anorg. Allg. Chem.,* 1982, **492**, 37.

21.   (a) D. A. Atwood, V. O. Atwood, A. H. Cowley, R. A. Jones, J. L. Atwood, S. G. Bott, *Inorg. Chem.,* 1994, **33**, 3251; (b) P. J. Brothers, R. J. Wehmschulte, M. M. Olmstead, K. Ruhlandt-Senge, S. R. Parkin, P. P. Power, *Organometallics,* 1994, **13**, 2792; (c) S. Kühner, R. Kuhnle, H.-D. Hausen, J. Weidlein, *Z. Anorg. Allg. Chem.,* 1997, **623**, 25.

22.   determined from a survey of the Cambridge Crystallographic Database, September, 2004.

23. M. A. Petrie, K. Ruhlandt-Senge, P. P. Power, *Inorg. Chem.,* 1992, **31**, 4038.

24. R. L. Wells, M. F. Self, R. A. Baldwin, P. S. White, *J. Coord. Chem.,* 1994, **33**, 279.

25. C. von Hänisch, O. Hampe, *Angew. Chem. Int. Ed.,* 2002, **41**, 2095.

26. B. Luo, V. G. Young Jr, W. L. Gladfelter, *J. Organomet. Chem.,* 2002, **649**, 268.

27. C. J. Carmalt, J. D. Mileham, A. J. P. White, D. J. Williams, J. W. Steed, *Inorg. Chem.,* 2001, **40**, 6035.

28. (a) P. J. O Malley, G. T. Babcock, *J. Am. Chem. Soc.,* 1986, **108**, 3995; (b) L. Kevan, P. A. Narayana, in *"Multiple Electron Resonance Spectroscopy"*, M. M. Dorio, J. H. Freed, Eds., Plenum Press, New York, 1979, Chap. 6, p. 229.

29. (a) H. Hurreck, B. Kirste, W. Lubitz, *Electron Nuclear Double Resonance Spectroscopy of Radicals in Solution; Applications to Organic and Biological Chemistry* 1988 VCH Publishers; (b) F. Gerson, *Acc. Chem. Res.,* 1994, **27**, 63; (c) J. S. Hyde, G. H. Rist, L. E. G. Ericksson, *J. Phys. Chem.,* 1968, **72**, 4269.

30. H. M. Tuononen, A. F. Armstrong, *Inorg. Chem.,* 2005, **44**, 443.

31. J. A. Weil, J. R. Bolton, J. E. Wertz, *Electron Paramagnetic Resonance; Elemental Theory and Practical Applications,* John Wiley and Sons, New York, 1994.

32. D. L. Clark, A. P. Sattelberger, *Inorg. Synth.,* 1997, **31**, 307.

33. G. Fritz, W. Hoelderich, *Z. Anorg. Allg. Chem.,* 1976, **422**, 104.

Chapter 5

# Group 14 and 15 Amidinate Complexes

1. Introduction

The use of amidinate ligands in coordination chemistry is well established, with complexes known for many transition and main group elements.[1-4] The amidinate ligand class, [R'NC(R)NR']−, R, R' = proton, aryl, alkyl, silyl; is extremely versatile due to its tuneability by varying the N- and backbone C- substituents. This tuneability, coupled with amidinates ability to coordinate in either i) monodentate, ii) σ,σ-symmetrical chelation, iii) σ,σ-unsymmetrical chelation or iv) bridging modes, has allowed for extensive coordination studies of this ligand class to be performed.[1,2]

i)   ii)   iii)   iv)
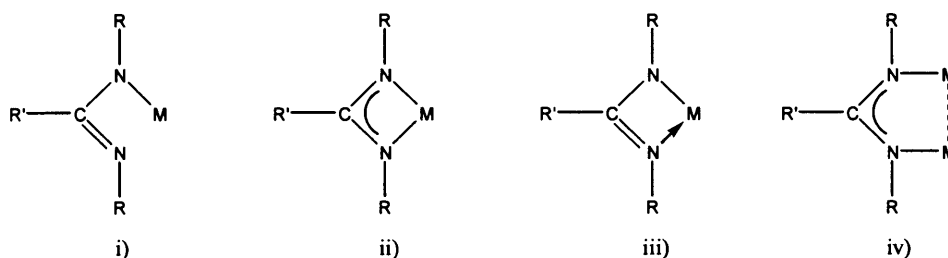
## 1.1 Group 14 amidinate complexes

Amidinate ligands have been shown to stabilise group 14 elements in the +2 and +4 oxidation states, as summarised below.[1-4] Group 14 amidinates are known for silicon,[5,6] germanium,[6] tin[7,8] and lead.[8] Syntheses of some silicon and germanium amidinate complexes are summarised in scheme 1.

Scheme 1
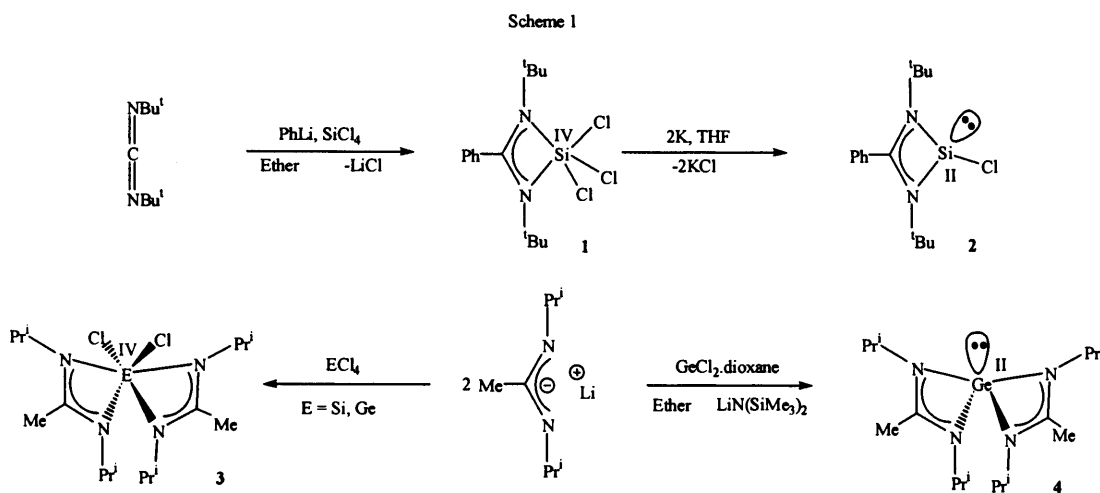
The reaction of *tert*-butylcarbodiimide with one equivalent of PhLi followed by treatment with SiCl$_4$ afforded complex 1.[5] Treatment of complex 1 with two equivalents of potassium yielded the novel monomeric chlorosilylene complex 2. This was the first example of a room temperature stable system containing a Si^{II}-Cl bond. Similarly, the treatment of MCl$_4$, where M = Si or Ge, with two equivalents of [Li][(Pr^i)NC(Me)N(Pr^i)] led to the isolation of the element(IV) complexes, 3. The treatment of GeCl$_2$.1,4-dioxane with two equivalents of [Li][(Pr^i)NC(Me)N(Pr^i)] led to the isolation of complex 4, where the germanium centre is formally in the +II oxidation state.[6] Examples of tin and lead amidinate syntheses are summarised in scheme 2. These salt metathesis reactions have enabled complexes with Sn^{IV} 5, Sn^{II} 6 and Pb^{II} 7 centres to be isolated.[7,8]

Scheme 2
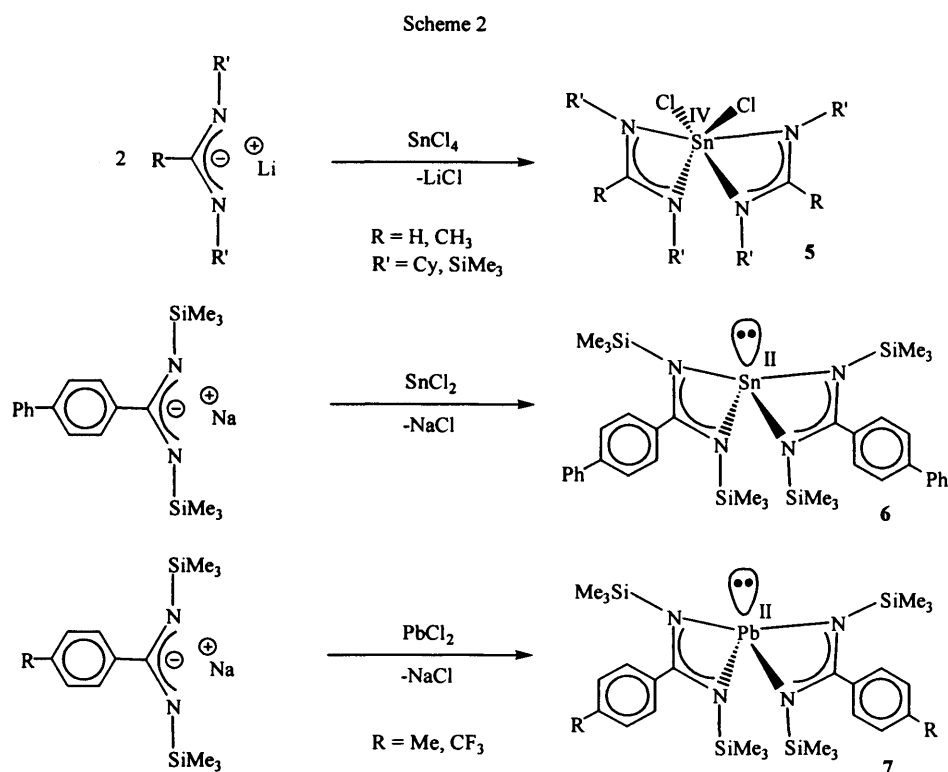
Theoretical (*ab initio*) calculations have been performed on the model complexes [{(H)NC(H)N(H)}$_n$M], where M = Si, Ge, Sn, Pb; n = 2 or 4; in which the metal centre is formally in either a divalent or tetravalent state. The results of this study pointed towards a donor-acceptor formulation with a delocalised NCN backbone in all cases.[9]
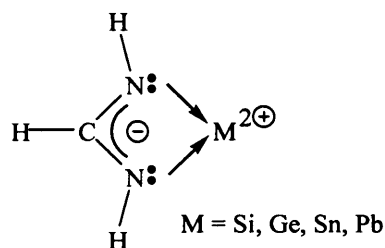
Furthermore, these calculations revealed that the formation of bis-amidinate group 14 element(II) complexes becomes increasingly more difficult for lighter group 14 elements. Additionally, the tetravalent species were found to be more stable than the divalent +II species.[9]

119

1.2 Group 15 amidinate complexes

Scheme 3 summarises some synthetic procedures for accessing group 15 amidinate complexes. It has been proposed that complex **8a** forms via carbodiimide insertion into a P-Cl bond of PCl_5 forming the four membered ring system. A subsequent treatment of **8a** with phenyllithium led to substitution of the chlorine of the ring system and not one of the phosphorus chlorides to give complex **8b** via salt metathesis.[10] Another example of group 15 amidinates involved their preparation via insertion mechanisms. ECl_3, E = P, As or Sb, inserts into the N-Cl bond of a chloro-amidine giving the 4-membered ring systems **9**.[11] In both **8** and **9**, the formal oxidation state of the group 15 centre is +V.
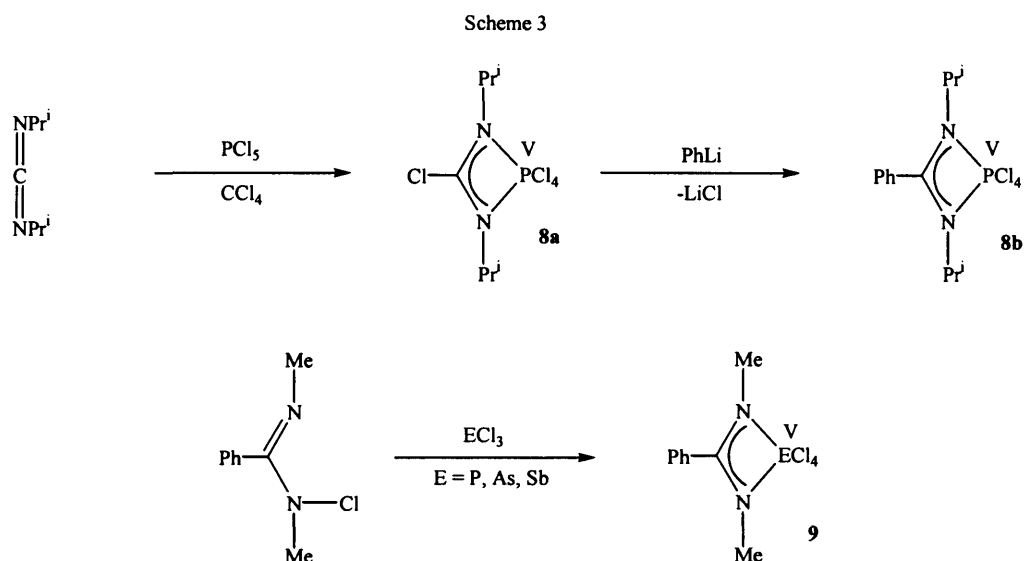
Scheme 3

Antimony amidinates have been synthesised with formal metal oxidation states +III and +V, examples are shown in scheme 4. Complexes **10** and **11** have been formed through salt metathesis where the formal oxidation state of the starting is retained in the product.[4] Complexes containing bismuth, where the formal metal oxidation state is +III, have also been accessed via the salt metathesis route, giving **12** and **13**.[12-14]

120

Scheme 4

$R = Me, Ph, R' = Bu^t, SiMe_3$
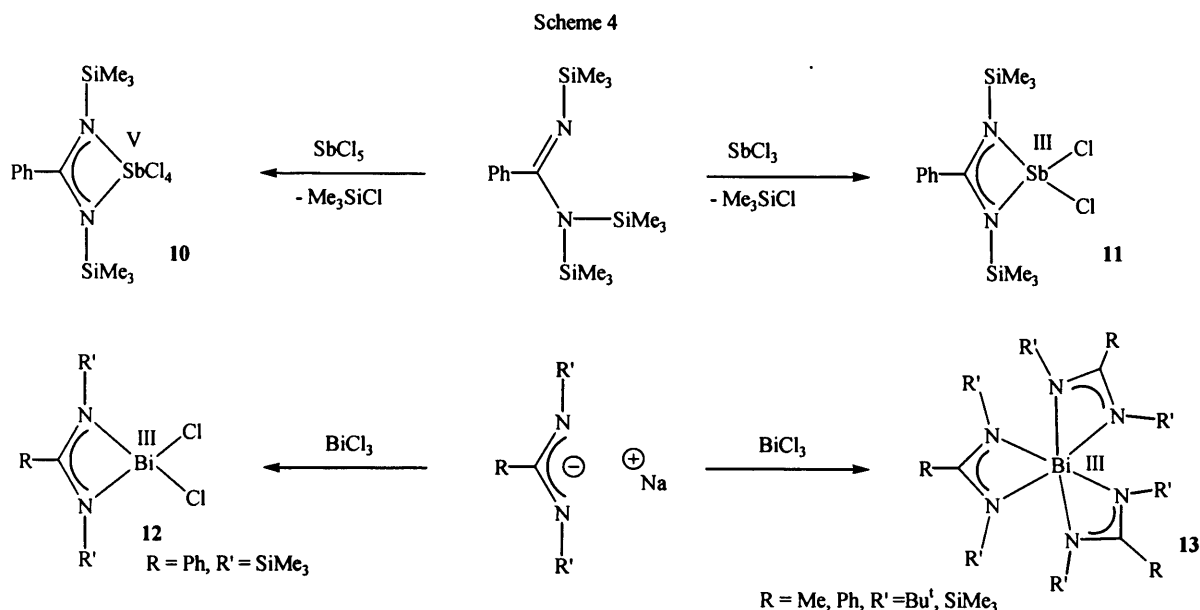
Bismuth amidinates, $[Bi\{(R')NC(R)N(R')\}_3]$, where $R' = Bu^t$; $R = Me$; have featured in patent applications as precursors for atomic layer deposition of bismuth oxide layers.[13] Further uses of bismuth amidinate complexes have been highlighted in a recent publication in which the reduction of $[\{(Ar)NC(H)N(Ar)\}BiCl_2]$, $Ar = 2,6-Pr^i_2C_6H_3$; with magnesium metal led to the isolation of a bulky magnesium amidinate, $[\{(Ar)NC(H)N(Ar)\}Mg(thf)Cl]_2$.[15]

2.   Research proposal

Group 14 amidinate complexes with very bulky N-substituents have rarely featured in the literature. With this in mind we felt there was scope to synthesise such species and investigate their reactivity. Further to this, a literature review revealed a scarcity of bismuth amidinate complexes. Therefore, it was our intention to prepare and characterise a series of such complexes and investigate their reductions. The results of these studies are presented below.

3.   Results and discussion

3.1   Reactivity of an amidinato germanium chloride complex

The bulky amidinato germanium complex used for this study was synthesised via a salt metathesis reaction, depicted in scheme 5.[16]

Scheme 5
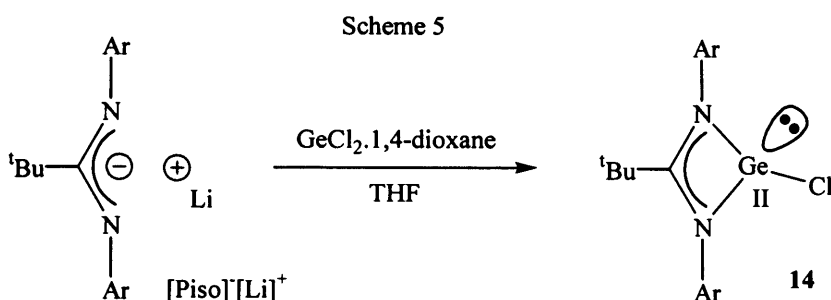
Complex **14** possess a germanium centre in the +II oxidation state. The Ge^{II} centre is coordinated by a σ,σ-symmetrical chelating amidinate ligand (Piso) and a chloride. Additionally, a lone pair of electrons resides on the metal centre. This complex has the potential to participate in a range of different reactivities and to this end **14** has been reacted with a series of main group and transition metal fragments in order to highlight the versatility of this system.

Initially, the salt metathesis reaction of **14** with group 15 salt fragments was explored. Complex **15** was synthesised from the treatment of **14** with lithium diisopropylamide (LDA) (scheme 6). This has presumably formed via salt metathesis whereby LiCl has been eliminated. It is worthy of note that the similar reaction of **14** with lithium diethylamide resulted in recovery of starting materials. Following from these results, the salt metathesis reactions of **14** was extended to include a transition metal salt fragment. The reaction of **14** with FpNa, where Fp = $[(\eta^5\text{-}Cp)Fe(CO)_2]^-$, Cp = cyclopentadienyl; gave complex **16** in moderate yield. As noted above, there is a lone pair of electrons residing at the germanium centre of **14**. This lone pair of electrons could form dative bonds with suitable fragments. To this end complex **17** was formed in good yield from the treatment of **14** with $W(CO)_5(THF)$, from which the THF is easily substituted. Additionally, the propensity of the germanium centre to be oxidised was explored. However, the treatment of **14** with propylenesulfide only gave the salt **18** in low yield, 18 %. The mechanism of this reaction is unknown, however **18** has been intentionally synthesised from the direct reaction of $[PisoH]^+[Cl]^-$ with $GeCl_2.1,4$-dioxane giving the desired material in a greater yield ca. 46%. In this case, there is presumably a chloride transfer from the amidinium salt to the germanium centre. Scheme 6 summarises the reactivity of **14**.

Scheme 6

Scheme with structures showing:

- Structure **16**: Ar–N, 'Bu, Ge II, Fe with Cp and two CO
- Fp = cyclopentadienirondicarbonyl
  Ar = 2,6-Pr$^i_2$C$_6$H$_3$
- Structure **15**: Ph, Ge II, N(iPr)$_2$, Ar–N
- Structure **14** (central)
- FpNa / THF
- LiN(Pr^i)$_2$ / THF
- W(CO)$_5$·THF / THF
- S (epoxide) / Toluene
- Structure **17**: Ar–N, 'Bu, Ge II, Cl, W(CO)$_5$
- Structure **18**: Ar–N$^{\oplus}$–H, 'Bu, N–H, Ar, GeCl$_3^{\ominus}$
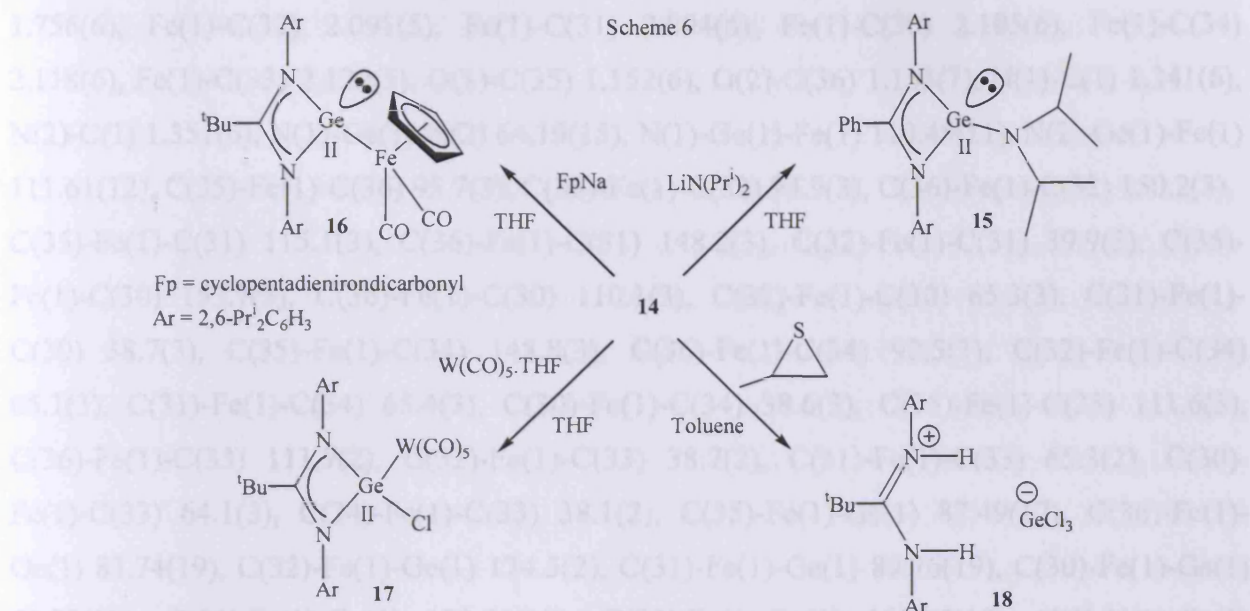
X-ray crystallographic studies were carried out on **16 - 18** and their molecular structures are depicted in figures 1 - 3 respectively.

Figure 1. Molecular structure of **16**. Selected bond lengths (Å) and angles (°): Ge(1)-N(1) 2.042(4), Ge(1)-N(2) 2.043(4), Ge(1)-Fe(1) 2.4415(11), Fe(1)-C(35) 1.750(6), Fe(1)-C(36)

1.756(6), Fe(1)-C(32) 2.091(5), Fe(1)-C(31) 2.094(6), Fe(1)-C(30) 2.105(6), Fe(1)-C(34) 2.118(6), Fe(1)-C(33) 2.122(5), O(1)-C(35) 1.152(6), O(2)-C(36) 1.153(7), N(1)-C(1) 1.341(6), N(2)-C(1) 1.351(6), N(1)-Ge(1)-N(2) 64.19(15), N(1)-Ge(1)-Fe(1) 110.45(11), N(2)-Ge(1)-Fe(1) 111.61(12), C(35)-Fe(1)-C(36) 95.7(3), C(35)-Fe(1)-C(32) 94.9(3), C(36)-Fe(1)-C(32) 150.2(3), C(35)-Fe(1)-C(31) 115.1(3), C(36)-Fe(1)-C(31) 148.2(3), C(32)-Fe(1)-C(31) 39.9(3), C(35)-Fe(1)-C(30) 153.7(3), C(36)-Fe(1)-C(30) 110.1(3), C(32)-Fe(1)-C(30) 65.3(3), C(31)-Fe(1)-C(30) 38.7(3), C(35)-Fe(1)-C(34) 148.8(3), C(36)-Fe(1)-C(34) 92.5(3), C(32)-Fe(1)-C(34) 65.1(3), C(31)-Fe(1)-C(34) 65.4(3), C(30)-Fe(1)-C(34) 38.6(3), C(35)-Fe(1)-C(33) 111.6(3), C(36)-Fe(1)-C(33) 111.7(2), C(32)-Fe(1)-C(33) 38.7(2), C(31)-Fe(1)-C(33) 65.3(2), C(30)-Fe(1)-C(33) 64.1(3), C(34)-Fe(1)-C(33) 38.1(2), C(35)-Fe(1)-Ge(1) 87.49(17), C(36)-Fe(1)-Ge(1) 83.74(19), C(32)-Fe(1)-Ge(1) 124.5(2), C(31)-Fe(1)-Ge(1) 89.76(19), C(30)-Fe(1)-Ge(1) 90.25(19), C(34)-Fe(1)-Ge(1) 123.31(19), C(33)-Fe(1)-Ge(1) 153.05(18), C(1)-N(1)-Ge(1) 93.2(3), C(1)-N(2)-Ge(1) 92.9(3), N(1)-C(1)-N(2) 107.5(4), O(1)-C(35)-Fe(1) 177.3(5), O(2)-C(36)-Fe(1) 175.8(7).
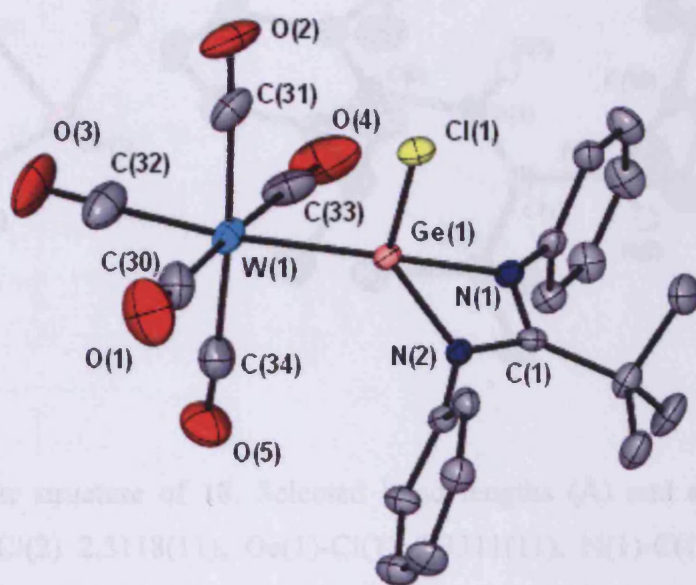

Figure 2. Molecular structure of **17** (isopropyl groups omitted for clarity). Selected bond lengths (Å) and angles (°): W(1)-C(32) 2.001(5), W(1)-C(33) 2.027(5), W(1)-C(30) 2.031(5), W(1)-C(34) 2.035(5), W(1)-C(31) 2.041(5), W(1)-Ge(1) 2.5564(6), Ge(1)-N(1) 1.961(3), Ge(1)-N(2) 1.978(3), Ge(1)-Cl(1) 2.2091(10), O(1)-C(30) 1.142(6), N(1)-C(1) 1.352(4), N(1)-C(6) 1.431(5),

C(1)-N(2) 1.340(4), O(2)-C(31) 1.134(5), O(3)-C(32) 1.148(5), O(4)-C(33) 1.156(6), O(5)-C(34) 1.151(5), C(32)-W(1)-C(33) 92.1(2), C(32)-W(1)-C(30) 91.5(2), C(33)-W(1)-C(30) 176.41(19), C(32)-W(1)-C(34) 88.47(18), C(33)-W(1)-C(34) 89.05(18), C(30)-W(1)-C(34) 91.39(19), C(32)-W(1)-C(31) 86.50(18), C(33)-W(1)-C(31) 89.15(19), C(30)-W(1)-C(31) 90.72(19), C(34)-W(1)-C(31) 174.59(16), C(32)-W(1)-Ge(1) 172.00(14), C(33)-W(1)-Ge(1) 90.32(15), C(30)-W(1)-Ge(1) 86.08(13), C(34)-W(1)-Ge(1) 99.21(12), C(31)-W(1)-Ge(1) 85.90(12), N(1)-Ge(1)-N(2) 66.42(12), N(1)-Ge(1)-Cl(1) 100.64(9), N(2)-Ge(1)-Cl(1) 95.93(9), N(1)-Ge(1)-W(1) 132.01(9), N(2)-Ge(1)-W(1) 138.78(8), Cl(1)-Ge(1)-W(1) 111.86(3), C(1)-N(1)-Ge(1) 93.7(2), N(2)-C(1)-N(1) 106.5(3), C(1)-N(2)-Ge(1) 93.3(2), O(1)-C(30)-W(1) 178.0(5), O(2)-C(31)-W(1) 177.4(4), O(3)-C(32)-W(1) 177.8(4), O(4)-C(33)-W(1) 179.1(5), O(5)-C(34)-W(1) 176.2(4).
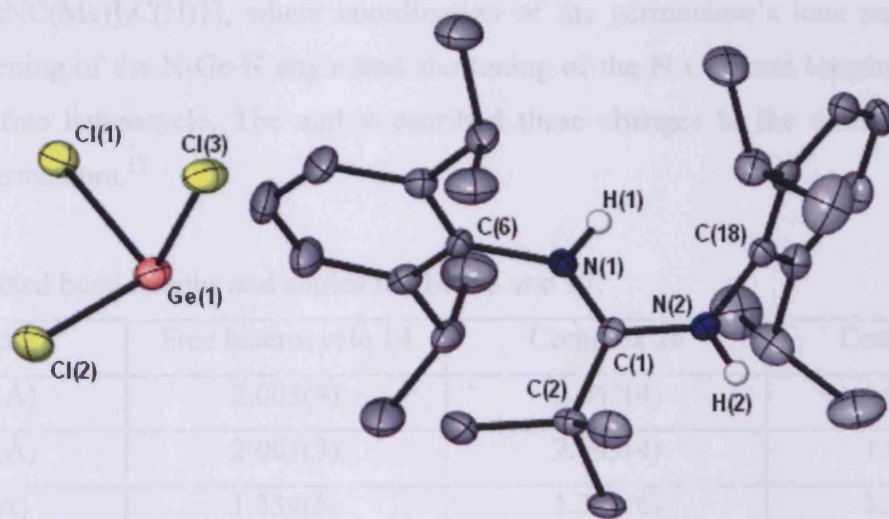
Figure 3. Molecular structure of **18**. Selected bond lengths (Å) and angles (°): Ge(1)-Cl(3) 2.2782(11), Ge(1)-Cl(2) 2.3118(11), Ge(1)-Cl(1) 2.3311(11), N(1)-C(1) 1.325(4), N(1)-C(6) 1.461(4), N(2)-C(1) 1.319(4), N(2)-C(18) 1.448(4), C(1)-C(2) 1.541(5), Cl(3)-Ge(1)-Cl(2) 97.02(5), Cl(3)-Ge(1)-Cl(1) 93.52(4), Cl(2)-Ge(1)-Cl(1) 95.97(5), C(1)-N(1)-C(6) 131.2(3), C(1)-N(2)-C(18) 126.9(3), N(2)-C(1)-N(1) 117.6(3), N(2)-C(1)-C(2) 115.1(3), N(1)-C(1)-C(2) 127.3(3).

The solid state structures of complexes **16** and **17** revealed some differences in comparison to the free heterocycle **14**, table 1. Complex **16** is formed via salt metathesis and as such the lone pair of electrons on the germanium plays no part in the reaction. It is apparent from table 1 that the N-Ge-N angle becomes more acute and N-Ge bond lengths become elongated in **16** compared with **14**. This is presumably caused by the development of a partial negative charge on the germanium and as such the ligand feels a greater repulsion. This charge development has presumably been caused by the lower electronegativity of the Fp fragment in comparison to the chloride it has replaced. These observations are further highlighted in the case of **17** where the opposite effect is seen. The donation of the germanium's lone pair of electrons towards the tungsten centre would necessitate the development of a partial positive charge, that is a diminished electron density at the germanium centre. Hence, a widening of the N-Ge-N angle and shortening of the N-Ge bond lengths occurs compared with those of the free heterocycle. This trend is consistent with that of the related β-diketiminate complex, $[(Cl)Ge\{[(Ph)NC(Me)]_2C(H)\}]$, where coordination of the germanium's lone pair to $W(CO)_5$ caused a widening of the N-Ge-N angle and shortening of the N-Ge bond lengths compared to those in the free heterocycle. The author ascribed these changes to the diminished electron densities at germanium.[17]

Table 1: Selected bond lengths and angles for **14**, **16** and **17**.

Bond	Free heterocycle **14**	Complex **16**	Complex **17**
Ge-N (Å)	2.003(4)	2.042(4)	1.961(3)
Ge-N (Å)	2.005(3)	2.043(4)	1.978(3)
C-N (Å)	1.334(5)	1.341(6)	1.340(4)
C-N (Å)	1.356(5)	1.351(6)	1.352(4)
N-Ge-N (°)	65.25(14)	64.19(15)	66.42(12)

Additionally, the solid state structure of complex **16** revealed the Fe-Ga bond length to be 2.4415(11) Å, which falls within normal bonding ranges.[18] Furthermore, the Ge-W bond length in complex **17** also falls within typical ranges.[18]

Complex **15** contains a group 14-15 bond formed via salt metathesis. A similar complex has been synthesised by Foley *et al.* where the stepwise treatment of $GeCl_2.1,4$-dioxane with a

lithium amidinates followed by addition of lithium amide resulted in the isolation of [[(Cy)NC(R)N(Cy)]GeN(SiMe$_3$)$_2$], Cy = cyclohexane, R = Bu^t or Me. These complexes were further reacted with elemental selenium to give terminal chalcogenido germanium complexes.[19]

The mechanism of formation for complex **18** is unknown, however a similar compound has been published in the literature [{(dpp-BIAN)(H)$_2$}$_2$(Cl)][GeCl$_3$].2.5(C$_6$H$_6$) where dpp-BIAN = 1,2-bis{(2,6-diisopropylphenyl)-imino}acenaphthene. This compound was formed from the metathetical reaction of (dpp-BIAN)GeCl with three equivalents of HCl where the dpp-BIAN became doubly protonated. The cationic ligand was found to be associated with a GeCl$_3$ anion in the solid state.[20]

Complexes **15** - **18** have been characterised by solution state NMR spectroscopy. The ^{1}H and ^{13}C{^{1}H} NMR spectra of all the complexes are as would be expected if the solid state structures were retained in solution. The solid state structures of **16** - **18** indicate that four different chemical environments should exist for the ^{i}PrCH$_3$ groups and two different chemical environments for the ^{i}PrCH groups of the aryl substituents. This has been qualified in their ^{1}H NMR spectra by the presence of four doublets corresponding to the ^{i}PrCH$_3$ groups and two septets which correspond to the ^{i}PrCH groups of the aryl substituents.

3.2 Formamidinato complexes of bismuth

A literature review highlighted a rarity of formamidinato bismuth complexes. Coupled with a survey of the Cambridge Crystallographic Database which revealed that no formamidinato bismuth complexes had been crystallographically characterised, it was our intention to synthesise and characterise a series of such complexes. To this end, the reactions of potassium formamidinate salts with BiBr$_3$, where the N-Aryl substituents of the formamidinate had been subtly modified, were carried out. It was thought that the subtle steric differences of the ligands might lead to a series of different structural motifs. Furthermore, some of the synthesised complexes may be suitable candidates for reduction, in order to form low valent, low oxidation state bismuth complexes.

The 1:1 reaction of BiBr$_3$ with [K][{(2,6-Pr$^i_2$C$_6$H$_3$)N}$_2$C(H)] gave complex **19** in low yield, 10 %. Presumably, this complex has been formed by salt metathesis. The 1:1 reaction of BiBr$_3$ with [K][{(2,6-Me$_2$C$_6$H$_3$)N}$_2$C(H)] gave a single isolated crystal of complex **20**. Despite

much effort in repeating this reaction, complex **20** could not be re-synthesised. The 1:2 reaction of BiBr$_3$ with [K][{(2,6-Me$_2$C$_6$H$_3$)N}$_2$C(H)] gave complex **22** in low yield, 27 %. Similarly, the 1:2 reaction of BiBr$_3$ with [K][{(2-PhC$_6$H$_4$)N}$_2$C(H)] gave the related complex **21** also in low yield, 31 %. The 1:3 reaction of BiBr$_3$ with [K][{(2,6-Et$_2$C$_6$H$_3$)N}$_2$C(H)] yielded complex **23** in moderate yield, 48 %. A related complex was also synthesised from the 1:3 reaction of BiBr$_3$ with [K][{(2,4,6-Me$_3$C$_6$H$_2$)N}$_2$C(H)] giving complex **24** in moderate yield, 38 %.

X-ray crystallographic studies were carried out on **19 - 24** and their molecular structures are depicted in figures 4 - 9 respectively.
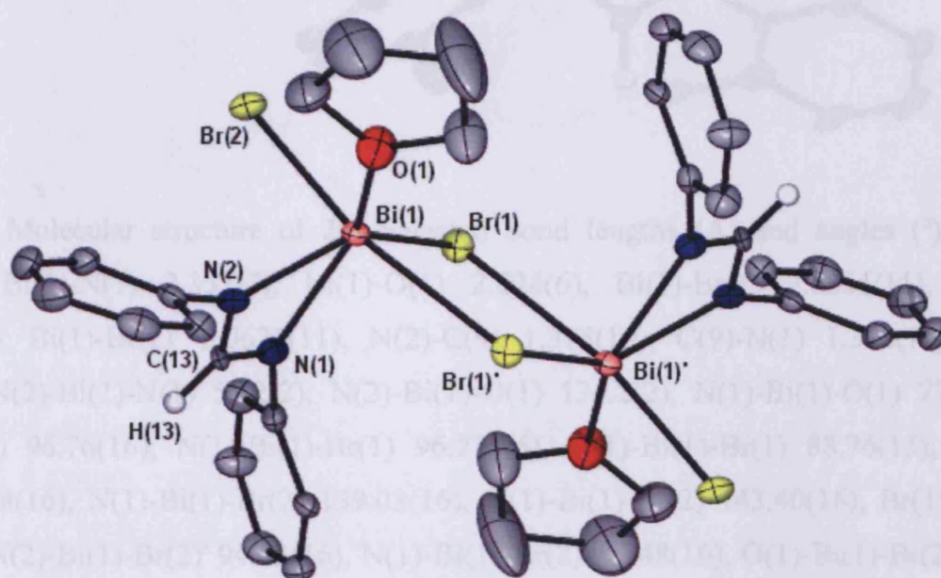
Figure 5. Molecular structure of **19** (isopropyl groups omitted for clarity). Selected bond lengths (Å) and angles (°): Bi(1)-N(1) 2.305(6), Bi(1)-N(2) 2.393(6), Bi(1)-O(1) 2.645(6), Bi(1)-Br(2) 2.6694(9), Bi(1)-Br(1) 2.8903(9), Bi(1)-Br(1)' 3.1151(9), N(2)-C(13) 1.310(9), C(13)-N(1) 1.306(10), C(13)-H(13) 0.9500, N(1)-Bi(1)-N(2) 56.7(2), N(1)-Bi(1)-O(1) 137.6(2), N(2)-Bi(1)-O(1) 81.6(2), N(1)-Bi(1)-Br(2) 96.23(16), N(2)-Bi(1)-Br(2) 92.12(16), O(1)-Bi(1)-Br(2) 91.98(15), N(1)-Bi(1)-Br(1) 85.24(17), N(2)-Bi(1)-Br(1) 141.92(16), O(1)-Bi(1)-Br(1) 136.03(15), Br(2)-Bi(1)-Br(1) 92.13(3), N(1)-Bi(1)-Br(1)' 94.90(16), N(2)-Bi(1)-Br(1)' 94.22(16), O(1)-Bi(1)-Br(1)' 79.92(15), Br(2)-Bi(1)-Br(1)' 168.86(3), Br(1)-Bi(1)-Br(1)' 88.52(2), Bi(1)'-Br(1)-Bi(1) 91.48(2), C(13)-N(2)-Bi(1) 91.1(5), N(1)-C(13)-N(2) 117.1(7), N(1)-C(13)-H(13) 121.5, N(2)-C(13)-H(13) 121.5, C(13)-N(1)-Bi(1) 95.2(5).
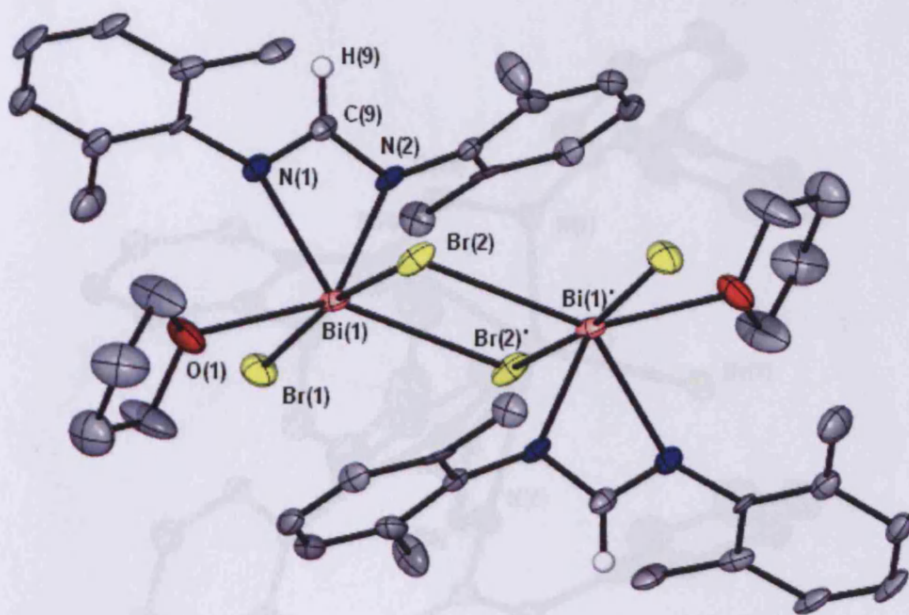
Figure 6. Molecular structure of **20**. Selected bond lengths (Å) and angles (°): Bi(1)-N(2) 2.291(7), Bi(1)-N(1) 2.353(7), Bi(1)-O(1) 2.634(6), Bi(1)-Br(1) 2.6856(11), Bi(1)-Br(2) 2.9281(11), Bi(1)-Br(2)' 3.0671(11), N(2)-C(9) 1.315(10), C(9)-N(1) 1.328(10), C(9)-H(9) 0.9500, N(2)-Bi(1)-N(1) 57.2(2), N(2)-Bi(1)-O(1) 134.2(2), N(1)-Bi(1)-O(1) 77.0(2), N(2)-Bi(1)-Br(1) 96.76(16), N(1)-Bi(1)-Br(1) 96.73(16), O(1)-Bi(1)-Br(1) 88.76(15), N(2)-Bi(1)-Br(2) 82.08(16), N(1)-Bi(1)-Br(2) 139.03(16), O(1)-Bi(1)-Br(2) 143.40(16), Br(1)-Bi(1)-Br(2) 91.96(4), N(2)-Bi(1)-Br(2)' 94.83(16), N(1)-Bi(1)-Br(2)' 92.48(16), O(1)-Bi(1)-Br(2)' 85.67(15), Br(1)-Bi(1)-Br(2)' 167.89(3), Br(2)-Bi(1)-Br(2)' 86.18(3), Bi(1)-Br(2)-Bi(1)' 93.82(3), C(9)-N(2)-Bi(1) 95.6(5), N(2)-C(9)-N(1) 114.6(7), N(2)-C(9)-H(9) 122.7, N(1)-C(9)-H(9) 122.7, C(9)-N(1)-Bi(1) 92.4(5), C(1)-N(1)-Bi(1) 142.7(5).
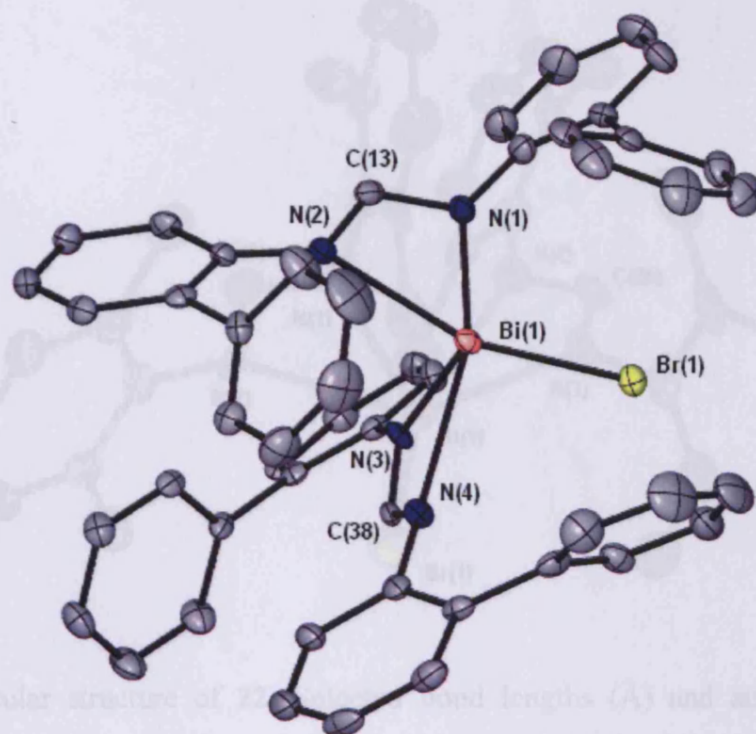
Figure 4. Molecular structure of **21**. Selected bond lengths (Å) and angles (°): Bi(1)-N(3) 2.266(3), Bi(1)-N(1) 2.340(3), Bi(1)-N(2) 2.473(3), Bi(1)-N(4) 2.613(4), Bi(1)-Br(1) 2.6908(5), N(1)-C(13) 1.335(5), N(2)-C(13) 1.300(5), N(3)-C(38) 1.337(5), N(4)-C(38) 1.296(5), N(3)-Bi(1)-N(1) 94.87(12), N(3)-Bi(1)-N(2) 80.32(12), N(1)-Bi(1)-N(2) 55.11(11), N(3)-Bi(1)-N(4) 54.39(11), N(1)-Bi(1)-N(4) 148.80(11), N(2)-Bi(1)-N(4) 108.22(11), N(3)-Bi(1)-Br(1) 86.55(8), N(1)-Bi(1)-Br(1) 86.75(9), N(2)-Bi(1)-Br(1) 137.84(8), N(4)-Bi(1)-Br(1) 95.59(8), C(13)-N(1)-Bi(1) 97.2(3), C(13)-N(2)-Bi(1) 92.1(2), C(38)-N(3)-Bi(1) 101.4(3), C(38)-N(4)-Bi(1) 86.7(2), N(2)-C(13)-N(1) 115.6(4), N(4)-C(38)-N(3) 117.5(4).
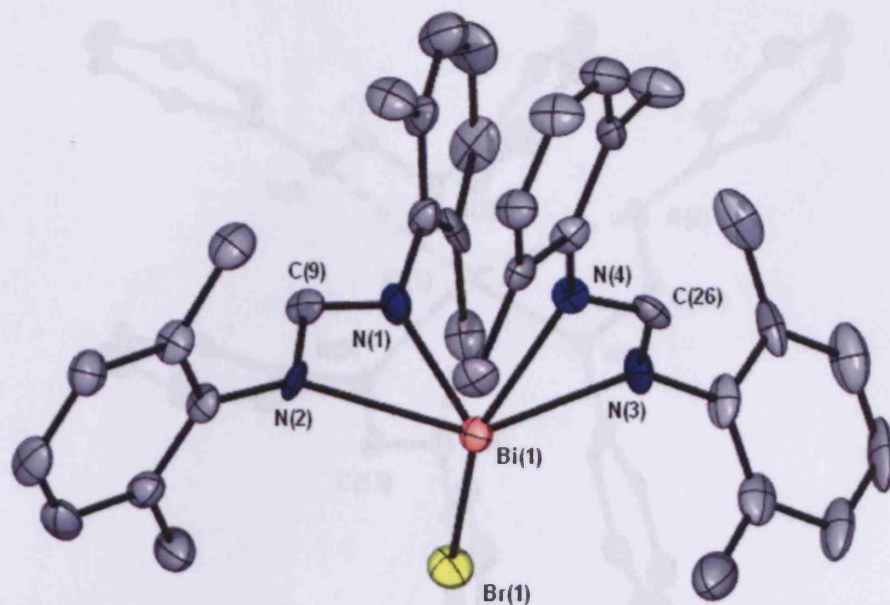
Figure 7. Molecular structure of **22**. Selected bond lengths (Å) and angles (°): Bi(1)-N(1) 2.279(10), Bi(1)-N(3) 2.340(8), Bi(1)-N(2) 2.488(8), Bi(1)-N(4) 2.488(8), Bi(1)-Br(1) 2.7395(11), N(1)-C(9) 1.343(14), N(2)-C(9) 1.301(14), N(3)-C(26) 1.295(13), N(4)-C(26) 1.299(14), N1 Bi1 N3 90.9(3), N(1)-Bi(1)-N(2) 55.6(3), N(3)-Bi(1)-N(2) 142.1(3), N(1)-Bi(1)-N(4) 84.3(3), N(3)-Bi(1)-N(4) 54.4(3), N(2)-Bi(1)-N(4) 100.5(3), N(1)-Bi(1)-Br(1) 93.2(2), N(3)-Bi(1)-Br(1) 98.2(2), N(2)-Bi(1)-Br(1) 100.8(2), N(4)-Bi(1)-Br(1) 152.3(2), C(9)-N(1)-Bi(1) 98.7(7), C(9)-N(2)-Bi(1) 90.3(7), C(26)-N(3)-Bi(1) 97.2(7), C(26)-N(4)-Bi(1) 90.2(6), N(2)-C(9)-N(1) 115.2(9), N(3)-C(26)-N(4) 116.8(9).
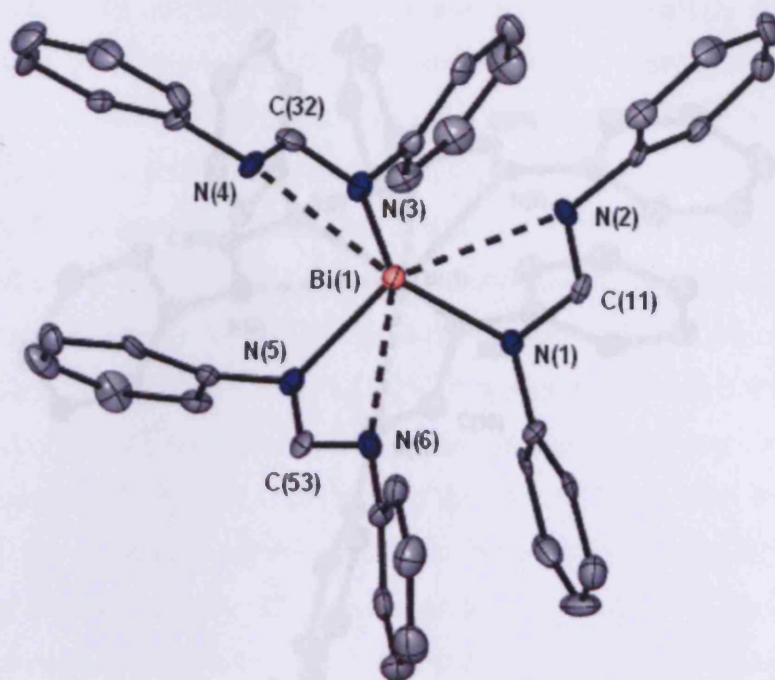
Figure 8. Molecular structure of **23** (ethyl groups omitted for clarity). Selected bond lengths (Å) and angles (°): Bi(1)-N(3) 2.256(5), Bi(1)-N(5) 2.264(5), Bi(1)-N(1) 2.273(5), Bi(1)-N(4) 2.750(5), Bi(1)-N(2) 2.761(5), Bi(1)-N(6) 2.834(5), N(1)-C(11) 1.348(7), N(2)-C(11) 1.297(7), N(3)-C(32) 1.339(7), N(4)-C(32) 1.306(7), N(5)-C(53) 1.353(7), N(6)-C(53) 1.294(7), N(3)-Bi(1) N5 95.48(17), N(3)-Bi(1)-N(1) 95.08(18), N(5)-Bi(1)-N(1) 95.85(17), N(3)-Bi(1)-N(4) 52.98(16), N(5)-Bi(1)-N(4) 84.37(16), N(1)-Bi(1)-N(4) 147.75(16), N(3)-Bi(1)-N(2) 84.72(16), N(5)-Bi(1)-N(2) 148.30(16), N(1)-Bi(1)-N(2) 52.73(15), N(4)-Bi(1)-N(2) 119.21(14), C(11)-N(1)-Bi(1) 103.9(4), C(11)-N(2)-Bi(1) 83.2(3), C(32)-N(3)-Bi(1) 104.4(4), C(32)-N(4)-Bi(1) 82.9(4), C(53)-N(5)-Bi(1) 104.5(4), N(2)-C(11)-N(1) 118.9(6), N(4)-C(32)-N(3) 118.8(6), N(6)-C(53)-N(5) 121.4(6).

Figure 9. Molecular structure of **24** (methyl groups omitted for clarity). Selected bond lengths (Å) and angles (°): Bi(1)-N(5) 2.202(3), Bi(1)-N(3) 2.368(3), Bi(1)-N(2) 2.382(3), Bi(1)-N(4) 2.585(3), Bi(1)-N(1) 2.629(3), Bi(1)-N(6) 2.730(3), N(1)-C(10) 1.300(4), N(3)-C(29) 1.348(4), N(5)-C(48) 1.352(4), N(6)-C(48) 1.289(4), N(2)-C(10) 1.346(4), N(2)-C(10) 1.346(4), N(4)-C(29) 1.292(4), N(5)-Bi(1)-N(3) 100.92(9), N(5)-Bi(1)-N(2) 92.58(10), N(3)-Bi(1)-N(2) 90.36(9), N(5)-Bi(1)-N(4) 90.25(9), N(3)-Bi(1)-N(4) 54.41(9), N(2)-Bi(1)-N(4) 144.47(9), N(5)-Bi(1)-N(1) 95.64(9), N(3)-Bi(1)-N(1) 141.55(9), N(2)-Bi(1)-N(1) 54.20(9), N(4)-Bi(1)-N(1) 160.28(9), N(5)-Bi(1)-N(6) 54.17(9), N(3)-Bi(1)-N(6) 132.96(9), N(2)-Bi(1)-N(6) 125.61(9), N(4)-Bi(1)-N(6) 83.73(8), N(1)-Bi(1)-N(6) 84.52(8).

A survey of the Cambridge Crystallographic Database revealed that **19 - 24** represent the first structurally characterised bismuth formamidinate complexes.[18] It is clear from the solid state structures that there are three distinct structural motifs. These are mono-formamidinato for complexes **19** and **20**, bis-formamidinato for complexes **21** and **22** and tris-formamidinato for complexes **23** and **24**. For complexes **19** and **20** dimerization has occurred where two bromine atoms bridge two bismuth centres. Presumably, a dimerization does not occur for complexes **21** and **22** due to greater steric crowding around the bismuth centre.

The solid state structures of complexes 19 and 20 possess heavily distorted octahedral geometries around their bismuth centres. The solid state structure of complex 21 shows a heavily distorted square based pyramidal molecular geometry in which N(3) is located in the apical position. A stereochemically active lone pair of electrons resides on the bismuth centre. In the related complex 22, the molecular geometry was also found to be heavily distorted square based pyramidal with N(1) in the apical position and a stereochemically active lone pair of electrons at the bismuth centre. Complex 23 could be considered as possessing a five coordinate bismuth centre due to the N(6)-Bi(1) distance being 2.834(5) Å which is almost 0.1 Å longer than any of the other N-Bi bonds. The N(6)-Bi(1) distance also falls outside of the sum of the covalent radii for Bi and N which is 2.22 Å. However, the sum of the van der Waals radii for Bi and N is 3.94 Å which indicates the possibility of an interaction between N(6) and Bi(1). It is therefore conceivable that the bismuth centre in 23 is five coordinate, with a stereo chemically active lone pair electrons and a heavily distorted square based pyramidal geometry with N(3) in the apical position. In stark contrast, complex 24 possesses a heavily distorted pentagonal pyramidal geometry which presumably occurs due to the lower steric strain of its ligand compared with that of 23. Additionally, in 24 a stereochemically active lone pair of electrons resides on the bismuth centre and N(5) was found in the apical position.

Table 2: Selected bond lengths for complexes 19 - 24.

Bond	19	20	21	22	23	24
Bi-N (Å)	2.305(6)	2.291(7)	2.340(3)	2.279(10)	2.273(5)	2.382(3)
Bi-N (Å)	2.393(6)	2.353(7)	2.473(3)	2.488(8)	2.761(5)	2.692(3)
N-C (Å)	1.306(10)	1.315(10)	1.300(5)	1.301(14)	1.297(7)	1.346(4)
N-C (Å)	1.310(9)	1.328(10)	1.335(5)	1.343(14)	1.348(7)	2.629(3)

Table 2 reveals some interesting trends that are linked to the three structural motifs. The Bi-N bond lengths for complexes 19 and 20 suggest a σ,σ-symmetrical chelation of the formamidinate ligand to the bismuth centres in these complexes. The N-C bond lengths for 19 and 20 are very similar and suggest the ligand system is fully delocalised. The Bi-N bond lengths in complexes 21 and 22 point towards an σ,σ-unsymmetrical chelation to the bismuth centre, however the N-C bond lengths of the formamidinate ligands are still suggestive of almost fully

delocalised systems. From the Bi-N bond lengths in complexes **23** and **24** it is very clear that the ligands are bonded in a σ,σ-unsymmetrical chelated fashion. Furthermore, the formamidinate N-C bond lengths are significantly different, showing that a delocalisation of the electron density across the ligands has not occurred and an imine / amine character presides. It is evident from the solid state structures that the increase in steric crowding on going from mono- to bis- to tris-formamidinate around the bismuth centre is the likely cause of the these observations.

Complexes **19 - 24** have been characterised by solution state NMR spectroscopy. The ^{1}H and ^{13}C{^{1}H} NMR spectra of all the complexes are as would be expected if free rotation around the N-aryl substituents is allowed on the NMR time scale, as suggested by the presence of only one ^{13}C signal for the *ortho-* and *meta*-aryl carbons of each complex. If rotation was restricted around the N-aryl substituents the spectra would be more complex.

It was felt that complexes **19** and **20** would be suitable candidates for reductions in order to form low oxidation state bismuth species. The reductions were attempted via the treatment of **19** and **20** with excess sodium metal in tetrahydrofuran. However, these attempts met with failure as decomposition of the starting materials occurred signified by the deposition of elemental bismuth.

4. Conclusion

In summary, a series of complexes have been synthesised from an amidinato-germanium-chloride complex. This work has highlighted the versatility of this system for the preparation of novel complexes. Furthermore, a series of formamidinato-bismuth complexes have been prepared via the salt metathesis reactions of BiCl$_3$ with potassium salts of formamidine ligands. The structures of these complexes have shown considerable variation dependent on the steric bulk of the formamidinate ligand.

5.   Experimental

General experimental procedures can be found in appendix 1. [(H)N(Ar)C(Bu^t)N(Ar)],[21] [{(2-PhC₆H₄)N(H)}C(H){N(2-PhC₆H₄)}],[22] GeCl₂.1,4-dioxane,[23] and W(CO)₅.THF[24] were synthesised according to literature procedures. [{(2,6-^{i}Pr₂C₆H₃)N(H)}C(H){N(2,6-^{i}Pr₂C₆H₃)}],[25] [{(2,6-Me₂C₆H₃)N(H)}C(H){N(2,6-Me₂C₆H₃)}],[25] [{(2,6-Me₂C₆H₃)N(H)}C(H){N(2,6-Me₂C₆H₃)}],[25] [{(2,6-Et₂C₆H₃)N(H)}C(H){(2,6-Et₂C₆H₃)N}][25] and [{(2,4,6-Me₃C₆H₂)N(H)}C(H){N(2,4,6-Me₃C₆H₂)}][25] were synthesised according to a modified literature procedure. [Na][(η⁵-Cp)Fe(CO)₂] was kindly donated by Dr S. Aldridge. All other reactants were obtained commercially and used as received.

Preparation   of   [Pr^{i}₂N[Ge{N(Ar)C(Bu^t)N(Ar)}]]   15. To   a   solution   of [ClGe{N(Ar)C(Bu^t)N(Ar)}] (0.25 g, 0.47 mmol) in THF (30 cm³) was added a solution of [Li][NPr^{i}₂] (0.05 g, 0.47 mmol) in THF (10 cm³) dropwise at –78 °C over 5 minutes. The resultant solution was warmed to room temperature and stirred overnight to yield a colourless solution. Volatiles were removed *in vacuo* and the residue extracted with hexane (15 cm³). Filtration, concentration and cooling to –50 °C overnight yielded colourless crystals of **15** (0.12 g, 42%). Mp = 138 – 140°C; ^{1}H NMR (400MHz, C₆D₆, 298K): δ = 0.68 (s, 9H, ^{t}Bu), 0.85 (d, $^3J_{HH}$ = 6.7 Hz, 6H, ^{i}PrCH₃), 0.94 (d, $^3J_{HH}$ = 6.7 Hz, 6H, ^{i}PrCH₃), 0.98 (d, $^3J_{HH}$ = 6.7 Hz, 6H, ^{i}PrCH₃), 1.05 (d, $^3J_{HH}$ = 6.7 Hz, 6H, ^{i}PrCH₃), 1.10 (d, $^3J_{HH}$ = 6.8 Hz, 12H, N-^{i}PrCH₃), 3.25 (sept, $^3J_{HH}$ = 6.8 Hz, 2H, N-^{i}PrCH), 3.40 (sept, $^3J_{HH}$ = 6.7 Hz, 2H, ^{i}PrCH), 3.68 (sept, $^3J_{HH}$ = 6.7 Hz, 2H, ^{i}PrCH), 6.75 – 6.86 (m, 6H, ArH); ^{13}C NMR (75MHz, C₆D₆, 298K): δ = 21.4 (N-^{i}PrCH₃), 23.4 (^{i}PrCH₃), 24.1 (^{i}PrCH₃), 27.4 (^{i}PrCH₃), 28.2 (^{i}PrCH₃), 28.6 (^{i}PrCH), 28.7 (^{i}PrCH), 29.1 (N-^{i}PrCH), 29.9 (^{t}BuCH₃), 42.1 (^{t}BuC), 123.0 (*m*-ArC), 124.0 (*m*-ArC), 124.8 (*p*-ArC), 138.3 (*ipso*-ArC), 141.0 (*o*-ArC), 142.0 (*o*-ArC), 166.5 (NCN); IR v/cm^{-1} (Nujol): s 1652, s 1616, s 1585, s 1321, s 1258, s 1211, s 1169, b 1097, b 1042, s 933; m/z (APCI): 593 [M⁺, 100%], 493 [M⁺ - N(^{i}Pr)₂, 90%], 421 [PisoH⁺, 100%]; CHN (%): C₃₅H₅₇N₃Ge₁ requires: C 70.95%, H 9.70%, N 7.09%, found C 70.69%, H 9.41%, N 6.86%.

Preparation   of   [{(CO)₂Fe(η⁵-Cp)}Ge{N(Ar)C(Bu^t)N(Ar)}]   16. To   a   solution   of [ClGe{N(Ar)C(Bu^t)N(Ar)}] (0.30 g, 0.57 mmol) in THF (15 cm³) was added a solution of [Na][(η⁵-Cp)Fe(CO)₂] (0.11 g, 0.57 mmol) in THF (15 cm³) dropwise at –78 °C over 5 minutes.

The resultant solution was warmed to room temperature and stirred overnight to yield a red solution. Volatiles were removed *in vacuo* and the residue extracted with hexane (10ml). Filtration, concentration and cooling to –30 °C overnight yielded red crystals of **16** (0.21g, 56%). Mp = 120 – 150°C; ^{1}H NMR (400MHz, C_6D_6, 298K): δ = 0.82 (s, 9H, ^tBu), 1.15 (d, $^3J_{HH}$ = 6.8 Hz, 6H, $^iPrCH_3$), 1.20 (d, $^3J_{HH}$ = 6.8 Hz, 6H, $^iPrCH_3$), 1.21 (d, $^3J_{HH}$ = 6.8 Hz, 6H, $^iPrCH_3$), 1.25 (d, $^3J_{HH}$ = 6.8 Hz, 6H, $^iPrCH_3$), 3.49 (sept, $^3J_{HH}$ = 6.8 Hz, 1H, ^iPrCH), 3.90 (s, 5H, Cp), 3.97 (sept, $^3J_{HH}$ = 6.8 Hz, 2H, ^iPrCH), 6.86 - 6.92 (m, 6H, ArH); ^{13}C NMR (75MHz, C_6D_6, 298K): δ = 22.9 ($^iPrCH_3$), 23.4 ($^iPrCH_3$), 27.4 ($^iPrCH_3$), 28.0 ($^iPrCH_3$), 28.7 (^iPrCH), 29.2 (^iPrCH), 29.4 ($^tBuCH_3$), 41.9 (^tBuC), 84.5 (Cp), 123.5 (*m*-ArC), 124.1 (*m*-ArC), 126.1 (*p*-ArC), 140.5 (*ipso*-ArC), 144.1 (*o*-ArC), 145.4 (*o*-ArC), 165.0 (NCN), 216.5 (CO); IR v/cm^{-1} (Nujol): s 1964, s 1921, s 1315, s 1253, s 1210, s 1172, s 1097, s 969; m/z (EI): 666 [M^+, 6%], 493 [M^+ - Fp, 42%], 421 [PisoH$^+$, 100%]; Accurate mass m/z (EI): Calc (666.2320), found (666.2328); CHN (%): $C_{36}H_{48}N_2Ge_1Fe_1O_2$ requires: C 64.61%, H 7.23%, N 4.18%, found: C 64.36%, H 7.15%, N 4.33%.

Preparation of [{(CO)$_5$W}(Cl)Ge{N(Ar)C(Bu^t)N(Ar)}] 17. To a solution of [ClGe{N(Ar)C(Bu^t)N(Ar)}] (0.30 g, 0.57 mmol) in THF (10 cm^3) was added a solution of W(CO)$_5$.THF (0.23 g, 0.57 mmol) in THF (40 cm^3) dropwise at –78 °C over 5 minutes. The resultant solution was warmed to room temperature and stirred overnight to yield a colourless solution. Volatiles were removed *in vacuo* and the residue extracted with hexane (15 cm^3). Filtration, concentration and cooling to –30 °C overnight yielded colourless crystals of **17** (0.27g, 56%). Mp = 138 – 142°C; ^{1}H NMR (400MHz, C_6D_6, 298K): δ = 0.48 (s, 9H, ^tBu), 0.96 (d, $^3J_{HH}$ = 6.8 Hz, 6H, $^iPrCH_3$), 1.01 (d, $^3J_{HH}$ = 6.8 Hz, 6H, $^iPrCH_3$), 1.09 (d, $^3J_{HH}$ = 6.8 Hz, 6H, $^iPrCH_3$), 1.23 (d, $^3J_{HH}$ = 6.8 Hz, 6H, $^iPrCH_3$), 3.35 (sept, $^3J_{HH}$ = 6.8 Hz, 2H, ^iPrCH), 3.82 (sept, $^3J_{HH}$ = 6.8 Hz, 2H, ^iPrCH), 6.72 – 6.80 (m, 6H, ArH); ^{13}C NMR (75MHz, C_6D_6, 298K): δ = 22.2 ($^iPrCH_3$), 23.6 ($^iPrCH_3$), 27.7 ($^iPrCH_3$), 28.4 ($^iPrCH_3$), 28.9 (^iPrCH), 29.1 (^iPrCH), 29.4 ($^tBuCH_3$), 41.9 (^tBuC), 124.1 (*m*-ArC), 124.7 (*m*-ArC), 125.6 (*p*-ArC), 135.8 (*ipso*-ArC), 146.3 (*o*-ArC), 146.8 (*o*-ArC), 185.1 (NCN), 196.0 (CO); IR v/cm^{-1} (Nujol): s 2073, b 1978, b 1948, sm 1318, s 1260, sm 1208, s 1185, b 1097, b 1015, s 933; m/z (APCI): 815 [M^+ - Cl, 25%], 421 [PisoH$^+$, 100%]; CHN (%): $C_{34}H_{43}N_2Ge_1Cl_1O_5$ requires: C 47.95%, H 5.09%, N 3.29%; found C 46.96%, H 5.14%, N 3.19%.

Preparation of **[Cl₃Ge]⁻[(H)N(Ar)C(Buᵗ)N(H)(Ar)}]⁺** **18.** To a solution of [ClGe{N(Ar)C(Buᵗ)N(Ar)}] (0.25 g, 0.47 mmol) in toluene (20 cm³) was added a solution of $H_3CHC(\mu^2\text{-S})CH_2$ (0.04g, 0.47 mmol) in toluene (20 cm³) dropwise at −78 °C over 5 minutes. The resultant solution was warmed to room temperature and stirred overnight to yield a pale yellow solution. Volatiles were removed *in vacuo* and the residue extracted with diethyl ether (20 cm³). Filtration, concentration and cooling to −30 °C overnight yielded pale yellow crystals of **18** (0.05 g, 18%). Mp = 194 - 196°C;

Alternative Preparation of [Cl₃Ge]⁻[(H)N(Ar)C(Buᵗ)N(H)(Ar)}]⁺ 18. To a solution of [(H)N(Ar)C(Buᵗ)N(H)(Ar)][Cl] (0.25 g, 0.55 mmol) in THF (20 cm³) was added a solution of GeCl₂.1,4-dioxane (0.13 g, 0.55 mmol) in THF (20 cm³) dropwise at −78 °C over 5 minutes. The resultant solution was warmed to room temperature and stirred overnight to yield a pale yellow solution. Volatiles were removed *in vacuo* and the residue extracted with dichloromethane (5ml). Filtration and layering with hexane yielded pale yellow crystals of **18** (0.15 g, 46%). Mp = 194 - 196°C; ¹H NMR (400MHz, C₆D₆, 298K): δ = 0.99 (d, $^3J_{HH}$ = 6.8 Hz, 6H, ʲPrCH₃), 1.30 (d, $^3J_{HH}$ = 6.8 Hz, 6H, ʲPrCH₃), 1.31 (d, $^3J_{HH}$ = 6.8 Hz, 6H, ʲPrCH₃), 1.33 (d, $^3J_{HH}$ = 6.8 Hz, 6H, ʲPrCH₃), 1.44 (s, 9H, ᵗBu), 2.86 (2 x coincidental sept, $^3J_{HH}$ = 6.8 Hz, 4H, ʲPrCH), 7.08 − 7.52 (m, 6H, ArH), 9.60 (s, 2H, CNH); ¹³C NMR (75MHz, C₆D₆, 298K): δ = 22.2 (ʲPrCH₃), 22.5 (ʲPrCH₃), 25.8 (ʲPrCH₃), 26.1 (ʲPrCH₃), 29.1 (ʲPrCH), 29.6 (ʲPrCH), 29.8 (ᵗBuCH₃), 40.1 (ᵗBuC), 124.7 (*m*-ArC), 125.6 (*m*-ArC), 129.6 (*p*-ArC), 132.3 (*ipso*-ArC), 145.6 (*o*-ArC), 146.7 (*o*-ArC), 175.2 (NCN); IR v/cm⁻¹ (Nujol): br. 3265 (N-H), s 1260, b 1095, b 1023, s 802; m/z (APCI): 421 [PisoH⁺, 100%].

Preparation of [[(μ²-Br)Bi(Br)[{(2,6-ʲPr₂C₆H₃)N}₂C(H)](THF)]₂] 19. To a solution of [(2,6-ʲPr₂C₆H₃)N(H)C(H)=N(2,6-ʲPr₂C₆H₃)] (0.20 g, 0.56 mmol) in THF (10 cm³) was added a solution of [K][N(SiMe₃)₂] (0.12 g, 0.59 mmol) in THF (30 cm³) at room temperature. The solution was stirred for two hours and then added dropwise to BiBr₃ (0.25 g, 0.56 mmol) in THF (10 cm³) at −78 °C, warmed to room temperature and stirred continually for 36 hours to yield a yellow solution with white precipitate. Volatiles were removed in vacuo, and the residue extracted with ether (30 cm³). Filtration, concentration and slow cooling to -30 °C overnight yielded yellow crystals of **19** (0.09 g, 10 %). Mp: 128 °C (dec). ¹H NMR (300 MHz, C₆D₆, 303K): δ 1.15 (d, $^3J_{HH}$ = 6.78 Hz, CH₃, 36 H), 1.38 (m, $^3J_{HH}$ = 6.67 Hz, CH₂-THF, 8 H), 3.10

(broad s, CH, 8 H), 3.43 (broad t, $^3J_{HH}$ = 6.51 Hz, OCH$_2$-THF, 8 H), 6.95 (s, ArH, 4 H), 7.07 (broad s, ArH, 8 H), 10.05 (broad s, NCH, 2 H); ^{13}C NMR (75 MHz, C$_6$D$_6$, 303K): δ 24.2 (CH$_3$^{i}Pr), 28.7 (CH^{i}Pr), 66.2 (CH$_2$THF), 68.2 (OCH$_2$THF), 123.8 (*m*-ArC), 126.3 (*p*-ArC), 144.3 (*i*-ArC), 146.4 (*o*-ArC), 155.3 (NCN); IR v/cm^{-1} (Nujol): 1664 (s), 1587 (s), 1541 (s), 1287 (s), 1181 (s), 800 (s), 753 (s); CHN (%): C$_{58}$H$_{86}$N$_4$Bi$_2$Br$_4$O$_2$ requires: C 44.13%, H 3.57%, N 3.55%, found: C 43.55%, H 5.41%, N 3.76%.

Preparation of [(μ^2-Br)Bi(Br)[{(2,6-Me$_2$C$_6$H$_3$)N}$_2$C(H)](THF)]$_2$ 20. To a solution of [(2,6-Me$_2$C$_6$H$_3$)N(H)C(H)=N(2,6-Me$_2$C$_6$H$_3$)] (0.14 g, 0.56 mmol) in THF (10 cm^3) was added a solution of [K][N(SiMe$_3$)$_2$] (0.12 g, 0.59 mmol) in THF (30 cm^3) at room temperature. The solution was stirred for two hours and then added dropwise to BiBr$_3$ (0.25 g, 0.56 mmol) in THF (10 cm^3) at −78 °C, warmed to room temperature and stirred continually for 36 hours to yield a yellow solution with white precipitate. Volatiles were removed in vacuo, and the residue extracted with ether (30 cm^3), and THF (30 cm^3). Filtration, concentration and slow cooling to − 30 °C overnight yielded a single yellow crystal of **20** from THF. No spectroscopic data could be obtained due to the very low yield (< 1%) of this complex.

Preparation of [[{(2-PhC$_6$H$_4$)N}$_2$C(H)]$_2$BiBr] 21. To a solution of [(2-PhC$_6$H$_4$)N(H)C(H)=N(2-PhC$_6$H$_4$)] (0.39 g, 1.12 mmol) in THF (10 cm^3) was added a solution of [K][N(SiMe$_3$)$_2$] (0.23 g, 1.17 mmol) in THF (30 cm^3) at room temperature. The solution was stirred for two hours and then added dropwise to BiBr$_3$ (0.25 g, 0.56 mmol) in THF (10 cm^3) at − 78 °C, warmed to room temperature and stirred continually for 36 hours to yield a yellow solution with a white precipitate. Volatiles were removed in vacuo, and the residue extracted with ether (30 cm^3). Filtration, concentration and slow cooling to -30 °C overnight yielded red crystals of **21** (0.17 g, 31 %). Mp: 162 – 164 °C. ^{1}H NMR (300 MHz, C$_6$D$_6$, 303K): δ 6.65 – 7.33 (m, ArH, 36 H), 10.64 (s, NCH, 2 H); ^{13}C NMR (75 MHz, C$_6$D$_6$, 303K): δ 129.0 (*m''*-ArC), 129.2 (*m*-ArC), 130.4 (*m'*-ArC), 130.7 (*p''*-ArC), 131.0 (*p*-ArC), 131.1 (*i''*-ArC), 137.3 (*i*-ArC), 141.1 (*o''*-ArC), 143.7 (*o*-ArC), 147.5 (*o'*-ArC), 159.8 (NCN); IR v/cm^{-1} (Nujol): 1663 (s), 1538 (s), 1278 (s), 1202 (s), 758 (s), 734 (s), 699 (s); CHN (%): C$_{50}$H$_{38}$N$_4$Bi$_1$Br$_1$ requires: C 61.05%, H 3.87%, N 5.70%, found: C 60.68%, H 4.31%, N 5.56%.

Preparation of [[{(2,6-Me₂C₆H₃)N}₂C(H)]₂BiBr] 22. To a solution of [(2,6-Me₂C₆H₃)N(H)C(H)=N(2,6-Me₂C₆H₃)] (0.28 g, 1.12 mmol) in THF (10 cm³) was added a solution of [K][N(SiMe₃)₂] (0.23 g, 1.17 mmol) in THF (30 cm³) at room temperature. The solution was stirred for two hours and then added dropwise to BiBr₃ (0.25 g, 0.56 mmol) in THF (10 cm³) at –78 °C, warmed to room temperature and stirred continually for 36 hours to yield a yellow solution with white precipitate. Volatiles were removed in vacuo, and the residue extracted with ether (30 cm³). Filtration, concentration and slow cooling to -30 °C overnight yielded yellow crystals of **22** (0.12 g, 27 %). Mp: 145 °C (dec). ¹H NMR (300 MHz, C₆D₆, 303K): δ 2.17 (s, CH₃, 24 H), 6.76 – 7.12 (m, ArH, 12 H), 10.00 (s, NCH, 2 H); ¹³C NMR (75 MHz, C₆D₆, 303K): δ 19.9 (CH₃), 125.4 (*m*-ArC), 134.4 (*p*-ArC), 144.3 (*i*-ArC), 146.2 (*o*-ArC), 161.8 (NCN); IR ν/cm⁻¹ (Nujol): 1651 (s), 1269 (s), 1200 (s), 1091 (s), 1029 (b), 768 (s); CHN (%): C₃₄H₃₈N₄Bi₁Br₁ requires: C 51.63%, H 4.85%, N 7.08%, found: C 51.59%, H 5.32%, N 6.55%.

Preparation of [[{(2,6-Et₂C₆H₃)N}₂C(H)]₃Bi] 23. To a solution of [(2,6-Et₂C₆H₃)N(H)C(H)=N(2,6-Et₂C₆H₃)] (0.52 g, 1.68 mmol) in THF (10 cm³) was added a solution of [K][N(SiMe₃)₂] (0.35 g, 1.76 mmol) in THF (30 cm³) at room temperature. The solution was stirred for two hours and then added dropwise to BiBr₃ (0.25 g, 0.56 mmol) in THF (10 cm³) at –78 °C, warmed to room temperature and stirred continually for 36 hours to yield a yellow solution with white precipitate. Volatiles were removed in vacuo, and the residue extracted with ether (30 cm³). Filtration, concentration and slow cooling to -30 °C overnight yielded yellow crystals of **23** (0.31 g, 48 %). Mp: 140 - 148 °C. ¹H NMR (300 MHz, C₆D₆, 303K): δ 1.02 (t, CH₃, ³J_HH = 7.49 Hz, 36 H), 2.66 (q, CH₂, ³J_HH = 7.44 Hz, 24 H), 6.83 – 7.20 (m, ArH, 18 H), 11.04 (s, NCH, 3 H); ¹³C NMR (75 MHz, C₆D₆, 303K): δ 16.2 (CH₃), 25.8 (CH₂), 125.7 (*m*-ArC), 126.3 (*p*-ArC), 140.1 (*i*-ArC), 147.7 (*o*-ArC), 164.2 (NCN); IR ν/cm⁻¹ (Nujol): 1667 (s), 1601 (s), 1567 (s), 1275 (s), 1181 (s), 812 (s), 761 (s); CHN (%): C₆₃H₈₁N₆Bi₁ requires: C 66.88%, H 7.22%, N 7.48%, found: C 64.76%, H 7.36%, N 7.15%.

Preparation of [[{(2,4,6-Me₃C₆H₂)N}₂C(H)]₃Bi] 24. To a solution of [(2,4,6-Me₃C₆H₂)N(H)C(H)=N(2,4,6-Me₃C₆H₂)] (0.47 g, 1.68 mmol) in THF (10 cm³) was added a solution of [K][N(SiMe₃)₂] (0.35 g, 1.76 mmol) in THF (30 cm³) at room temperature. The solution was stirred for two hours and then added dropwise to BiBr₃ (0.25 g, 0.56 mmol) in THF

(10 cm^3) at -78 °C, warmed to room temperature and stirred continually for 36 hours to yield a yellow solution with white precipitate. Volatiles were removed in vacuo, and the residue extracted with ether (30 cm^3). Filtration, concentration and slow cooling to -30 °C overnight yielded yellow / orange crystals of **24** (0.22 g, 38 %). Mp: 126 °C (dec). ^{1}H NMR (300 MHz, C$_6$D$_6$, 303K): δ 2.20 (s, 4-CH$_3$, 18 H), 2.23 (s, 2,6-CH$_3$, 36 H), 6.65 (s, ArH, 12 H), 10.47 (s, NCH, 3 H); ^{13}C NMR (75 MHz, C$_6$D$_6$, 303K): δ 20.2 (4-CH$_3$), 21.2 (2,6-CH$_3$), 129.8 (*m*-ArC), 133.8 (*p*-ArC), 134.0 (*i*-ArC), 145.0 (*o*-ArC), 164.1 (NCN); IR *v*/cm^{-1} (Nujol): 1647 (s), 1302 (s), 1265 (s), 1213 (s), 849 (s), 722 (s); CHN (%): C$_{57}$H$_{69}$N$_6$Bi$_1$ requires: C 65.38%, H 6.64%, N 8.03%, found: C 64.84%, H 6.89%, N 7.88%.

6. References

1. M. P. Coles, *Dalton Trans.*, 2006, 985, and references therein.

2. J. Barker, M. Kilner, *Coord. Chem. Revs.*, 1994, **133**, 219, and references therein.

3. W. Bradley, I. Wright, *J. Chem. Soc.*, 1956, 640.

4. F. T. Edelmann, *Coord. Chem. Revs.*, 1994, **137**, 403, and references therein.

5. C.-W. So, H. W. Roesky, J. Magull, R. B. Oswald, *Angew. Chem. Int. Ed.*, 2006, **45**, 1.

6. H. H. Karsch, P. A. Schlüter, M. Reisky, *Eur. J. Inorg. Chem.*, 1998, 433.

7. Y. Zhou, D. S. Richeson, *Inorg. Chem.*, 1997, **36**, 501.

8. U. Kilimann, M. Noltemeyer, F. T. Edelmann, *J. Organomet. Chem.*, 1993, **443**, 35.

9. W. W. Schoeller, A. Sundermann, M. Reiher, *Inorg. Chem.*, 1999, **38**, 29.

10. D. K. Kennepohl, B. D. Santarsiero, R. G. Cavell, *Inorg. Chem.*, 1990, **29**, 5081.

11. W. Höneise, W. Schwarz, G. Heckmann, A. Schmidt, *Z. Anorg. Allg. Chem.*, 1986, **533**, 55.

12. K. Dehnicke, C. Ergezinger, E. Hartmann, A. Zinn, K. Hösler, *J. Organomet. Chem.*, 1988, **352**, C1.

13. R. G. Gordon, B. S. Lim, *PCT int. Appl.*, 2004, 52pp.

14. J.-K. Buijink, M. Noltemeyer, F. T. Edelmann, *Z. Naturforsch.*, 1991, **46b**, 1328.

15. P. C. Andrews, M. Brym, C. Jones, P.C. Junk, M. Kloth, *Inorg. Chem. Acta.*, 2006, **359**, 355.

16.   S. P. Green, C. Jones, P. C. Junk, K.-A. Lippert, A. Stasch, *Chem. Commun.*, 2006, **38**, 3978.

17.   I. Saur, G. Rima, K. Miqueu, H. Gornitzka, J. Barrau, *J. Organomet. Chem.*, 2003, **672**, 77.

18.   As determined by a survey of the Cambridge Crystallographic Database, September 2006.

19.   S. R. Foley, C. Bensimon, D. S. Richeson, *J. Am. Chem. Soc.*, 1997, **119**, 10359.

20.   I. L. Fedushkin, N. M. Khvoinova, A. Y. Baurin, G. K. Fukin, V. K. Cherkasov, M. P. Bubnov, *Inorg. Chem.*, 2004, **43**, 7807.

21.   A. Xia, H. El-Kaderi, M. J. Heeg, C. H. Winter, *J. Organomet. Chem.*, 2003, **682**, 224.

22.   M. L. Cole, G. B. deacon, C. M. Forsyth, K. Konstas, P. C. Junk, *Dalton Trans.*, 2006, 3360.

23.   T. Fjeldberg, A. Haaland, B. E. R. Schilling, M. F. Lappert, A. J. Thorne, *J. Chem. Soc., Dalton Trans.*, 1986, 1551.

24.   H. B. Davis, F. W. B. Einstein, P. G. Glavina, T. Jones, R. K. Pomeroy, P. Rushman, *Organomet.*, 1989, **8**, 1030.

25.   R. M. Roberts, *J. Org. Chem.*, 1949, 277.

Chapter 6

Synthesis and Characterisation of Tempo-Group 13 Hydride Complexes

1.   Introduction

1.1   Group 13 trihydrides

Boron trihydride complexes have been extensively investigated for uses in organic[1] and inorganic[2] chemistry. Since the early 90's there has been a vast amount of literature published on the synthesis, chemistry and uses of the heavier group 13 trihydrides, especially the Lewis base adducts of aluminium trihydride (alane) and gallium trihydride (gallane).[3-7] Towards the end of the 90's the accumulation of knowledge on Al and Ga hydride species aided the isolation of Lewis base adducts of indium trihydride (indane).[8] Due to the extensive nature of this area and its thorough documentation, only a brief overview of some aspects of group 13 trihydride chemistry will be presented here.

The accumulation of knowledge for alane and gallane has highlighted that similarities and major differences exist between their coordination modes. These differences arise from the stronger tendency for aluminium to form 'hyper'-valent structures compared to gallium.[9] Although the covalent radii of aluminium and gallium are similar (1.25 Å), aluminium is more electropositive than gallium (chapter 1, table 1).[8] This discrepancy results from the 'd-block' contraction that occurs for gallium. The AlH_3 unit is therefore more Lewis acidic than the GaH_3 unit and thus prefers coordination numbers of five or six to satisfy its electron deficiency.[3,8] The gallane unit is generally found possessing a coordination number of four in its complexes. For example, complexes 2 and 7 (below) possess differing structures which can be attributed to the differing Lewis acidity between the alane and gallane fragments.

Lewis base adducts of alane and gallane have found uses in organic, inorganic and materials chemistry.[3,6,10,11] There physical characteristics have made them ideal molecular precursors for the production of electronic devices. Alane and gallane lack metal-carbon bonds, where metal-hydride bonds are found instead. This, therefore, reduces the amount of carbon impurities formed during production of electronic materials when using them as precursors. Furthermore, the thermal frailty of the metal-hydride bond and the often high volatility of alane

and gallane complexes results in a reduction of the temperatures and pressures required for the production of electronic devices by chemical vapour deposition processes.[11] For example, dimethylethylamine alane has been shown to deposit thin aluminium films at low temperatures using procedures such as metal organic chemical vapor deposition (MOCVD).

1.2 Synthetic routes to Lewis base adducts of group 13 trihydrides

Several synthetic routes have been employed for accessing Lewis base adducts of alane and gallane. For example, complex 1 has been synthesised from the direct reaction of elemental aluminium and triethylenediamine in the presence of H_2 gas (scheme 1).[12] High pressure H_2 gas and elevated temperatures are required for this preparation to proceed. A similar compound, quinuclidine alane (quinAlH$_3$), has been synthesised from the metathetical reaction between lithium tetrahydroaluminate and quinuclidine hydrochloride at 0°C.[13] Elimination of LiCl and evolution of H_2 gas occurs as the reaction proceeds yielding the thermally sensitive material quinAlH$_3$. Due to thermal sensitivity of quinAlH$_3$, the direct reaction route can not be used to prepare this material.

Scheme 1

tmeda = N,N,N',N'-tetramethylethylenediamine
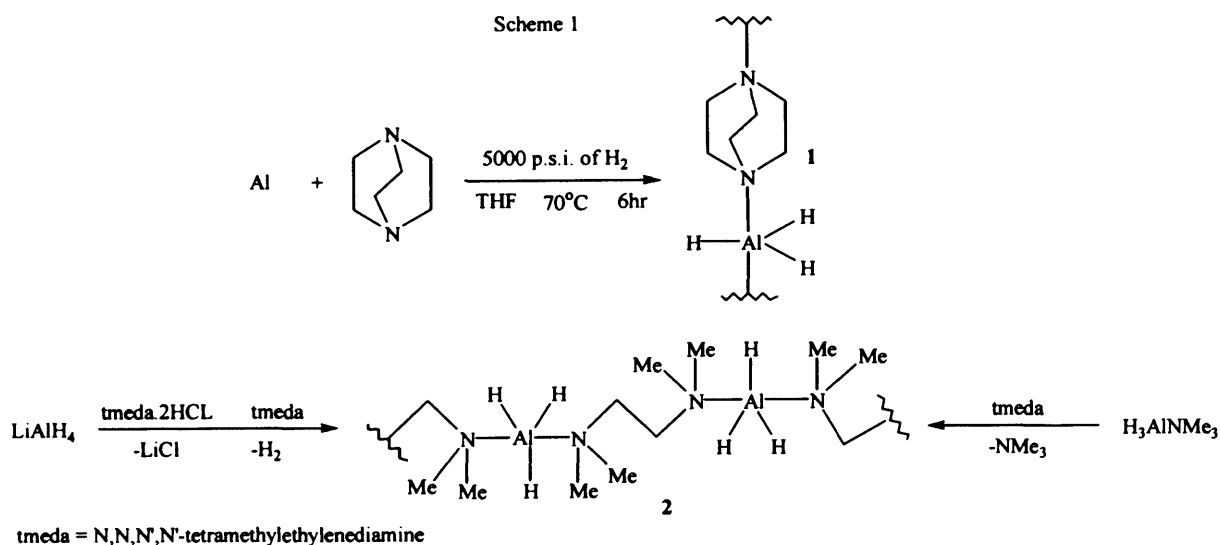
The metathesis pathway has been extensively used in the formation of tertiary amine adducts of alanes. A further example is in the preparation of the five coordinate complex 2.[14] The authors of its report demonstrated how a ligand substitution pathway could also be used for the production of Lewis base adducts of alanes. The reaction of trimethylamine alane with tmeda

resulted in the substitution of trimethylamine by the stronger donor group, tmeda, at the aluminium centre.

A common alane complex utilised for ligand substitutions is the Lewis base adduct Me_3NAlH_3. This has been synthesised from 3 $LiAlH_4$ and 4 NMe_3 giving 2 Me_3NAlH_3 and Li_3AlH_6. However, the similar reaction of $LiAlH_4$ with NEt_3 does not proceed.[15]

Tertiary phosphine adducts of alane and gallane have been synthesised and examples are shown in scheme 2. Complexes **3** were isolated from metathesis and ligand substitution pathways.[13,16] Identical preparatory methods have been used for other alane and gallane complexes.[17,18] Interestingly, the treatment of trimethylamine alane with dimethylphosphinoethane yielded the mixed donor complex **4**, instead of ligand substitution products, cf. **3**.[13]
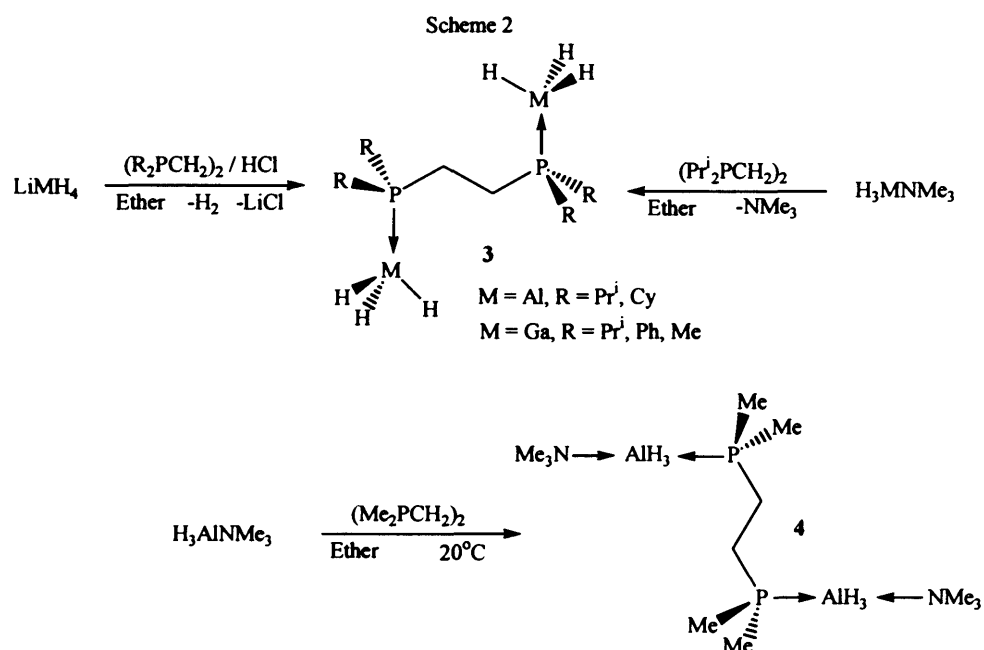
Scheme 2

Further tertiary amine adducts of alane and gallane, **5**, have been synthesised from the two common routes, ligand substitution and metathesis, and are shown in scheme 3.[16-18] Complex **6** was synthesised by treatment of trimethylamine hydrochloride with lithium gallium hydride.[19] Complex **6** has been used as a starting material for the synthesis of other gallane containing compounds. For example, complex **7** was synthesised by ligand substitution in the treatment of **6** with tmeda.[20] Complex **8** was synthesised from the metathesis reaction between lithium gallium hydride and quinuclidine hydrochloride.[20]

145
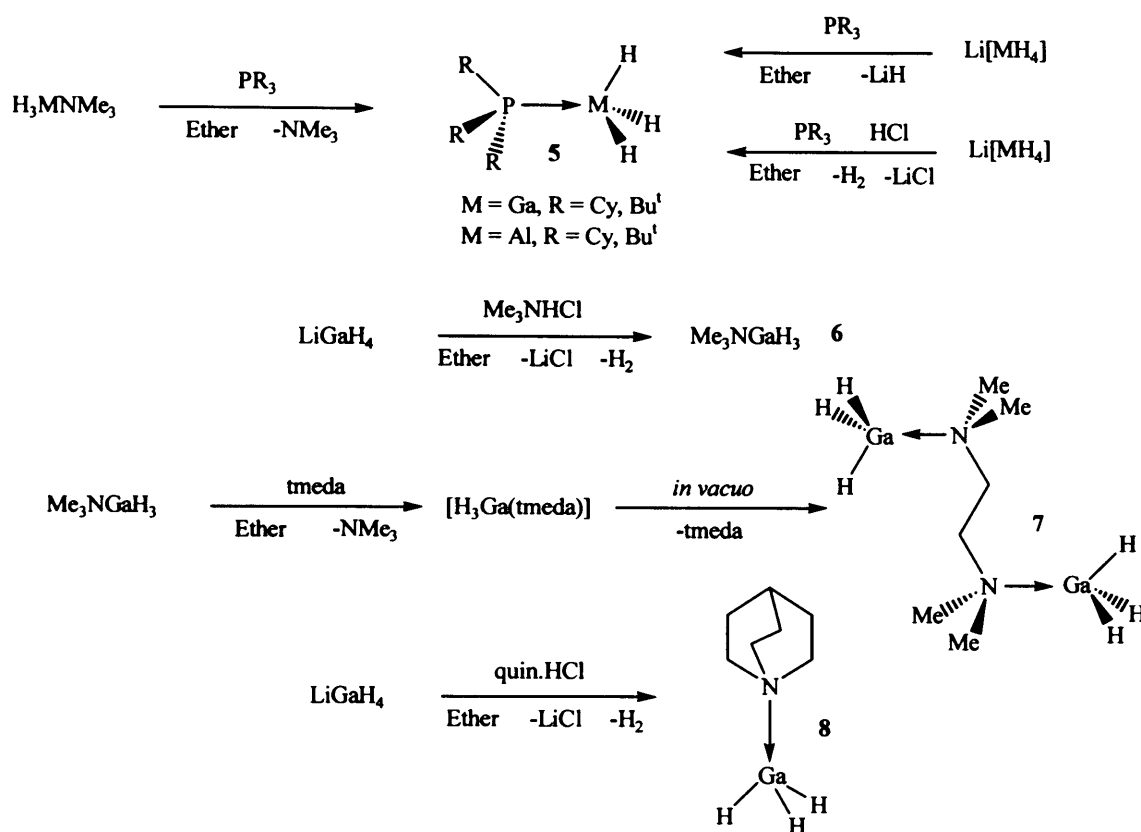
Scheme 3

More recently the isolation of a Lewis base adduct of an indium trihydride compound was published, scheme 4. The N-heterocyclic carbene indane, **9**, can be synthesised via ligand substitution of in-situ prepared trimethylamine indium trihydride by the N-heterocyclic carbene (NHC). Alternatively, the addition of the NHC to lithium indium hydride also yielded complex **9**.[21] Related NHC complexes of alane[22,23] and gallane[22] have also been reported. Tertiary phosphine adducts of indane have also been accessed via ligand displacement from the treatment of Me₃NInH₃ with, for example, PCy₃, Cy = cyclohexyl; giving complex **10**.[24]

Scheme 4
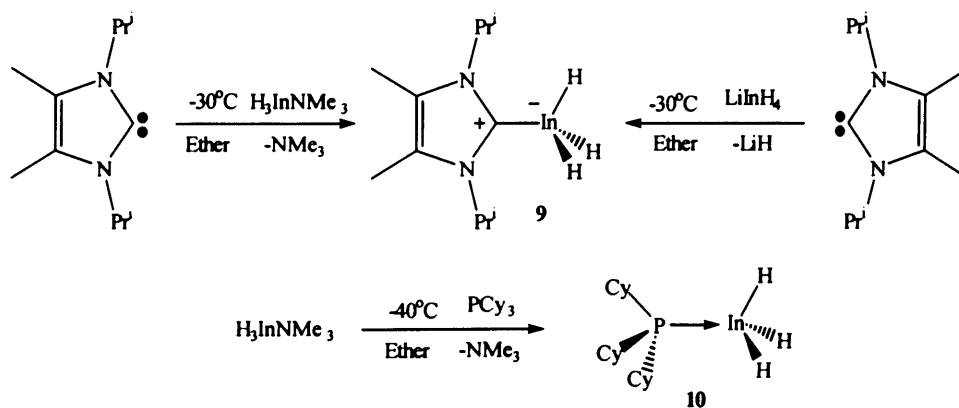
1.3   Sub-valent Group 13 cluster formation

Schnockel and co-workers have been prevalent in the exploration of sub-valent group 13 cluster compound formation. They have shown that by using a specially designed reactor, the temperature controlled disproportionation of metastable M(I)halides, M = Al, Ga; in the presence of a suitable ligand or coordinating solvent leads to an array of fascinating cluster compounds.[25,26] For example, the $[Al_{77}R_{20}]^{2-}$ and $[Ga_{84}R_{20}]^{4-}$, R = $N(SiMe_3)_2$; clusters were formed from the reactions of Al(I)Cl or Ga(I)Br with $LiN(SiMe_3)_2$. These cluster compounds have provided great insight into the formation of metals and group 13 elemental topologies. Recently, Jones and co-workers isolated a In_5 cluster from the controlled decomposition of quinInH$_3$, quin = quinuclidine; in the presence of LiBr, where evolution of H$_2$ gas occured.[27] Interestingly, there is no precedence for the formation of similar cluster materials for aluminium or gallium using a similar procedure.
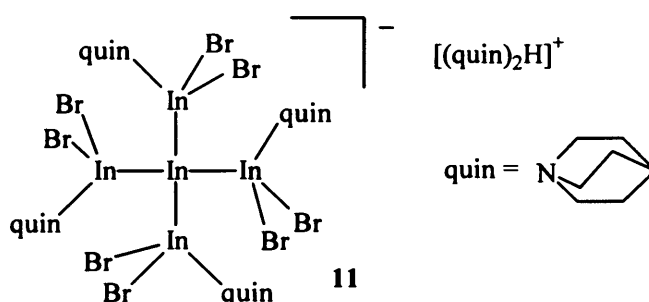

2.   Research Proposal

We wished to extend the pursuit of sub-valent group 13 metal-metal bond and subsequent cluster formation to the reduction of +III oxidation state group 13 hydrides. Group 14 mono hydrides have been shown to yield radical coupled metal-metal bonded species from the reactions of 2,2,6,6-tetramethyl-1-piperidinyloxy free radical (tempo) with either Bu$_3$SnH or Ph$_3$GeH. However, these species have only been detected by GC/MS.[28] It was thought that the treatment of a group 13 metal tri-hydride complexes, {L}MH$_3$, where L = Lewis base; M = Al, Ga, In; with a radical abstraction agent would promote homolytic cleavage of the M-H bond in {L}MH$_3$ giving {L}M˙H$_2$. A second equivalent of {L}M˙H$_2$ could conceivably bond through a radical coupling mechanism giving a metal(II)-metal(II) bonded species. Furthermore, it was

thought that the addition of further equivalents of radical abstraction agents may facilitate the formation of sub-valent group 13 metal hydride clusters, which are unknown.

3. Results and discussion

Quinuclidine adducts of alane, gallane and indane were selected for radical coupling investigations due to their general ease of synthesis and moderate thermal stability. Furthermore, quinuclidine indane has been used for the synthesis of a mixed oxidation state In cluster complex 11, as described above.[27] A series of radical abstraction agents have been reacted with quniAlH₃, quinGaH₃ and quinInH₃ to attempt the synthesis of metal-metal bonded species. The results of this study are summarised in scheme 5.

Scheme 5
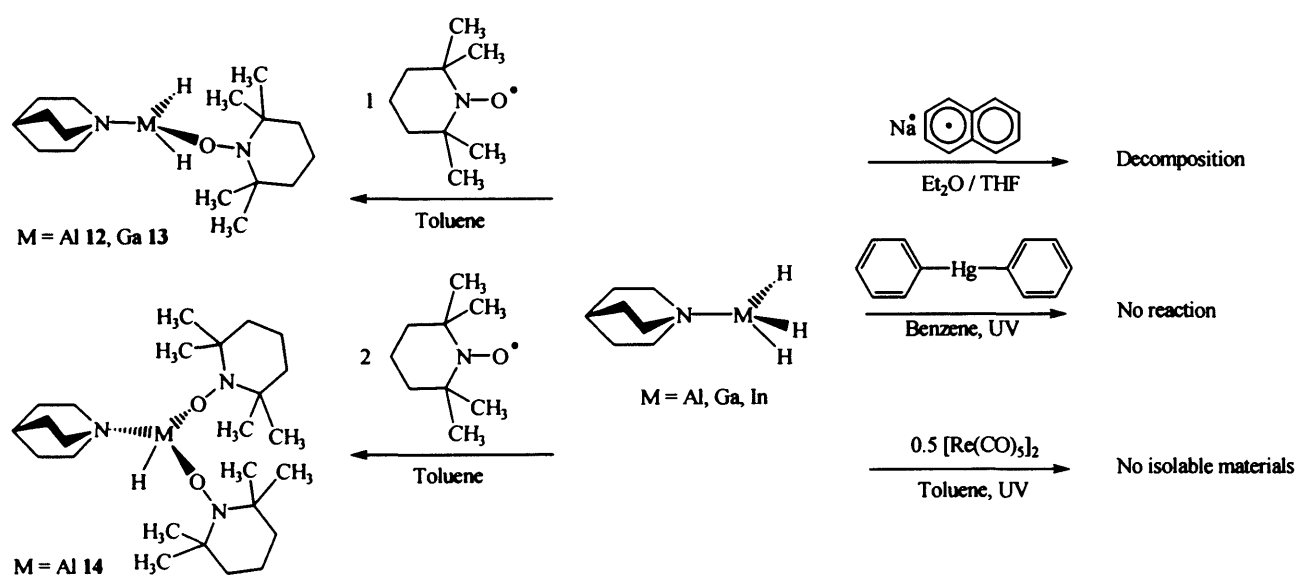
The 1:1 treatment of quniAlH₃ and quinGaH₃ with tempo yielded the complexes 12 and 13 in low yield. During the reaction, hydrogen evolution was seen to occur which suggests that hydrogen was displaced by tempo yielding the observed products. The same mechanism was also thought to facilitate the formation of complex 14 which was synthesised from the 2:1 treatment of quinAlH₃ by tempo. Complex 14 was isolated in moderate yield. In all cases the oxidation state of the metal centre remains unchanged. The reaction of tempo and quinInH₃ resulted in decomposition of the indane complex signified by the deposition of elemental indium.

X-ray crystallographic studies were carried out on **12 - 14** and their molecular structures are depicted in figures 1 - 3 respectively.
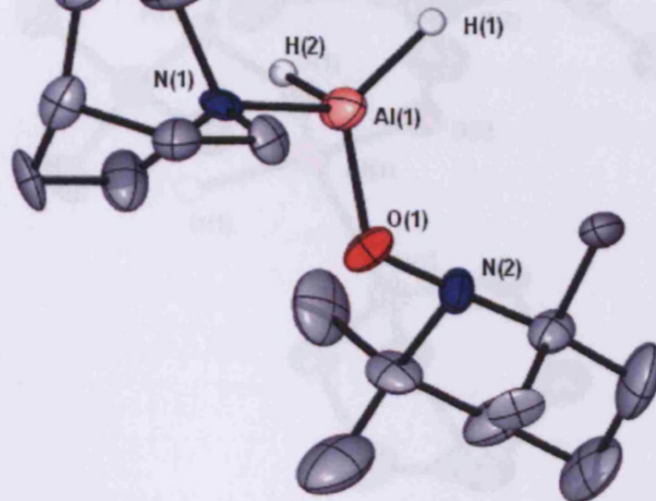
Figure 1. Molecular structure of **12**. Selected bond lengths (Å) and angles (°): Al(1)-O(1) 1.754(3), Al(1)-N(1) 2.003(3), Al(1)-H(1) 1.61(5), Al(1)-H(2) 1.57(6), O(1)-N(2) 1.456(4), O(1)-Al(1)-N(1) 94.03(14), O(1)-Al(1)-H(1) 119.3(19), N(1)-Al(1)-H(1) 100.6(19), O(1)-Al(1)-H(2) 116(2), N(1)-Al(1)-H(2) 106(2), H(1)-Al(1)-H(2) 116(2), N(2)-O(1)-Al(1) 113.4(2).
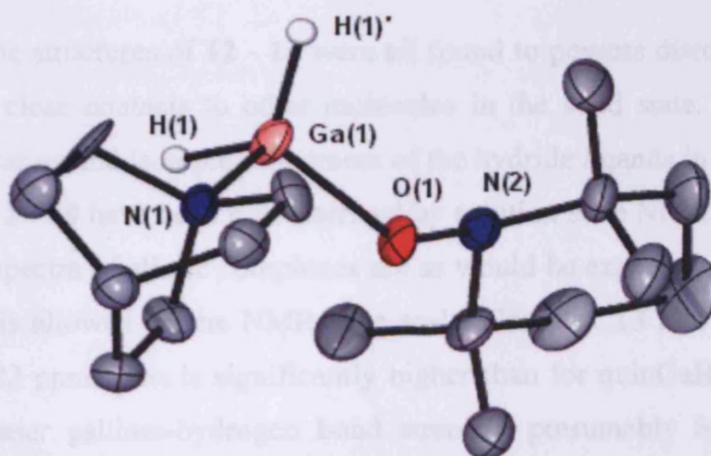
Figure 2. Molecular structure of **13**. Selected bond lengths (Å) and angles (°): Ga(1)-O(1) 1.850(5), Ga(1)-N(1) 2.078(7), Ga(1)-H(1) 1.43(6), O(1)-N(2) 1.447(8), O(1)-Ga(1)-N(1) 90.8(2), O(1)-Ga(1)-H(1) 117(2), N(1)-Ga(1)-H(1) 103(2), N(2)-O(1)-Ga(1) 112.7(4).
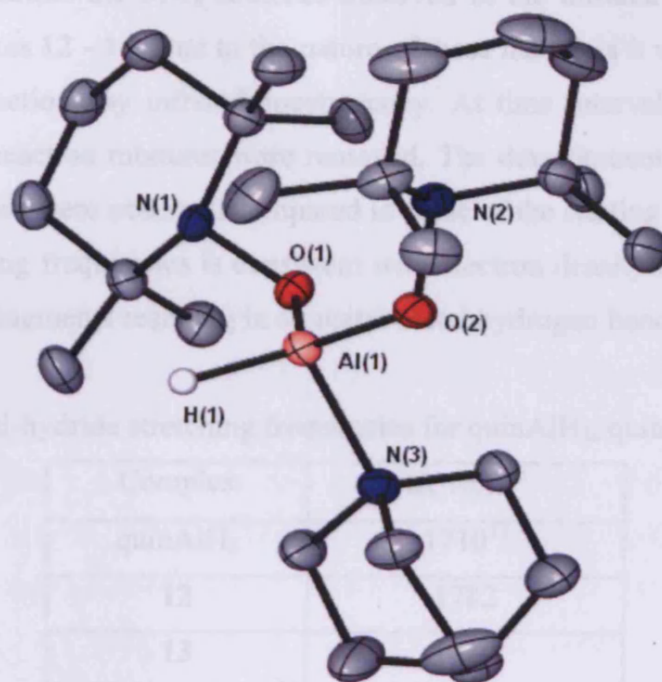
Figure 3. Molecular structure of **14**. Selected bond lengths (Å) and angles (°): Al(1)-O(1) 1.7423(15), Al(1)-O(2) 1.7535(15), Al(1)-N(3) 2.0215(17), Al(1)-H(1) 1.55(2), O(1)-N(1) 1.4602(19), O(2)-N(2) 1.453(2), O(1)-Al(1)-O(2) 119.89(7), O(1)-Al(1)-N(3) 101.38(7), O(2)-Al(1)-N(3) 93.68(7), O(1)-Al(1)-H(1) 116.5(8), O(2)-Al(1)-H(1) 115.8(8), N(3)-Al(1)-H(1) 103.1(8), N(1)-O(1)-Al(1) 121.37(11), N(2)-O(2)-Al(1) 120.48(10).

The solid state structures of **12 - 14** were all found to possess distorted tetrahedral metal geometries with no close contacts to other molecules in the solid state. The geometries were confirmed by the location and isotopic refinement of the hydride ligands in each case.

Complexes **12 - 14** have been characterised by solution state NMR spectroscopy. The ^{1}H and ^{13}C$\{^1$H$\}$ NMR spectra of all the complexes are as would be expected if free rotation around ligand-metal bonds is allowed on the NMR time scale. Complex **13** also shows a broad metal hydride signal at 5.22 ppm. This is significantly higher than for quinGaH$_3$ (4.80 ppm)[20] and is suggestive of a greater gallium-hydrogen bond strength, presumably because of a negative inductive effect of the tempo ligand. No Al-H resonances were observed in the ^{1}H NMR spectra of **12** and **14** due to the quadrapolar nature of the metal. Where the quadrapolar moment of Al is greater than that of Ga, 5/2 and 3/2 respectively.

Table 1 summarises the M-H stretches observed in the infrared spectra of the starting materials and complexes **12 - 14**. Due to the nature of these materials it was possible to monitor progression of the reactions by infrared spectroscopy. At time intervals during the reactions, small aliquots of the reaction mixtures were removed. The development of new, higher energy hydride stretching bands were observed compared to those of the starting materials. The increase in the hydride stretching frequencies is consistent with electron density removal from the metal centres by the tempo fragments resulting in a greater metal hydrogen bond strengths.

Table 1: Infrared metal-hydride stretching frequencies for quinAlH$_3$, quinGaH$_3$ and **12 - 14**

Complex	IR v/cm^{-1}
quinAlH$_3$	1710[13]
12	1782
13	1819
quinGaH$_3$	1810[20]
14	1850

4.   Conclusion

In summary, a series of complexes have been synthesised from the elimination of hydrogen from Lewis base-group 13 trihydride adducts by treatment with a radical abstraction agent, tempo. Despite multiple efforts to form metal-metal bonded species with radical abstraction agents, no such materials could be synthesised. Generally, these reactions met with failure where decomposition of starting materials occurred or intractable mixtures of products were formed.

5. Experimental

General experimental procedures can be found in appendix 1. quinAlH$_3$[13] and quinGaH$_3$[20] were synthesised by literature procedures. All other reactants were obtained commercially and used as received.

Preparation of QuinAl(H)$_2$[tempo] 12. To a solution of QuinAlH$_3$ (0.12 g, 1.25 mmol) in toluene (15 cm^3) was added a solution of tempo (0.19 g, 1.25 mmol) in toluene (15 cm^3) dropwise at -78 °C over 5 minutes. The resultant solution was warmed to room temperature and stirred overnight to yield a pale yellow solution. Volatiles were removed *in vacuo* and the residue extracted with hexane (10 ml). Filtration, concentration and cooling to -30 °C overnight yielded colourless crystals of **12** (0.05 g, 15%) Mp = 97– 100 °C. ^{1}H NMR (400MHz, C$_6$D$_6$, 298K): δ = 0.92 (br. s, 12H, Tempo CH$_3$), 1.26 – 1.53 (m, 6H, Tempo CH$_2$), 1.58 (m, 6h, Quin CH$_2$), 1.78 (m, 1H, Quin CH), 2.47 (m, 6H, Quin NCH$_2$), AlH not observerved; ^{13}C NMR (75MHz, C$_6$D$_6$, 298K): δ = 18.3 (Tempo C(4)H$_2$), 20.0 (Quin CH), 22.3, 36.7 (Tempo *Gem* CH$_3$), 24.5 (Quin CH2), 40.6 (Tempo C(3,5)H$_2$), 46.9 (Quin NCH$_2$), 59.7 (Tempo C(2,6)N); IR v/cm^{-1} (Nujol): b 1782 (AlH), s 1260, s 1208, s 1129, s 1045, s 1012, s 979; m/z (EI): 158 [TEMPOH$^+$, 78%], 141 [TempoH$^+$-O, 100%].

Preparation of QuinGa(H)$_2$[tempo] 13. To a solution of QuinGaH$_3$ (0.39 g, 2.15 mmol) in toluene (15 cm^3) was added a solution of tempo (0.34 g, 2.15 mmol) in toluene (15 cm^3) dropwise at -78 °C over 5 minutes. The resultant solution was warmed to room temperature and stirred overnight to yield a pale yellow solution. Volatiles were removed *in vacuo* and the residue extracted with hexane (10ml). Filtration, concentration and cooling to -30 °C overnight yielded colourless crystals of **13** (0.17g, 23%) Mp = 243 °C. ^{1}H NMR (400MHz, C$_6$D$_6$, 298K): δ = 1.02 (br. s, 12H, Tempo CH$_3$), 1.28 – 1.52 (m, 6H, Tempo CH$_2$), 1.56 (m, 6h, Quin CH$_2$), 1.82 (m, 1H, Quin CH), 2.80 (m, 6H, Quin NCH$_2$), 5.22 (br. s, 2H, GaH); ^{13}C NMR (75MHz, C$_6$D$_6$, 298K): δ = 17.8 (Tempo C(4)H$_2$), 19.9 (Quin CH), 24.4, 38.7 (Tempo *Gem* CH$_3$), 25.1 (Quin CH2), 40.3 (Tempo C(3,5)H$_2$), 47.6 (Quin NCH$_2$), 59.2 (Tempo C(2,6)N); IR v/cm^{-1} (Nujol): b 1850 (GaH), s 1262, s 1206, s 1132, b 1053, s 986, s 956; m/z (APCI): 339 [M$^+$ - H, 100%], 158 [TEMPOH$^+$, 70%].

Preparation of QuinAl(H)[tempo]₂ 14. To a solution of QuinAlH₃ (0.31 g, 2.16 mmol) in toluene (15 cm³) was added a solution of tempo (0.68 g, 4.33 mmol) in toluene (15 cm³) dropwise at −78 °C over 5 minutes. The resultant solution was warmed to room temperature and stirred overnight to yield a pale yellow solution. Volatiles were removed *in vacuo* and the residue extracted with hexane (10 ml). Filtration, concentration and cooling to −30 °C overnight yielded colourless crystals of **14** (0.38 g, 39%) Mp = 159 − 162 °C. ¹H NMR (400MHz, C₆D₆, 298K): δ = 1.03 (br. s, 24H, Tempo CH₃), 1.30 − 1.59 (m, 12H, Tempo CH₂), 1.58 (m, 6H, Quin CH₂), 1.91 (m, 1H, Quin CH), 3.11 (m, 6H, Quin NCH₂), AlH not observed; ¹³C NMR (75MHz, C₆D₆, 298K): δ = 18.3 (Tempo C(4)H₂), 20.4 (Quin CH), 25.2, 36.3 (Tempo *Gem* CH₃), 24.5 (Quin CH2), 40.1 (Tempo C(3,5)H₂), 47.0 (Quin NCH₂), 59.7 (Tempo C(2,6)N); IR v/cm⁻¹ (Nujol): b 1819 (AlH), s 1260, s 1240, s 1131, s 1045, s 1002, s 967; m/z (EI): 158 [TEMPOH⁺, 58%], 141 [TempoH⁺-O, 100%].

6. References

1. I. Beletskaya, A. Pelter, *Tetrahedron,* 1997, **53**, 4957.

2. T. P. Fehlner, *J. Chem. Soc., Dalton Trans.,* 1998, 1525.

3. C. Jones, G. A. Koutsantonis, C. L. Raston, *Polyhedron,* 1993, **12**, 1829.

4. C. L. Raston, *J. Organomet. Chem.,* 1994, **475**, 15.

5. A. J. Downs, C. R. Pulham, *Chem. Soc. Rev.,* 1994, **3**, 175.

6. M. G. Gardiner, C. L. Raston, *Coord. Chem. Revs.,* 1997, **166**, 1.

7. A. J. Downs, *Coord. Chem. Revs.,* 1999, **189**, 59.

8. C. Jones, *Chem. Commun.,* 2001, 2293, and references therein.

9. B. J. Duke, C. Liang, H. F. Schaefer III, *J. Am. Chem. Soc.,* 1991, **113**, 2884.

10. *"Chemistry of Aluminium, Gallium, Indium and Thallium"* Ed. A. J. Downs, Blakie, Glasgow, 1993.

11. J. A. Jegier, W. L. Gladfelter, *Coord. Chem. Revs.,* 2000, **206-207**, 631.

12. E. C. Ashby, *J. Am. Chem. Soc.,* 1964, **86**, 1882.

13. J. L. Atwood, K. W. Butz, M. G. Gardiner, C. Jones, G. A. Koutsantonis, C. L. Raston, K. D. Robinson, *Inorg. Chem.,* 1993, **32**, 3482.

14. J. M. Davidson, T. Wartik, *J. Am. Chem. Soc.,* 1960, **82**, 5506.

15.   J. A. Dilts, E. C. Ashby, *Inorg. Chem.,* 1970, **9**, 855.

16.   F. R. Bennett, F. M. Elms, M. G. Gardiner, G. A. Koutsantonis, C. L. Raston, N. K. Roberts, *Organomet.,* 1992, **11**, 1457.

17.   J. L. Atwood, K. D. Robinson, F. R. Bennett, F. M. Elms, G. A. Koutsantonis, C. L. Raston, D. J. Young, *Inorg. Chem.,* 1992, **31**, 2673.

18.   F. M. Elms, M. G. Gardiner, G. A. Koutsantonis, C. L. Raston, J. L. Atwood, K. D. Robinson, *J. Organomet. Chem.,* 1993, **449**, 45.

19.   N. N. Greenwood, A. Storr, M. G. H. Wallbridge, *Inorg. Chem.,* 1963, **2**, 1036.

20.   J. L. Atwood, S. G. Bott, F. M. Elms, C. Jones, C. L. Raston, *Inorg. Chem.,* 1991, **30**, 3793.

21.   D. E. Hibbs, M. B. Hursthouse, C. Jones, N. A. Smithies, *Chem. Commun.,* 1998, 869.

22.   M. D. Francis, D. E. Hibbs, M. B. Hursthouse, C. Jones, N. A. Smithies, *J. Chem. Soc., Dalton. Trans.,* 1998, 3249.

23.   R. J. Baker, A. J. Davies, C. Jones, M. Kloth, *J. Organomet. Chem.,* 2002, **656**, 203.

24.   D. E. Hibbs, C. Jones, N. A. Smithies, *Chem. Commun.,* 1999, 185.

25.   G. Linti, H. Schnöckel, *Coord. Chem. Revs.,* 2000, **206-207**, 285.

26.   A. Schnepf, H. Schnöckel, *Angew. Chem. Int. Ed.,* 2002, **41**, 3532.

27.   M. L. Cole, C. Jones, M. Kloth, *Inorg. Chem.,* 2005, **44**, 4909.

28.   M. Lucarini, E. Marcheis, G. F. Pedulli, C. Chatgilialoglu, *J. Org. Chem.,* 1998, **63**, 1687.

Appendix 1

General experimental procedures.

All manipulations were carried out using standard Schlenk and glove box techniques under an atmosphere of high purity argon or dinitrogen in flame dried glassware. All apparatus was cleaned by overnight immersion in a isopropyl alcohol solution with potassium hydroxide followed by rinsing with hydrochloric acid, distilled water and acetone before oven drying at $110^{\circ}C$.

The solvents diethyl ether, hexane, tetrahydrofuran and toluene were pre-dried over sodium wire whereas acetonitrile and dichloromethane were pre-dried over calcium hydride. All solvents were distilled under an atmosphere of high purity dinitrogen for 12 hours prior to collection. Toluene, tetrahydrofuran and hexane were distilled over potassium metal whilst diethyl ether was distilled over Na/K alloy. Acetonitrile and dichloromethane were distilled over calcium hydride.

Melting points were determined in sealed glass capillaries under argon and are uncorrected. Mass spectra were recorded using a VG Fisons Platform II instrument under APCI conditions, or were obtained from the EPSRC National Mass Spectrometric Service at Swansea University. Microanalyses were obtained from Medac Ltd. IR spectra were recorded using a Nicolet 510 FT-IR spectrometer as Nujol mulls between NaCl plates.

^{1}H and ^{13}C NMR spectra were recorded on either a Bruker DXP400 spectrometer operating at 400.13 and 100 MHz respectively, or a Jeol Eclipse 300 spectrometer operating at 300.52 and 75.57 MHz respectively and were referenced to the resonances of the solvent used. The ^{31}P NMR spectra were recorded on a Jeol Eclipse 300 spectrometer operating at 121.5 MHz and referenced to 85 % H_3PO_4. The ^{51}V NMR spectra were recorded on a Jeol Eclipse 300 spectrometer operating at 78.91 MHz and referenced relative to external $VOCl_3$ ($\delta = 0$ ppm).

Publications

Reactions of a Gallium(II)-Diazabutene Dimer, [{{[(H)C(Bu^t)N]$_2$}GaI}$_2$], with [ME(SiMe$_3$)$_2$] (M = Li or Na; E = N, P, or As): Structural, EPR and ENDOR Characterisation of Paramagnetic Gallium(III) Pnictide Complexes, K. L. Antcliff, R. J. Baker, C. Jones, D. M. Murphy, R. P. Rose, *Inorg. Chem.*, 2005, **44**, 2098.

η^6-Triphosphabenzene, η^5-Triphosphacyclohexadienyl, and η^5-Diphosphacyclopentadienyl Complexes of Group 8 and 9 Metals: Heterocycle Transformations at the Metal Center, M. D. Francis, C. Holtel, C. Jones, R. P. Rose, *Organomeallics.*, 2005, **24**, 4216.

Oxidative Addition of an Imidazolium Cation to an Anionic Gallium(I) N-Heterocyclic Carbene Analogue: Synthesis and Characterisation of Novel Gallium Hydride Complexes, Cameron Jones, D. P. Mills, R. P. Rose, *J. Organomet. Chem.*, 2006, **691**, 3060.

Complexes of a Gallium Heterocycle with Transition Metal Sandwich, Half Sandwich and Dialkyl Fragments, S. Aldridge, R. J. Baker, N. D. Coombs, C. Jones, R. P. Rose, A. Rossin, D. J. Willock, *Dalton Trans.*, 2006, 3313.

Synthesis, Structural Characterization, and Theoretical Studies of Complexes of Magnesium and Calcium with Gallium Heterocycles, C. Jones, D. P. Mills, J. A. Platts, R. P. Rose, *Inorg. Chem.*, 2006, **45**, 3146.

'GaI' : A New Reagent for Chemo- and Diastereoselective C-C Bond Forming Reactions, S. P. Green, C. Jones, R. P. Rose, A. Stasch, *New J. Chem.*, submitted.